UDK 66:54(05) CODEN HMIDA 8 ISSN 0367–598 X

4

Hemijska industrija

Vol. 67

Časopis Saveza hemijskih inženjera

Chemical Industry

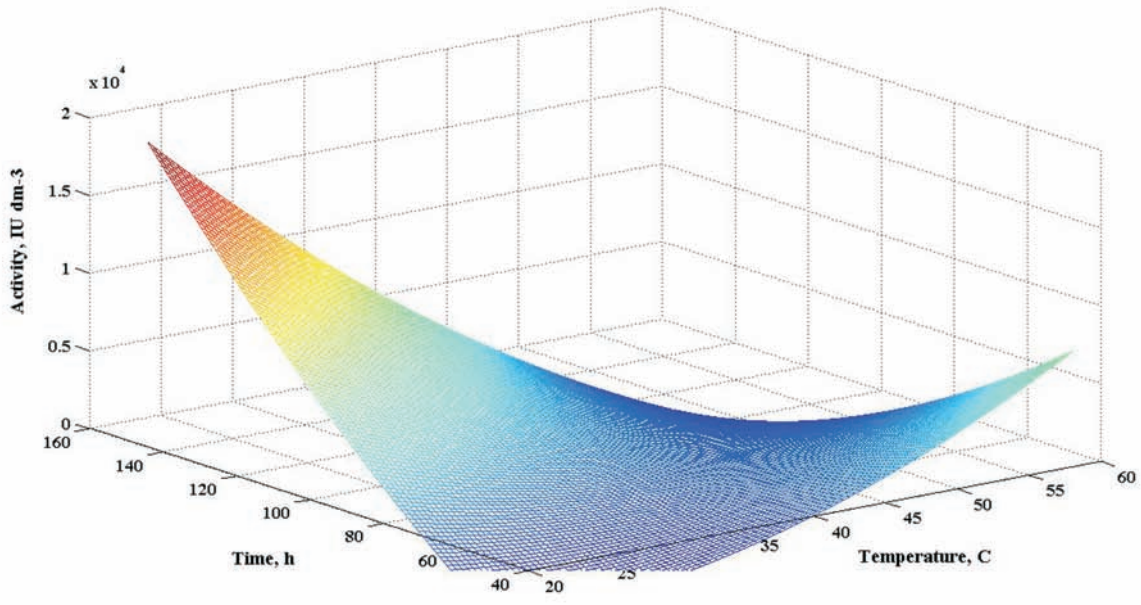

BEOGRAD, JUL-AVGUST 2013. HMIDA 8, 67 (4) 559-701 (2013)

Beograd Srbija SHI

Chemical Industry
Химическая промышленность

Hemijska industrija

Časopis Saveza hemijskih inženjera Srbije
Journal of the Association of Chemical Engineers of Serbia
Журнал Союза химических инженеров Сербии

VOL. 67 **Beograd, jul–avgust 2013** **Broj 4**

Izdavač
Savez hemijskih inženjera Srbije
Beograd, Kneza Miloša 9/I

Glavni urednik
Branko Bugarski
Urednici
Katarina Jeremić, Ivana Banković-Ilić, Maja Obradović, Dušan Mijin

Članovi uredništva
Milorad Cakić, Željko Čupić, Željko Grbavčić, Katarina Jeremić, Miodrag Lazić, Slobodan Petrović, Milovan Purenović, Aleksandar Spasić, Dragoslav Stoiljković, Radmila Šećerov-Sokolović, Slobodan Šerbanović, Nikola Nikačević, Svetomir Milojević

Članovi uredništva iz inostranstva
Dragomir Bukur (SAD), Jiri Hanika (Češka Republika), Valerij Meshalkin (Rusija), Ljubiša Radović (SAD), Constantinos Vayenas (Grčka)

Likovno-grafičko rešenje naslovne strane
Milan Jovanović

Redakcija
11000 Beograd, Kneza Miloša 9/I
Tel/fax: 011/3240-018
E-pošta: shi@yubc.net
www.ache.org.rs

Izlazi dvomesečno, rukopisi se ne vraćaju

Za izdavača
Tatijana Dudukoviċ

Sekretar redakcije
Slavica Desnica

Izdavanje časopisa pomaže
Republika Srbija, Ministarstvo prosvete, nauke i tehnološkog razvoja

Uplata pretplate i oglasnog prostora vrši se na tekući račun Saveza hemijskih inženjera Srbije, Beograd, broj 205-2172-71, Komercijalna banka a.d., Beograd

Kompjuterska priprema
Vladimir Panić

Štampa
Razvojno-istraživački centar grafičkog inženjerstva, Tehnološko-metalurški fakultet, Univerzitet u Beogradu, Karnegijeva 4, 11000 Beograd

Indeksiranje
Radovi koji se publikuju u časopisu *Hemijska Industrija* ideksiraju se preko *Thompson Reuters Scietific®* servisa *Science Citation Index - Expanded™* i *Journal Citation Report (JCR)*, kao i domaćeg *SCIndeks* servisa Centra za evaluaciju u obrazovanju i nauci

SADRŽAJ

Miloš M. Kostić, Miljana D. Radović, Jelena Z. Mitrović, Danijela V. Bojić, Dragan D. Milenković, Aleksandar Lj. Bojić, **Application of new biosorbent based on chemicaly modified *Lagenaria vulgaris* shell for the removal of copper(II) from aqueous solutions: Effects of operational parameters** 559

Midhat Suljkanović, Milovan Jotanović, Elvis Ahmetović, Goran Tadić, Nidret Ibrić, **Formalizovana metodologija za separaciju trokomponentnih elektrolitičkih sistema. Parcijalna separacija sistema** 569

Saša S. Ranđelović, Danijela A. Kostić, Aleksandra R. Zarubica, Snežana S.Mitić, Milan N. Mitić, **The correlation of metal content in medicinal plants and their water extracts** 585

Zoran I. Petrović, Vlado B. Teodorović, Mirjana R. Dimitrijević, Sunčica Z. Borozan, Miloš T. Beuković, Dragica M. Nikolić, Aurelija T. Spirić, **Environmental cadmium and zinc concentrations in liver and kidney of european hare from different serbian regions** 593

Ferenc E. Kiš, Goran C. Bošković, **Ocenjivanje uticaja životnog ciklusa biodizela ReCiPe metodom** 601

Danijela Z. Šuput, Vera L. Lazić, Ljubinko B. Lević, Nevena M. Krkić, Vladimir M. Tomović, Lato L. Pezo, **Characteristics of meat packaging materials and their environmental suitability assessment** 615

Goran Radosavljević, Andrea Marić, Michael Unger, Nelu Blaž, Walter Smetana, Ljiljana Živanov, **Električna, mehanička i temperaturna karakterizacija komercijalno dostupnih LTCC dielektričnih materijala** 621

Radoslav D. Mićić, Milan D. Tomić, Mirko Đ. Simikić, Aleksandra R. Zarubica, **Biodiesel from rapeseed variety "Banaćanka" using KOH catalyst** 629

Sunčica D. Kocić-Tanackov, Gordana R. Dimić, **Gljive i mikotoksini – kontaminenti hrane** 639

Nada V. Bojić, Ružica R. Nikolić, Branimir Z. Jugović, Zvonimir S. Jugović, Milica M. Gvozdenović, **Uniaxial tension of drying sieves** 655

Živko T. Sekulić, Aleksandra S. Daković, Milan M.Kragović, Marija A. Marković, Branislav B.Ivošević, Božo M. Kolonja, **Kvalitet zeolita iz ležišta Vranjska Banja po klasama krupnoće** 663

Liljana Koleva Gudeva, Sasa Mitrev, Viktorija Maksimova, Dusan Spasov, **Content of capsaicin extracted from hot pepper (*Capsicum annuum* ssp. *microcarpum* L.) and its use as an ecopesticide** 671

Sonja M. Jakovetić, Zorica D. Knežević-Jugović, Sanja Ž. Grbavčić, Dejan I. Bezbradica, Nataša S. Avramović, Ivanka M. Karadžić, **Rhamnolipid and lipase production by *Pseudomonas***

SADRŽAJ nastavak

***aeruginosa* san-ai: The process comparison analysis by statistical approach** 677
Milica Ž. Pavlićević, Slađana P. Stanojević, Biljana V. Vucelić-Radović, **Influence of extraction method on protein profile of soybeans** 687
Branka Hadžić, Nebojša Romčević, Maja Romčević, Izabela Kuryliszyn-Kudelska, Witold D. Dobrowolski, Ursula Narkiewicz, Daniel Sibera, **Raman study of surface optical phonons in ZnO(Co) nanoparticles prepared by hydrothermal method** 695

CONTENTS

Miloš M. Kostić, Miljana D. Radović, Jelena Z. Mitrović, Danijela V. Bojić, Dragan D. Milenković, Aleksandar Lj. Bojić, **Application of new biosorbent based on chemicaly modified *Lagenaria vulgaris* shell for the removal of copper(II) from aqueous solutions: Effects of operational parameters** 559
Midhat Suljkanović, Milovan Jotanović, Elvis Ahmetović, Goran Tadić, Nidret Ibrić, **Formalized methodology for the separation of three component electrolytic systems. Partial separation of the system** 569
Saša S. Ranđelović, Danijela A. Kostić, Aleksandra R. Zarubica, Snežana S.Mitić, Milan N. Mitić, **The correlation of metal content in medicinal plants and their water extracts** 585
Zoran I. Petrović, Vlado B. Teodorović, Mirjana R. Dimitrijević, Sunčica Z. Borozan, Miloš T. Beuković, Dragica M. Nikolić, Aurelija T. Spirić, **Environmental cadmium and zinc concentrations in liver and kidney of european hare from different serbian regions** 593
Ferenc E. Kiš, Goran C. Bošković, **Life cycle impact assessment of biodiesel using the ReCiPe Method** 601
Danijela Z. Šuput, Vera L. Lazić, Ljubinko B. Lević, Nevena M. Krkić, Vladimir M. Tomović, Lato L. Pezo, **Characteristics of meat packaging materials and their environmental suitability assessment** 615
Goran Radosavljević, Andrea Marić, Michael Unger, Nelu Blaž, Walter Smetana, Ljiljana Živanov, **Electrical, mechanical and themperature characterization of commercialy available LTCC dielectric materials** 621
Radoslav D. Mićić, Milan D. Tomić, Mirko Đ. Simikić, Aleksandra R. Zarubica, **Biodiesel from rapeseed variety "Banaćanka" using KOH catalyst** 629
Sunčica D. Kocić-Tanackov, Gordana R. Dimić, **Fungi and mycotoxins – food contaminants** 639
Nada V. Bojić, Ružica R. Nikolić, Branimir Z. Jugović, Zvonimir S. Jugović, Milica M. Gvozdenović, **Uniaxial tension of drying sieves** 655
Živko T. Sekulić, Aleksandra S. Daković, Milan M.Kragović, Marija A. Marković, Branislav B.Ivošević, Božo M. Kolonja, **Quality of zeolit from Vranjska Banja deposit according to size classes** 663
Liljana Koleva Gudeva, Sasa Mitrev, Viktorija Maksimova, Dusan Spasov, **Content of capsaicin extracted from hot pepper (*Capsicum annuum* ssp. *microcarpum* L.) and its use as an ecopesticide** 671
Sonja M. Jakovetić, Zorica D. Knežević-Jugović, Sanja Ž. Grbavčić, Dejan I. Bezbradica, Nataša S. Avramović, Ivanka M. Karadžić, **Rhamnolipid and lipase production by *Pseudomonas***

CONTENTS Continued

aeruginosa **san-ai: The process comparison analysis by statistical approach** 677

Milica Ž. Pavlićević, Slađana P. Stanojević, Biljana V. Vucelić-Radović, **Influence of extraction method on protein profile of soybeans** 687

Branka Hadžić, Nebojša Romčević, Maja Romčević, Izabela Kuryliszyn-Kudelska, Witold D. Dobrowolski, Ursula Narkiewicz, Daniel Sibera, **Raman study of surface optical phonons in ZnO(Co) nanoparticles prepared by hydrothermal method** 695

Application of new biosorbent based on chemicaly modified *Lagenaria vulgaris* shell for the removal of copper(II) from aqueous solutions: Effects of operational parameters*

Miloš M. Kostić[1], Miljana D. Radović[1], Jelena Z. Mitrović[1], Danijela V. Bojić[1], Dragan D. Milenković[2], Aleksandar Lj. Bojić[1]

[1]*University of Niš, Faculty of Sciences and Mathematics, Department of Chemistry, Niš, Serbia*
[2]*High Chemical Technological School, Department of Chemical Technology, Kruševac, Serbia*

Abstract

In the present study, a low cost biosorbent derived from the *Lagenaria vulgaris* plant by xanthation, was tested for its ability to remove copper from aqueous solution. The effect of contact time, initial pH, initial concentration of copper(II) ions and adsorbent dosage on the removal efficiency were studied in a batch process mode. The optimal pH for investigated metal was 5. A dosage of 4 g dm^{-3} of xanthated *Lagenaria vulgaris* biosorbent (xLVB) was found to be effective for maximum uptake of copper(II). The kinetic of sorption of metal was fast, reaching at equilibrium in 50 min. The kinetic data were found to follow closely the pseudo-second-order model. The adsorption equilibrium was described well by the Langmuir isotherm model with maximum adsorption capacity of 23.18 mg g^{-1} copper(II) ions on xLVB. The presence of sulfur groups on xLVB was identified by FTIR spectroscopic study. Copper removal efficiency was achieved at 81.35% from copper plating industry wastewater.

Keywords: xanthated *Lagenaria vulgaris*, copper(II) ions, biosorption.

Available online at the Journal website: http://www.ache.org.rs/HI/

SCIENTIFIC PAPER

UDC 544.723:544.47:546.56

Hem. Ind. **67** (4) 559–567 (2013)

doi: 10.2298/HEMIND120703097K

Copper is widely used in electrical wiring, plumbing, gear wheel, selenium rectifier and roofing industries, due to its excellent properties such as electrical and thermal conductivity, good corrosion resistance, ease of fabrication and installation [1]. The potential sources of copper in industrial effluents include metal cleaning and plating baths, pulp, paperboard mills, wood pulp production, and the fertilizer industry. Copper(II) is known to be one of the heavy metals most toxic to living organisms and it is one of the more widespread heavy metal contaminants of the environment [2].

The conventional methods for removing copper(II) from aqueous solutions include precipitation, oxidation/reduction, electrochemical treatments, evaporative recovery, coagulation/flocculation, filtration methods, ion-exchange and membrane technologies. These processes may have different limitations: high cost, process complexity and sludge formation, or may be ineffective, especially when the metals in solution are in range of 1-100 mg dm^{-3} [3–5]. Biosorption processes are being employed as an attractive alternative technique for the decontamination of industrial effluents and for the recovery of the retained metals [6]. The major advantages of biosorption over conventional methods include low cost, high efficiency, minimization of chemical or biological sludge and possibility of bio–sorbent regeneration [7]. A low cost sorbent is defined as one which is abundant in nature, or is a by-product or waste material from another industry [8]. Recently, Bailey *et al*. [9] reviewed a wide variety of low cost sorbents for the removal of heavy metals.

Among the adsorbents used to remove heavy metals, those containing sulfur-bearing groups have a high affinity for heavy metals but low affinity for light metals. From the different sulfur bearing compounds, xanthates are found to be the most prominent because they are easy to prepare with relatively inexpensive reagents, highly insoluble and have high stability constants of metal complex formed according to HSAB classification system. *Lagenaria vulgaris* biosorbent is mostly composed of cellulose and lignin. These components contain many hydroxyl functional groups, which makes it a potential matrix to synthesize xanthate [10–12].

The objective of this research was to investigate the copper removal efficiency of xanthated *L. vulgaris* biosorbent (xLVB) by adsorption from aqueous media. The effect of contact time, initial pH, initial concentration of copper(II) ions and adsorbent dosage were examined. Batch experiments were carried out to investigate the

Correspondence: M.D. Radović, Department of Chemistry, Faculty of Sciences and Mathematics, University of Niš, Visegradska 33, 18000 Niš, Serbia.

E-mail: mimaradovic@gmail.com

Paper received: 3 July, 2012

Paper accepted: 26 September, 2012

* Some results of this study were communicated at the meeting: 9th Symposium "Novel technologies and economic development" (with international participation), 21–22 October 2011, Leskovac, Serbia.

adsorption kinetics and isotherms of Cu(II) ions adsorption onto xLVB from aqueous solutions.

EXPERIMENTAL

Reagents

All chemicals were of analytical reagent grade and were used without further refinement. HNO_3, NaOH, CS_2, $Cu(NO_3)_2$ were purchased from Merck (Germany). All solutions were prepared with deionized water. Standard metal stock solution was prepared by dissolving given amounts of analytical grade $Cu(NO_3)_2$. All standard solutions were stored in a refrigerator at 4 °C.

Preparation of xanthated biosorbent

Lagenaria vulgaris is a creeping, hardy plant. It belongs to the Cucurbitaceae family. The outer shell is recognized to be hard and ligneous covering the spongy white pith characterized by bitter taste [13]. The experiments in this study have been carried out using a shell of *L. vulgaris*, grown in the south area of Serbia (near the town of Niš) at about 200 m altitude. Plants were grown under controlled conditions with irrigation and without fertilization, planted at the same time in mid-April and harvested in the mid-October, also all at the same time.

L. vulgaris shell was roughly crushed, washed with deionized water and grounded by laboratory mill. Biomass was soaked in 0.3 M HNO_3 for 24 h to remove metals bio-accumulated in the plant during growing. After that, biomass was washed with deionized water to remove excess acid and treated with 0.1 M NaOH in period of 30 min. Excess alkali was removed by thoroughly washing and sorbent was dried in the oven at 55±5 °C to constant weight. Dried biomass was fractionised using standard sieves (Endecotts, England). The prepared adsorbent was abbreviated as basic *L. vulgaris* biosorbent (LVB) hereafter for convenience.

Xanthation was carried out by following procedure: LVB, with granulation from 0.8 to 1.25 mm, was soaked in 4 M NaOH and stirred for 3 h and another 3 h after adding CS_2. Xanthated material was allowed to settle for 1 h and separated by decantation and filtration. After that, the biomass was washed with deionized water. Xanthated *L. vulgaris* biosorbent (xLVB) prepared on this way was additionally washed in two times with acetone and dried at room temperature. As a result, xLVB was prepared for removing heavy metals from aqueous solutions.

Batch biosorption experiments

The stock solution of Cu(II) was prepared in 1.00 g dm^{-3} concentration using $Cu(NO_3)_2$ and working standard solutions were prepared just before use by the appropriate dilution of the stock solutions. The pH of each solution was adjusted to the required value with 0.1/0.01 mol dm^{-3} $NaOH/HNO_3$ solutions pH-metrically (SensIon5, HACH, USA), before biosorption treatment.

Studies on the adsorption of metal ions by xLVB were carried out in batch conditions, by agitating 250 cm^3 of 50.0 mg dm^{-3} metal ion solutions of Cu(II), contacted with 1.00 g biosorbent. A parallel experiment was a blank system, a treatment of the same solution without biosorbent. We used the blank system for testing the loss of metal on glass dishes. At required time intervals, 4.0 cm^3 of samples were withdrawn and analyzed using a flame atomic adsorption spectrometer AAnalyst 300 (Perkin Elmer, USA). The amount of metal adsorbed q_t (mg g^{-1}) was determined by using the following equation:

$$q_t = \frac{(c_0 - c_t)V}{m} \quad (1)$$

where c_0 and c_t are the initial and final concentrations of the metal ion in solution (mg dm^{-3}), V is the solution volume (dm^3) and m is the mass of the sorbent (g).

The removal efficiency (RE) of metal ions by biosorbent was calculated using the equation:

$$\mathrm{RE} = \frac{c_0 - c_t}{c_0} \times 100 \quad (2)$$

RESULTS AND DISCUSSION

Contact time effect

The effect of contact time on the removal efficiency of Cu(II) ions by xanthated *Lagenaria vulgaris* biosorbent (xLVB), was investigated in time intervals 0, 1, 5, 10, 20, 40, 60, 90, 120 and 240 min.

Typical biosorption kinetics exhibit a rapid initial uptake, followed by a slower process. The experimental results show that maximum adsorption efficiency was observed in the first 20 min of sorbent-sorbate contact, when removal of Cu(II) ions was 81.92%. The sorption equilibrium was attained after about 50 min of contact time, when 97.92% of total Cu(II) ions were removed. The initial concentration of Cu(II) ions decreased from 50.0 to level of 1.04 mg dm^{-3} when equilibrium was attained. To the end of the treatment, changes of metal concentrations in the solution are negligible. It can be seen that after 240 min of treatment, 98.92% of total Cu(II) ions were removed from aqueous solution (Figure 1).

The effect of contact time on the adsorption of Cu(II) by unmodified *L. vulgaris* biosorbent indicated that initial concentration of metal ions decreases from 50.0 to 29.38 mg dm^{-3} after 50 min of contact time when equilibrium was attained. It can be seen that xLVB gave significantly better removal efficiency than unmodified biosorbent: 98.92 with regard to 62.59%.

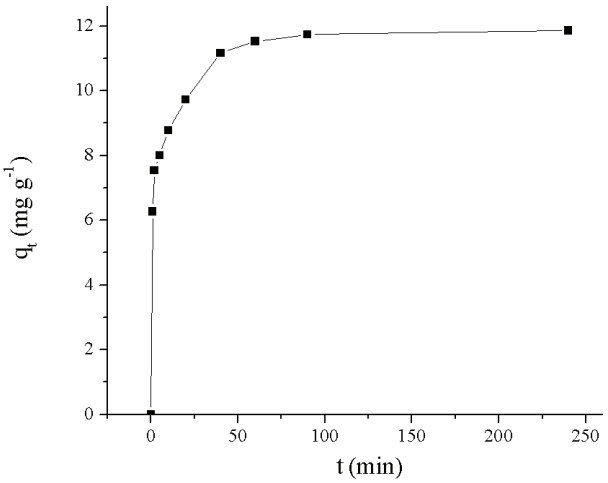

Figure 1. Removal of Cu(II) ions from aqueous solutions by xLVB. Initial pH: 5, $[Cu(II)]_0$ = 50.0 mg dm^{-3}, sorbent dose: 4.0 g dm^{-3}, temperature: 25.0±0.5 °C.

Effect of pH

Generally, the pH of solution is recognized as a very important parameter that governs the adsorption process. It was established that pH affected the surface change of the adsorbent. The influence of initial pH on the removal of Cu(II) ions from aqueous solution was investigated at five different initial pH values: 2, 3, 4, 5 and 6. An increase in the solution pH from 2 to 5 led to an increase of removal efficiency for the adsorption of Cu(II) ions (Figure 2), and then slightly decreases at pH 6. Values for removal efficiency at pH 6 (results not shown) were obtained by subtraction change of Cu(II) concentration in the blank from residual concentration in biosorption treatment. At pH value 5, removal efficiency achieved maximum values (98.92%). When the pH decreased, concentrations of protons increased and competition in binding the active sites on the surface of biosorbent, between the H^+ and metal ions, started. Protonated active sites were incapable of binding the bind metal ions, leading to free ions remaining in the solution.

With the increase of pH, the overall surface on xLVB became negative and adsorption was increased. The competing effect of hydronium ions decreased and the positively charged metal ions took up the free binding sites. Dominant species of copper in the pH range 3–5 are Cu^{2+} and $CuOH^+$, while the copper at above 6.3 occurs as insoluble $Cu(OH)_{2(s)}$ [14–16]. Above pH 6, insoluble copper hydroxide starts precipitating from the solution [17]. For these reasons, further metal sorption studies were carried out at pH 5, which is well below the pH level where Cu(II) ions are precipitated.

During the adsorption process on xLVB, the equilibrium pH values increased because the buffer solution is not used in any experimental solutions (Figure 3). This phenomenon can probably be explained by releasing OH^- from $CuOH^+$ at pH between 5 and 6 [15]. In addition, Na^+ were also released into the solution according to ion exchange, then combined with OH^- to form alkali, which strengthened the alkalinity of the solutions [11].

Effect of initial Cu(II) concentration

Biosorption of metals by any biosorbent is highly dependent on the initial concentration of metal ions [18]. The effect of concentration on sorption of Cu(II) was investigated with initial Cu(II) concentrations of 10, 20, 50, 100, 200 and 400 mg dm^{-3}. The experiments

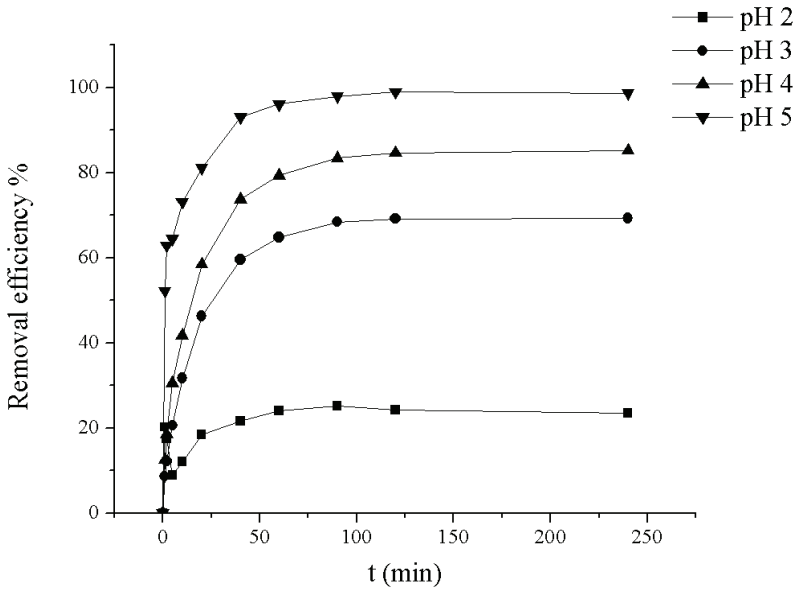

Figure 2. Effect of initial pH on the removal efficiency of Cu(II) ions from aqueous solutions by xLVB. $[Cu(II)]_0$ = 50.0 mg dm^{-3}, sorbent dose: 4.0 g dm^{-3}, temperature: 25.0±0.5 °C.

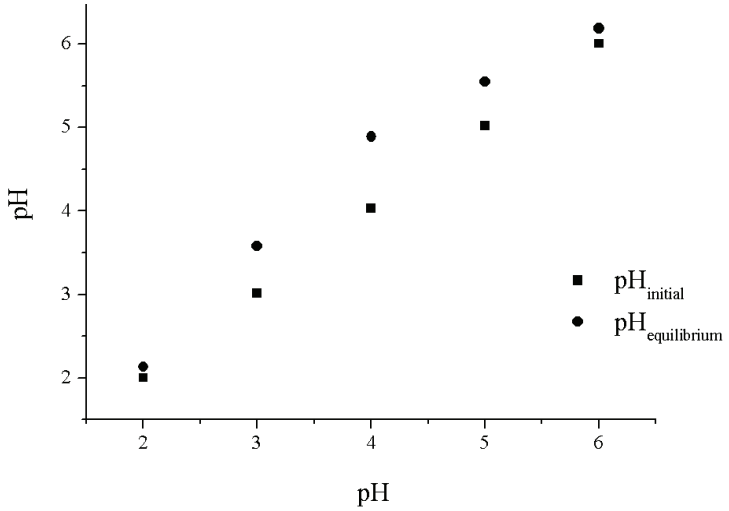

Figure 3. A plot of $pH_{initial}$ and $pH_{equilibrium}$; $[Cu(II)]_0$ = 50.0 mg dm^{-3}, sorbent dose: 4.0 g dm^{-3}, temperature: 25.0±0.5 °C.

were performed by adding 250 cm^3 solution of each concentration to six different 250 mL flasks each containing 1.0 g of biosorbent. The results are shown in Figure 4. When the initial metal ions concentration was increased from 10 to 400 mg dm^{-3}, at pH 5, the loading capacity of adsorbent increased from 2.59 to 23.18 mg of Cu(II) per gram of xLVB (Figure 4). Examination of this parameter is important because wastewater from various processes such as electroplating processes contains metal ions in a wide range of concentrations [19,20].

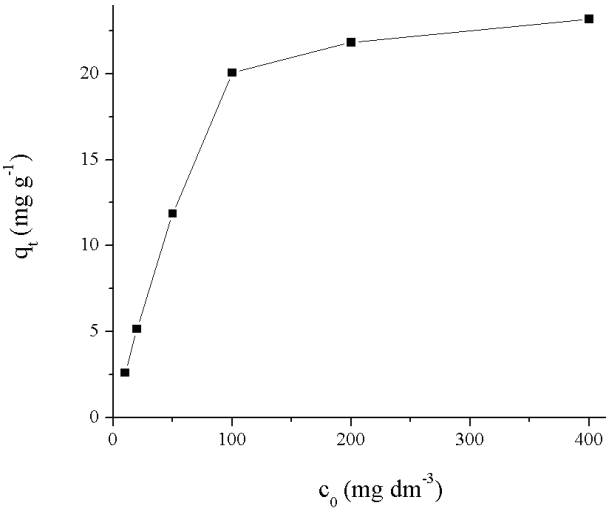

Figure 4. Effect of initial metal concentration on the removal efficiency of Cu(II) ions from aqueous solutions by xLVB. Initial pH: 5, sorbent dose: 4.0 g dm^{-3}, temperature: 25.0±0.5 °C.

Effect of adsorbent dosage

For the assessment of adsorbent dosage of the adsorption, 50.0 mg dm^{-3} Cu(II) solutions were stirred for 240 min with different amounts of xLVB (0.5, 1, 2, 4 and 8 g dm^{-3}). The results of experiments with varying biosorbent concentration are presented in Figure 5. With an increase in biosorbent concentration from 0.5 to 8 g dm^{-3}, the percentage of biosorbed Cu(II) removal increased from 12.74 to 98.98% as the number of possible binding sites is increased. It is obvious that the removal efficiency is not increased considerably when biosorbent concentrations are higher than 4.0 g dm^{-3}. Thus, the optimum dosage of xLVB for biosorption of Cu(II) ions was found to be 4.0 g dm^{-3}.

Kinetic study

One of the most important features of the biosorbent is the rate at which the solid phase adsorbs metal ions from the aqueous solutions and attains equilibrium. In our case, two different kinetic models were applied in order to establish which of them shows the best fit with experimental results. All kinetic data for the adsorption of Cu(II) ions onto xLVB are reported in Table 1. Comparison of the r^2 values for different models suggested that metal sorption by xLVB followed the pseudo-second-order reaction.

It can be seen from Figure 6 that the adsorption of Cu(II) on xLVB at an initial metal ion concentration of 50.0 mg dm^{-3} can attain equilibrium within 50 min. The fast adsorption rate reflect good accessibility of the binding sites of xLVB to Cu(II) ions. Data were modeled using pseudo-second-order model, which assumes that the rate is proportional to the square of the number of remaining free surface sites [21].

$$\frac{t}{q_t} = \frac{1}{k_2 q_e^2} + \frac{1}{q_e} t \qquad (3)$$

The plot of t/q_t *versus* t (Figure 6) is a straight line where the slope and intercept are respectively $1/q_e$ and $1/(k_2 q_e^2)$. The rate constant, k_2, and the equilibrium sorption capacity, q_e, are calculated from these para-

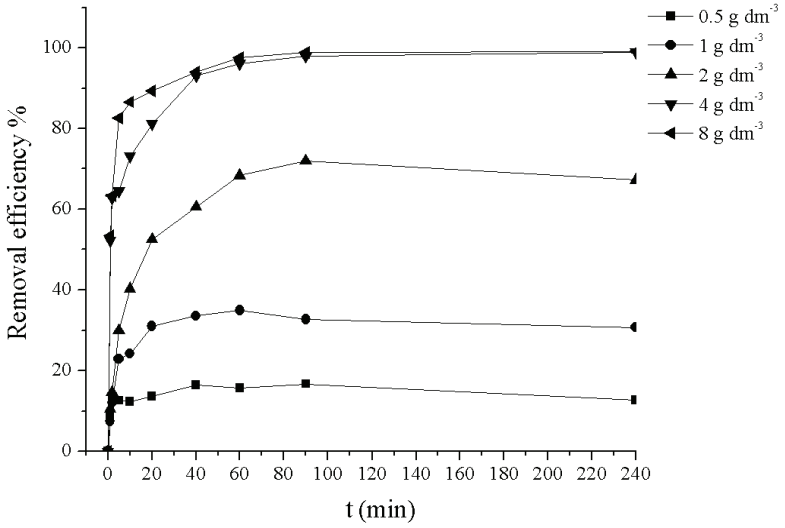

Figure 5. Effect of sorbent dosage on the removal efficiency of Cu(II) ions from aqueous solutions by xLVB. Initial pH: 5, $[Cu(II)]_0$ = 50.0 mg dm^{-3}, temperature: 25.0±0.5 °C.

meters [22]. Obviously, the biosorption process could be well described by the pseudo-second-order equation, indicating the process mechanism to be chemical adsorption.

Sorption isotherms

Sorption equilibrium can be described by a number of models available in the literature. In this study, the equilibrium data obtained for the adsorption of Cu(II) ions were analyzed by considering the Langmuir, Freundlich and Temkin isotherm models. The isotherm parameters for the adsorption of Cu(II) ions onto xLVB are given in Table 2. The Langmuir adsorption model provides the best fit with experimentally obtained data (r^2 = 0.9984, Figure 7).

The linear form of Langmuir isotherm equation is given as:

$$\frac{c_e}{q_e} = \frac{c_e}{q_{max}} + \frac{1}{q_{max} K_L} \quad (4)$$

where q_e (mg g^{-1}) is the amount of metal removed per gram of sorbent, q_{max} (mg g^{-1}) is the maximum sorption capacity, c_e (mg dm^{-3}) is concentration in the equilibrium solution, and K_L (mg dm^{-3}) is the Langmuir constant related to the adsorption energy [22–24]. The biosorption followed the Langmuir isotherm model with the maximum biosorption capacity of 23.18 mg g^{-1}.

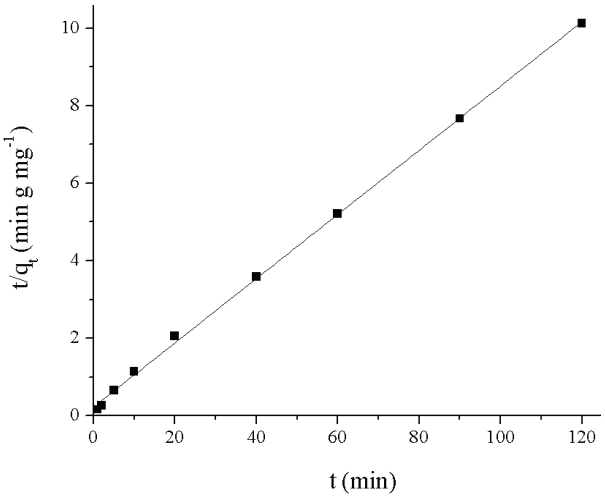

Figure 6. Pseudo-second-order kinetic model of adsorption Cu(II) ions onto xLVB. Initial pH: 5, $[Cu(II)]_0$ = 50.0 mg dm^{-3}, sorbent dose: 4.0 g dm^{-3}, temperature: 25.0±0.5 °C.

Table 1. Kinetic model parameters for adsorption of Cu(II) onto xLVB

Kinetic model	Parameter	Value
Pseudo-first-order	k_1 / g mg^{-1} min^{-1}	0.0576
	r^2	0.9452
	q_e / mg g^{-1} (exp)	11.7375
	q_e / mg g^{-1} (calculated)	6.2361
Pseudo-second-order	k_2 / g mg^{-1} min^{-1}	0.0306
	r^2	0.9991
	q_e / mg g^{-1} (exp)	11.7375
	q_e / mg g^{-1} (calculated)	12.0700

Table 2. Equilibrium model parameters for adsorption of Cu(II) onto xLVB

Equilibrium model	Parameter	Value
Langmuir isotherm	K_L / dm^3 mg^{-1}	0.2886
	q_{max} / mg g^{-1}	23.175
	r^2	0.9984
Freundlich isotherm	K_F / dm^3 g^{-1}	6.839
	n	4.066
	r^2	0.8310
Temkin isotherm	K_t	1.0036
	b_T / kJ mol^{-1}	0.9599
	r^2	0.9643

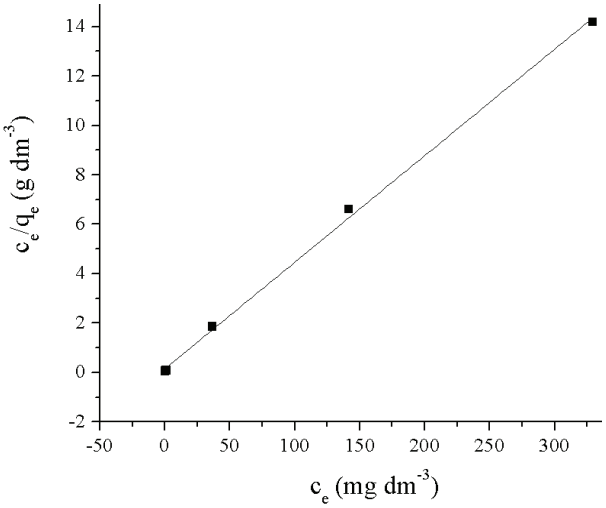

Figure 7. Langmuir isotherm for Cu(II) adsorption onto xLVB. Initial pH: 5, $[Cu(II)]_0$ = 50.0 mg dm^{-3}, sorbent dose: 4.0 g dm^{-3}, temperature: 25.0±0.5 °C.

Analysis of Fourier transform infrared spectroscopy (FTIR)

The FTIR spectrum of xLVB is shown in Figure 8. In xLVB spectrum, the broad and intense absorption peaks at around 3414.9 cm^{-1} correspond to the O–H stretching vibrations due to inter- and intra-molecular hydrogen bonding of polymeric compounds (macromolecular associations), such as alcohols, phenols and carboxylic acids, as in cellulose and lignin [25]. The peaks at 2922.1 cm^{-1} are attributed to the symmetric and asymmetric C–H stretching vibration of aliphatic acids [26]. The peaks at 1654.0 and 1458.8 cm^{-1} are due to asymmetric and symmetric stretching vibration of C=O in ionic carboxylic groups (-COO$^-$), respectively. Aliphatic acid group vibration at 1267.8 cm^{-1} may be assigned to deformation vibration of C=O and stretching formation of –OH of carboxylic acids and phenols [27]. The broad peak is at 3414.9 cm^{-1} in the xLVB, which indicates that the hydroxyl groups have com-

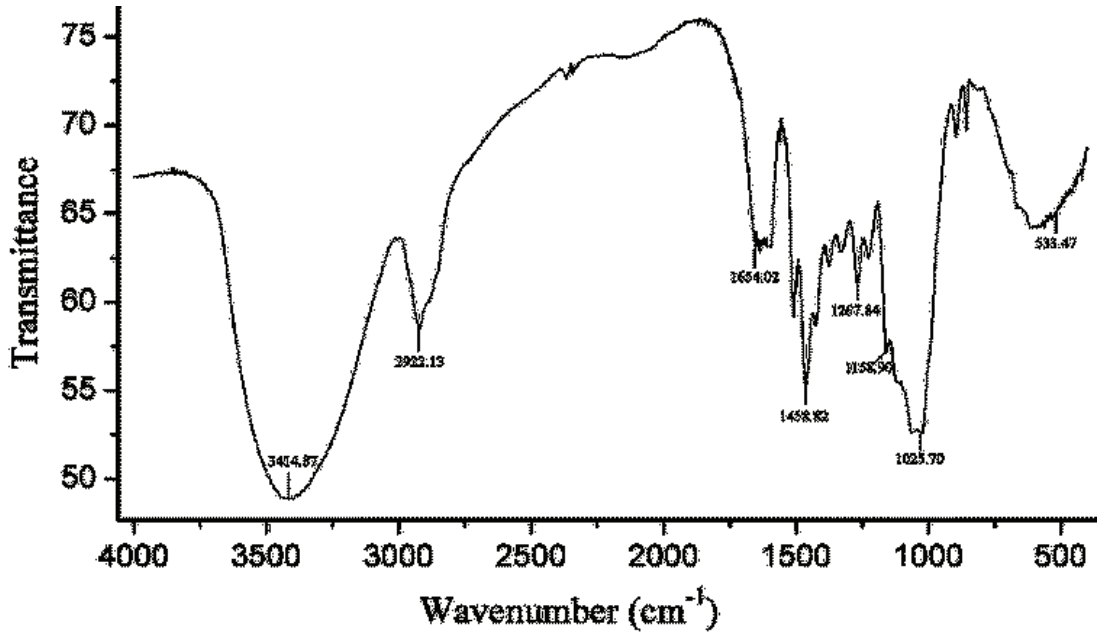

Figure 8. FTIR Spectrum of xLVB.

bined with CS_2. The presence of sulfur groups in the xLVB has been identified by the appearance of peaks at 533.5, 1025.7 and 1158.9 cm^{-1} corresponding to ν_{C-S}, $\nu_{C=S}$ and ν_{S-C-S} [11].

Testing under copper plating industry effluent condition

In recent years, the production of metal-containing waste has been continuously increasing. The level of copper in electroplating effluent is from less 100 to almost 1000 mg dm^{-3} while pH ranged from 2.5 to 5.0 [19,28]. The Environmental Protection Agency (EPA) sets a limit of 1.3 mg dm^{-3} of copper in drinking water and the allowed industrial discharges level of copper should not exceed 1 mg dm^{-3}, otherwise the water has a metallic taste [29]. Therefore, the concentration of this metal must be reduced to the level that satisfies environmental regulations for various bodies of water.

The applicability of the xanthated *L. vulgaris* biosorbent (xLVB) was demonstrated by removing Cu(II) from copper plating industry wastewater. The metal content of copper plating industry effluent is shown in Table 3. For preparing a model effluent, copper plating industry wastewater was diluted to have a new solution with 50.0 mg dm^{-3} of copper. To determine the dependence of metal sorption on time, 1.0 g of xLVB was exposed to a 250 cm^3 model effluent with initial pH 5.0. Despite the presence of competitive effect of cadmium, chromium, zinc and nickel metal ions, about 81.35% reduction in Cu(II) concentration was achieved as a result of treatment with developed adsorbent. It was observed that the copper removal efficiency decreased by 17.57% comparing to a single metal solution of copper.

Table 3. The metal content of copper plating industry effluent

Metal ion	Concentration, mg dm^{-3}
Cu(II)	380.0
Cd(II)	6.0
Cr(VI)	41.0
Zn(II)	130.0
Ni(II)	116.0
Na^+	600.0
K^+	18.0
Ca^{2+}	16.0
pH	3.8

CONCLUSION

Xanthated *Lagenaria vulgaris* biosorbent (xLVB) was employed as an adsorbent for removal of Cu(II) ions from aqueous solution. The maximum biosorption capacity of biosorbent for the removal of Cu(II) was obtained at pH 5. The loading capacity of xLVB increased from 2.59 to 23.18 mg of Cu(II) per gram of xLVB, as the initial concentration of Cu(II) ions increased from 10 to 400 mmol dm^{-3}. The optimum adsorbent dosage was established to be 4 g dm^{-3}. Kinetics experiments proved that the biosorption process was rapid with equilibrium attained within 50 min. The kinetics of the process were best described using the pseudo-second order model. The Langmuir adsorption model was used to represent the experimental data and equilibrium data fitted very well to the Langmuir isotherm model (r^2 = 0.9984). FTIR Spectra confirm the presence of sulphur groups on the *L. vulgaris* xanthate. Batch studies with 81.35% copper removals from a copper plating industry effluent wastewater revealed the practical utility of the developed biosorbent.

The obtained results and their comparison to various biosorbents reported in the literature showed that xanthated *L. vulgaris* biosorbent (xLVB) was an efficient biosorbent for Cu(II) ions.

Acknowledgement

The authors would like to acknowledge the Serbian Ministry of Education, Science and Technological Development for financial support (Grant No. TR34008).

REFERENCES

[1] Z. Aksu, L.A. Isoglu, Removal of copper(II) ions from aqueous solution onto agricultural waste sugar beet pulp, Process Biochem. **40** (2005) 3031–3044.

[2] G. DÖnmez, Z. Aksu, The effect of copper(II) ions on the growth and bioaccumulation properties of some yeasts, Process Biochem. **35** (1999) 135–142.

[3] A. Witek-Krowiak, R.G. Szafran, S. Modelski, Biosorption of heavy metals from aqueous solutions onto peanut shell as a low-cost biosorbent, Desalination **265** (2011) 126–134.

[4] J. Febrianto, A.N. Kosasih, J. Sunarso, Y.H. Ju, N. Indraswati, S. Ismadji, Equilibrium and kinetic studies in adsorption of heavy metals using biosorbent: A summary of recent studies, J. Hazard. Mater. **162** (2009) 616–645.

[5] S.S. Ahluwalia, D. Goyal, Microbial and plant derived biomass for removal of heavy metals from wastewater, Bioresour. Technol. **98** (2007) 2243–2257.

[6] B. Volesky, Sorption and Biosorption, BV Sorbex, Inc., Montreal – St. Lambert, Quebec, Canada, 2003.

[7] M. Zhao, J.R. Duncan, R.P. van Hille, Removal and recovery of zinc from solution and electroplating effluent using *Ayolla filiculoides*, Water Res. **33 (6)** (1999) 1516––1522.

[8] K.S. Low, C.K. Lee, S.C Liew, Sorption of cadmium and lead from aqueous solutions by spent grain, Process Biochem. **36** (2000) 59–64.

[9] S.E. Bailey, T.J. Olin, R.M. Bricka, D.D. Adrian, A review of potentially low-cost sorbents for heavy metals, Water. Res. **33** (1999) 2469–2479.

[10] A. Kumar, N.N. Rao, S.N. Kaul, Alkali-treated straw and insoluble straw xanthate as low cost adsorbents for heavy metal removal – preparation, characterization and application, Bioresour. Technol. **71** (2000) 133–142.

[11] G.C. Panda, S.K. Das, A.K. Guha, Biosorption of cadmium and nickel by functionalized husk of *Lathyrus sativus*, Colloids Surfaces, B **62** (2008) 173–179.

[12] S. Liang, X. Guo, N. Feng, Q. Tian, Application of orange peel xanthate for the adsorption of Pb^{2+} from aqueous solution, J. Hazard. Mater. **170** (2009) 425–429.

[13] D-L. Mitić-Stojanović, A. Zarubica, M. Purenovic, D. Bojic, T. Andjelkovic, A. Bojic, Biosorptive removal of Pb^{2+}, Cd^{2+} and Zn^{2+} ions from water by Lagenaria vulgaris shell, Water SA **37**(3) (2011) 303–312.

[14] E. Demirbasa, N. Dizgeb, M.T. Sulakb, M. Kobyab, Adsorption kinetics and equilibrium of copper from aqueous solutions using hazelnut shell activated carbon, Chem. Eng. J. **148** (2009) 480–487.

[15] H.A. Eliot, C.P. Huang, Adsorption characteristic of some Cu(II) complexes on aluminosilicates, Water Res. **15** (1981) 849–855.

[16] M. Asmal, A.H. Khan, S. Ahmad, A. Ahmad, Cole of sawdust in the removal of copper(II) from industrial waters, Water Res. **32** (1998) 3085–3091.

[17] T. Mathialagon, T. Viraraghavan, Adsorption of cadmium from aqueous solution by perlite, J. Hazard. Mater., B **94** (2002) 291–303.

[18] N. Ahalya, R.D. Kanamacdi, T.V. Ramachandra, Biosorption of chromium(VI) from aqueous solution by the husk of Bengal gram (*Cicer arientinum*), Eur. J. Biotechnol. **8** (2005) 258–264.

[19] C. Peng, Y. Liu, J. Bi, H. Xu, A-S. Ahmed, Recovery of copper and water from copper electroplating wastewater by the combination process of electrolysis and electrodialysis, J. Hazard. Mater. **189** (2011) 814–820.

[20] M. Kul, Ü. Çetinkaya, Recovery of copper by LIX 984N-C from electroplating rinse bath solution, Hydrometallurgy **98** (2009) 86–91.

[21] Y.S. Ho, G. Mckay, The kinetics of sorption of basic dyes from aqueous solution by sphagnum moss peat, Can. J. Chem. Eng. **76** (1998) 822–827.

[22] A. Aziz, M.S. Ouali, E.H. Elandaloussi, L.C. De Menorval, M. Lindheimer, Chemically modified olive stone: A low-cost sorbent for heavy metals and basic dyes removal from aqueous solutions, J. Hazard. Mater. **163** (2009) 441–447.

[23] S. Altenor, B. Carene, E. Emmanuel, J. Lambert, J.J. Ehrhardt, S. Gaspard, Adsorption studies of methylene blue and phenol onto vetiver roots activated carbon preparedby chemical activation, J. Hazard. Mater. **165** (2009) 1029–1039.

[24] M. Iqbal, A. Saeed, S. I. Zafar, FTIR spectrophotometry, kinetics and adsorption isotherms modeling, ion exchange, and EDX analysis for understanding the mechanism of Cd^{2+} and Pb^{2+} removal by mango peel waste, J. Hazard. Mater. **164** (2009) 161–171.

[25] R. Gnanasambandam, A. Protor, Determination of pectin degree of esterification by diffuse reflectance Fourier transform infrared spectroscopy, Food Chem. **68** (2000) 327–332.

[26] [26] F.T. Li, H. Yang, Y. Zhao, R. Xu, Novel modification pectin for heavy metal adsorption, Chin. Chem. Lett. **18** (2007) 325–328.

[27] Z. Reddad, C. Gerente, Y. Andres, P. Le Cloirec, Adsorption of several metal ions onto a low-cost biosorbent: Kinetic and equilibrium studies, Env. Sci. Technol. **36** (2002) 2067–2073.

[28] F.J. Cerino-Córdova, A.M. García-León, E. Soto-Regalado, M.N. Sánchez-González, T. Lozano-Ramírez, B.C. García-Avalos, J.A. Loredo-Medrano, Experimental design for the optimization of copper biosorption from aqueous solution by Aspergillus terreus, J. Environ. Manage. **95** (2012) S77–S82.

[29] H. Harmita, K.G. Karthikeyan, X.J. Pan, Copper and cadmium sorption onto kraft and organosolv lignins, Bioresour. Technol. **100**(24) (2009) 6183–6191.

IZVOD

PRIMENA NOVOG BIOSORBENTA NA BAZI HEMIJSKI MODIFIKOVANE KORE *Lagenaria vulgaris* ZA UKLANJANJE BAKRA(II) IZ VODENIH RASTVORA: UTICAJ PARAMETARA PROCESA

Miloš M. Kostić[1], Miljana D. Radović[1], Jelena Z. Mitrović[1], Danijela V. Bojić[1], Dragan D. Milenković[2], Aleksandar Lj. Bojić[1]

[1]*Departman za hemiju, Prirodno–matematički fakultet, Univerzitet u Nišu, Srbija*
[2]*Visoka hemijsko–tehnološka škola strukovnih studija, Departman za hemijsku tehnologiju, Kruševac, Srbija*

(Naučni rad)

Kora biljke *Lagenaria vulgaris* korišćena je za dobijanje novog biosorbenta procesom ksantovanja u alkalnoj sredini. Dobijeni ksantovani materijal primenjen je kao adsorbent za uklanjanje jona bakra iz vodenih rastvora. Ispitivan je uticaj kontaktnog vremena, pH, inicijalne koncentracije bakra(II) i količine adsorbensa na efikasnost procesa uklanjanja metala. Pokazano je da sorpcioni proces dostiže ravnotežu za 50 min, a najveća vrednost sorpcionog kapaciteta (23,18 mg g^{-1}) postignuta je pri početnoj vrednosti pH rastvora 5. Sa povećanjem početne koncentracije metalnog jona od 10 do 400 mg dm^{-3} raste i količina metala adsorbovanog po gramu sorbenta. Rezultati ispitivanja uticaja količine sorbenta na efikasnost uklanjanja bakra(II) pokazuju da je optimalna količina sorbenta 4 g dm^{-3}. Kinetika adsorpcije se najbolje opisuje modelom pseudo-drugog reda, dok je najbolje slaganje eksperimentalnih rezultata dobijeno sa Langmuir-ovom adsorpcionom izotermom. Funkcionalne grupe na površini ksantovanog biosorbenta su ispitivane FTIR metodom. Ksantovani *L. vulgaris* biosorbent može se primeniti za uklanjanje bakra iz otpadnih voda industrija prevlaka bakra sa efikasnošću od 81,35%.

Ključne reči: Ksantovani *Lagenaria vulgaris* • Bakar(II) joni • Biosorpcija

Formalizovana metodologija za separaciju trokomponentnih elektrolitičkih sistema. Parcijalna separacija sistema

Midhat Suljkanović[1], Milovan Jotanović[2], Elvis Ahmetović[1], Goran Tadić[2], Nidret Ibrić[1]

[1]*Univerzitet u Tuzli, Tehnološki fakultet, Tuzla, Bosna i Hercegovina*
[2]*Univerzitet u Istočnom Sarajevu, Tehnološki fakultet, Zvornik, Bosna i Hercegovina*

Izvod

U ovom radu predstavljena je formalizovana metodologija za separaciju soli iz trokomponentnih elektrolitičkih sistema. U osnovi metodologije je multivarijantni modelirajući blok, poopštenog kristalizacionog procesa, čije opcije simuliraju granične uslove egzistencije ravnotežnih procesa i elemente kristalizacionih tehnika: hlađenje sistema preko kontaktne površine, hlađenje uz smanjenje pritiska, kristalizaciju isoljavanjem, kristalizaciju uz isparavanje vode i kombinaciju navedenih kristalizacionih tehnika. Mogućnosti kreiranog procesnog simulatora pokazane su na primjerima separacije soli iz sistema, NaCl–Na_2SO_4–H_2O, sa različitim sadržajem soli u polaznom sistemu.

Ključne reči: sinteza procesa kristalizacije, matematičko modelovanje i simulacija, separacija elektrolitičkih sistema.

Dostupno na Internetu sa adrese časopisa: http://www.ache.org.rs/HI/

NAUČNI RAD

UDK 544.6:54:519.87:66

Hem. Ind. **67** (4) 569–583 (2013)

doi: 10.2298/HEMIND120808099S

Sinteza procesnih struktura, hemijsko–tehnoloških sistema, predstavlja jednu od osnovnih faza u razvoju novih ili pak optimizaciji postojećih procesa. Kako je uvijek u pitanju relativno veliki broj alternativnih varijanti procesa, po kojima se fizički može realizovati zahtijevana transformacija polaznih spojeva u konačan proizvod, problemi njihovog generisanja, analize i poređenja izuzetno su aktuelni. Danas je, hemijskim inžinjerima, na raspolaganju čitav niz procesnih simulatora za sintezu mreža razmjenjivača toplote, sekvenci separacionih i reaktorskih podsistema. Osnovni separacioni procesi, čija se sinteza i analiza može provesti primjenom komercijalnih procesnih simulatora pripadaju destilacionim procesima, a istraživanja vezana za kreaciju procesnih simulatora za separaciju elektrolitičkih sistema su novijeg datuma.

U prvom publikovanom radu [1], u kome je tretirana problematika sinteze procesa kristalizacije soli iz višekomponentnih elektrolitičkih sistema, sistematizovani su procesni putevi za kristalizaciju ciljne soli iz tro- i četverokomponentnih sistema. Za procjenu elemenata materijalnog bilansa korištena je grafička metoda – pravilo poluge. Rad je, u osnovi, preglednog karaktera i njegova osnovna karakteristika je u formulisanoj tvrdnji da se proces sinteze procesnih struktura, frakcione kristalizacije soli iz višekomponentnih sistema, teško može poopštiti. Na ovu konstataciju će se pozivati, svi istraživači, čiji je objekat interesa bila kompjuterska sinteza kristalizacionih procesa. Profesor J. M. Douglas, sa Univerziteta *Massachusetts*, utemeljitelj opšte prihvaćenog konceptualnog pristupa projektovanju hemijsko–procesnih sistema, je 1986 god. publicirao, u saradnji sa A.P. Rossiter-om, seriju od tri rada u kojima tretira problematiku projektovanja i optimizacije procesa sa čvrstom materijom [2–4].

U prvom radu [2], koji je posvećen hijerarhijskoj proceduri sinteze procesa sa čvstom fazom, Douglas je prezentirao novi postupak za sintezu procesnih struktura i utvrđivanje osnovnih režimskih uslova za procese sa čvrstom materijom. Po svojoj prirodi postupak je razvojni i donošenje odluka podrazumijeva prolazak kroz niz hijerarhijskih nivoa pri čemu se, na svakom nivou, procesna struktura postepeno usložnjava. U drugom radu [3] prezentiran je novi pristup optimizaciji procesne šeme sa fiksnom tehnološkom topologijom. Verifikacija metodologije izvedena je na primjeru izotermičke kristalizacije natrijum hlorida, iz njegovog binarnog rastvora, što je prezentovano u trećem radu [4]. U navedenim radovima predmet interesa nije bila kreacija procesnih struktura sa alternativnim kristalizacionim tehnikama i tek se, u prvom radu, navodi da procesi kristalizacije mogu biti realizovani: izotermskim isparavanjem vode iz rastvora, hlađenjem (preko razmjenjivačke površine i flešovanjem sistema), isoljavanjem i kao rezultat odvijanja hemijske reakcije. Luis A. Cisternas i Dale F. Rudd su 1993 godine publicirali rad vezan za projektiranje procesa frakcione kristalizacije, neorganskih soli, iz vodenih rastvora [5].

Na osnovu karakteristika fizičko–hemijske ravnoteže, za konkretne sisteme, utvrđena je procedura za identifikaciju alternativnih procesnih struktura za kristalizaciju pojedinih soli iz sistema. Razmotreni su višekomponentni sistemi iz kojih kristališu bezvodne soli, kristalohidrati i dvojne soli. Karakteristike razvijene

Prepiska: M. Suljkanović, Tehnološki fakultet, Univerzitet u Tuzli, Univerzitetska 8, 75000 Tuzla, Bosna i Hercegovina.
E-pošta: midhat.suljkanovic@untz.ba
Rad primljen: 8. avgust, 2012
Rad prihvaćen: 11. oktobar, 2012

metodologije su prezentovane na razdvajanju sistema Na_2SO_4–Na_2CO_3–H_2O i nju autori ograničavaju na sisteme sa sličnom faznom ravnotežom.

Važan doprinos formalizaciji sinteze kristalizacionih procesa neorganskih soli, iz vodenih rastvora, dali su Gani i saradnici [6,7]. Mogućnosti predložene metodologije, koja se temelji na korištenju računske fazne ravnoteže za određene sisteme (Na_2SO_4–K_2SO_4–H_2O i NaCl–KCl–H_2O), demonstrirane su na dva granična slučaja: pri zadatom tipu kristalizacione opreme utvrđuju se zahtijevane komponente vektora polaznog sistema uz zadovoljenje ograničenja na količinu kristalnog produkta i, u drugom slučaju, za poznati vektor parametra pojnog toka utvrđuje se procesna konfiguracija, i parametri procesnih tokova, potrebni za ostvarivanje zadatog kapaciteta sistema u odnosu na kristalni produkt. Autori jednaku važnost pridaju problematici sinteze novih procesa i problematici vezanoj za reinžinjering ("*process retrofit*") sistema koji su u eksploataciji. Za simulaciju i optimizaciju procesnih struktura autori koriste sopstvene, predhodno razvijene, simulatore za rješavanje sistema jednačina velikog formata. U drugom radu [7] prezentirani su, predhodno razvijeni, termodinamički modeli neidealnih elektrolitičkih sistema i njihova primjena u simulaciji i optimizaciji procesa frakcione kristalizacije. Kao primjeri uzeti su sistemi NaCl–KCl–H_2O i NaCl–$NaNO_3$–KCl–H_2O.

U navedenim publikacijama kreacija polaznih procesnih struktura, kao i njihovo izvođenje u procesu razvoja procesa, proizilašla je iz grafički prezentirane ravnoteže u višekomponentnim elektrolitičkim sistemima. Grafičke metode koje koriste različite tipove ravnotežnih dijagrama, sastav-osobina sistema, u kombinaciji sa analitičkim metodama, predstavljaju najzastupljenije metode koje se koriste u inženjerskoj praksi projektovanja procesa produkcije mineralnih soli i tretmana višekomponentnih elektrolitičkih sistema. Ove metode izuzetno dobro vizueliziraju ukupne procese i njihova primjena je relativno jednostavna za slučaj posjedovanja znanja studiranja i identificiranja procesnih sekvenci u ravnotežnim dijagramima. Kada su u pitanju viševarijantni procesi i procesi sa unutrašnjim reciklima, tečnih i čvrstih materijala, ove metode su teško primjenjljive, a potpuno neprimjenjljive postaju za procese čija se fizička izvodljivost mora verifikovati u rezultatu simultanog rješavanja sistema jednačina materijalnog i toplotnog bilansa.

Pored navedenih metoda, za sintezu i optimizaciju procesa kristalizacije mogu se koristiti i metode koje se baziraju na matematičkom programiranju. Cisternas i saradnici [8–11] su među prvim autorima koji su predstavili metodologiju kristalizacionih procesa koja se bazira na matematičkom programiranju. Oni su razvili model mreže za procese separacije soli i njihova metodologija se može uspješno primjeniti za sintezu procesa frakcione kristalizacije uključujući i integraciju topline. Pored njih, i drugi autori [12–15] su koristili metode matematičkog programiranja za sintezu procesa kristalizacije. Njihovi modeli su formulisani kao problemi nelinearnog programiranja [13,15] ili pak miješanog cjelobrojnog nelinearnog programiranja [12,14] za slučaj kada se pored radnih uslova optimira i topologija procesa kristalizacije. Više informacija o pregledu metoda i dostignućima u području sinteze i optimizacije procesa kristalizacije je dostupno u preglednim radovima [16,17].

U realnim uslovima, separacija višekomponentnih sistema uvijek podrazumijeva, kao osnovu, primjenu jedne ili više kristalizacionih tehnika što ove procese sa stanovišta fizičke izvodljivosti procesa, u samom polazištu čini strukturno viševarijantnim. Utvrđivanje parametarski i strukturno optimizirane procesne strukture, za procese parcijalne ili potpune separacije višekomponentnih elektrolitičkih sistema, podrazumijeva predhodno utvrđivanje skupa dozvoljenih procesnih topologija nad čijim se elementima provode optimizacione procedure. Zadatak, formalizovanog, utvrđivanja fizički izvodljivih procesnih struktura za parcijalnu i potpunu separaciju hipotetičkog trokomponentnog elektrolitičkog sistema postavljen je kao neposredan cilj u prezentovanim istraživanjima.

U smislu navedenog kao objekat istraživačkog interesa, u ovom radu, uzet je hipotetski trokomponentni elektrolitički sistem AX–BX–H_2O a neposredni predmet interesa predstavlja kreacija i algoritmizacija formalizirane metodologije kojom se utvrđuju i verifikuju fizički izvodljivi procesi separacije sistema.

TEORETSKA OSNOVA

U realnim uslovima, na zadatak separacije trokomponentnih elektrolitičkih sistema, može se postaviti neki od slijedećih zahtjeva:

- iz sistema treba izdvojiti jednu so, npr. AX,
- iz sistema treba izdvojiti smjesu soli, (AX+BX) i
- izvodi se frakciona kristalizacija soli, AX i BX.

U teoretskom slučaju ako se nezasićenom sistemu iz okoline, pri konstantnom pritisku, dovodi toplotna energija on će, pri određenoj temperaturi, proključati i isparavanjem vode najprije će postati zasićen u odnosu na so AX, i daljim isparavanjem vode doći će do kristalizacije soli AX. Proces isparavanja vode, iz sistema, može se završiti u trenutku kad je sistem postao zasićen u odnosu i na drugu so ili pak biti nastavljen uz kristalizaciju smjese soli (AX+BX). Ako se iz sistema, koji je dostigao uslove dvojnog zasićenja za konstantan pritisak, izdvoji so AX i zaostali matični rastvor podvrgne identičnom tretmanu, ali pri nekoj drugoj vrijednosti pritiska, iz sistema će kristalisati so BX. Nakon izdvajanja soli BX, iz sistema koji je dostigao uslove dvojnog zasićenja, zaostali matični rastvor, zavisno od ograniče-

nja postavljenih na funkcionisanje separacionog sistema, može biti vraćen na početak procesa i pomiješan sa polaznim sistemom, ili pak izveden preko granica sistema. U skladu sa prezentovanim, na konceptualnom nivou, mogu se sintetizirati slijedeće strukture procesa separacije sistema AX-BX-H_2O, slika 1.

Procesna struktura, sa slike 1, a), odražava proces separacije sistema na smjesu soli i vodu i u pitanju je trivijalna struktura čija trivijalnost proizilazi iz činjenice da se isparavanjem vode iz sistema, do suha, u rezultatu ima smjesa soli u odnosu koji je identičan njihovom odnosu u polaznom sistemu. Razvoj procesne strukture, za navedeni slučaj separacije sistema, važan je stanovišta dekompozicije procesa na podsistem zasićavanja i kristalizacije i mogućnosti njihove energetske integracije [18].

U procesu sa slike 1, b), isparavanje vode praćeno je kristalizacijom samo soli AX i identitet soli koja kristališe određen je, pored izobare na kojoj se izvodi proces, odnosom sadržaja soli u polaznom sistemu. Procesne strukture sa slike 1, c) i d), predstavljaju procese parcijalne i ukupne frakcione kristalizacije i sa stanovišta konceptualnog određenja podrazumijevaju „uređivanje“ para kristalizacionih podsistema u smislu utvrđivanja pritisaka i redoslijeda po kome dolazi do kristalizacije, pojedinih soli iz sistema.

FORMULACIJA POLAZNOG ZADATKA

Za hipotetski elektrolitički sistem, AX–BX–H_2O, potrebno je kreirati i algoritmizirati formaliziranu metodologiju za sintezu konceptualnih procesnih puteva za procese parcijalne i frakcione kristalizacije soli iz sistema.

Na funkcionisanje procesnog sistema postavljena su ograničenja na područja pritisaka/temperatura pri kojima se izvode procesi kristalizacije pojedinih soli iz sistema.

Utvrđivanje polazne procesne strukture

Iz određenja polaznog zadatka sinteze proizilazi da je objekat istraživačkog interesa kreacija alternativnih procesa kristalizacije soli, iz trokomponentog elektrolitičkog sistema, i za konceptualni nivo procesa sinteze potrebno je, najprije, utvrditi polaznu procesnu strukturu koja će, u procesu sinteze, biti izvedena.

Kada se sintetitiziraju alternativne procesne strukture za procese kristalizacije soli, iz binarnih sistema, polazna struktura je trivijalna i njena trivijalnost proizilazi iz činjenice da do izdvajanja soli, iz nezasićenog polaznog sistema, mora doći ako se:

- iz sistema izdvoji voda u količini koja je veća od količine potrebne da sistem primi stanje zasićenja za posmatranu temperaturu i
- ako se sistem hladi, preko izmjenjivačke površine, na temperaturu koja je niža od temperature zasićenja, za sadržaj soli u polaznom sistemu.

Kada su u pitanju procesi kristalizacije soli, iz trokomponentnih sistema, onda se trivijalnost procesne strukture gubi budući da stanje polaznog sistema određuje kako mogućnost kristalizacije ciljne soli iz sistema a takođe i konceptualnu procesnu strukturu procesnog sistema.

Za utvrđivanje polazne procesne strukture za polazište je uzeto određenje trokomponentnog elektrolitičkog rastvora kao sistema.

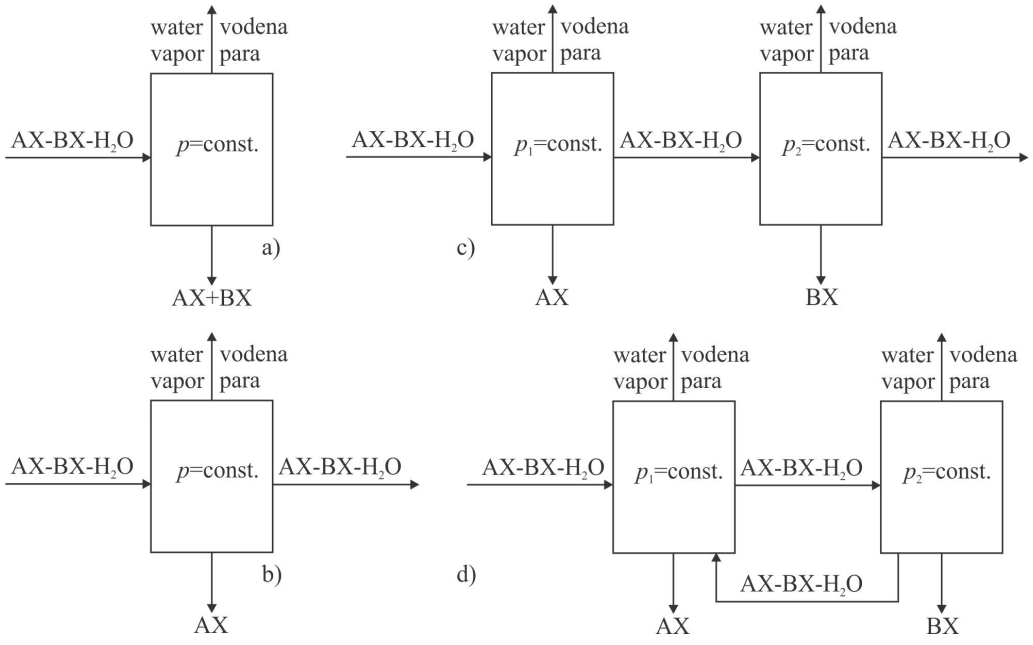

Slika 1. Konceptualne procesne strukture separacije sistema AX–BX–H_2O.
Figure 1. Conceptual process structures for the separation of AX–BX–H_2O system.

Naime, iz hipotetskog trokomponentnog sistema, AX–BX–H_2O, moguće je izdvojiti željenu so AX, bez predhodnog izdvajanja soli BX, pri temperaturi t_{KR} samo za slučaj da je odnos sadržaja soli AX i soli BX, u polaznom sistemu veći od odgovarajućeg odnosa za sistem koji je u stanju dvojnog zasićenja pri temperaturi kristalizacije. Nadalje, ako je u polaznom sistemu sadržaj soli AX, veći od ravnotežnog sadržaja, za temperaturu kristalizacije i sadržaj soli BX (sistem je prezasićen u odnosu na so AX s obzirom na izotermu t_{KR}), do kristalizacije soli AX dolazi samo uslijed hlađenja sistema.

Suprotno, ako sistem nije prezasićen u odnosu na ciljnu so, nad sistemom se moraju izvesti odgovarajući procesi u cilju postizanja uslova sistema potrebnih za kristalizaciju soli AX.

Ako se, sa polazišta sistemskog pristupa, sistem AX-BX-H_2O posmatra kao skup međusobno povezanih elemenata (AX, BX i H_2O) onda će kondicioniranje sistema, u cilju postizanja uslova potrebnih za kristalizaciju soli AX, podrazumijevati komunikaciju sistema, sa okolinom, preko materijalnih tokova koji predstavljaju, ostatne elemente sistema, vodu i so BX. Dostizanje uslova polaznog sistema, sa kojih je moguće izvesti kristalizaciju soli AX hlađenjem sistema preko izmjenjivačke površine, obezbjeđuje se:

- izdvajanjem vode iz sistema,
- uvođenjem vode u sistem,
- uvođenjem soli BX u sistem i
- određenom kombinacijom navedenih postupaka.

Za razvoj metodologije za utvrđivanje fizički izvodljivih procesa kristalizacije soli AX, iz hipotetskog trokomponentnog sistema AX–BX–H_2O kao polazište uzeta je hipoteza da hlađenjem polaznog sistema, na temperaturu određenu polaznim zadatkom sinteze procesa, u kristalizatoru sa razmjenjivačkom površinom dolazi do kristalizacije ciljne soli AX.

Kako se u realnim uslovima, u cilju zadovoljena ograničenja polaznog zadatka sinteze, polazni sistem najčešće mora kondicionirati u narednom dijelu rada navedene su osnovne tehnike kondicioniranja sistema.

Kondicioniranje sistema uz isparavanje vode

Ako je stanje polaznog sistema, u ravnotežnom dijagramu, određeno tačkom 0 (slika 2) proizilazi da je sistem, u odnosu na radnu izotermu t_{KR}, nezasićen i da do kristalizacije ciljne soli može doći ako se sistem kondicionira uz isparavanje vode. U ovom slučaju, u procesu kondicioniranja, sistem sa okolinom komunicira preko toka izdvojene vodene pare i stanje sistema se mijenja po odsječku 0–1, na zraku koncentrisanja sistema koji prolazi kroz koordinatni početak ravnotežnog dijagrama i tačku polaznog sistema. Granična stanja kondicioniranog sistema su određena, sa donje strane, stanjem zasićenja sistema (tačka 3) i sa gornje strane tačkom 4 koja predstavlja sistem čijim se hlađenjem postižu uslovi dvojnog zasićenja sistema za radnu izotermu t_{KR}.

Hlađenjem kondicioniranog sistema, čije je stanje određeno tačkom 1 ravnotežnog dijagrama, dolazi do kristalizacije ciljne soli. Proces kristalizacije je predstavljen odsječkom 1–2, na zraku kristalizacije soli, koji prolazi kroz vrh soli AX i tačku kondicioniranog sistema 1. Stanje matičnog rastvora, koji je u ravnoteži sa nastalim kristalnim produktom, određen je tačkom 2 na radnoj izotermi.

Kondicioniranje sistema uz uvođenje vode

Izdvajanje soli AX iz polaznog sistema, čije je stanje određeno tačkom 0 (slika 3), zahtijeva uvođenje vode u sistem u cilju njegovog dovođenja u polje kristalizacije ciljne soli. Proces kondicioniranja sistema, u ovom slučaju je, u ravnotežnom dijagramu predstavljen odsječkom 0–1 na zraku razrijeđivanja sistema vodom. Ovaj zrak je identičan zraku koncentrisanja sistema, uz isparavanje vode, ali je sa suprotnim usmjerenjem.

Fizička izvodljivost procesa kristalizacije određena je graničnim količinama vode uvedene u polazni sistem. Tako je minimalna količina vode vezana za dovođenje sistema u stanje (tačka 3) čijim hlađenjem sistem postiže stanje dvojnog zasićenja za radnu izotermu. Maksimalna količina uvedene vode vezana je za dostizanje

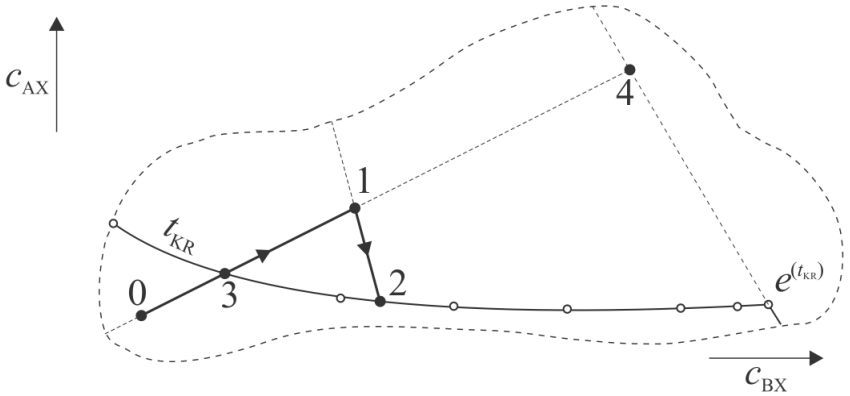

Slika2. Kristalizacija soli AX uz predhodno koncentrisanje sistema isparavanjem dijela vode.
Figure 2. Crystallization of AX salt with previous system concentration by partial water evaporation.

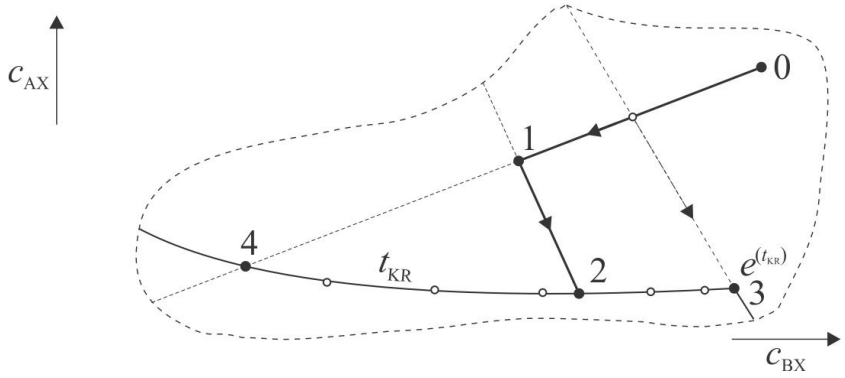

Slika 3. Kristalizacija soli AX uz uvođenje vode u sistem.
Figure 3. Crystallization of AX salt with the introduction of water.

stanja zasićenja sistema, u odnosu na so AX, na radnoj izotermi (tačka 4).

Kondicioniranje sistema uz uvođenje soli BX

Ako je stanje polaznog sistema određeno tačkom 0, u ravnotežnom dijagramu sa slike 4, onda se stanje sistema, pri dozasićavanju uz uvođenje čvrste soli BX, mijenja po zraku rastvaranja koji prolazi kroz vrh soli BX i tačku polaznog sistema. U ovom slučaju sistem sa okolinom komunicira preko čvrste soli BX, uvedene u sistem, i njena minimalna količina odgovara postizanju stanja zasićenja sistema (tačka 1, za radnu izotermu). Uvođenje u sistem veće količine soli BX, od minimalne, praćeno je kristalizacijom soli AX. Maksimalna količina uvedene soli BX odgovara matičnom rastvoru za stanje dvojnog zasićenja pri radnoj izotermi.

Za polazni sistem čije je stanje, u ravnotežnom dijagramu, određeno tačkom 2 postizanje konačnog stanja sistema postiže se u procesu dozasićavanja (pravac 2–3) i hlađenja sistema na radnu izotermu (pravac 3–*e*).

Multivarijantni kristalizacioni moduo

U cilju razvoja metodologije, čiji je zadatak definisan u formulaciji problema, kristalizacioni proces izdvajanja soli AX izveden je u kristalizatoru poopštene strukture (slika 5).

Kristalizatoru su incidentni slijedeći tokovi: 1 – tok polaznog sistema; 2 – kristalni produkt AX; 3 – tok matičnog rastvora; 4 – tok izmijenjene vode sa okolinom i 5 – kristalna so BX.

Osnova koncepta analitičke metodologije, za utvrđivanje mogućih procesnih struktura za kristalizaciju soli AX, je u slijedećem: u matematičkom opisu poopštenog kristalizacionog procesa figuriše veći broj promjenjljivih od broja relacija koje povezuju te promjenjljive i svaka od varijanti kristalizacionog procesa, ili pak njegovih sekvenci, biće određena elementima podskupa slobodnih promjenjljivih kojima se, u cilju rješivosti matematičkog opisa, moraju dodijeliti vrijednosti. Cilj je kreirati procesni simulator koji, u svom konceptu, rješavajući višekratno matematički opis kristalizacionog procesa, za različitu strukturu skupa slobodnih promjenjljivih, daje realne procesne strukture za različite parametre polaznog sistema.

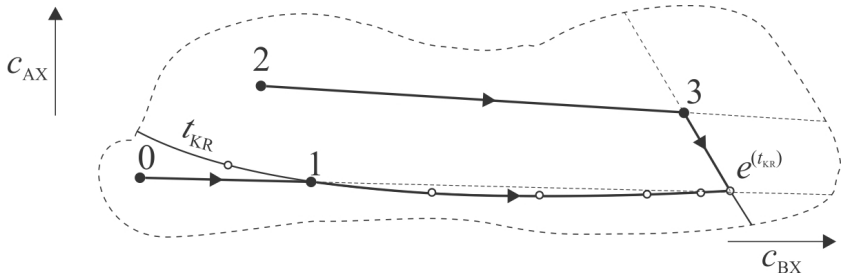

Slika 4. Kristalizacija AX isoljavanjem uz uvođenje soli BX.
Figure 4. Crystallization of AX salt with the introduction of BX salt.

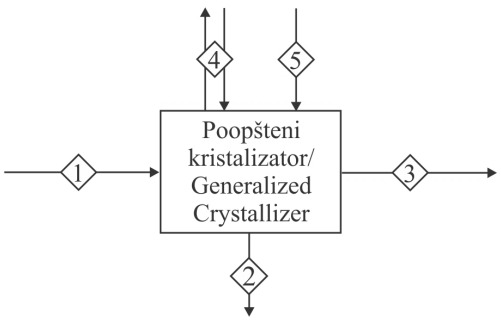

Slika 5. Ulazno-izlazna struktura poopštenog kristalizatora.
Figure 5. Inlet-outlet structure of the generalized crystallizer.

Matematički opis poopštenog kristalizacionog procesa

U skladu sa ulazno–izlaznom procesnom strukturom, sa slike 5, dobija se slijedeći sistem jednačina matematičkog opisa:

Jednačina ukupnog materijalnog bilansa:

$$\bar{m}_1 + \bar{m}_5 = \bar{m}_2 + \bar{m}_3 + \bar{m}_4 \quad (1)$$

Jednačina materijalnog bilansa u odnosu na so koja kristališe:

$$\bar{m}_1 c_{AX}^{(1)} = \bar{m}_2 c_{AX}^{(KR)} + \bar{m}_3 c_{AX}^{(3)} \quad (2)$$

Jednačina materijalnog bilansa u odnosu na so koja ne kristališe:

$$\bar{m}_1 c_{BX}^{(1)} + \bar{m}_5 = \bar{m}_3 c_{BX}^{(3)} \quad (3)$$

Tok matičnog rastvora je sistem zasićen u odnosu na so AX, pri temperaturi kristalizacije t_{KR}, i sadržaji soli su povezani relacijom ravnoteže u sistemu:

$$c_{AX} = f(c_{BX}, t_{KR})$$

odnosno za stanje matičnog rastvora dobija se:

$$c_{AX}^{(3)} = f(c_{BX}^{(3)}, t_{KR}) \quad (4)$$

Maksimalna vrijednost sadržaja soli BX, u matičnom rastvoru, dobija se u stanju dvojnog zasićenja sistema pri temperaturi u kristalizatoru. U opštem slučaju sadržaji soli u sistemu, za stanje dvojnog zasićenja, su funkcija temperature:

$$c_{BX}^{(dz)} = f(t_{KR}) \quad (5)$$

Sadržaj soli u sistemu matičnog rastvora se najčešće opisuje preko varijable λ koja predstavlja stepen dostizanja stanja dvojnog zasićenja:

$$c_{BX}^{(3)} = \lambda c_{BX}^{(dz)} \quad (6)$$

Stepen dostizanja dvojnog zasićenja sistema može primiti vrijednost iz intervala $\lambda \in [\lambda_{min}, 1)$ pri čemu je:

$$\lambda_{min} = \frac{c_{BX}^{(1)}}{c_{BX}^{(dz)}} \quad (7)$$

Sadržaj bezvodne soli, u kristalnom produktu, određen je tipom kristalnog produkta i može primiti vrijednost $c_{AX}^{(KR)} = 1$, za bezvodnu so, dok je sadržaj soli u kristalohidratnom produktu određen relacijom:

$$c_{AX}^{(KR)} = \frac{M_{AX}}{M_{AX}^{(KRH)}}$$

pri čemu su: $M_{AX}, M_{AX}^{(KRH)}$ – molekulske mase bezvodne i kristalohidratne soli.

U formiranom sistemu jednačina, poopštenog kristalizacionog procesa, šest relacija ((1)–(6)) povezuje slijedećih 13 varijabli:

$$\bar{m}_i, i = 1, 5; c_{AX}^{(1)}, c_{AX}^{(3)}, c_{AX}^{(KR)}, c_{BX}^{(1)}, c_{BX}^{(3)}, c_{BX}^{(dz)}, t_{KR}, \lambda$$

i broj stepeni slobode sistema jednačina matematičkog opisa modula je:

$$F = 13 - 6 = 7$$

Kako je varijabla $c_{AX}^{(KR)}$ sadržaj bezvodne soli u kristalnom produktu, parametar, i uz varijable čije vrijednosti proizilaze iz formulacije polaznog zadatka:

- parametri polaznog sistema, $\bar{m}_1, c_{AX}^{(1)}, c_{BX}^{(1)}$ i
- temperatura pri kojoj se izvodi proces kristalizacije, t_{KR}. Proizilazi da je, u cilju svođenja matrice sistema jednačina na kvadratni oblik, potrebno dodijeliti vrijednosti za još dvije promjenljive.

Elementi realnih kristalizacionih procesa proizilaze u rezultatu rješavanja multivarijantnog kristalizacionog modula (MKM) za partikularne slučajeve strukture dvočlanog podskupa slobodnih informacionih promjenljivih, S_{IP}. U tekstu što slijedi prikazani su elementarni koraci razvijene, formalizirane, metodologije za utvrđivanje alternativnih procesnih struktura za kristalizaciju soli soli AX iz trokomponentnog sistema.

Metodologija za utvrđivanje procesnih struktura

Osnovi metodologije su predstavljeni kroz slijedeće elementarne korake:

Korak br. 1. Za sadržaj soli u polaznom sistemu $c_{AX}^{(1)}, c_{BX}^{(1)}$ i temperaturu izvođenja procesa kristalizacije, t_{KR}, utvrđuju se mogućnosti kristalizacije soli AX iz sistema. U tom smislu upoređuju se vrijednosti odnosa sadržaja soli AX i BX u polaznom sistemu α_0 i sistemu koji je u stanju dvojnog zasićenja α_{dz}, za temperaturu u kristalizatoru. Za $\alpha_0 > \alpha_{dz}$ iz polaznog sistema se, primjenom neke kristalizacione tehnike, može separisati so AX. U suprotnom, u cilju separacije soli AX, iz sistema se prethodno mora izvesti djelimična separacija soli BX.

Korak br. 2. Utvrđuje se fizička izvodljivost procesa kristalizacije soli AX hlađenjem sistema preko razmjenjivačke površine. Procesni simulator, MKM, rješava sistem jednačina matematičkog opisa za skup slobodnih informacionih promjenljivih u koga, pored parametara polaznog sistema, ulazi količina izdvojene vode i količina dodate soli BX. Ovim promjenljivim se, u skladu sa posmatranim tipom kristalizacionog procesa, dodijeljuju vrijednosti nule. Podskup S_{IP} je:

$$S_{IP}^{(I)} = \{\bar{m}_4 = 0, \bar{m}_5 = 0\}$$

i on određuje prvu varijantu MKM. Skup izlaznih promjenljivih je:

$\bar{m}_2, \bar{m}_3, c_{AX}^{(3)}, c_{BX}^{(3)}, c_{BX}^{(dz)}$ i λ

Fizička izvodljivost procesa kristalizacije određena je vrijednostima dvaju promjenljivih:

- količinom kristalnog produkta $\bar{m}_2$ i
- stepenom dostizanja stanja dvojnog zasićenja, λ.

Realno su, s obzirom na različite parametre polaznog sistema, slika 6, moguće slijedeće vrijednosti za uređen par promjenljivih $\bar{m}_2$ i λ.

Za polazni sistem određen tačkom 1, u ravnotežnom dijagramu sistema AX–BX–H_2O, dobija se stanje matičnog rastvora, na izotermi hlađenja, t_{KR}, određeno tačkom 1^1 i rješavanjem MKM za elemente $S_{IP}^{(I)}$ dobija se $\bar{m}_2 > 0$ i $\lambda < 1$. U pitanju je fizički izvodljiv proces.

Za polazni sistem, određen tačkom 2, dobija se $\bar{m}_2 > 0$ i $\lambda > 1$. Matični rastvor, čije je stanje određeno tačkom 2^2, fizički ne može egzistirati za izotermu t_{KR} i u cilju kristalizacije soli AX, polazni sistem se mora kondicionirati uz uvođenje vode u sistem.

Polazni sistem, određen tačkom 3, je u odnosu na izotermu kristalizacije nezasićen i u rezultatu rješenja MKM se ima $\bar{m}_2 < 0$ i $\lambda < \lambda_{min}$. U cilju kristalizacije soli AX polazni sistem se mora kondicionirati uz izdvajanje vode iz sistema.

Korak br. 3. Procesi kristalizacije uz kondicioniranje polaznog sistema uvođenjem vode.

Za polazni sistem čijim se hlađenjem preko izmjenjivačke površine ima $\bar{m}_2 > 0$ i $\lambda < \lambda_{min}$, jedino mogući postupak njegovog kondicioniranja predstavlja uvođenje vode u sistem.

Sistem jednačina MKM se, u ovom slučaju, rješava za slijedeći S_{IP}:

$$S_{IP}^{(II)} = \left\{ \bar{m}_5 = 0, c_{BX}^{(3)} \right\}$$

Promjenljiva $c_{BX}^{(3)}$, za fizički izvodljiv proces kristalizacije, može primiti vrijednost iz intervala $c_{BX}^{(3)} \in (c_{BX}^{(min)}, c_{BX}^{(max)})$, pri čemu minimalna vrijednost odgovara slučaju dovođenja polaznog sistema u stanje zasićenja, u odnosu na so AX, uvođenjem vode u sistem, slika 7.

Minimalna vrijednost promjenljive $c_{BX}^{(3)}$ proizilazi u rezultatu rješavanja sistema jednačina MKM za slijedeću strukturu S_{IP}:

$$S_{IP}^{(III)} = \left\{ \bar{m}_2 = 0, \bar{m}_5 = 0 \right\}$$

Korak br. 4. Procesi kristalizacije uz kondicioniranje sistema uvođenjem soli BX.

Zavisno od parametara polaznog sistema fizička izvodljivost kristalizacionog procesa može podrazumijevati uvođenje čvste soli BX, do postizanja stanja zasićenja sistema po soli AX, na nekoj izotermi t_{zas}, ili je pak

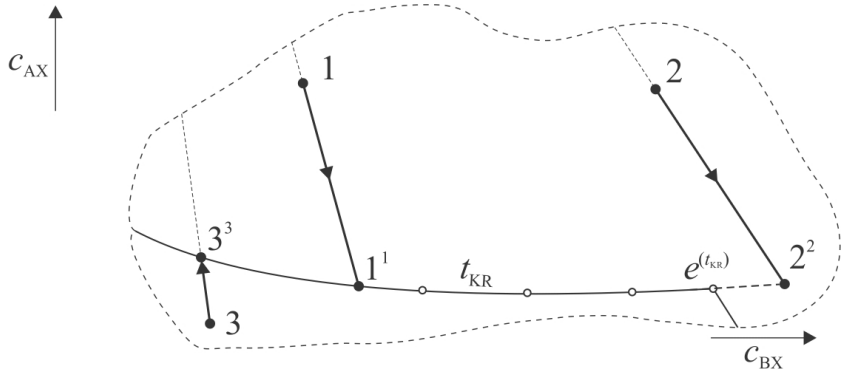

Slika 6. Procesi hlađenja sistema, različitih parametara, preko razmjenjivačke površine.
Figure 6. Processes of system cooling with different initial parameters through heat exchanger surface.

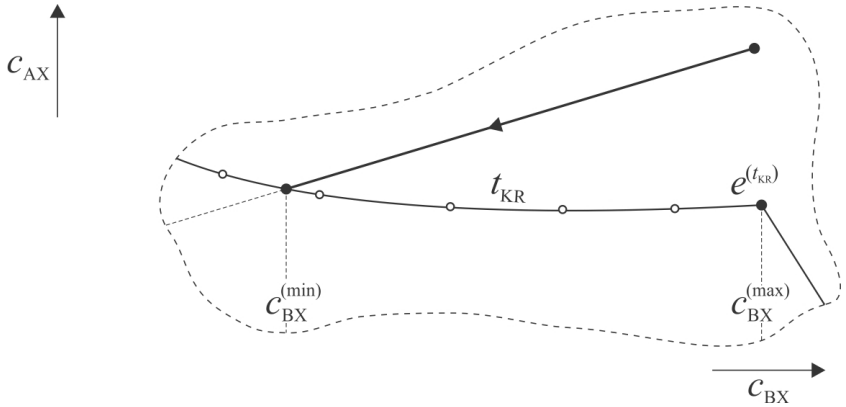

Slika 7. Utvrđivanje granica fizičke egzistencije procesa uz uvođenje vode.
Figure 7. Determination of feasible process bounds with water introduction.

fizička izvodljivost procesa moguća samo uz nezasićen kondicionirani sistem (slika 8).

Tako je, za polazni sistem čije je stanje u ravnotežnom dijagramu određeno tačkom 1, fizički izvodljiv kristalizacioni proces uz kondicioniranje sistema uvođenjem čvrste soli BX do postizanja zasićenja sistema pri izotermi t_{zas} (tačka 2). Ako je pak, polazni sistem, određen tačkom 1^1 onda se, hlađenjem do zasićenog sistema (tačka 2^1) na izotermu t_{KR}, fizički ne može izvesti proces kristalizacije soli AX. Fizička izvodljivost procesa, u ovom slučaju, moguća je samo iz sistema koji je djelomično zasićen i maksimalna količina uvedene soli u sistem određena je tačkom 2^2 kondicioniranog sistema. U ovom slučaju MKM se rješava za $S_{IP}^{(III)}$.

Fizički izvodljivim procesima kristalizacije, uz kondicioniranje sistema uvođenjem čvrste soli BX, odgovara tačno određen interval promjene stanja matičnog rastvora. Ako se stanje matičnog rastvora opisuje sa sadržajem soli BX i pripadajućom izotermom t_{KR} onda je donja granica intervala, sadržaja soli BX, određena sadržajem soli koji se ima za matični rastvor sistema dobijen hlađenjem polaznog sistema bez njegovog kondicioniranja. Utvrđivanje maksimalne vrijednosti sadržaja soli BX, u matičnom rastvoru, proizilazi iz procedure koja podrazumijeva slijedeće:

1. Utvrđuje se varijanta procesa dozasićavanja koja obezbjeđuje fizičku izvodljivost kristalizacionog procesa kroz slijedeće korake:

a. Rješavanjem sistema jednačina MKM, za slijedeću opciju S_{IP}:

$$S_{IP}^{(III)} = \{\bar{m}_2 = 0, \bar{m}_4 = 0\}$$

utvrđuju se parametri zasićenog sistema, pri zadatoj izotermi t_{zas}, dobijenog uvođenjem soli BX.

b. Za dobijene parametre zasićenog sistema, u prethodnom koraku, rješava se MKM, za $S_{IP}^{(I)}$, čiji rezultati jednoznačno određuju varijantu procesa dozasićavanja polaznog sistema (tačka 2 na slici 8).

2. Ako se polazni sistem kondicionira do stanja zasićenja onda je dozvoljeni interval promjene vrijednosti sadržaja soli BX, u matičnom rastvoru, dat kao $c_{BX}^{(max)} > c_{BX}^{(3)} > c_{BX}^{(min)}$ a u suprotnom maksimalna vrijednost sadržaja soli BX, u matičnom rastvoru, odgovara njenom sadržaju u stanju dvojnog zasićenja sistema.

Korak br. 5. Kondicioniranje sistema uz isparavanje dijela prisutne vode.

Za utvrđivanje elemenata procesa kristalizacije, uz kondicioniranje sistema isparavanjem dijela prisutne vode, rješava se MKM za slijedeću varijantu S_{IP}:

$$S_{IP}^{(IV)} = \{\bar{m}_5 = 0, c_{BX}^{(3)}\}$$

Kao i za proces kondicioniranja sistema, dozasićavanjem sa čvrstom soli BX, i u ovom slučaju je interval vrijednosti sadržaja soli BX, u matičnom rastvoru, za koga je fizički izvodljiv proces kristalizacije soli AX, je funkcija sadržaja soli u polaznom sistemu (slika 9).

Za polazni sistem koji je, na izotermi kristalizacije t_{KR}, nezasićen (tačka 1 na dijagramu sa slike 9) minimalna vrijednost $c_{BX}^{(3)}$ određena je kao ravnotežni sastav koji odgovara zasićenom sistemu dobijenom izdvajanjem vode, iz polaznog sistema, za izotermu u kristalizatoru, tačka 2. Za utvrđivanje vrijednosti navedene promjenljive rješava se MKM za elemente $S_{IP}^{(III)}$.

Ako je polazni sistem određen tačkom 1^1, onda je minimalan sadržaj soli BX određen kao sadržaj u matičnom rastvoru iz koga je kristalisala so AX, hlađenjem polaznog sistema preko izmjenjivačke površine, pri izotermi t_{KR}. U ovom slučaju se ima opcija MKM za elemente $S_{IP}^{(I)}$. Donja granica promjene vrijednosti $c_{BX}^{(3)}$

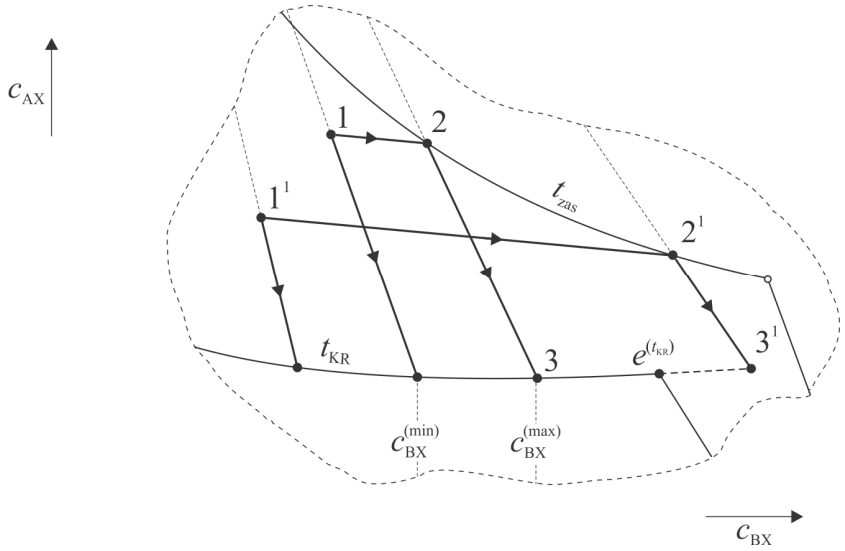

Slika 8. Procesi kristalizacije soli AX uz uvođenje soli BX u sistem.
Figure 8. Crystallization processes of AX salt with introduction of BX salt.

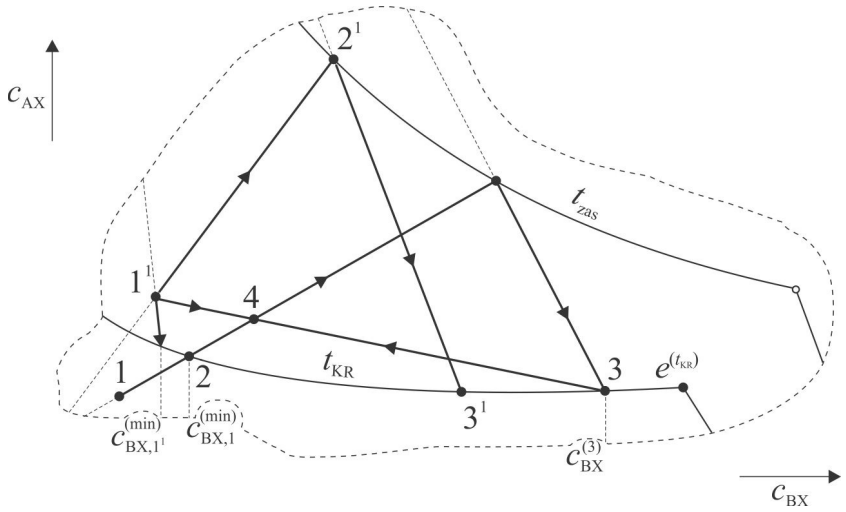

Slika 9. Utvrđivanje granica fizičke izvodljivosti procesa isparavanjem dijela prisutne vode.
Figure 9. Determination of feasible process bounds with partial water evaporation.

određena je sadržajem soli, u uslovima dvojnog zasićenja, pri izotermi kristalizacije.

Nakon utvrđivanja elemenata globalnog materijalnog bilansa, kristalizacionog procesa, slijedi postupak utvrđivanja procesne strukture. Konačno stanje sistema može se postići u acikličnoj odnosno cikličnoj procesnoj strukturi slika 10 i zahtijevana struktura je u potpunosti određena stanjem polaznog sistema.

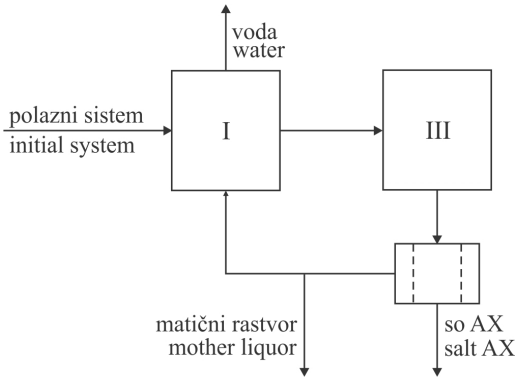

Slika 10. Procesna struktura sa isparavanjem vode.
Figure 10. Process structure with water evaporation.

Za polazni sistem određen tačkom 1, u ravnotežnom dijagramu sa slike 9, proces se može izvesti u acikličnoj strukturi uz ograničenje da sistem postiže stanje zasićenja, isparavanjem vode, na izotermi t_{zas}.

Za polazni sistem čije je stanje određeno tačkom 1^1, zahtijevano konačno stanje sistema se može postići samo u cikličnoj procesnoj strukturi u kojoj je pojni tok koncentratora nastao miješanjem polaznog sistema i dijela toka matičnog rastvora, tačka 4 u dijagramu sa slike 9.

Procedura utvrđivanja zahtijevane procesne strukture podrazumijeva slijedeće:

- Rješava se MKM za elemente $S_{IP}^{(IV)}$ i u rezultatu se dobijaju vrijednosti kapaciteta sistema u odnosu na matični rastvor $\bar{m}_3$, kristalni produkt $\bar{m}_2$ i izdvojenu vodu $\bar{m}_4 = 0$.
- Rješava se sistem jednačina kristalizacionog modula koji predstavlja podsistem kristalizator-separator. MKM se rješava za elemente S_{IP}:

$$S_{IP}^{(VI)} = \{\bar{m}_2, \bar{m}_3\}$$

U rezultatu se dobijaju parametri pojnog toka kristalizatora i protok recirkulacionog toka matičnog rastvora. Kako je, na stanje pojnog toka kristalizatora, postavljeno ograničenje da je u pitanju zasićen sistem, pri nekoj temperaturi/pritisku, onda dobijena vrijednost protoka recirkulacionog toka odgovara minimalnoj vrijednosti $\bar{m}_{REC}^{(min)}$ za koju je izvodljiv proces u cikličnoj procesnoj strukturi.

Proces u cikličnoj strukturi funkcioniše sa nezasićenim sistemom, kao pojnim tokom kristalizatora, pri protocima recirkulacionog toka $\bar{m}_{REC} > \bar{m}_{REC}^{(min)}$.

Ako se u rezultatu rješenja sistema jednačina kristalizacionog modula dobije negativna vrijednost za protok recirkulacionog toka onda je fizički izvodljiv proces u acikličnoj procesnoj strukturi i sa nezasićenim sistemom kao pojnim tokom kristalizatora.

Korak br. 6. Kondicioniranje sistema kombinacijom procesa koncentrisanja uz isparavanje vode i uvođenja čvste soli BX.

Procesna struktura kristalizacionog procesa predstavljena je na slici 11; I – kondicioniranje sistema uz izdvajanje vode; II – kondicioniranje sistema uz dozasićavanje sa soli BX; III – kristalizator hlađen preko razmjenjivačke površine i IV – centrifuga.

Utvrđivanje parametara kristalizacionog sistema izvodi se u skladu sa slijedećom procedurom:

- Utvrđuje se minimalni sadržaj soli BX, slika 12, u matičnom rastvoru kristalizatora, sekvencijskim rješavanjem MKM za elemente S_{IP}: $S_{IP}^{(III)}$, $S_{IP}^{(I)}$.
- U iterativnoj proceduri, za dodijeljenu početnu vrijednost protoku toka izdvojene vode $\bar{m}_4$, rješavaju se sistemi jednačina MKM, za izdvojene podsisteme (slika 13), u skladu sa slijedećom sekvencom: MKM_I, MKM_{II}, MKM_{III}.

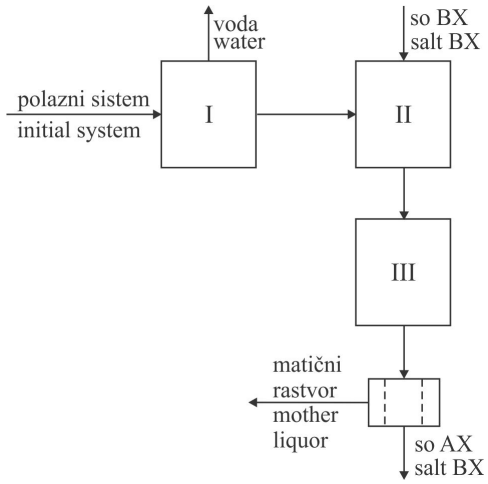

Slika 11. Procesna struktura sa kombinovanim kondicioniranjem sistema.
Figure 11. Process structure with combined system conditioning.

Elementi kristalizacionog procesa se dobijaju uz ograničenje na postizanje zasićenja, pojnog toka kristalizatora, pri temperaturi zasićenja, t_{zas}.

PRIMJENA RAZVIJENE METODOLOGIJE

Primjer 1

U jednom termoenergetskom sistemu, u podsistemu za pripremu vode, pri regeneraciji jonoizmjenjivačkih masa generiše se otpadni tok za koga se aproksimativno može uzeti da predstavlja sistem NaCl–Na_2SO_4–H_2O. Primjenom prezentovane metodologije utvrditi fizički izvodljive procese izdvajanja natrijum sulfata iz sistema. Na funkcionisanje sistema postavlja se ograničenje vezano za minimalnu temperaturu u procesu od 0 °C i maksimalni pritisak, pri kome se koncentriše sistem, od 1 bar.

Sistem NaCl–Na_2SO_4–H_2O ima dvije određujuće karakteristike koje ga diferenciraju od većine trokomponentnih sistema. Pri temperaturama većim od 17,9 °C iz sistema kristališe bezvodna so a pri temperaturama manjim od 17,9 °C u čvrstu fazu prelazi kristalohidrat sa deset molekula vode. U temperaturnom intervalu (32,4–110 °C) rastvorljivost natrijum-sulfata se smanjuje sa povećanjem temperature.

Na osnovu tabelarnih podataka, o ravnoteži u sistemu NaCl–Na_2SO_4–H_2O [19], izvršena je aproksimacija politerme sistema, za sisteme zasićene u odnosu na natrijum-sulfat, za područja u kojima je u čvstoj fazi bezvodna so odnosno kristalohidrat. U području kristalizacije bezvodnog natrijum-sulfata sadržaj natrijum-sulfata u sistemu, u zavisnosti od sadržaja natrijum-hlorida aproksimiran je polinomalnom relacijom trećeg reda:

$$c_{Na_2SO_4} = \sum_{i=0}^{3} a_i c_{NaCl}^{i}$$

Parametri a_i, u polinomalnoj zavisnosti, su linearna funkcija temperature i dati su u tabeli 1.

U području ravnotežnog dijagrama, iz koga natrijum-sulfat kristališe kao dekahidrat, sadržaj natrijum-sulfata u sistemu, u zavisnosti od sadržaja natrijum-hlorida aproksimiran je polinomom drugog stepena:

$$c_{Na_2SO_4} = a_0 + a_1 c_{NaCl} + a_2 c_{NaCl}^2$$

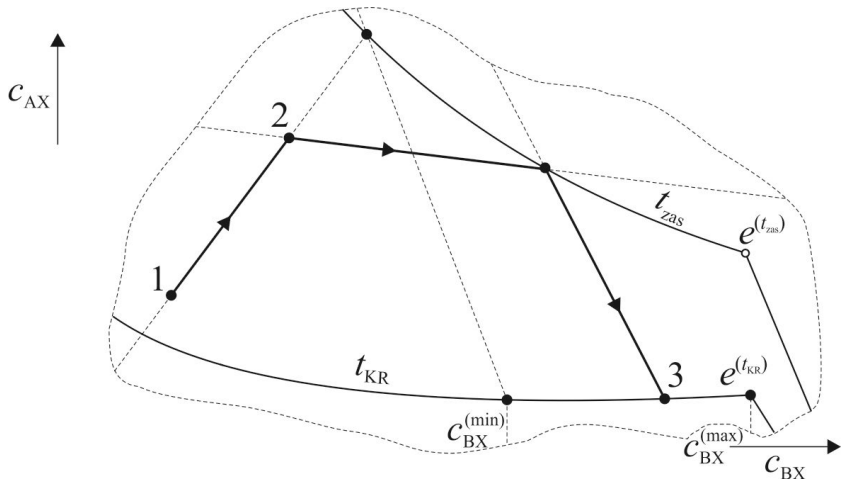

Slika 12. Proces kristalizacije uz kombinovano kondicioniranje polaznog sistema.
Figure 12. Crystallization process with combined initial system conditioning.

Parametri a_0, a_1 i a_2 su funkcija temperature i takođe su aproksimirani polinomom drugog stepena:

$$a_i = \sum_{i=0}^{2} b_i t^i$$

Vrijednosti parametara b_i, $i = 0,2$ date su u tabeli 2.

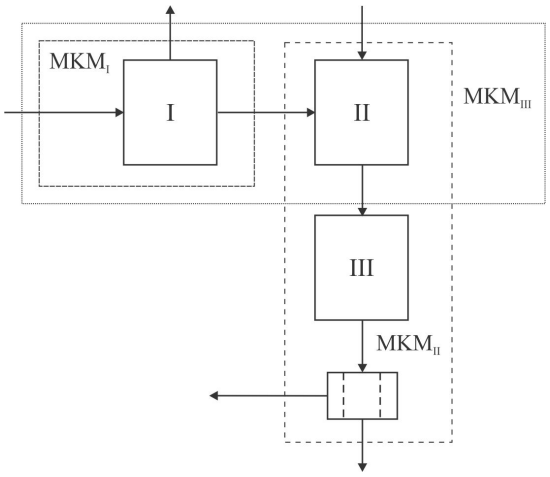

Slika 13. Podsistemi dekompoziranog procesnog sistema.
Figure 13. Subsystems of decomposed process system.

Tabela 1. Parametri u relaciji:

$$c_{Na_2SO_4} = \sum_{i=0}^{3} a_i c_{NaCl}^{i}$$

sistema NaCl–Na_2SO_4–H_2O; temperaturni interval: 40–120 °C
Table 1. Parameters in equation:

$$c_{Na_2SO_4} = \sum_{i=0}^{3} a_i c_{NaCl}^{i}$$

for the NaCl–Na_2SO_4–H_2O system; temperature range: 40–120 °C

Parametar	Relacija
a_0	$0,3394 - 4,2695\times10^{-4} t$
a_1	$-1,3247 - 1,2528\times10^{-4} t$
a_2	$-0,8391 + 1,1851\times10^{-3} t$
a_3	$6,3205 + 1,8698\times10^{-2} t$

Tabela 2. Vrijednosti parametara b_i u relaciji za ravnotežu u sistemu
Table 2. Value of parameters b_i in the equilibrium equation

Parametar a_i	Parametar b_i		
	b_0	b_1	b_2
	$c_{NaCl} < 15\%$		
a_0	$4,2425\times10^{-2}$	$2,370834\times10^{-3}$	$1,68166\times10^{-4}$
a_1	–0,3715	–0,5615	$1,63\times10^{-3}$
a_2	1,15	0,2980	0,012333
	$c_{NaCl} > 15\%$		
a_0	$3,0769\times10^{-2}$	$4,2329\times10^{-4}$	$2,935572\times10^{-4}$
a_1	–0,204	$1,2939\times10^{-2}$	$-1,891576\times10^{-3}$
a_2	0,525628	$4,07816\times10^{-2}$	$5,785697\times10^{-3}$

Sadržaj soli u sistemu, za uslove dvojnog zasićenja sistema, u zavisnosti od temperature opisan je relacijama:

- Za temperaturni režim 0–17,9 °C:

$$c_{NaCl}^{(e)} = 0,24544 + 2,03641\times10^{-3} t - 1,87513\times10^{-4} t^2$$

$$c_{Na_2SO_4}^{(e)} = 1,32106\times10^{-2} + 1,88382\times10^{-4} t + 1,85176\times10^{-4} t^2$$

- Za temperaturni režim 45–150 °C:

$$c_k = \sum_{i=0}^{3} a_i t \ , \ k = \text{NaCl, } Na_2SO_4; \ i = 0,3$$

i odgovarajući parametri u polinomalnoj relaciji dati su u tabeli 3.

Tabela 3. Parametri u relaciji za ravnotežu u uslovima dvojnog zasićenja
Table 3. Parameters in equation for equilibrium of dual saturation conditions

Parametar	Sadržaj soli	
	NaCl	Na_2SO_4
a_0	21,0896	8,53
a_1	$7,1378\times10^{-2}$	$9,238\times10^{-2}$
a_2	$2,975\times10^{-4}$	$6,4293\times10^{-4}$
a_3	$7,0785\times10^{-7}$	$1,231\times10^{-6}$

Sadržaji soli, u navedenim relacijama, figurišu u masenim udjelima.

Za parametre polaznog sistema: maseni protok 12000 kg/h, sadržaj NaCl 1,3 mas.%, sadržaj natrijum-sulfata 2,5 % i uz ograničenja na temperaturu procesa kristalizacije od 5 °C i pritisak pri kome se izvodi koncentrisanje sistema, uz isparavanje vode, od 0,7 bar imaju se slijedeći rezultati:

- Hlađenjem sistema preko razmjenjivačke površine, na zadatu temperaturu u kristalizatoru, dobija se količina kristalnog produkta manja od nule ($\bar{m}_2 < 0$) što upućuje na potrebu kondicioniranja sistema.
- Isparavanjem vode do sadržaja soli u sistemu od $c_{NaCl} = 1,88\%$ i $c_{Na_2SO_4} = 3,59\%$ dobija se zasićenje sistema, u odnosu na natrijum sulfat, pri temperaturi od 5 °C. Navedeni sadržaj NaCl predstavlja donju granicu intervala, mogućih sadržaja NaCl u matičnom rastvoru kristalizatora.
- Dovođenjem sistema, u stanje zasićenja, isparavanjem vode pri pritisku 0,7 bar i hlađenjem zasićenog sistema na temperaturu u kristalizatoru dobija se matični rastvor sa sadržajem NaCl od 14,95%.
- Kako je sadržaj NaCl, u matičnom rastvoru manji od maksimalno mogućeg (uslovi dvojnog zasićenja) to proizilazi da se ima, u acikličnoj procesnoj strukturi, fizički izvodljiv proces kristalizacije.

Parametri procesnog sistema predstavljeni su na slici 14.

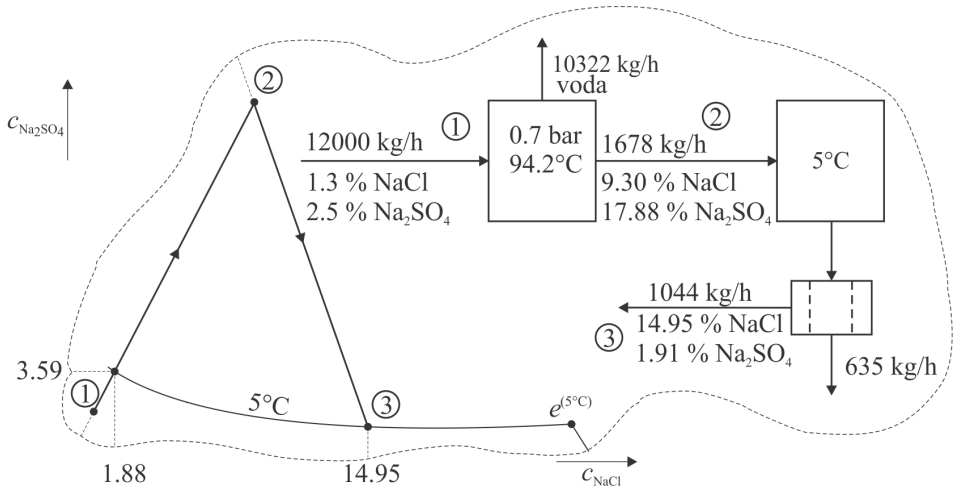

Slika 14. Aciklična procesna struktura uz isparavanje vode.
Figure 14. Noncyclic process structure with water evaporation.

Kako je u acikličnoj procesnoj strukturi ostvarena relativno mala vrijednost stepena dostizanja dvojnog zasićenja to, u narednom koraku, procesni simulator utvrđuje elemente cikličnog procesa za zadati stepen dostizanja dvojnog zasićenja sistema.

Za proces, u kome je matični rastvor postigao uslove dvojnog zasićenja, imaju se elementi procesa prikazani na slici 15.

Za proces u kome se priprema polaznog sistema izvodi kombinacijom procesa koncentrisanja, uz isparavanje vode, i dozasićavanja uz uvođenje čvstog NaCl donju granicu intervala, dozvoljenih sadržaja NaCl u matičnom rastvoru kristalizatora, određuju parametri zasićenog sistema postignutog uz isparavanje vode. U posmatranom slučaju uzeto je da se zasićavanje sistema, uz isparavanje vode, a i uz uvođenje čvrstog NaCl izvodi pri izotermi 45 °C. Ovoj izotermi odgovara sadržaj NaCl, u matičnom rastvoru, od 16,3%.

Elementi procesnog sistema za sadržaj NaCl, u matičnom rastvoru kristalizatora, predstavljeni su slici 16.

Primjer 2

U jednom realnom procesu produkcije NaCl, u kome je sirovina rastvor nastao podzemnim rastvaranjem sonog ležišta, kao otpadni tok se javlja sistem NaCl–Na_2SO_4–H_2O slijedećeg sastava: 24,0 mas.% NaCl i 5,2 mas.% Na_2SO_4.

Iz sistema je, uz identične zahtjeve kao u primjeru 1, moguće izdvojiti natrijum sulfat dekahidrat u procesu čiju su elementi predtavljeni na slici 17.

Hlađenjem sistema, preko razmjenjivačke površine, dobija se količina kristalnog produkta veća od nula ($\bar{m}_2 > 0$) i sadržaj NaCl u matičnom rastvoru od 26,03% koji je veći od, za fizički izvodljiv proces, maksimalno mogućeg (25,09% za sistem u stanju dvojnog zasićenja). Jedini mogući način kondicioniranja polaznog sistema je uz uvođenje vode u sistem. Tako sistem postaje zasi-

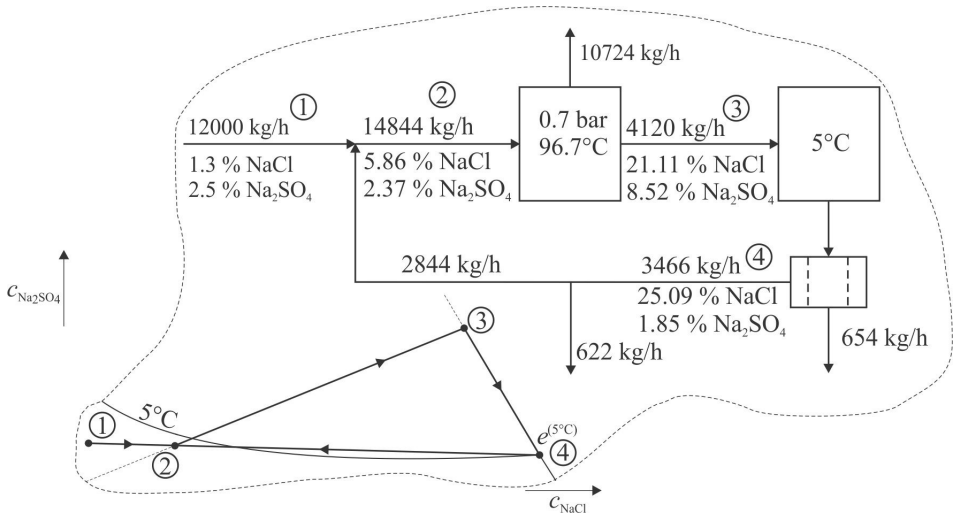

Slika 15. Ciklična procesna struktura uz isparavanje vode.
Figure 15. Cyclic process structure with water evaporation.

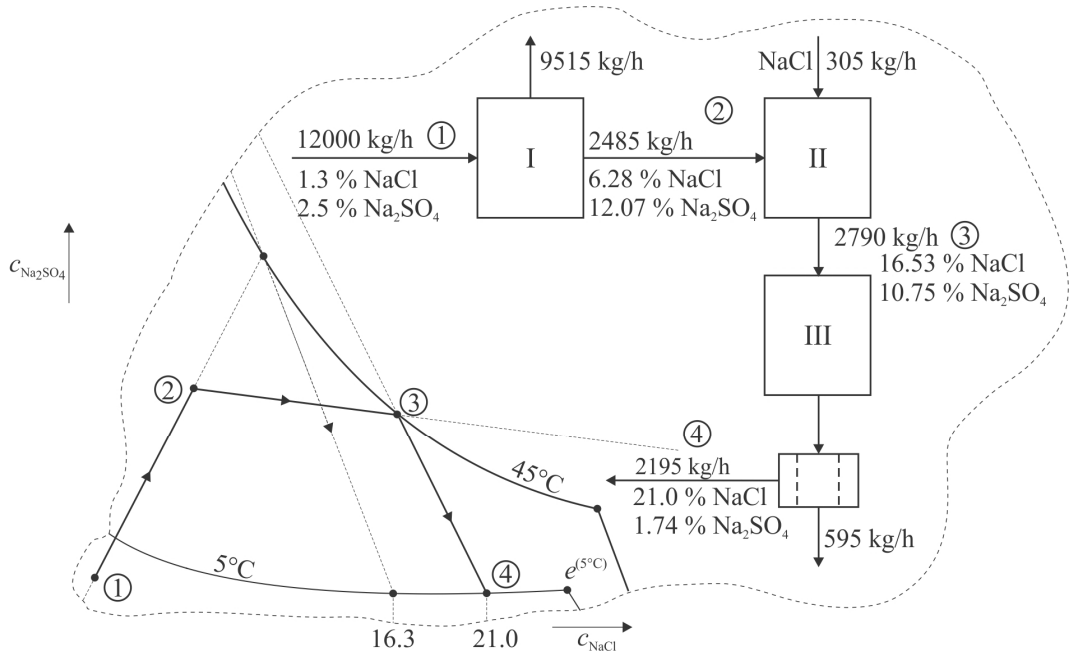

Slika 16. Struktura sa koncentrisanjem uz isparavanje vode i dozasićavanje sa NaCl.
Figure 16. Structure with concentration by water evaporation and additional saturation with NaCl.

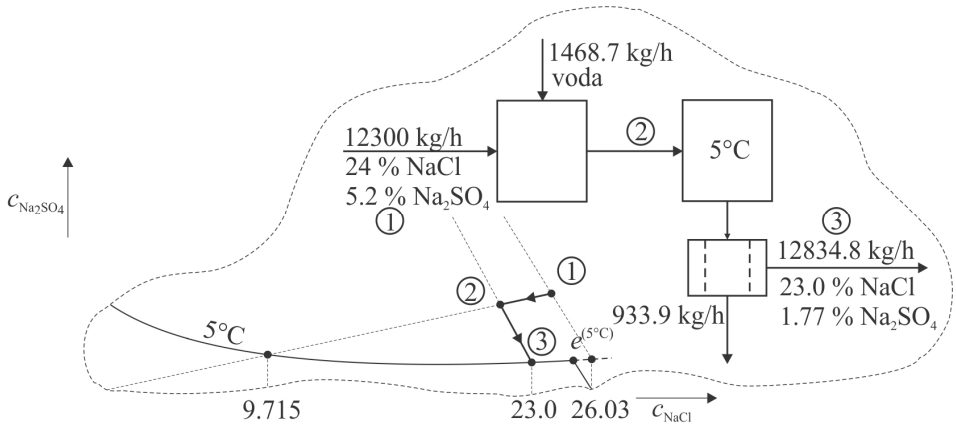

Slika 17. Struktura sa uvođenjem vode u sistem.
Figure 17. Structure with water introduction into system.

ćen, u odnosu na Na_2SO_4 na 5 °C, uz uvođenje 18087 kg/h vode pri čemu se ima donja granična vrijednost sadržaja NaCl, u zasićenom sistemu, od 9,715%. Elementi procesa sa slike 17 simulirani su za sadržaj NaCl u matičnom rastvoru kristalizatora od 23,0%.

ZAKLJUČAK

Razvijena je formalizirana metodologija sistemske analize, za kristalizaciju soli AX iz hipotetskog elektrolitičkog sistema AX–BX–H_2O, koja podrazumijeva utvrđivanje procesnih varijanti komunikacijom sistema sa okolinom preko izmijenjene vode i kristalne soli BX. Kreirani procesni simulator čiju osnovu predstavlja multivarijanti kristalizacioni moduo, pored utvrđivanja konceptualnih procesnih struktura, određuje i intervale promjene vrijednosti, ključnih tehnoloških parametara, u kojima fizički egzistiraju utvrđeni procesi. Ovim je izgrađena pouzdana osnova za parametarsku i strukturnu optimizaciju industrijskih kristalizacionih procesa što i predstavlja logičan nastavak budućih istraživanja. Primjenom razvijenog procesnog simulatora za utvrđivanje procesnih struktura kristalizacije kristalohidratnog natrijum-sulfata, iz dvaju realnih sistema NaCl–Na_2SO_4–H_2O, utvrđeno je da procesnu strukturu, pored karakteristika ravnoteže, determinira i sadržaj soli u polaznom sistemu.

LITERATURA

[1] B. Fitch, How to Design Fractional Crystallization Processes, Ind. Eng. Chem. **62**(6) (1970) 6–33.

[2] A.P. Rossiter, J.M. Douglas, Design and Optimization of Solids Processes: Part 1 – A Hierarchical Decision Procedure for Synthesis of Solids Systems, Chem. Eng. Res. Des. **67** (1986) 175–183.

[3] A.P. Rossiter, J.M. Douglas, Design and Optimization of Solids Processes: Part 2: Optimisation of Crystallizer, Centrifuge and Dryer Systems, Chem. Eng. Res. Des. **64** (1986) 184–190.

[4] A.P. Rossiter, Design and Optimization of Solids Processes: Part 3: Optimisation of Crystalline Salt Plant Using a Novel Procedure, Chem. Eng. Res. Des. **64** (1986) 191––195.

[5] L.A. Cisternas, D.F. Rudd, Process Design for Fractional Crystallization from Solution, Ind. Eng. Chem. Res. **32**(9) (1993) 1993–2005.

[6] K. Thomsen, R. Gani, P. Rasmunssen, Synthesis and Analysis of Processes with Electrolyte Mixtures, Comput. Chem. Eng. **19** (1995) 527–532.

[7] K. Thomsen, R. Gani, P. Rasmunssen, Simulation and Optimization of Fractional Crystallization Processes, Chem. Eng. Sci **53**(8) (1998) 1551–1564.

[8] L.A. Cisternas, R.E. Swaney, Separation System Synthesis for Fractional Crystallization from Solution Using a Network Flow Model, Ind. Eng. Chem. Res. **37** (1998) 2761––2769.

[9] L.A. Cisternas, Optimal Design of Crystallization-Based Separation Schemes, AIChE J. **45**(7) (1999) 1477–1487.

[10] L.A. Cisternas, C.P. Guerrero, R.E. Swaney, Separation System Synthesis of Fractional Crystallization Processes with Heat Integration, Comp. Chem. Engng. **25** (2001) 595–602.

[11] L.A. Cisternas, J. Cueto, R.E. Swaney, Flowsheet Synthesis of Fractional Crystallization Processes with Cake Washing, Comp. Chem. Engng. **28** (2004) 613–625.

[12] C. Méndez, J. Myers, S. Roberts, J. Logdson, A. Vaia, I. E. Grossmann, MINLP model for synthesis of paraxylene separation processes based on crystallization technology, in: L. Puigjaner (Ed.), European Symposium on Computer Aided Process Engineering (ESCAPE)-15, Elsevier, 2005.

[13] R. Isopescu, L. Filipescu. Optimization of the Crystallization Based Separation Flowcharts. 15th International Symposium on Industrial Crystallization, Napoli, Italy, 2002, pp. 849–854.

[14] R.M. Lima, I.E. Grossmann, Optimal Synthesis of *p*-Xylene Separation Processes Based on Crystallization Technology, AIChE J. **55**(2) (2008) 354–373.

[15] L.M. Nader, Design of Optimal Process Flowsheet for Fractional Crystallization Separation Process, Iran. J. Chem. Chem. Eng. **28**(2) (2009) 63–73.

[16] J.C. Person, Literature Survey for fractional Crystallization Study, CH2M HILL Hanford Group, Inc., Richland, WA, 2004.

[17] L.A. Cisternas, Vásquez, R.E. Swaney, On the Design of Crystallization-Based Separation Processes: Review and Extension, AIChE J. **52**(5) (2006) 1754–1769.

[18] M. Suljkanović, E. Ahmetović, Verifikacija struktura za utilizovanje otpadnih višekomponentnih elektrolitičkih sistema, Hem. ind. **62**(1) (2008) 4-12.

[19] Справочник по растворимости солевых систем, Том I--1, Химия, 1973.

SUMMARY

FORMALIZED METHODOLOGY FOR THE SEPARATION OF THREE COMPONENT ELECTROLYTIC SYSTEMS. PARTIAL SEPARATION OF THE SYSTEM

Midhat Suljkanović[1], Milovan Jotanović[2], Elvis Ahmetović[1], Goran Tadić[2], Nidret Ibrić[1]

[1]*Uiversity of Tuzla, Faculty of Technology, Tuzla, Bosnia and Herzegovina*
[2]*University of East Sarajevo, Faculty of Technology, Zvornik, Bosnia and Herzegovina*

(Scientific paper)

This work presents a formalized methodology for salt separation from three-component electrolytic systems. The methodology is based on the multi-variant modelling block of a generalized crystallization process, with options for simulating the boundary conditions of feasible equilibrium processes and the elements of crystallization techniques. The following techniques are considered: cooling crystallization, adiabatic evaporative-cooling crystallization, salt-out crystallization, isothermal crystallization, and a combination of the mentioned techniques. The multi-variant options of the crystallization module are based on different variable sets with assigned values for solving mathematical models of generalized crystallization processes. The first level of the methodology begins with the determination of salt crystallization paths from a hypothetical electrolytic AX–BX––H_2O system, following by an examination of salt-cooling crystallization possibilities. The second level determines feasible processes by the communication of a feed-system with the environment through a stream of evaporated water, or introduced water with introduced crystallized BX salt. The third level determines the value intervals of the variables for feasible processes. The methodological logic and possibilities for the created process simulator are demonstrated on examples of sodium sulphate separation from the NaCl–Na_2SO_4–H_2O system, using different salt concentrations within the feed system.

Keywords: Synthesis of crystallization process • Mathematical modelling and simulation • Separation of electrolytic systems

The correlation of metal content in medicinal plants and their water extracts

Saša S. Ranđelović, Danijela A. Kostić, Aleksandra R. Zarubica, Snežana S.Mitić, Milan N. Mitić

University of Niš, Faculty of Science and Mathematics, Department of Chemistry, Višegradska 33, 18000 Niš, Serbia

Abstract

The quality of some medicinal plants and their water extracts from southeast Serbia was determined on the basis of metal content using atomic absorption spectrometry. Two methods were used for the preparation of water extracts in order to examine the impact of the preparation on the content of metals in the samples. The contents of investigated metals in both water extracts were markedly lower than in medicinal plants, but were higher in the water extract prepared by method (I), with the exception of lead. The coefficients of extraction for the observed metal can be represented in the following order: Zn > Mn > Pb > Cu > Fe. Correlation coefficients between the metal concentration in the extract and total metal content in plant material varied in the range from 0.6369 to 0.9956. This indicates the need for plants to be collected and grown in unpolluted areas, and to examine the metal content. The content of heavy metals in the investigated medicinal plants and their water extracts is below the maximum allowable values, so they are safe to use.

Keywords: medicinal plants, water extracts, AAS.

Available online at the Journal website: http://www.ache.org.rs/HI/

PROFESSIONAL PAPER

UDC 615.89:633.88(497.11):543.42:54

Hem. Ind. **67** (4) 585–591 (2013)

doi: 10.2298/HEMIND120703098R

Beverages and extracts prepared from medicinal plants are commonly consumed in the world for their desirable aroma, taste and putative positive physiological functions. The growing interest in plant beverages all over the world would be connected with polyphenol antioxidative activity, fighting the harmful influence of environmentally generated free radicals [1]. Medicinal plants and their extracts containing many essential and nonessential elements provided from the soil were grown. The human body requires both metallic and non-metallic elements within certain permissible limits for growth and good health (Table 1) [2]. Many elements play a vital role in the metabolic processes and in the general well-being of humans, but some can be toxic.

Heavy metals such as copper (Cu) are essential to maintain metabolism of the human body, but at higher concentration they can lead to poisoning and can cause kidney and liver damage. Nickel (Ni) is also needed in small amounts to produce red blood cells, but at higher concentration it becomes mildly toxic. It can cause heart and liver damage. Cadmium (Cd) is associated with renal dysfunction and it may also produce bone defects such as osteoporosis. Beside copper (Cu), chromium (Cr) can be can accumulated in the kidney and liver and can cause severe damage to those systems. In addition, this metal can also damage the circulatory and nerve tissue. High levels of lead (Pb) may result in toxic biochemical effects in humans, which in turn cause problems in the synthesis of hemoglobin, effects on the kidneys, gastrointestinal tract, joints and reproductive system and acute or chronic damage to the nervous system and also can cause mental retardation. Owing to the importance of metals present in medicinal plants, many studies were carried out to determine their levels in medicinal plants and their extracts. The broadest view contents of the trace element in tea leaves, made tea and tea infusion was given in a review by Karak. The presence of trace elements in all analyzed tea samples surveyed in this review was within the safe limits towards human beings, but it appeared that it still provides a significant additional source of trace elements [3].

A number of herbs grown in southeastern Serbia are used in traditional medicine. Razić *et al.* in their works determined the metal content in the soil, herb and herbal drags. Elemental composition of soil, of different parts of plant of *Echinacea purpurea* (Asteracae) and ethanolic extract were determined by flame atomic absorption and flame atomic emission spectrometry. The trace element data were evaluated by multivariate methods, i.e. principal component analysis and hierarchical cluster analysis [4]. Similar analyses were carried out for many herbs from Serbia [5-8]. Determination of heavy metal concentrations in tea samples taken from Belgrade market (Serbia) were provided, too [9]. Trace metals in medicinal plants and their extracts were determined by Kostic *et al.* [10].

Correspondence: S.S. Randjelović, Department of Chemistry, Faculty of Science and Mathematics, University of Niš, Višegradska 33, 18000 Niš, Serbia.

E-mail: despotovicsasa@yahoo.com

Paper received: 3 July, 2012

Paper accepted: 15 October, 2012

Table 1. Recommended daily intakes of various minerals

Mineral	Recommended daily intake	Over dosage
Boron	< 20 mg	No information found
Calcium	1000 mg	Doses larger than 1500 mg may cause stomach problems for sensitive individuals
Chlorine	3400 mg (in chloride form)	No information found
Chromium	120 μg	Doses larger than 200 μg are toxic and may cause concentration problems and fainting
Copper	2 mg	As little as 10 mg of copper can have a toxic effect
Fluorine	3,5 mg	No information found
Iodine	150 μg	No information found
Iron	15 mg	Doses larger than 20 mg may cause stomach upset, constipation and blackened stools
Magnesium	350 mg	Doses larger than 400 mg may cause stomach problems and diarrhea
Manganese	5 mg	Excess manganese may hinder iron adsorption
Molybdenum	75 μg	Doses larger than 200 μg may cause kidney problems and copper deficiencies
Nickel	< 1 mg	Products containing nickel may cause skin rash in case of allergies
Phosphorus	1000 mg	Contradiction: the FDA states that doses larger than 250 mg may cause stomach problems for sensitive individuals
Potassium	3500 mg	Large doses may cause stomach upsets, intestinal problems or heart rhythm disorder
Selenium	35 μg	Doses larger than 200 μg can be toxic
Sodium	2400 mg	No information found
Vanadium	< 1,8 mg	No information found
Zinc	15 mg	Doses larger than 25 mg may cause anaemia and copper deficiency

Determination of trace elements in tea is important from two aspects: a) to judge their nutritional value and b) to guard against any possible ill-effects due to intake of heavy metals. The content of heavy metals is one of the criteria deciding on the acceptability of the herb material for the production of herbal beverages or the other traditional medicaments. Therefore, the control of heavy metals contents in herbs and herbal beverages is required [11,12].

In this work, heavy metal contents in the following plants and their teas: *Hipericum perforatum* L., *Saturea Montana* L., *Calendula officinalis* L., *Origanum vulgare* L., *Crataegus leavigata* L., and *Prunus spinosa* L were determined. These plants have been used in traditional Serbian medicine for the treatment of many diseases.

Hipericum perforatum L. (St. John's wort) is a plant from the Hypericaceae family. It has antidepressant, sedative and antibiotic effects [13].

Saturea montana L. (Winter savory) is a plant from the Lamiaceae family. It has an extremely strong antiseptic effect, and as such is used for the treatment of respiratory and digestive organs illnesses, and the inflammations of skin and mucosa [14].

Calendula officinalis L. (Marigold) is a plant from the Asteraceae family. It has antibacterial and bactericidal effects; therefore, it is used for the treatment of wounds, psoriasis, etc. [15]. *Origanum vulgare* L. (Oregano) is a plant from the Lamiaceae family. It has antispasmodic, bronchodilating, and diuretic effects [16].

Crataegus oxyacantha L. (Hawthorn) is a plant from the Rosaceae family. It is used for the treatment of arteriosclerosis, heart diseases, and mild nervous disorders [17].

Prunus spinosa L. (Blackthorn) is a plant from the Rosaceae family. It is used for the treatment of skin problems, to alleviate stomach colic, etc. [18].

EXPERIMENTAL

Reagents

All the reagents used were of analytical purity (Merck, Germany). The working solutions were prepared immediately before the analysis from the basic solution with 1000 mg/l concentration for all metals. For the preparation of standard solutions high purity Milli-Q water was used. The glassware and polyethylene containers used for analysis were washed with tap water, then soaked over the night in 6 M HNO_3 solution and rinsed several times with ultra-pure water to eliminate absorbance due to detergent.

Apparatus

Atomic absorption measurements were made using a Varian SpectraAA 10 with background correction and hollow cathode lamps. Air–acetylene flame was used

for determination of all the elements. The calibration interval, wavelength, slit, and detection level are given in Table 2.

Sample preparation

The plant material was collected in the flowering phase from the natural habitats of the plants *Hipericum perforatum* L., *Saturea Montana* L., *Calendula officinalis* L., *Origanum vulgare* L. and fruit of *Crataegus leavigata* L., i *Prunus spinosa* L, in the stage of full maturity, in the region of southeast Serbia in July 2010. The study area is located in the surroundings of the city of Nis, which has about 300,000 inhabitants and is the third-largest city in the country after Belgrade and Novi Sad. However, the industry in this area is poorly developed. Sample sites were selected in accordance with the methods used in the European moss monitoring project [19]. A minimum distance of 300 m to major roads and larger settlements was required, as well as a minimum distance of 100 m to minor roads and houses and a minimum distance of 5 m to forest roads. Plants were first washed with distilled water and then dried at a temperature of 105 °C for 24 h. The herbs materials were then homogenized.

Procedures

Mineralization. The standard procedure described by the Association of Official Analytical Chemists (AOAC) was followed for the preparation of the samples for the analysis of heavy metals [20]. Accurately weighed (1 g) sample was transferred into a silica crucible and kept in a muffle furnace for ashing at 450 °C for 3 h and then 5 ml of 6 M HCl was added to the crucible. Care was taken to ensure that all the ash came into contact with acid. Further, the crucible containing acid solution was kept on a hot plate and digested to obtain a clean solution. The final residue was dissolved in 0.1 M HNO_3 solution and made up to 25 ml. Working standard solutions were prepared by diluting the stock solution with 0.1 M nitric acid for checking the linearity.

Preparation of water extracts. The two methods commonly used for preparation of water extracts were applied for this study, in order to assess the actual amount of heavy metal reach human body trough drinking such beverages.

Method I

Brew. In this method, 2 g of herb was boiled with 100 ml of destiled water for 5 min. The mixture was held for 5 min at room temperature and then filtered. After that, 2.5 ml HCl:H_2O (1:1) and 2.5 ml HNO_3:H_2O (1:1) were added. The thus obtained solution was used for the analysis of heavy metals.

Method II

*Infusio*n. In this method, 100 ml of hot destilled water was added to 2 g of herb. The mixture was left to cool at room temperature for 5 min and then filtered to obtain a clear solution for futher procesing.

Statistical analysis

The data were reported as mean ± standard deviation (SD) for triplicate determinations. Significance of inter-group differences was determined by the analysis of variance (ANOVA). A p value of less than 0.05 was considered statistically significant.

RESULTS AND DISCUSION

Contents of metals in medicinal plants are shown in Table 3. Metals are accumulated from the soil on which the plants were grown, especially Fe, followed by Mn, Zn, and Cu.

The iron concentration in the investigated plant samples was the highest and ranged from 65.3 to 490.6 mg/kg. The contents of zinc, manganese, and copper in herbs varied from 11.8 to 32.3 mg/kg for zinc, from 6.00 to 46.64 mg/kg for manganese, and from 13.0 to 46.5 mg/kg for copper. The contents of non-essential heavy metals, Pb, Ni and Cd was exceptionally low in herbs, decreasing in the following order: Pb (7.8–0.1 mg/kg) > Ni (2.0–4.0 mg/kg) > Cd (0.6–1.8 mg/kg).

The Cd and Ni concentration in water extracts prepared by methods I and II was too low to be detected by AAS. Lead concentrations in investigated water extract were very low and amounted from 2.3 to 6.1 mg/kg (method I), and from 3.0 to 8.4 mg/kg (method II). On the other hand, the contents of essential metals (Fe, Mn, Zn and Cu) in the investigated water extracts were relatively high.

Concentration of Fe in beverages prepared according to method I was from 11.1 to 42.1 mg/kg, and in

Table 2. Analytical characteristics of the AAS determination

Element	Working range, mg/l	*LOD* / mg l^{-1}	Wavelength, nm	Slit	Correlation coefficient
Fe	0.00-10.00	0.015	248.3	0.2	0.9987
Cu	0.00-1.00	0.007	213.9	1.0	0.9999
Zn	0.00-5.00	0.021	324.8	0.5	0.9990
Pb	0.00-1.00	0.002	217.0	1.0	0.9993
Cd	0.00-1.00	0.003	228.8	0.5	0.9991
Mn	0.00-2.00	0.005	279.5	0.2	0.9987
Ni	0.00-1.00	0.002	232.0	0.2	0.9994

Table 3. Concentration of metals (mg/kg dry mass, mean of three values) in medicinal plants and their water extracts

Plant		Zn	Mn	Fe	Pb	Ni	Cu	Cd
Hipericum perforatum L.	Plant	32.2±0.6	33.3±1.0	65.3±2.0	7.8±0.2	3.0±0.1	21.8±0.4	0.8±0.1
	Method I	28.0±0.6	15.2±0.5	13.0±0.4	2.6±0.1	–	5.1±0.1	–
	Method II	26.2±0.5	12.0±0.4	10.1±0.3	3.1±0.1	–	3.1±0.1	–
Saturea Montana L.	Plant	31.0±0.6	28.3±0.9	156.8±4.7	16.6±0.3	2.5±0.1	28.8±0.6	1.8±0.1
	Method I	25.2±0.5	11.2±0.3	17.6±0.5	3.8±0.1	–	1.1±0.1	–
	Method II	18.1±0.4	7.1±0.2	12.4±0.4	4.4±0.1	–	0.9±0.1	–
Calendula officinalis L.	Plant	31.5±0.6	33.3±1.0	490.6±14.7	9.8±0.2	4.0±0.1	46.5±0.9	0.8±0.1
	Method I	28.0±0.6	14.0±0.4	42.0±1.3	3.1±0.1	–	10.1±0.2	–
	Method II	21.1±0.4	12.4±0.4	25.2±0.6	3.1±0.1	–	9.0±0.2	–
Origanum vulgare L.	Plant	17.1±0.3	46.6±1.4	93.7±2.9	20.1±0.4	2.0±0.1	23.1±0.5	0.6±0.1
	Method I	12.1±0.2	27.5±0.8	11.1±0.3	6.1±0.1	–	3.1±0.1	–
	Method II	8.0±0.12	24.1±0.7	8.9±0.3	8.4±0.2	–	2.6±0.1	–
Crataegus leavigata L.	Plant	11.8±0.2	6.0±0.2	119.4±3.6	8.3±0.2	2.4±0.1	13.2±0.3	0.8±0.1
	Method I	8.2±0.2	3.0±1.0	28.1±0.8	2.5±0.1	–	3.0±0.1	–
	Method II	5.04±0.1	2.5±0.1	25.6±0.8	3.0±0.1	–	2.9±0.1	–
Prunus spinosa L.	Plant	14.5±0.3	9.5±0.3	130.8±3.9	8.8±0.2	3.2±0.1	13.0±0.3	0.8±0.1
	Method I	9.5±0.2	4.6±0.1	15.4±0.5	2.3±0.1	–	2.6±0.1	–
	Method II	6.9±0.1	3.9±0.1	14.0±0.4	3.0±0.1	–	2.1±0.1	–

those prepared according to method II from 8.95 to 25.60 mg/kg. Zinc concentration varied in the range from 8.15 to 28.02 mg/kg (method I), and from 5.05 to 26.15 mg/kg (method II).

Manganese concentration was from 3.0 to 27.5 mg/kg (method I), while for method II it amounted from 2.5 to 24.1 mg/kg. In herbal extracts, copper had the lowest content, and varied from 2.6 to 10.1 mg/kg (method I), and from 2.0 to 9.0 mg/kg (method II).

The contents of heavy metals in water extracts prepared by method I and method II decreased in the following order: Fe > Zn > Mn > Cu > Pb. Metal concentrations in beverages prepared by method I were slightly higher. Only the concentration of Pb was higher in beverages prepared by method II.

The heavy metals concentrations in water extracts prepared by medicinal plants are affected by numerous factors, such as: organic matter contained in individual herbs that can chelate heavy metals, solubility of mineral and organic matter in water, minerals content and pH value of the water used for the preparation of extracts. In order to avoid the influence of water quality on the heavy metals concentration in the extracts, demineralized water was used for their preparation.

The extraction coefficient of the investigated metals was calculated as the relation between the metal concentration in the herbal beverages and the total metal content in the herb.

As seen in Table 4, the extraction coefficients vary in the range from 3.27 to 88.86%. Based on the

Table 4. Extraction coefficients (%) of metals

Plant	Water extracts	Zn	Mn	Fe	Pb	Cu
Hipericum perforatum L.	Method I	86.90	47.74	19.98	33.55	23.22
	Method II	81.05	36.12	15.51	40.13	14.34
Saturea Montana L.	Method I	81.31	39.40	11.25	23.02	3.83
	Method II	58.42	24.98	7.90	26.59	3.27
Calendula officinalis L.	Method I	88.86	42.19	8.57	31.69	21.63
	Method II	66.86	37.29	5.14	31.79	19.39
Origanum vulgare L.	Method I	70.70	59.00	11.43	30.54	13.43
	Method II	46.78	51.73	9.26	56.90	11.09
Crataegus leavigata L.	Method I	69.36	50.17	23.53	33.94	22.64
	Method II	42.89	41.67	21.44	36.36	21.58
Prunus spinosa L.	Method I	61.95	48.32	11.81	25.83	19.85
	Method II	47.38	40.97	10.68	34.17	15.69

obtained results of the extraction coefficient, the analyzed elements can be classified into three groups: those with a low extraction coefficient (less than 20%) – Fe and Cu; elements with a medium extraction coefficient (20–60%) – Pb and Mn, and elements with the extraction coefficient higher than 60% – Zn. The extraction coefficients of the investigated metals can be presented in the declining order: Fe > Zn > Mn > Cu > Pb.

The data from Table 3 indicate a great transfer of metals, which is higher in herbal beverages prepared with method I (Pb being the only exception in this case). The obtained results are in accordance with those obtained by Abou-Arab *et al.* [13].

Correlation coefficients of heavy metals content in medicinal plants and their water extracts were also determined. The correlation coefficients of heavy metals contents in plants and their extracts (given in Table 4) were calculated using the following equation [14]:

$$R = \frac{\sum_i (x_i - \overline{x})(y_i - \overline{y})}{\sqrt{\sum_i (x_i - \overline{x})^2 \sum_i (y_i - \overline{y})^2}} \quad (1)$$

The values of correlation coefficients existed between the metals content (mean value of three measurements) in medicinal plants and their water extracts prepared by method I were: Fe (0.8853), Zn (0.9956), Mn (0.9586), and Pb (0.8680) and Cu (0.7924).

A significant correlation also existed between the metals content in medicinal plants and their water extracts prepared by method II, amounting to: Zn (0.9650), Mn (0.9255), Pb (0.9384), Fe (0.6370) and Cu (0.7693) (Table 5).

Table 5. Correlation coefficients between the concentrations of metals in medicinal plants and their water extracts

Method	Metal				
	Zn	Mn	Fe	Pb	Cu
I	0.9956	0.9586	0.8853	0.8680	0.7924
II	0.9650	0.9255	0.6370	0.9384	0.7693

A number of authors from various countries have determined the content of heavy metals in different plants and their extracts.

Table 6 shows the survey of metals contents in various plants from various regions. A conclusion can be drawn that there are significant differences in the heavy metals contents in the investigated plants, which can be a consequence of different soil quality on which the plants had been grown, having in mind the geographical distances between the regions on one hand, and on the other hand, the ability of the plants species themselves to accumulate the individual heavy metals. It is well known that some plants have an extraordinary ability to accumulate heavy metals and are used for bioremediation of the soil.

When the results of heavy metals contents in the investigated extracts are compared with those of other authors, the accordance level is slightly lower regarding the absolute heavy metals concentration, while the accordance is higher with respect to extraction coefficients.

Based on the data on heavy metals contents in plant extracts from various regions (Table 7), one can recognize that the results are very much congruent with the exception of Thailand, where the extracts have very high values for Mn, and Egypt with very high values for Zn and Mn. These can be a consequence of the geochemical composition of the soil where the plants have been grown, causing a high content of these metals in the plant materials and, consequently, in their water extracts. The accordance is significantly higher with respect to the extraction coefficient and coefficient of correlation between the heavy metals content in medicinal plants and their water extracts.

A comparative study of the results of heavy metals content in medicinal plants and their water extracts (Table 3) with recommended daily intake of elements for an adult person (Table 1) we can see that herbal teas can represent a good source of essential elements. However, their use should be under strict control because of possible presence of toxic elements, such as

Table 6. Comparison of metal contents (mg/kg dry mass) of Serbian medicinal plants with other plants from different areas

State	Zn	Mn	Fe	Pb	Ni	Cu	Cd	Reference
Serbia	11.75–32.25	6.00–46.61	65.25–490.62	7.75–20.07	1.97–3.95	13.0–46.5	0.62–1.75	Present study
Serbia	31–34	106–111	–	4.5–5.5	27–58	19–22	0.5–0.75	[24]
Serbia	15.0–43.0	25.0–111.0	75.0–546	–	–	5.92–14.79	–	[5]
Pakistan	55.3–70	24.6–28.9	125.2–151.1	–	–	12.2–14.3	–	[23]
Pakistan	17.38–65.85	34.14–105.56	181.63–6796.88	3.15–10.63	2.6–15.8	7.06–19.19	0.59–1.66	[25]
India	–	–	–	0.48–1.03	1.1–5.3	15.9–32.2	0.05–0.38	[18]
Iran	–	–	–	2.08–2.59	–	17.59–32.8	–	[27]
Egypt	8–68.8	9.8–289	26.96–1046	0.5–14.4	0.61–2.85	1.8–11.4	1.06–2.44	[21]
Turkey	21.9–48.4	23–244	224.8–810	0.26–4.80	0.90–5.4	3.92–35.8	0.004–0.44	[11]
Ethiopia	20.2–21.6	1242–1421	319–467	—	–	9.1–11.5	–	[1]

Table 7. Comparison of metal contents (mg/kg d.w.) in extracts prepared from Serbian medicinal plants and plant extracts from different areas

Area	Zn	Mn	Fe	Pb	Cu	Reference
Serbia	8.15–28.2	3.01–27.05	11.05–42.05	0.37–4.67	2.58–10.6	This paper
Thailand	1.37–29.77	4.79–370.85	2.22–29.77	–	12.2–14.3	[12]
Turkey	3.9–18.0	–	2.45–107.4	–	2.45–8.10	[11]
Egypt (spice and medicinal plants)	30.56–112.45	130.77–220	30.56–122.45	—	3.34–20.12	[28]
Egypt (tea)	5.5–48.25	–	–	0.37–4.65	1.05–9.15	[21]
Iran	–	–	–	–	1.15–1.65	[27]

Pb and Cd. Nevertheless, values given in Table 3 are the concentrations of elements in plants and water extracts given for 1 kg of any medicinal herb per day. Having in mind that the medicinal herbs are packed in bags containing averagely 2 g of plant material, that means that only 10 g of any plant is used if the herbal tea is consumed five times per day. Consequently, there is no danger from toxic elements originating from the herbal tea.

CONCLUSION

Metal contents in medicinal plants from the region of southeast Serbia (*Hypericum perforatum* L., *Saturea montana* L., *Calendula officinalis* L., *Origanum vulgare* L., *Crataegus laevigata* L., and *Prunus spinosa* L.) and water extracts prepared from them by two methods were investigated by AAS. In medicinal plants founded the presence of the following metals : Fe, Zn, Mn, Cu, Pb, Cd and Ni, and their concentration was determined The contents of metals in the herbal beverages, regardless of the preparation method, were significantly lower than their concentration in the herbs and decreased in this order: Fe > Zn > Mn > Cu > Pb. The contents of Ni and Cd were below the detection limit and were not possible to determine by the AAS method. It was found that the extract preparation method had an effect on the heavy metals content. Contents of investigated metals in both water extracts were markedly lower then in medicinal plants, but higher in water extract prepared by method (I), with exception of lead content. Accordingly, the extraction coefficients varied in the range from 0.0 to 88.86%.

Correlation analysis by ANOVA statistical program proved that there is great transfer of metals from the herbs into the herbal beverages. The correlation coefficients of heavy metals contents in the herbs and their beverages are very high and amount from 0.6369 to 0.9956.

The results represent a significant contribution to the study of metal content in medicinal plants, transferring them to the water extracts and the potential effect on human health as a result of their consumption. The investigated medicinal plants and their water extracts can be safely used in food, in terms of metal content.

Acknowledgements

This work was supported under the projects No.OI 172047 by the Ministry of Education, Science and Technological Development of the Republic of Serbia.

REFERENCES

[1] D. W. Gebretsadik, B. S. Chandravanshi, Levels of metals in commercially available Ethiopian black teas and their infusion, Bull.Chem.Soc.Ethiop. **24** (3) (2010), 339–349.

[2] Lenntech B.V, http://www.lenntech.com/recommended-daily-intake.htm#ixzz27P3CVWjr (accessed on 3.9.2013).

[3] T. Karak, R.M. Bhagat, Trace elements in tea leaves, made tea and tea infusion: A Review, Food Res. Int. **43** (2010) 2234–2252.

[4] S. Ražić, A. Onja, B. Potkonjak, Trace elements analysis of Echinacea purpurea – herbal medicinal, J. Pharmaceut. Biomed. **33** (2003) 845–850.

[5] S. Ražić, A. Onja, S. Đogo, L. Slavković, A. Popović, Determination of metal content in some herbal drugs—Empirical and chemometric approach, Talanta **67** (2005) 233–239.

[6] S. Ražić, A. Onjia, S. Đogo, L. Slavković, Inorganic analysis of herbal drugs. Part I. Metal determination in herbal drugs originating from medicinal plants of the family *Lamiacae,* J.Serb.Chem.Soc. **70**(11) (2005) 1347–1355.

[7] S. Ražić, S. Đogo, L. Slavković, Multivariate characterization of herbal drugs and rhizosphere soil samples according to their metallic content, Microchem. J. **84**(1–2) (2006) 93–101.

[8] S. Ražić, S. Đogo, L. Slavković, Inorganic analysis of herbal drugs. Part II. Plant and soil analysis – diverse bioavailability and uptake of essential and toxic elements, J. Serb. Chem. Soc. **71**(10) (2006) 1095–1105.

[9] A.Perić-Grujić, V. Pocajt, M. Ristić, Determination Of Heavy Metal Concentrations In Tea Samples Taken From Belgrade Market, Serbia, Hem. Ind. **63** (2009) 433–436.

[10] D. Kostic, S. Mitic, A. Zarubica, M.Mitic, J. Velickovic, S. Randjelovic, Determination of trace metals in medicinal plants and their extracts, Hem. Ind. **65** (2) (2010) 165––170.

[11] S. Basgel, S. B. Erdemoglu, Determination of mineral and trace elements in some medicinal herbs and their

infusions consumed in Turkey, Sci. Total Environ. **359** (2006) 82–89.

[12] S. Nookabkaew, N. Rangkadilok, J. Satayavivad, Determination of Trace Elements in Herbal Tea Products and Their Infusions Consumed in Thailand, J. Agric. Food Chem. **54** (2006) 6939–6944.

[13] S. Kasper, *Hypericum perforatum* – a review of clinical studies. Pharmacopsychiatry **34** (2001) 51–55.

[14] V. Slavkovska, R. Jancic, S. Bojovic, S. Milosavljevic, D. Djokovic, Variability of essential oils of *Satureja montana* L. and *Satureja kitaibelii* wierzb. Ex Heuff. from the central part of the Balkan peninsula. Phytochemistry **57** (2001) 71–76.

[15] A. Raal, K. Kirsipuu, Total flavonoid content in varieties of *Calendula officinalis* L. originating from different countries and cultivated in Estonia, Nat. Prod. Res. **25** (2011) 658–662.

[16] B. M. Lawrence, The botanical and chemical aspects of oregano, Perfum. Flavor **9** (1984) 41–52.

[17] World Health Organization (WHO). Monographs on selected medicinal plants, *Folium cum Flore Crataegi*, Vol. 2, World Health Organization (WHO), Geneva, 2002, p. 66.

[18] K. Browics, *Prunus*, In: Davis P.H. (ed.), Flora of Turkey and East Eagean Islands. Vol 4. University Press, Edinburgh, 1972, pp. 8–12.

[19] H. G. Zechmeister, D. Hohenwallner, A. Riss, A. Hanus-Illnar, Variations in heavy metal concentrations in the moss species *Abietinella abietina* (Hedw.) Fleisch. According to sampling time, within site variability and increase in biomass, Sci. Total. Environ. **301** (2003) 55––65.

[20] A.O.A.C. 2000, Official Methods of Analysis, Association of Official Analytical Chemist, EUA.

[21] A.K. Abou-Arab, M.A. Abou Donia, Heavy metals in Egyptian spicies and medicinal plants and the effect of processing on their levels, J. Agric. Food Chem **48** (2000) 2300–2304.

[22] Stats Tutorial, University of Toronto, http:// //www.chem.utoronto.ca/coursenotes/analsci/StatsTutorial/CorrCoeff.html (Accessed on 3.9.2013).

[23] J. Pirzada, W. Shaikh, K.U. Ghani,. K.A. Laghari, Study of anti fungal activity and some basic elements of medicinal plant *cressa cretica* linn against fungi causing skin diseases, Sindh Univ. Res. Jour. (Sci. Ser.). **41**(2) (2009) 15–20.

[24] D. Radanović, S. Antić Mladenović, M. Jakovljević, M. Kresović, Content of heavy metals in Gentiana lutea L. roots and galenic forms, J. Serb. Chem. Soc. **72**(2) (2007) 133–138.

[25] S. Jabeen, M. Tahir Shah, S. Khan, M. Qasim Hayat, Determination of major and trace elements in ten important folk therapeutic plants of Haripur basin, Pakistan, J. Med. Plants Res. **4**(7) (2010) 559–566.

[26] S. Seenivasan, N. Manikandan, N. N. Muraleedharan, R. Selvasundaram, Heavy metal content of black teas from south India, Food control. **19** (2008) 746–749.

[27] G. Karimi, M.K. Hasanzadeh, A. Nili, Z. Khashayarmanesh, Z. Samiei, F. Nazari, M. Teimuri, Concentrations and Health risk of heavy metals in tea samples marketed in Iran, Pharmacology **3** (2008) 164–174.

[28] Y.F. Lasheen, N.S. Awwad, A. El-Khalafawy, A.A. Abdel-Rassoul, Annual effective dose and concentration levels of heavy metals in different types of tea in Egypt, Int. J. of Phys. Sci. **3** (2008) 112–119.

IZVOD

KORELACIONA ANALIZA SADRŽAJA METALA U LEKOVITIM BILJKAMA I NJIHOVIM VODENIM EKSTRAKTIMA

Sasa S. Ranđelović, Danijela A. Kostić, Aleksandra R. Zarubica, Snežana S. Mitić, Milan N. Mitić

Univerzitet u Nišu, Prirodno–matematički fakultet, Department za hemiju, Višegradska 33, 18000 Niš, Srbija

(Stručni rad)

Kvalitet biljaka i njihovih vodenih ekstrakata sa područja Jugoistočne Srbije odredjen je na osnovu sadržaja metala korišćenjem atomske absorpcione spektrometrije. Korišćene su dve metode za pripremu vodenih ekstrakata, kako bi se ispitao uticaj pripreme na sadržaj metala u njima. U vodenim ekstraktima sadržaj metala je niži od sadržaja u biljkama, ali u vodenom ekstraktu pripremljenom sa toplom vodom (metod I) koncentracije metala su veće, sa izuzetkom sadržaja olova. Ekstrakcioni koeficijenti posmatranih teški metala mogu biti predstavljni sledećim redosledom: Zn > Mn > Pb > Cu > Fe. Korelacionom analizom su utvrđeni korelacioni koeficijenti između koncentracije teških metala u biljkama i njihovim ekstraktima i kreću se u granicama od 0,6369 do 0,9956. S obzirom na to neophodno je da se lekovito bilje gaji i bere na nezagadjenom području, i da se ispituje sadržaj metala. Sadržaj metala u ispitivanim biljkama i njihovim vodenim ekstraktima je ispod maksimalno dozvoljene vrednosti, tako da su bezbedni za korišćenje.

Ključne reči: Lekovito bilje • Vodeni ekstrakti • AAS

Environmental cadmium and zinc concentrations in liver and kidney of european hare from different serbian regions

Zoran I. Petrović[1], Vlado B. Teodorović[2], Mirjana R. Dimitrijević[2], Sunčica Z. Borozan[3], Miloš T. Beuković[4], Dragica M. Nikolić[1], Aurelija T. Spirić[1]

[1]*Institute of Meat Hygiene and Technology, Kacanskog 13, Belgrade, Serbia*
[2]*University of Belgrade, Faculty of Veterinary Medicine, Department of Food Hygiene and Technology, Belgrade, Serbia*
[3]*University of Belgrade, Faculty of Veterinary Medicine, Department for Chemistry, Belgrade, Serbia*
[4]*University of Novi Sad, Faculty of Agriculture, Department of Animal Husbandry, Novi Sad, Serbia*

Abstract

The assayed hares (n = 84) were divided into five age groups: 3–6, 12, 12–24, 24–36 and 36+ months. Between all sampling regions (11) significant differences of Cd levels were found in kidney and liver (p values of 0.001 and 0.007, respectively). Significant statistical differences (p = 0.001) are registered between Cd content in the kidney and liver of hares among all represented age groups. Looking at all investigated hare samples, moderately higher concentrations of Zn were found in the liver (median value: 25.4 mg/kg w.w.) compared to those in the kidney (21.4 mg/kg). These differences were statistically significant (p = 0.001). Zinc concentrations in the liver, between all age groups, did not differ significantly (p = 0.512) but in the kidney these differences were statistically significant (p = = 0.001). Significant differences between Zn concentrations in liver in comparison to kidney (pairwise differences) were found within every single age group with the exception of the oldest (36+). Strong statistically significant correlations *(Ps* – Pearson's correlation) between Cd concentrations in kidney and liver were registered in three groups older than 12 months (*Ps* = 0.81, p = 0.001; *Ps* = 0.78, p = 0.001 and *Ps* = 0.79, p = 0.001, respectively). Negative correlation between Zn and Cd concentrations were found in liver samples within the age group of 12 months (*Ps* = –0.67, p = 0.004).

Keywords: cadmium, zinc, kidney, liver, hare.

Available online at the Journal website: http://www.ache.org.rs/HI/

PROFESSIONAL PAPER

UDC 504.5:546.48]:639.112

Hem. Ind. **67** (4) 593–599 (2013)

doi: 10.2298/HEMIND120815100P

One of the major mechanisms of metal input to plants and soils is atmospheric deposition (for example in the forest ecosystems) while anthropogenic sources include agriculture (fertilizers, animal manures, pesticides), metallurgy (mining, smelting and metal finishing), energy production (power plants) and sewage sludge and scrap disposal [1]. Agricultural intensification results in increased mechanization and agro-chemical use, and changes in habitats such as a reduction in diversity [2]. Phosphate fertilizers are known to contain varying levels of heavy metals such as cadmium, lead, nickel and chromium [3]. Cadmium (Cd) and zinc (Zn) are elements that have similar geochemical and environmental properties [4,5]. The chemically and physically similar but essential element zinc (Zn) is also strongly enriched in precipitation over different areas [6]. The co-occurrence of these two metals in the natural environment and their possible interactions in biological systems are therefore of particular interest.

Toxicity in wildlife from metals exposures is generally poorly understood and is rarely quantified in field settings. Animal tissue levels can provide important data regarding the fate and bioavailability of heavy metals within natural ecosystems [7–9]. In general, the gastrointestinal tract and the liver regulate the uptake and transfer of Zn. Interactions between essential and non-essential metals are very common (*e.g.*, Cd uptake can mimic that of Zn).

The objectives of this study were to evaluate the environmental Cd and Zn concentrations in European hare from different Serbian regions. The tissue samples acquired bring up a concept of using hares as promising Cd and Zn biomonitors as well as to investigate how the different age distribution within hare population affects comparison between Cd and Zn levels among sampling regions and age groups. The present study was also projected to estimate bioaccumulation trends of Cd and Zn during the lifetime of European hares and interactions between Cd and Zn in hare organs if any exists and try to model the dependency of liver Cd and Zn concentrations.

Correspondence: Z. Petrović, Institute of Meat Hygiene and Technology, Kacanskog 13, 11000 Belgrade, Serbia.
E-mail: zoran@inmesbgd.com
Paper received: 15 August, 2012
Paper accepted: 15 October, 2012

EXPERIMENTAL

Materials and methods

A total of 168 tissue samples (84 kidneys and 84 livers) obtained from all hunted free-range hares (*Lepus europaeus*) were investigated for Cd and Zn presence. The hares were acquired from eleven regions of western, central and southern parts of Serbia during regular hunting season 2010/2011. The geographical locations from which samples had been collected are shown in Figure 1.

The eye samples were used for estimating the age of the hares. The weight of the eye lens increases because of insoluble proteins that accumulate in it and this process correlates with the animal's age. After extraction, eye samples were placed in marked plastic bags with zipper open/close system, and immediately transported to the laboratory. The eye lenses were fixed in 5% formalin for 72 h and then dried at 37 °C for 96 h, under normal pressure. After they were dried, the lenses were weighed on a precise analytical scale (Mettler AE 200) to 1 mg precision. For further data analysis, the hares were sub-divided according to their age into five groups: 3–6 months old (100–200 mg), 12 months old (200–280 mg), 12–24 months old (280–310 mg); 24–36 months old (310–370 mg) and older than 36 months (≥ 370 mg).

The whole liver and kidney were sampled from each animal. The liver and kidney samples were stored at –20 °C until analysis. After homogenization, tissue samples (1 g) were digested with 8 ml of HNO_3 (65% v/v, analytical grade, JT Baker, Center Valley, USA) and 2 ml of H_2O_2 (30%, analytical grade, Kemika, Zagreb, Croatia) using the method of acid microwave digestion. The samples were digested in a microwave digestion unit (Milestone TC, EVISA, EU) with temperature control. The digestion program began at a potency of 1000 W, then it was ramped for 10 min to 200 °C, after which the samples were held at 1000 W and a temperature of 180 °C for 20 min. Calibration standards were prepared from commercial solutions in HNO_3 (0.2%) with 1.000 mg/l of each element (JT Baker, Center Valley, PA, USA). All results are expressed on wet weight basis (w/w).

Cadmium concentrations were determined by the AAS graphite furnace technique at 228.8 nm using a Varian SpectrAA 220 atomic absorption spectrophotometer, equipped with a Varian GTA 110 furnace with constant temperature zone. Zinc concentrations were measured by flame atomic absorption spectrophotometry (FAAS) at 213.9 nm with deuterium background correction. The maximum allowable relative standard deviation between three replicates was set to 5%. The trueness of the method was tested with standard reference material – pig kidney (BCR No.186) from the Community Bureau of Reference and recoveries. Cd in standard reference material deviated at most by ±10% from the certified mean values, whereas Zn deviated at

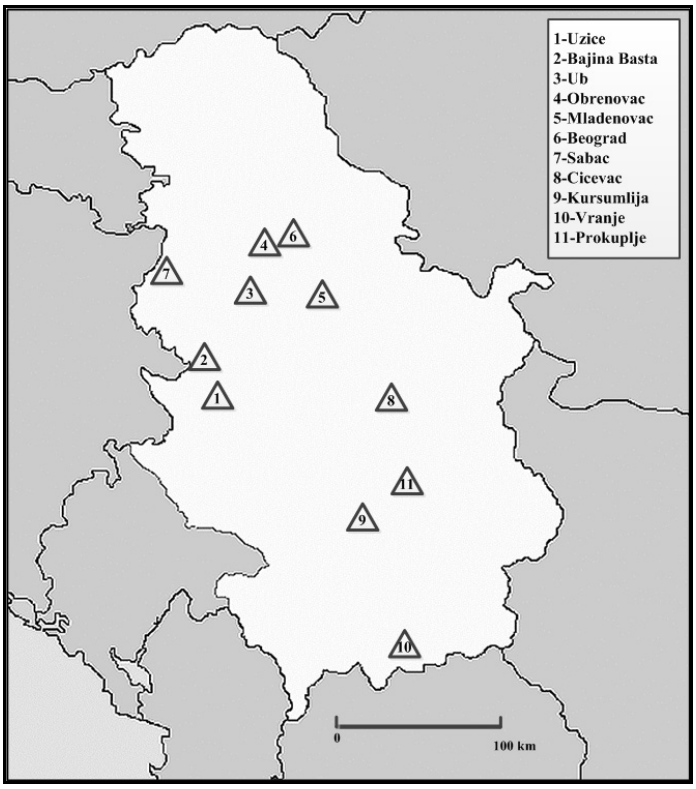

Figure 1. Map of sampling regions.

most by +8%. The recovery of Cd and Zn was determined by adding a known amount of a particular standard solution into the samples. Recoveries of added Cd and Zn standards in the analyses were controlled in randomly selected samples, and fell within the range of 95–102%. The detection limits for Cd and Zn were 0.005 and 0.2 mg/kg, respectively.

Data analysis

Statistical analysis was performed using the MINITAB software package, version 16.0. Concentrations were expressed as median values and range of minimum to maximum. The Kruskal-Wallis test and the post-hoc Man-Whitney non parametric test were used to examine statistical differences of heavy metal concentrations among groups. The Wilcoxon signed rank test was used to examine differences between Cd and Zn concentrations in kidney and liver within age groups. The significance of correlations between Cd and Zn levels were calculated using Pearson's correlation (*Ps*). The differences were considered statistically significant when the *p* value was less than 0.05.

RESULTS AND DISCUSSION

Accumulation of toxic and essential elements in hare organs has been studied by a number of authors [10–15]. Considering values obtained by sampling regions (Table 1) we noticed that the median values, of both the metals, are probably affected by random individual variations, age structure of collected animals and the sample size from the particular sampling region.

The concentrations of Cd and Zn in brown hare organs in relation to sampling regions are listed in Table 1.

Looking at all sampling regions (Figure 1) significant differences of median values were noted in Cd levels in kidney and liver (p = 0.001 and p = 0.007, respectively). Significant statistical differences (p=0.001) were registered between Cd content in the kidney and in the liver (p = 0.001) of hares among all represented age groups. Age trends of Cd and Zn concentrations in various organs of European hare are shown in Table 2.

For Zn, within the investigated hare samples (n = 84), higher concentrations (expressed as median values) were found in liver (25.4 mg/kg w.w.) and slightly lower Zn concentrations (21.4 mg/kg w.w.) were found in kidney samples. These differences were statistically significant (p = 0.001).

Based on non-parametric analysis between sampling localities, we found significant differences of Zn concentrations in the kidney (p = 0.001) while in the liver these differences were not statistically siginificant (p = 0.155). Zinc concentrations in the liver, between all

Table 1. Metal concentrations (mg/kg w.w.) in kidney and liver of hares from different Serbian sampling regions (n=84)

Region	*n*		Cd		Zn	
			Kidney	Liver	Kidney	Liver
1-Uzice	10	Median	1.65	0.13	23.2	25.8
		Range	0.27–3.10	0.06–0.17	20.5–30.8	21.3–31.7
2-Bajina Basta	6	Median	1.85	0.11	21.8	25.0
		Range	0.38–7.54	0.01–0.85	19.3–31.5	18.6–26.4
3-Ub	10	Median	1.96	0.12	24.0	25.6
		Range	0.64–4.97	0.05–0.45	17.8–37.0	17.3–33.5
4-Obrenovac	6	Median	3.15	0.26	22.6	25.5
		Range	0.18–5.12	0.05–0.32	17.8–25.7	22.5–32.7
5-Mladenovac	10	Median	1.33	0.11	18.2	24.7
		Range	0.15–2.97	0.02–0.33	14.1–24.2	18.7–28.0
6-Beograd	7	Median	1.63	0.24	21.3	21.8
		Range	0.49–5.36	0.08–0.32	18.0–22.2	15.5–26.9
7-Sabac	9	Median	2.05	0.14	16.8	20.9
		Range	0.66–5.30	0.04–0.35	16.0–26.6	17.8–32.2
8-Cicevac	7	Median	2.39	0.25	22.2	24.8
		Range	1.83–3.10	0.17–0.29	19.6–23.8	22.0–28.8
9-Kursumlija	6	Median	0.96	0.04	16.4	26.6
		Range	0.16–2.00	0.01–0.14	13.9–21.6	23.6–27.7
10-Vranje	6	Median	3.73	0.28	22.4	29.0
		Range	0.53–5.10	0.08–0.70	17.9–22.9	19.5–33.5
11-Prokuplje	7	Median	0.32	0.07	18.3	25.4
		Range	0.09–0.95	0.02–0.23	12.6–20.4	22.9–31.1

Table 2. Cd and Zn content (mg/kg w.w.) in kidney and liver by age groups

Age, months	*n*		Cd		Zn	
			Kidney	Liver	Kidney	Liver
3–6	11	Median	0.32	0.05	17.2	24.6
		Range	0.15–0.71	0.01–0.24	12.6–30.8	17.8–31.1
12	16	Median	0.93	0.09	19.8	25.1
		Range	0.21–2.21	0.02–0.31	16.0–24.7	15.9–27.1
12–24	17	Median	1.78	0.14	22.1	25.7
		Range	0.71–2.97	0.09–0.33	15.6–26.8	18.6–31.7
24–36	28	Median	2.8	0.26	22.2	24.9
		Range	1.83–4.97	0.07–0.70	16.2–24.8	15.5–33.5
36+	12	Median	4.91	0.32	23.7	25.8
		Range	3.08–7.84	0.17–0.85	16.8–37.1	21.8–32.1

age groups, did not differ significantly (p = 0.512) but in the kidney these differences were statistically significant (p = 0.001).

Pairwise differences between Zn concentrations in liver and kidney within every single age group are given in Table 3.

*Table 3. Pairwise differences of Zn content in liver and kidney within age groups; * – statistically significant differences ($p < 0.05$)*

Age, months	*p* Value
3–6	0.001*****
12	0.002*****
12–24	0.015*****
24–36	0.002*****
36+	0.926

The significant correlation between Cd and Zn concentrations in the kidney (CdK-ZnK) within the investigated hare samples and in different tissue samples are presented in Table 4.

Strong statistically significant correlations between Cd concentrations in kidney and liver were found in three groups older than 12 months. Negative correlation ZnL-CdL was found in the liver within the age group of 12 months.

However, changes in the slope constant Zn/Cd for the liver samples, sorted by age, may reflect environmental Cd exposure during the individual development of European hares (Figure 2).

Looking at the slope constants Zn/Cd among age groups presented in Figure 2, in a form of linear regression equation $Y_{ZnL} = kX_{CdL} + b$ (ZnL – zinc concentration in liver; CdL – cadmium concentration in liver; b – intercept value with *Y* axis), we registered a sharp decline of the regression line (k = –30.1) in age group of 12 months. This trend is also supported by taking into account the strong negative correlation found within this age group. It seems that Cd amplifies Zn deficiency in yearlings but also reduces or delays toxic effects of Cd at presented levels. The significant correlations of Cd concentration in different tissue (CdK-CdL) are registered in age groups older than 12 months (12–24 months: Ps = 0.81, p = 0.01; 24–36 months: Ps = 0.78, p = 0.001; ≥36 months: Ps = 0.79, p = 0.004). These correlations were not registered in age groups 3–6 and 12 months (Ps = 0.142; p = 0.552 and Ps = 0.06; p = = 0.826, respectively). Further, the slope constants Zn/Cd given in Figure 2 arise in subsequent age groups in order: -5.33, –1.6 and 3.1. Such difference between bioaccumulation rates of Zn and Cd in the liver can be used as an indicator of Cd exposure [16]. In principle, there has been a distinct increase of bioaccumulation

*Table 4. Significant correlations between and within tissue metal concentrations (in all investigated samples and by age groups); Ps – Pearson's correlation coefficient; * – statistically significant correlations ($p < 0.05$); r^2 – coefficient of determination; CdK – cadmium in kidney; ZnK – zinc in kidney; CdL – cadmium in liver; ZnL – zinc in liver; 12–24; 24–36; 36+ (age groups)*

	CdK	CdL
ZnK	Ps = 0.57; p = 0.001*****; r^2 = 0.32	Ps = 0.52; p = 0.001*****; r^2 = 0.27
CdL	Ps=0.81; p=0.001*****; r^2 = 0.70	–
ZnL	–	Ps = –0.67; p=0.004*; r^2 = 0.46
	$CdK_{12–24}$	$CdK_{24–36}$	CdK_{36+}
CdL_{12-24}	Ps = 0.81; p = 0.001*****	–	–
CdL_{24-36}	–	Ps = 0.78; p = 0.001*****	–
CdL_{36+}	–	–	Ps = 0.79; p = 0.004*****

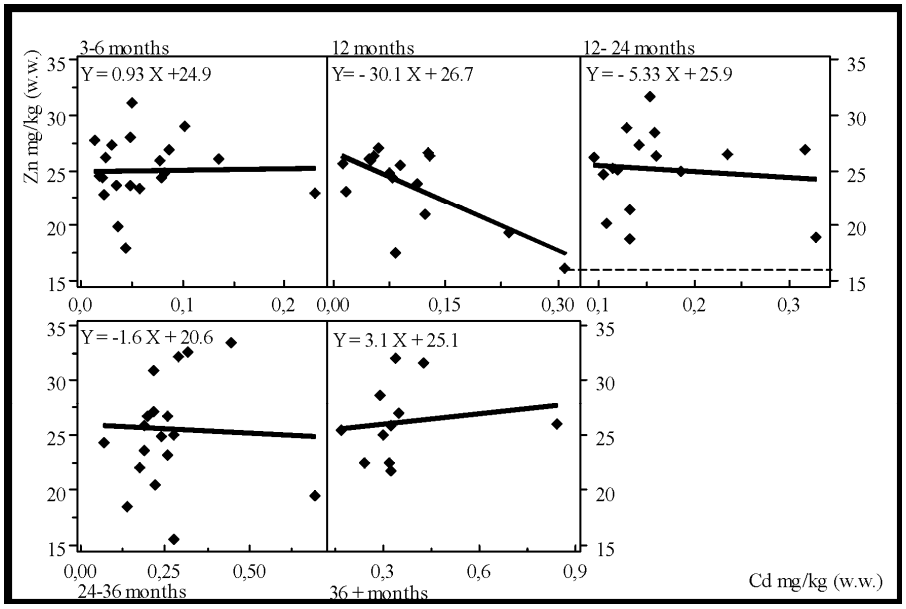

Figure 2. Relationship between Zn and Cd concentrations in liver with regression line by age groups; Y-axis: Zn concentrations in liver; X-axis: Cd concentrations in liver.

of Cd in hare organs during subsequent stages of life (Table 2). A somewhat higher increase of hepatic Zn related to Cd was registered in the oldest age group (≥ 36 months). It can be interpreted that Zn, as an essential element, has a homeostatic mechanism that maintains optimum tissue levels over a range of exposure to environmental Cd. It can also be speculated, considering the obtained results of hepatic and renal Zn concentrations in yearlings, that Cd is simply transferred to metallothionein (MT) according to their binding affinity with subsequent displacement of Zn [17].

Intercepts calculated form equations (Figure 2) related to hepatic Zn-Cd correlations by age groups are: 24.9, 26.7, 25.9, 20.6 and 25.1, respectively. It can be stated that these values may correspond to the physiological concentrations in the liver of the hares studied. Registered background tissue levels of Zn refers to those concentrations of metals that derive from natural as well as anthropogenic sources that are not the focus of the risk assessment. Distinct age trends of Zn concentration in liver of European hare have not been established. It is probably because of the native liver MTs of most animals predominantly contain Zn bounded tightly, and are less able to be substituted by Cd.

The relationship with respect to Zn and Cd concentrations in liver and kidney within all investigated hare samples are given in Figure 3.

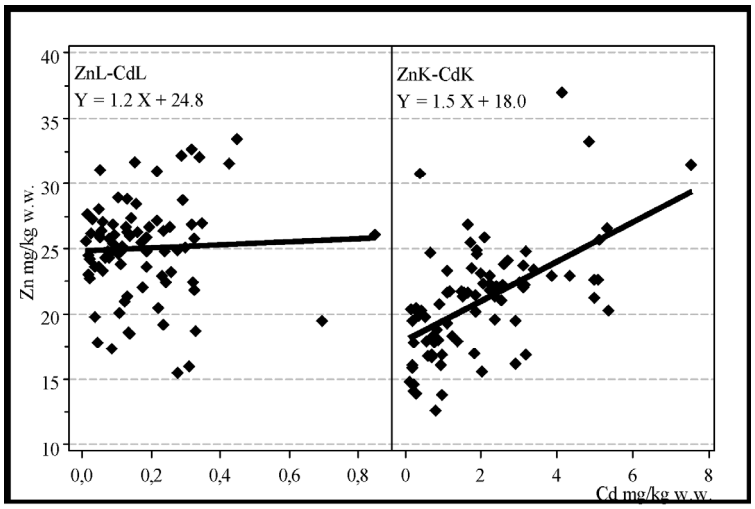

Figure 3. Relationship between Zn and Cd concentrations in liver and kidney with regression line within all investigated hare samples (n = 84); ZnL-CdL: scatter plot with regression line and fitted intercept of Zn and Cd concentrations in liver; ZnK-CdK: scatter plot with regression line and fitted intercept of Zn and Cd concentrations in kidney.

The increase of Zn content with elevated Cd concentrations in the kidney, looking at the investigated hare samples, was more distinct in comparison to the liver (Figure 3). However, the reason why the less distinct increase of Zn in relation to Cd at high concentrations in the same organ is unknown at present.

The difference between particular values of Zn in liver probably results from the different sex, age, diet and inhabitation conditions. Although the hare relies largely on grasses for food, its diet composition may vary markedly from one area to the next [18]. Under stressful conditions, hares consume increased quantities of browse and plant biomass of very low nutritional value, such as bark, pine needles, etc. [19,20]. Seasonal variations in the diet may vary from periods when animals eat more plants with wood stems or when they eat more grass. The grass regenerates yearly, whereas, for example, willow and birch are exposed to the influence of air pollution for longer periods, during which they accumulate heavy metals.

CONCLUSIONS

It can be noted that the biological role of Zn metabolism during development and growth of European hare is very important. Considering the concentrations of Cd, during the individual development of European hare, it should be stated that there is a distinct increase of bioaccumulation of Cd during subsequent stages of life. Observing the relationship between Cd and Zn levels within various age groups, it can be concluded that the bioaccumulation process comes after the first year of life. It may be important information if the hare organs are intended to be used for environmental biomonitoring of Cd. Furthermore, age distribution suggests that the samples can be censored for age to include those of animals with an exposure period of 2 or 3 years, collected from the regions of interest, and the obtained results compared with yearlings. Such age censoring would increase the monitoring precision in sampling a specific exposure period in a long-term monitoring program. Metals uptake, therefore, likely reflects metals availability through diets based on the composition and structure of specific ecosystems as affected by current stressors. Observed animals inhabiting the studied areas in Serbia show similar to lower Cd and Zn bioaccumulation compared to other biotopes in Europe. The strong age dependency due to Cd accumulation in hare organs precludes direct comparison of different groups (areas etc.), unless the age distributions are fairly equal.

Acknowledgement

The authors would like to thank the colleagues from the Department of residue analysis of the Institute of Meat Hygiene and Technology for reviewing the quality assurance for metals analyses. We thank the Hunting Association of Serbia for assisting in carcass acquisition and the hunters who contributed to this study. We also thank the staff at the Vojvodina Hunting Association Central Laboratory for conducting age analyses and for their helpful suggestions on a draft of the manuscript.

REFERENCES

[1] D.L. Sparks, Toxic Metals in the Environment: The Role of Surfaces, Elements **4** (2005) 193–197.

[2] R.K. Smith, N.V. Jennings, S.A. Harris, Quantitative analysis of the abundance and demography of European hares (*Lepus europaeus*) in relation to habitat type, intensity of agriculture and climate, Mamm. Rev. **35** (2005) 1–24.

[3] A. Fairbrother, R. Wenstel, K. Sappington, W. Wood, Framework for Metals Risk Assessment, Ecotox. Environ. Safety **68** (2007) 145–227.

[4] N.K. Moustakas, A. Akoumianaki-Ioannidou, P.E. Barouchas, The effects of cadmium and zinc interactions on the concentration of cadmium and zinc in pot marigold (*Calendula officinalis* L.), Aust. J. Crop. Sci. **5** (2011) 277––282.

[5] R.S. Nikolić, J.M Jovanović, G.M Kocić, T.P. Cvetković, S.R. Stojanović, T.D. Anđelković, N.S. Krstić, Monitoring the effects of exposure to lead and cadmium in working and living environment through standard biochemical blood parameters and liver endonucleases activity, Hem.Ind. **65** (2011) 403–409 (in Serbian).

[6] A. Brekken, E. Steinnes. Seasonal concentrations of cadmium and zinc in native pasture plants: consequences for grazing animals, Sci. Tot. Environ. **326** (2004) 181–195.

[7] D.C. Wren, Mammals as Biological Monitors of Environmental Metal Levels, Environ. Monit. Assess. **6** (1986) 127–144.

[8] M. Lazaruš, T. Orct, M. Blanuša, I. Vicković, B. Šoštarić, Toxic and essential metal concentrations in four tissues of red deer (*Cervus elaphus*) from Baranja, Croatia, Food Addit. Contam. **25** (2008) 270–283.

[9] N. Bilandžić, M. Sedak, M. Đokić, B. Šimić, Wild Boar Tissue Levels of Cadmium, Lead and Mercury in Seven Regions of Continental Croatia, Bull. Environ. Contam. Toxicol. **84** (2010) 738–743.

[10] E.R. Venalainen, A. Niemi, T. Hirvi, Heavy metals of hares in Finland 1980-82 and 1992–93, Bull. Environ. Contam. Toxicol. **56** (1996) 251–258.

[11] C. Eiraa, J. Torresa, J.Vingadab, J. Miquela, Concentration of some toxic elements in *Oryctolagus cuniculus* and in its intestinal cestode *Mosgovoyia ctenoides*, in Dunas de Mira (Portugal), Sci. Tot. Environ. **346** (2005) 81–86.

[12] M. Kramarova, P. Massanyi, A. Jancova, R. Toman, J. Slamecka, F. Tataruch, J. Kovacik, J. Gasparik, P. Nad, M. Skalicka, B. Korenekova, R. Jurcik, J. Cubon, P. Hascik, (2005) Concentration of cadmium in the liver and kidneys of some wild and farm animals, B. Vet. I. Pulawy **49** (2005) 465–469.

[13] P.Myslek, E. Kalisinska, Contents of selected heavy metals in the liver, kidneys and abdominal muscle of the brown hare (*Lepus europaeus Pallas*) in Central Pomerania, Poland, Pol. J. Vet. Sci. **9** (2006) 31–41.

[14] S. Pedersen, S. Lierhagen, Heavy metal accumulation in arctic hares (*Lepus arcticus*) in Nunavut, Canada, Sci. Tot. Environ. **368** (2006) 951–955.

[15] A. Kolesarova, J. Slamecka, R. Jurcik, F. Tataruch, N. Lukac, J. Kovacik, M. Capcarova, M. Valent, P. Massanyi, Environmental levels of cadmium, lead and mercury in brown hares and their relation to blood metabolic parameters, J. Environ. Sci. Heal., A **43** (2008) 646–650.

[16] K. Honda, R.Tatsukawa, Distribution of cadmium and zinc in tissues and organs, and their age-related changes in striped dolphins, *Stenella coeruleoalba*, Arch. Environ. Cont. Tox. **12** (1983) 543–550.

[17] S. Onosaka, K. Tanaka, M.G. Cherian, Effects of Cadmium and Zinc in Tissue Levels of Metallothionein. Environ. Health Persp. **54** (1984) 67–92.

[18] T. Reichlin, E. Klansek, K. Hackländer, Diet selection by hares (*Lepus europaeus*) in arable land and its implications for habitat management, Eur. J. Wildl. Res. **52** (2006) 109–118.

[19] H.G. Rödel, W. Volkl, H. Kilias, Winter browsing of brown hares: evidence for diet breadth expansion, Mamm. Biol. **6** (2004) 410–419.

[20] P. Stott, Comparisons of digestive function between the European hare (*Lepus europaeus*) and the European rabbit (*Oryctolagus cuniculus*): Mastication, gut passage, and digestibility, Mamm. Biol. **73** (2008) 276–286.

IZVOD

SADRŽAJ KADMIJUMA I CINKA IZ ŽIVOTNE SREDINE U JETRI I BUBREZIMA DIVLJIH ZEČEVA SA RAZLIČITIH PODRUČJA SRBIJE

Zoran I. Petrović[1], Vlado B.Teodorović[2], Mirjana R. Dimitrijević [2], Sunčica Z. Borozan[3], Miloš T. Beuković[4], Dragica M. Nikolić, Aurelija T. Spirić[1]

[1]*Institut za higijenu i tehnologiju mesa, Beograd, Srbija*
[2]*Univerzitet u Beogradu, Fakultet veterinarske medicine, Katedra za higijenu i tehnologiju namirnica animalnog porekla, Beograd, Srbija*
[3]*Univerzitet u Beogradu, Fakultet veterinarske medicine, Katedra za hemiju, Beograd, Srbija*
[4]*Univerzitet u Novom Sadu, Poljoprivredni fakultet, Departman za stočarstvo, Novi Sad, Srbija*

(Naučni rad)

Ukupno je ispitano 168 uzoraka tkiva (jetra i bubrezi) sa 84 divlja zeca sakupljenih iz 11 različitih područja Srbije na prisustvo kadmijuma (Cd) i cinka (Zn). Jaka statistička povezanost između količina kadmijuma registrovanih u bubrezima i jetri je registrovana kod životinja starijih od 12 meseci, što ukazuje na prisutnost ovog metala u njihovom okruženju. Značanje statističke razlike između koncentracija cinka u jetri u odnosu na bubrege su utvrđene unutar svih prisutnih starosnih grupa, izuzimajući najstariju. Negativna korelacija (*Ps* - Pirsonov korelacioni koeficijent) je registrovana unutar starosne grupe od 12 meseci (*Ps* = –0,67, *p* = = 0.004). Utvrđeno je da cink kod ispitane populacije divljeg zeca pokazuje homeostatski mehanizam koji u prisustvu toksičnog elementa, kao što je kadmijum, održava optimalni nivo ovog esencijalnog elementa u ispitanim tkivima. Uočeno je da se sadržaj cinka, izražen kao vrednost medijane u jetri po starosnoj dobi, ne menja značajno dok je u bubregu u blagom porastu, mada su individualne varijacije jako prisutne. Izmerene vrednosti cinka u ciljnom organu – jetri se nalaze u okviru normalnih vrednosti za hepatično tkivo. Pouzdano je utvrđeno da su medijan vrednosti ispitanih metala pod jakim uticajem starosne strukture uzoraka divljeg zeca kao i regionalnih razlika u prisutnosti kadmijuma i cinka u životnoj sredini. Utvrđen je odličan biomonitorski potencijal tkiva divljeg zeca za sistemski monitoring i praćenje aerodepozicije kadmijuma obzirom na način ishrane, životni vek, radijus kretanja, težinu, adaptibilnost, dostupnost i pokrivenost u velikom broju staništa Srbije, uključujući i oblasti u neposrednoj blizini zagađivača (termoelektrane, pepelišta, površinski kopovi uglja, rafinerije) i poljoprivrednih područja sa raširenom primenom fosfatnih đubriva i agrohemikalija.

Ključne reči: Kadmijum • Cink • Bubreg • Jetra • Divlji zec

Ocenjivanje uticaja životnog ciklusa biodizela ReCiPe metodom

Ferenc E. Kiš, Goran C. Bošković

Univerzitet u Novom Sadu, Tehnološki fakultet, Novi Sad, Republika Srbija

Izvod

U radu su prikazani rezultati ocenjivanja uticaja životnog ciklusa biodizela proizvedenog od ulja uljane repice ReCiPe metodom. Funkcionalna jedinica (FJ) je definisana kao 3750 km pređenog puta kamionom na biodizel gorivo. Od ukupno 18 ispitivanih kategorija uticaja svega 4 je odgovorno za 99% ukupnog uticaja životnog ciklusa biodizela. Zauzimanje poljoprivrednih površina (0,67 ha·god./FJ) je odgovorno za oko polovine ukupnog negativnog uticaja životnog ciklusa biodizela. Emisije gasova sa efektom staklene bašte (3000 kg $CO_{2\ ekv.}$/FJ) i emisija materija koje utiču na formiranje suspendovanih čestica (12,4 kg $PM_{ekv.}$/FJ) prouzrokuju 37% negativnog uticaja životnog ciklusa. Preostali deo negativnog uticaja životnog ciklusa je uglavnom posledica smanjenja rezervi fosilnih goriva (21168 MJ/FJ).

Ključne reči: biodizel, uljana repica, ocenjivanje životnog ciklusa, ReCiPe metod.

Dostupno na Internetu sa adrese časopisa: http://www.ache.org.rs/HI/

NAUČNI RAD

UDK 662.756.3:633.85

Hem. Ind. **67** (4) 601–613 (2013)

doi: 10.2298/HEMIND120801102K

Transesterifikacijom triglicerida biljnih ulja u prisustvu alkohola i katalizatora dobija se biodizel, obnovljivo pogonsko gorivo sa značajnom zastupljenošću u zemljama Evropske unije [1]. Preovladava mišljenje da je upotreba biodizela na bazi biljnih ulja umesto dizel goriva fosilnog porekla opravdana sa aspekta zaštite životne sredine [2,3]. Brojna istraživanja su pokazala da su sastav i koncentracija štetnih jedinjenja u izduvnim gasovima motora sa unutrašnjim sagorevanjem (SUS) sa aspekta zaštite životne sredine povoljniji u slučaju korišćenja biodizela umesto fosilnog dizela [4].

Ocena podobnosti biodizela sa aspekta zaštite životne sredine, međutim, ne sme se oslanjati isključivo na uporednu analizu produkata sagorevanja alternativnih goriva. Sagorevanje biodizela u motorima SUS je samo jedna od faza, i to poslednja, u kompleksnom životnom ciklusu (ŽC) biodizela. Proizvodnja biodizela odvija se nizom sukcesivnih aktivnosti koje neminovno prati emisija zagađujućih materija i korišćenje prirodnih resursa, a kao posledica nastaju promene u životnoj sredini sa posledicama po ljudsko zdravlje, ekosistem i raspoloživost prirodnih resursa. Poslednjih godina se sve više pažnje posvećuje proceni uticaja biodizela na životnu sredinu tokom njegovog celokupnog životnog ciklusa [5–8]. Zahtev da se uticaj motornih goriva na životnu sredinu ispituje tokom njihovog celokupnog životnog ciklusa je postavljen i u Direktivi 2009/28/EC Evropskog Parlamenta i Saveta o promociji upotrebe energije iz obnovljivih izvora.

Cilj rada je ocenjivanje uticaja životnog ciklusa biodizela, proizvedenog u uslovima koji se mogu ekstrapolisati na uslove proizvodnje u Vojvodini/Srbiji, na životnu sredinu. Analiza je ograničena na biodizel proizveden od ulja uljane repice, jer od važnijih biljnih ulja proizvedenih u Srbiji jedino ulje uljane repice zadovoljava zahteve srpskog standarda za biodizel (SRPS EN 14214) u pogledu maksimalno dozvoljenog jodnog broja sirovine.

METOD RADA I IZVORI PODATAKA

Ocenjivanje uticaja životnog ciklusa biodizela na životnu sredinu se zasniva na metodi „Ocenjivanje životnog ciklusa (eng. *Life Cycle Assessment* – LCA)“ definisanog standardom SRPS ISO 14040:2008 [9]. Prema ovom standardu LCA se izvodi u četiri faze: *i)* određivanje cilja, predmeta i područja primene, *ii)* inventarisanje životnog ciklusa, *iii)* ocenjivanje uticaja životnog ciklusa i *iv)* interpretacija rezultata.

Cilj, predmet i područje primene

Cilj je, kako je istaknuto u Uvodu, ocenjivanje uticaja životnog ciklusa biodizela proizvedenog od ulja uljane repice na životnu sredinu. U okviru predmeta i područja primene potrebno je odrediti bitne metodske pretpostavke, pre svega funkciju i funkcionalnu jedinicu ispitivanog sistema, granice sistema i postupak alokacije.

Funkcija ispitivanog sistema proizvoda je definisana kao „obezbeđivanje primenjive energije za pogon motora SUS“. Eventualne druge funkcije kao što su „smanjenje poljoprivrednih površina za proizvodnju prehrambenih useva“ ili „dobijanje kvalitetne stočne hrane“ nisu uzete u obzir i samim tim njihov potencijalni efekat nije meren kroz funkcionalnu jedinicu. Funkcionalna jedinica (FJ) je određena kao 3750 km pređenog puta kamionom ukupne težine 28 t sa ugrađenim EURO 3 motorom pri realnim uslovima kretanja (ETC – European Transient Cycle) i prosečnog iskorišćenja tovarnog kapaciteta od 50%. Kamion kao gorivo koristi čist biodizel, B-100 (tj. bez namešavanja sa dize-

Prepiska: F.E. Kiš, Univerzitet u Novom Sadu, Tehnološki fakultet, Bul. Cara Lazara 1, 21000 Novi Sad, Srbija.
E-pošta: ferenc1980@gmail.com
Rad primljen: 1. avgust, 2012
Rad prihvaćen: 19. oktobar, 2012

lom fosilnog porekla), proizveden od ulja uljane repice. Prosečna potrošnja biodizela referentnog kamiona pri datim uslovima iznosi 0,2667 kg/km [10], što definiše referentnu količinu biodizela od 1000 kg po FJ. Granice sistema definišu jedinične procese koji čine životni ciklus proizvoda, a koji su uključeni u LCA [9]. U ovom radu, granice sistema su definisane na način da uključuju najveći deo jediničnih procesa za koje je u prethodnim LCA biodizela dokazano da imaju značajan uticaj na formiranje rezultata analize [7,8,11-14]. Granicama sistema nisu obuhvaćeni procesi u vezi sa izgradnjom, održavanjem i demontažom građevinskih objekata i opreme korišćenih pri proizvodnji i sušenju zrna, proizvodnji ulja i transesterifikaciji. Prema rezultatima ranijih istraživanja ovi procesi imaju samo manji uticaj na formiranje rezultata LCA [11–13]. Faze životnog ciklusa biodizela koje su obuhvaćene analizom kao i osnovni materijalni tokovi iskazani u odnosu na FJ su prikazani na slici 1.

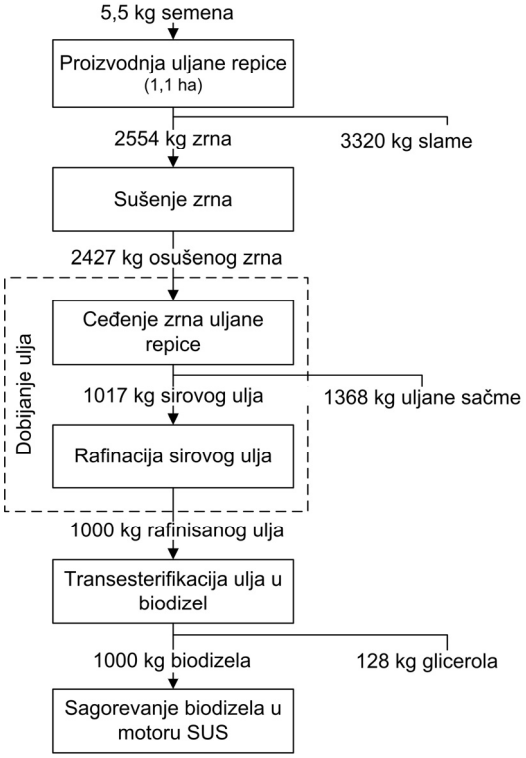

Slika 1. Osnovni materijalni tokovi u životnom ciklusu 1000 kg biodizela [15].
Figure 1. Main material flows in the life cycle of 1000 kg of biodiesel [15].

Kada kao rezultat nekog proizvodnog procesa nastaje više od jednog proizvoda javlja se problem alokacije, odnosno kako ukupan uticaj proizvodnog procesa raspodeliti na glavni i jedan ili više sporednih proizvoda. Na primer, u pojedinim fazama životnog ciklusa biodizela pored glavnog proizvoda nastaju i sporedni proizvodi kao što su slama, uljana sačma i glicerol (slika 1). S obzirom na to da je istraživanje usmereno isključivo na ocenjivanje uticaja biodizela potrebno je nekom od metoda alokacije iz rezultata isključiti uticaje vezane za sporedne proizvode [9]. Deo ukupne količine elementarnog toka *i* u životnom ciklusu biodizela (elementarni tok je emisija koja se ispušta u životnu sredinu ili prirodni resurs koji se uzima iz životne sredine), koji se pripisuje biodizelu ($E_{\text{biodizel.total},i}$), utvrđuje jednačinom (1):

$$E_{\text{biodizel.total},i} = E_{1,i} f_1 f_2 f_3 + E_{2,i} f_2 f_3 + E_{3,i} f_3 + E_{4,i} \quad (1)$$

gde je $E_{1,i}$ količina elementarnog toka *i* u fazi proizvodnje zrna uljane repice; f_1 je deo (u %) $E_{1,i}$ koji se pripisuje zrnu uljane repice; $E_{2,i}$ je količina elementarnog toka *i* u fazama sušenja zrna i ekstrakcije i rafinacije ulja; f_2 je deo $E_{2,i}$ koji se pripisuje rafinisanom ulju uljane repice; $E_{3,i}$ je količina elementarnog toka *i* u fazi transesterifikacije; f_3 je deo $E_{3,i}$ koji se pripisuje biodizelu; $E_{4,i}$ je količina elementarnog toka *i* u fazi sagorevanja biodizela u motoru SUS.

Vrednosti $E_{x,i}$ se dobijaju kao rezultat inventarisanja, dok se faktori alokacije (f_x) utvrđuju metodom alokacije. Faktori alokacije pokazuju koji deo elementarnog toka $E_{x,i}$ se pripisuje glavnom proizvodu u pojedinim fazama životnog ciklusa biodizela. U ovom radu se primenjuje ekonomska alokacija što znači da je vrednost f_x jednaka udelu prihoda od prodaje glavnog proizvoda u ukupnom prihodu faze. Na osnovu mase (slika 1) i tržišnih cena glavnih i sporednih proizvoda [15] (265 EUR/t zrna uljane repice; 28 EUR/t slame uljane repice; 730 EUR/t rafinisanog ulja; 170 EUR/t sačme; 900 EUR/t biodizela; 80 EUR/t glicerola) dobijene su sledeće vrednosti faktora alokacije: f_1 = 88%, f_2 = 76% i f_3 = 99%. Jednačina (1) se primenjuje na sve elementarne tokove izuzev CO_2 biološkog porekla (objašnjeno u daljem delu teksta).

Inventarisanje životnog ciklusa

Inventarisanje životnog ciklusa biodizela se radi u dva koraka, u skladu sa principima opisne LCA. U prvom se prikupljaju podaci o vrsti i količini materijalnih i energetskih ulaza (u daljem tekstu „ulazi“) u pojedinim fazama životnog ciklusa biodizela (npr. koja vrsta i količina mineralnih đubriva se koristi pri proizvodnji uljane repice). U drugom se prikupljaju podaci o emisijama u životnu sredinu i korišćenju prirodnih resursa u celokupnom životnom ciklusu svakog pojedinačnog ulaza definisanog u prethodnom koraku inventarisanja (npr. koja vrsta i količina zagađujućih materija se emituje u životnu sredinu tokom proizvodnog lanca i upotrebe mineralnih đubriva). Konačan rezultat inventarisanja sadrži podatke o vrstama i količinama materija koje se emituju u životnu sredinu, kao i podatke o vrstama i količinama prirodnih resursa upotrebljenih u životnom ciklusu biodizela.

Podaci o emisijama i vrsti i količini prirodnih resursa u životnom ciklusu ulaza koji se koriste u životnom ciklusu biodizela preuzeti su iz Ecoinvent 2.0 baze podataka. Pri inventarisanju životnog ciklusa korišćen je SimaPro 7.3 LCA računarski program u čijem sastavu je i pomenuta baza podataka.

Ukupna količina elementarnog toka *i* (E_i) u životnom ciklusu biodizela se utvrđuje jednačinom (2):

$$E_i = \sum_{j=1}^{n} I_j E_{i,j} \quad (2)$$

gde su: I_j – količina ulaza *j* u životnom ciklusu biodizela (npr. kg heksana/FJ), $E_{i,j}$ – količina elementarnog toka *i* u životnom ciklusu jedinice ulaza *j* (npr. kg CH_4/kg heksana) i *n* – broj (vrsta) različitih ulaza u životnom ciklusu biodizela

Podaci o vrsti i količini ulaza po pojedinim fazama životnog ciklusa biodizela kao i izvor podataka o elementarnim tokovima u životnom ciklusu pojedinih ulaza dati su u nastavku poglavlja.

Proizvodnja zrna uljane repice. U proračunima se uzima da je prinos uljane repice 2305 kg/ha na osnovu petogodišnjeg (2005–2009) proseka u Vojvodini [16]. Materijalni i energetski tokovi proizvodnje zrna uljane repice u uslovima Vojvodine su preuzeti iz [15]. Norma setve iznosi 5 kg semena po ha. Uljana repica se prihranjuje sa 140 kg N, 40 kg P_2O_5 i 80 kg K_2O po ha. Azot se u zemljište unosi u vidu amonijum-nitratnog đubriva (35% N) dok se potrebna količina fosfora i kalijuma unosi putem trostrukog superfosfata (48% P_2O_5) i kalijum-hlorida (60% K_2O). Deo azota unetog u zemljište se gubi usled volatizacije slobodnog amonijaka i denitrifikacije. Gasoviti gubici iznose 74 g NH_3, 35 g N_2O i 16 g NO po kg unetog azota [15]. Od pesticida koristi se „Fusilade forte“, „BOSS 300 SL“ i „Megatrin 2.5 EC“. Kao gorivo u poljoprivrednoj mehanizaciji se koristi fosilni dizel. Ukupna potrošnja dizel goriva prilikom izvođenja agrotehničkih operacija je 90 l/ha. Potrošnja maziva u motorima poljoprivrednih mašina proporcionalna potrošnji goriva i iznosi 0,62 vol.% goriva [17]. Nakon žetve zrno uljane repice se prevozi do sušare udaljene 37,5 km kamionima na dizel gorivo fosilnog porekla.

Sušenje zrna uljane repice. U procesu sušenja sadržaj vode u zrnu uljane repice se smanjuje sa početnih 13,5 na 9%. Pretpostavlja se da se sušenje odvija u vertikalnoj gravitacionoj sušari Strahl 5000 (Officine Minute, Italija) koja kao gorivo koristi lako ulje za loženje. Ova tehnologija sušenja zrna ratarskih useva je rasprostanjena u Vojvodini [18]. Specifična potrošnja energije po toni osušenog zrna iznosi 260 MJ toplotne energije i 2,8 MJ električne energije [15]. Osušeno zrno se prevozi do uljare udaljene 37,5 km kamionima na dizel gorivo fosilnog porekla.

Ekstrakcija ulja i rafinacija. Usled nedostatka podataka o relevantnim materijalnim i energetskim tokovima uljara u Srbiji analiza se oslanja na podatke danske uljare „AarhusKarlshamn“ iz Aarhusa [19]. Ekstrakcija ulja se zasniva na kombinovanom postupku, koji podrazumeva najpre presovanje zrna uljane repice, a zatim ekstrakciju preostalog ulja iz uljane pogače heksanom. Kombinovani postupak dobijanja ulja je karakterističan za većinu uljara u Srbiji [1]. Potrošnja heksana po toni presovanog i ekstrahovanog ulja u uljari „AarhusKarlshamn“ je 1,19 kg. Potrebe procesa u toplotnoj energiji se zadovoljavaju energijom vodene pare koja se dobija sagorevanjem lakog ulja za loženje (donja toplotna moć goriva je 41,8 MJ/kg). U procesu ekstrakcije ulja po toni sirovog ulja troši se 43 kg lakog lož ulja, kao i 419 MJ električne energije po toni sirovog ulja.

U procesu rafinacije sirovog ulja slobodne masne kiseline se konvertuju u sapune dodatkom natrijum-hidroksida i uklanjaju centrifugiranjem. Ostale nečistoće se uklanjaju filtracijom primenom kiselinom tretirane gline za izbeljivanje. U procesu rafinacije troši se 6,1 kg lakog lož ulja i 104 MJ električne energije po toni sirovog ulja. Rafinisano ulje se prevozi do pogona za transesterifikaciju udaljenog 1 km kamionima na dizel gorivo fosilnog porekla.

Transesterifikacija ulja u biodizel. Transesterifikacija se zasniva na nemačkoj tehnologiji (Lurgi AG) pri kojoj se transesterifikacija ulja u biodizel izvodi metanolom u prisustvu alkalnog katalizatora natrijum-metilata. Ova tehnologija se primenjuje i u fabrici biodizela „Victoria-Oil“ u Šidu. Materijalni i energetski tokovi procesa su dostupni iz literature [20]. Nakon transesterifikacije biodizel gorivo se distribuira cisternama na fosilno dizel gorivo do benzinskih pumpi koje su prosečno udaljene 50 km.

Pregled materijalnih i energetskih ulaza proizvodnog lanca biodizela iskazanih u odnosu na FJ, odnosno referentnu količinu od 1000 kg biodizela, zajedno sa podacima o emisijama i upotrebi prirodnih resursa u životnom ciklusu pojedinih ulaza, dat je u tabeli 1. Za one ulaze za koje je procenjeno da je uticaj faze upotrebe na životnu sredinu zanemarljiv (npr. električna energija), ili za koje ne postoje pouzdani i kompletni podaci o eventualnim uticajima faze upotrebe (npr. fosforna i kalijumova đubriva), razmatrani su samo uticaji koji nastaju u njihovom proizvodnom lancu.

Sagorevanje biodizela. Kao reprezentativni inventar emisije gasova motora SUS na biodizel gorivo za kamion i uslove opisanih u FJ, koriste se podaci iz literature [10], koji su delimično korigovani [15]. Pri sagorevanju 1000 kg biodizela u motoru referentnog kamiona emituje se 2849 kg CO_2. Od ukupne količine CO_2 koja nastaje pri sagorevanju biodizela 2700 kg je biološkog porekla, dok je preostali deo fosilni CO_2 poreklom iz metanola [15]. Ugljenik biološkog porekla u biodizelu

Tabela 1. Ulaz materijala i energije u proizvodnom lancu 1000 kg biodizela; ŽC – uzet u obzir ceo životni ciklus; PL – uzet u obzir samo proizvodni lanac
Table 1. Material and energy inputs in the production chain of 1000 kg of biodiesel

Faza životnog ciklusa	Procesi obuhvaćeni analizom	Ulaz materijala i energije (pre alokacije)		Izvor podataka o inventaru ŽC ili PL
		Jedinica	Količina	
Proizvodnja zrna uljane repice	ŽC amonijum-nitrata	kg N	155,1	[6,15]
	PL trostrukog superfosfata	kg P_2O_5	44,3	[21]
	PL kalijum-hlorida	kg K_2O	88,6	[21]
	PL pesticida	kg	1,4	[21]
	PL semena	kg	5,5	[21]
	ŽC dizel goriva u polj. maš.	kg	84,8	[10,21]
	ŽC maziva u polj. mašinama	kg	0,52	[10]
	Transport zrna do sušare	tkm	191,0	[22]
Sušenje zrna	ŽC lakog lož ulja	kg	15,1	[23]
	PL električne energije	MJ	23,6	[23]
	Transport zrna do uljare	tkm	182,0	[22]
Presovanje i ekstrakcija ulja	ŽC lakog lož ulja	kg	43,7	[10]
	PL električne energije	MJ	426,1	[23]
	PL heksana	kg	1,2	[24]
Rafinacija ulja	PL električne energije	MJ	104,0	[23]
	ŽC lakog lož ulja	kg	6,2	[10]
	PL fosforne kiseline (85%)	kg	0,8	[25]
	PL natrijum-hidroksida (50%)	kg	2,1	[25]
	PL sumporne kiseline (100%)	kg	1,9	[25]
	PL gline za izbeljivanje	kg	9,0	[26]
	Transport rafinisanog ulja	tkm	1,0	[22]
Transesterifikacija	PL električne energije	MJ	43,2	[23]
	ŽC zemnog gasa u parnom kotlu	m^3	33,4	[27]
	PL natrijum-metilata (100%)	kg	5,0	[28]
	PL natrijum-hidroksida (50%)	kg	1,5	[25]
	PL sone kiseline (36%)	kg	10,0	[24]
	PL metanola	kg	96,0	[25]
	Transport biodizela	tkm	50,0	[22]

vodi poreklo od atmosferskog ugljenika koji je bio apsorbovan u zrnu uljane repice u procesu fotosinteze, te se ova količina CO_2 (2700 kg) oduzima od ukupne emisije CO_2 u fazi proizvodnje zrna uljane repice. Pored CO_2 u procesu sagorevanja 1000 kg biodizela u vazduh se oslobađa 3,37 kg CO, 28,8 kg NO_x (oksidi azota), 26,4 g N_2O, 335 g $PM_{2.5}$ (čestice sa prečnikom manjim od $2{,}5\cdot10^{-6}$ m), 49,2 g PM_{co} (čestice sa prečnikom većim od $2{,}5\cdot10^{-6}$ m), 0,61 kg NMVOC (nemetanska lakoisparljiva organska jedinjenja), 14,3 g CH_4, 18,7 g NH_3 i 4,3 g benzena [10,15].

Metod za ocenjivanje uticaja životnog ciklusa

Rezultat inventarisanja sadrži podatke o vrstama i količinama emisija i prirodnih resursa vezanih za životni ciklus biodizela ali ne i o mogućim uticajima ovih elementarnih tokova na životnu sredinu. U kontekstu LCA mogući uticaj proizvoda na životnu sredinu se utvrđuje nekom od metoda za ocenjivanje uticaja životnog ciklusa (eng. *Life Cycle Impact Assessment method* – LCIA metod).

Za ocenjivanje uticaja životnog ciklusa biodizela u radu se koristi ReCiPe metod [29]. ReCiPe metod je nastao kombinacijom i usavršavanjem dva popularna LCIA metoda: CML2000 [30] i Eco-indicator 99 [31]. Ono što izdvaja ovaj metod od ostalih jeste mogućnost vrednovanja uticaja kako na međupozicijama, tako i na krajnjim pozicijama mehanizma životne sredine (tj. na nivou štete). Uticaj životnog ciklusa proizvoda se meri kroz rezultat 18 indikatora na međupozicijama i 3 indikatora na krajnjim pozicijama mehanizma životne sredine. U većini kategorija uticaja na međupozicijama, ukupan uticaj svakog elementarnog toka se iskazuje u odnosu na ekvivalentan uticaj referentnog elementarnog toka. Na primer, u okviru kategorije uticaja „globalno zagrevanje“ uticaj svakog gasa sa efektom sta-

klene bašte (CO_2, CH_4, N_2O, itd.) se iskazuje zbirno, kroz ekvivalentan uticaj referentne supstance, koja je u slučaju ReCiPe metoda CO_2 (slika 2).

Indikatori na krajnjim pozicijama se nazivaju i indikatori štete jer se kroz njih meri šteta koja nastaje kao posledica emisija i korišćenja prirodnih resursa u životnom ciklusu ispitivanog proizvoda. ReCiPe metod razmatra uticaje u okviru sledeće tri kategorije uticaja na krajnjim pozicijama mehanizma životne sredine:

- *Šteta naneta ljudskom zdravlju* – računa se kao zbir izgubljenih godina života zbog prevremene smrti i izgubljenih godina „zdravog“ života usled oštećenja zdravlja zbog izloženosti osobe zagađenju. Jedinica mere je DALY *(eng. Disability Adjusted Life Year).*
- *Šteta naneta raznolikosti ekosistema* – meri se kroz gubitak biodiverziteta, a obim štete se iskazuje kroz broj vrsta koji će nestati tokom određenog vremenskog perioda usled zagađenja životne sredine ili korišćenja zemljišta. Jedinica mere je „br. vrsti×god.“.
- *Šteta zbog umanjene raspoloživosti mineralnih resursa* – procenjuje se na osnovu predviđenog rasta graničnih troškova eksploatacije mineralnih rezervi u

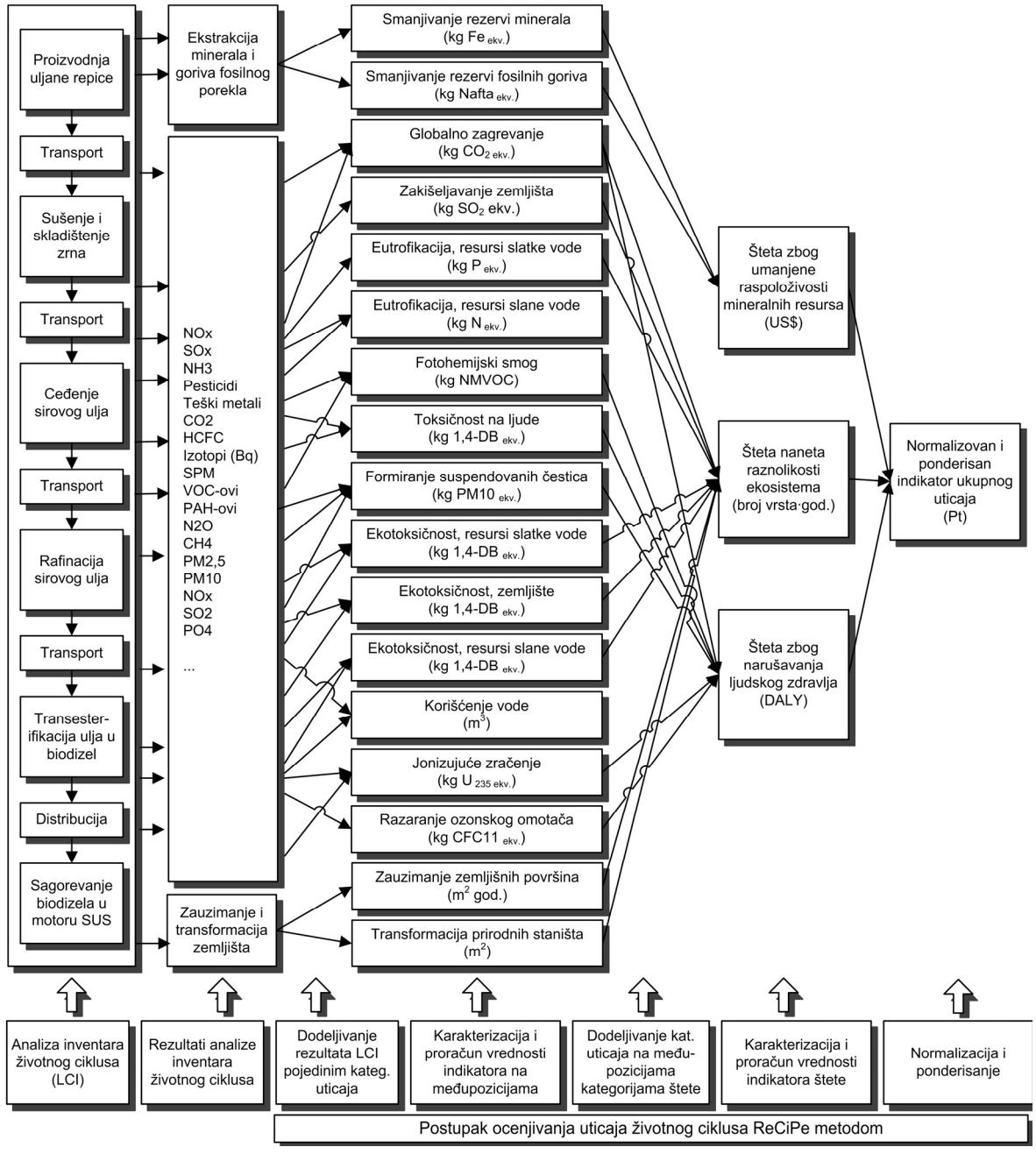

Slika 2. Šematski prikaz ReCiPe metode.
Figure 2. Scheme of the ReCiPe method.

budućnosti i efekta ovog rasta na troškove globalne ekonomije. Jedinica mere je US$.

ReCiPe metod omogućuje iskazivanje ukupnog uticaja u vidu jednog sintetičkog indikatora sa jedinicom mere Pt. Ovaj indikator je rezultat normalizacije i ponderisanja (u literaturi se češće koristi i izraz „odmeravanja“) između indikatora tri pomenute kategorije štete i omogućuje njihovo neposredno poređenje i utvrđivanje njihovih udela u ukupnom uticaju životnog ciklusa. Prema SRPS ISO 14040:2008 normalizacija i ponderisanje su opcioni elementi LCIA i korišćenje ovako izvedenih indikatora nije dozvoljena u uporednim analizama.

Pregled kategorija uticaja obuhvaćenih ReCiPe metodom i postupak vrednovanja dati su na slici 2. Interesantno je napomenuti da od 18 indikatora na međupozicijama, dva, *eutrofikacija – slana voda* i *korišćenje vode*, nije moguće meriti na nivou indikatora na krajnjim pozicijama mehanizma životne sredine [29]. To pokazuje da, iako je metod nastao usavršavanjem dva prethodna metoda, još uvek ne omogućava vrednovanje svih uticaja životnog ciklusa na krajnjim pozicijama.

Vrednovanje rezultata indikatora kategorija uticaja rađeno je uz pomoć računarskog programa SimaPro 7.3, korišćenjem verzije ReCiPe metoda koja u ovom računarskom programu nosi oznaku „ReCiPe Endpoint (H), Europe ReCiPe H/A“.

REZULTATI I DISKUSIJA

Rezultati istraživanja se iskazuju na dva nivoa: *i)* na nivou rezultata inventarisanja, koji sadrži podatke o vrsti i količini elementarnih tokova u životnom ciklusu biodizela i *ii)* na nivou rezultata ocenjivanja uticaja životnog ciklusa. Ukoliko nije drugačije navedeno svi rezultati se iskazuju u odnosu na FJ (1000 kg biodizela).

Rezultat inventarisanja životnog ciklusa

U životnom ciklusu biodizela se u životnu sredinu emituje više stotina različitih supstanci i upotrebljava nekoliko stotina različitih oblika ruda minerala, neobnovljivih izvora energije, zemljišta i drugih prirodnih resursa. Zbog nemogućnosti prikazivanja svih elementarnih tokova vezanih za životni ciklus biodizela, prikaz podataka je ograničen na manji broj elementarnih tokova (tabele 2–4). Pregledom su obuhvaćene emisije u životnu sredinu koje su određene Pravilnikom o graničnim vrednostima emisije, načinu i rokovima merenja i evidentiranja podataka (Sl. glasnik RS, br. 30/97) i

Tabela 2. Odabrani rezultati inventarisanja ŽC 1000 kg biodizela – emisije u vazduh
Table 2. Partial life cycle inventory results of 1000 kg of biodiesel – emissions to air

Emisije u vazduh	Jed.	Proizvodnja zrna	Sušenje zrna	Dobijanje ulja	Transesterifikacija	Sagorevanje biodizela	Ukupno ŽC
CO_2[a]	kg	–2,08E+03	6,47E+01	2,66E+02	1,87E+02	2,85E+03	1,28E+03
N_2O	kg	5,56E+00	7,03E-04	2,98E-03	1,70E-03	2,64E-02	5,60E+00
CH_4	kg	9,98E-01	6,63E-02	1,82E-01	6,72E-01	1,43E-02	1,93E+00
NO_x	kg	6,27E+00	2,08E-01	3,66E-01	2,74E-01	2,88E+01	3,59E+01
SO_2	kg	1,82E+00	1,44E-01	1,75E+00	3,64E-01	0,00E+00	4,08E+00
CO	kg	1,12E+00	6,21E-02	8,43E-02	1,18E-01	3,37E+00	4,75E+00
PM, ukupno[b]	kg	9,62E-01	3,31E-02	3,48E-01	9,07E-02	3,85E-01	1,82E+00
PM, <2,5 μm	kg	4,72E-01	1,69E-02	2,26E-01	3,74E-02	3,36E-01	1,09E+00
PM, između 2,5 i 10 μm	kg	1,82E-01	5,40E-03	3,19E-02	1,42E-02	3,25E-02	2,66E-01
PM, >10 μm	kg	3,08E-01	1,07E-02	9,00E-02	3,91E-02	0,00E+00	4,47E-01
NH_3	kg	8,27E+00	4,41E-04	7,72E-04	1,05E-03	1,88E-02	8,29E+00
HF	kg	6,58E-03	1,98E-04	3,62E-03	7,98E-04	0,00E+00	1,12E-02
HCl	kg	1,11E-02	7,64E-04	1,19E-02	3,22E-03	0,00E+00	2,71E-02
NMVOC[c]	kg	5,70E-01	5,42E-02	1,01E-01	1,66E-01	6,14E-01	1,51E+00
Benzen	kg	3,03E-03	1,68E-04	5,91E-04	9,98E-04	4,37E-03	9,15E-03
Benzo(*a*)piren	kg	4,43E-06	1,09E-07	1,78E-07	5,97E-07	0,00E+00	5,32E-06
Pah	kg	2,75E-04	3,09E-06	5,27E-06	2,48E-05	0,00E+00	3,08E-04
Arom. Hc	kg	1,43E-03	4,98E-05	6,70E-05	5,18E-04	0,00E+00	2,06E-03
Metali[d]	kg	4,06E-03	7,62E-04	5,68E-04	2,44E-04	0,00E+00	5,63E-03

[a]Ukupna emisija CO_2 u životnom ciklusu biodizela je umanjena za količinu atmosferskog CO_2 koja je apsorbovana u zrnu uljane repice u procesu fotosinteze i koja je nakon prerade zrna dospela u biodizel; [b]ukupne suspendovane čestice (PM, ukupno) obuhvataju suspendovane čestice sa prečnikom manjim od 2,5 μm, čestice sa prečnikom između 2,5 i 10 μm i čestice sa prečnikom većim od 10 μm; [c]grupa NMVOC u vazduh obuhvata oko 90 jedinjenja ili skupa jedinjenja uključujući i benzen, benzo(*a*)piren, PAH i aromatične ugljovodonike. Zbog značaja sa aspekta kvaliteta vazduha, benzen, benzo(*a*)piren, PAH i aromatični ugljovodonici se iskazuju i posebno; [d]teški metali obuhvataju cink, nikl, bakar, barijum, olovo, arsen, mangan, kobalt, kadmijum i živu

Tabela 3. Odabrani rezultati inventarisanja ŽC 1000 kg biodizela – emisije u vodu i zemljište
Table 3. Partial life cycle inventory results of 1000 kg of biodiesel – emissions to water and soil

Komponenta	Jed.	Proizvodnja zrna	Sušenje zrna	Dobijanje ulja	Transesterifikacija	Sagorevanje biodizela	Ukupno ŽC
Emisije u vodu							
NH_3	kg	7,71E-02	9,99E-05	2,93E-04	3,15E-04	0,00E+00	7,78E-02
NO_3^-	kg	2,68E-01	2,85E-04	9,29E-04	1,91E-03	0,00E+00	2,72E-01
PO_4^{3-}	kg	1,23E+00	7,36E-04	1,64E-02	2,10E-03	0,00E+00	1,25E+00
P	kg	1,34E-03	6,55E-06	4,67E-05	9,84E-04	0,00E+00	2,37E-03
HPK	kg	1,95E+00	1,80E-01	4,47E-01	2,83E-01	0,00E+00	2,86E+00
BPK	kg	1,75E+00	1,74E-01	4,49E-01	2,41E-01	0,00E+00	2,62E+00
HC[a]	kg	1,04E-02	1,21E-03	4,17E-03	2,64E-02	0,00E+00	4,22E-02
Metali[b]	kg	3,33E-02	2,79E-03	1,68E-02	4,40E-03	0,00E+00	5,73E-02
Emisije u zemljište							
Metali[(2)]	kg	3,20E-03	3,14E-04	6,79E-04	5,32E-04	0,00E+00	4,73E-03

[a]Grupa ugljovodonika (HC) emitovanih u vodu obuhvata oko 40 jedinjenja ili skupa jedinjenja iz inventara životnog ciklusa biodizela; [b]teški metali obuhvataju cink, nikl, bakar, barijum, olovo, arsen, mangan, kobalt, kadmijum i živu

Tabela 4. Odabrani rezultati inventarisanja ŽC 1000 kg biodizela – prirodni resursi
Table 4. Partial life cycle inventory results of 1000 kg of biodiesel – natural resources

Resurs	Jed.	Proizvodnja zrna	Sušenje zrna	Dobijanje ulja	Transesterifikacija	Sagorevanje biodizela	Ukupno ŽC
Korišćenje neobnovljivih izvora energije							
Sirova nafta, u zemlji[a]	kg	1,26E+02	1,80E+01	4,18E+01	3,89E+00	0,00E+00	1,89E+02
Zemni gas, u zemlji[b]	m^3	1,13E+02	1,57E+00	4,32E+00	1,33E+02	0,00E+00	2,52E+02
Mrki ugalj, u zemlji[c]	kg	2,57E+01	7,06E+00	1,48E+02	2,67E+01	0,00E+00	2,07E+02
Kameni ugalj, u zemlji[d]	kg	2,95E+01	1,07E+00	2,16E+00	7,06E+00	0,00E+00	3,98E+01
Uranijum[e]	kg	1,08E-03	5,44E-05	1,40E-04	4,40E-04	0,00E+00	1,71E-03
Zauzimanje površina							
Poljoprivredno zemljište	m^2·god.	6,71E+03	1,13E-01	4,20E-01	7,13E-01	0,00E+00	6,71E+03
Građevinsko zemljište	m^2·god.	6,18E+00	2,62E-01	7,56E-01	4,62E-01	0,00E+00	7,66E+00
Korišćenje vode							
Voda	m^3	5,45E+00	1,67E-01	1,08E+00	6,26E-01	0,00E+00	7,33E+00

[a]Sirova nafta čija je gornja toplotna moć 45,80 MJ/kg; [b]zemni gas čiji je gornja toplotna moć 38,3 MJ/m^3; [c]mrki ugalj čiji je gornja toplotna moć 9,9 MJ/kg; [d]kameni ugalj čiji je gornja toplotna moć 19,1 MJ/kg; [e]uranijum iz koga se dobija 560000 MJ električne energije po 1 kg

Uredbom o uslovima za monitoring i zahtevima kvaliteta vazduha (Sl. glasnik RS, br. 11/10), kao i neki drugi elementarni tokovi koji bi mogli pomoći prilikom tumačenja rezultata LCIA.

Rezultat ocenjivanja uticaja životnog ciklusa

Rezultati ocenjivanja uticaja životnog ciklusa biodizela se iskazuju najpre na nivou rezultata indikatora pojedinih kategorija uticaja, a zatim i na nivou normalizovanog i ponderisanog indikatora ukupnog uticaja.

Pregled rezultata indikatora kategorija uticaja na međupozicijama i krajnjim pozicijama mehanizma životne sredine dat je u tabeli 5.

Iz rezultata se vidi da je svega nekoliko kategorija uticaja odgovorno za najveći deo ukupnog uticaja u okviru pojedinih kategorija uticaja na krajnjim pozicijama, a to su: globalno zagrevanje, formiranje suspendovanih čestica, zauzimanje poljoprivrednih površina i smanjenje rezervi fosilnih goriva.

Šteta zbog narušavanja ljudskog zdravlja se skoro u celosti pripisuje emisiji gasova sa efektom staklene bašte (56%) i emisijama u vazduh koje doprinose formiranju čestica (43%). Kumulativan doprinos rezultata indikatora ostalih kategorija uticaja (jonizujuće zračenje, formiranje fotohemijskog smoga, razaranje ozonskog omotača i toksičnost po ljude) ukupnom uticaju na ljudsko zdravlje je svega 1% (tabela 5). Uticaj emisija u životnom ciklusu biodizela na globalno zagrevanje je procenjen na 3000 kg $CO_{2,ekv.}$ (tabela 5), što je manje nego što se emituje u životnom ciklusu iste mase fosilnog dizela (3700 kg $CO_{2,ekv.}$ prema [10]). Interesantno je napomenuti da u životnom ciklusu biodizela CO_2 nije gas koji je najviše odgovoran za globalno zagrevanje već je to N_2O. Naime, iako se u životnom ciklusu biodizela emituje svega 5,6 kg N_2O naspram 1280 kg CO_2 (tabela

Tabela 5. Rezultati vrednovanja uticaja životnog ciklusa 1000 kg biodizela na nivou pojedinih kategorija uticaja
Table 5. Life cycle impact assessment results of 1000 kg of biodiesel

R.b.	Kategorije uticaja	Rezultati indikatora na međupozicijama		Rezultati indikatora na krajnjim pozicijama (veličina štete)		
		Jed. mere	Vrednost	Ljudsko zdravlje (DALY)	Ekosistem (br. vrsta·god.)	Resursi, US$
1.	Globalno zagrevanje	kg $CO_{2,ekv.}$	3,00E+03	4,19E-03	2,37E-05	
2.	Razaranje ozonskog omotača	kg CFC-$11_{ekv.}$	1,51E-04	4,00E-07		
3.	Toksičnost na ljude	kg 1,4 $DB_{ekv.}$	9,87E+01	6,91E-05		
4.	Fotohemijski smog	kg $NMVOC_{ekv.}$	3,62E+01	1,41E-06		
5.	Formiranje susp. čestica	kg $PM2.5_{ekv.}$	1,24E+01	3,21E-03		
6.	Jonizujuće zračenje	kg $U235_{ekv.}$	9,58E+01	1,57E-06		
7.	Zakišeljavanje zemljišta	kg $SO_{2ekv.}$	4,36E+01		2,53E-07	
8.	Eutrofikacija, slatka voda	kg $P_{ekv.}$	4,15E-01		1,82E-08	
9.	Eutrofikacija, slana voda	kg $N_{ekv.}$	1,43E+01			
10.	Ekotoksičnost, zemljište	kg 1,4 $DB_{ekv.}$	8,36E-01		1,07E-07	
11.	Ekotoksičnost, slatka voda	kg 1,4 $DB_{ekv.}$	2,14E+00		5,56E-10	
12.	Ekotoksičnost, slana voda	kg 1,4 $DB_{ekv.}$	3,24E+00		2,60E-12	
13.	Zauzimanje polj. zemljišta	m^2·god.	6,71E+03		1,23E-04	
14.	Zauzimanje građ. zemljišta	m^2·god.	7,66E+00		1,48E-07	
15.	Transfor. prirodnih staništa	m^2	4,28E-01		8,57E-07	
16.	Korišćenje vode	m^3	7,33E+00			
17.	Smanjivanje rezervi minerala	kg $Fe_{ekv.}$	8,25E+01			5,89E+00
18.	Smanjivanje rezervi fosilnih goriva	kg $Nafta_{ekv.}$	5,04E+02			8,10E+03
Ukupna šteta prouzrokovana životnim ciklusom biodizela				7,48E-03	1,48E-04	8,11E+03

2), zbog 293 puta većeg uticaja prethodnog kao gasa sa efektom staklene bašte u odnosu na CO_2, emisija N_2O je odgovorna za 55% uticaja u okviru globalnog zagrevanja. U životnom ciklusu biodizela N_2O uglavnom nastaje u procesu denitrifikacije amonijum-nitratnog đubriva. Doprinos pojedinih faza životnog ciklusa ukupnoj emisiji značajnijih gasova sa efektom staklene bašte dat je u tabeli 2. Prema ReCiPe metodu emisije koje doprinose formiranju čestica su amonijak, oksidi azota, oksidi sumpora i suspendovane čestice (PM). Ukupan uticaj u okviru kategorije uticaja „formiranje suspendovanih čestica“ je procenjen na 12,4 kg $PM_{2.5,ekv.}$ (tabela 5), i posledica je emisije oksida azota (61%), amonijaka (21%), suspendovanih čestica (12%) i oksida sumpora (6%). Emisija ovih jedinjenja se u najvećoj meri pripisuje fazama proizvodnje zrna uljane repice i sagorevanju biodizela u motorima SUS (tabela 2).

Šteta naneta raznolikosti ekosistema se u ReCiPe metodi vrednuje kroz gubitak biodiverziteta na određenoj teritoriji. Gubitak biodiverziteta u životnom ciklusu biodizela je uglavnom posledica zauzimanja poljoprivrednih površina (83%) i globalnog zagrevanja izazvanog emisijama gasova sa efektom staklene bašte u životnom ciklusu biodizela (16%). Kumulativan doprinos rezultata indikatora ostalih kategorija uticaja (zakišeljavanje zemljišta, eutrofrikacija vodnih resursa, ekotoksičnost i transformacija prirodnih staništa) ukupnom uticaju na raznolikost ekosistema je svega 1% (tabela 5). Procesi u vezi sa životnim ciklusom 1000 kg biodizela zauzimaju 0,67 ha poljoprivrednog zemljišta (tabela 5).

Šteta zbog umanjene raspoloživosti mineralnih resursa je skoro u potpunosti posledica smanjenja mineralnih rezervi fosilnih goriva (99%). U proizvodnom lancu 1000 kg biodizela koriste se fosilna goriva u količini od 504 kg $Nafta_{ekv.}$ (tabela 5). U ReCiPe metodi se uzima da je energetski sadržaj 1 kg $Nafta_{ekv.}$ 42 MJ što znači da je za dobijanje 1000 kg biodizela potrebno iskoristiti 21168 MJ energije iz fosilnih izvora. Odnosno, za dobijanje 1 MJ energije u biodizelu potrebno je iskoristiti 0,56 MJ energije iz fosilnih izvora (računato na osnovu donje toplotne moći biodizela od 37,8 MJ/kg), što je znatno manje energije nego što se iskoristi za dobijanje iste količine energije u fosilnom dizelu (1,29 MJ prema [10]).

Slika 3 pokazuje doprinos pojedinih faza životnog ciklusa biodizela rezultatu indikatora na međupozicijama mehanizma životne sredine. Rezultati indikatora svih kategorija uticaja su uglavnom određeni fazama proizvodnje zrna i sagorevanja biodizela.

Šteta koja nastaje po funkcionalnoj jedinici u kategoriji uticaja „šteta zbog narušavanja ljudskog zdravlja“ je procenjena na 7,48E-03 DALY ekvivalenta, u kategoriji uticaja „šteta naneta raznolikosti ekosistema“ na 1,48E-04 br. vrsti·god., a u kategoriji uticaja „šteta zbog umanjene raspoloživosti mineralnih resursa“ na 8,11E+03 US$ (tabela 5). Doprinos pojedinih faza život-

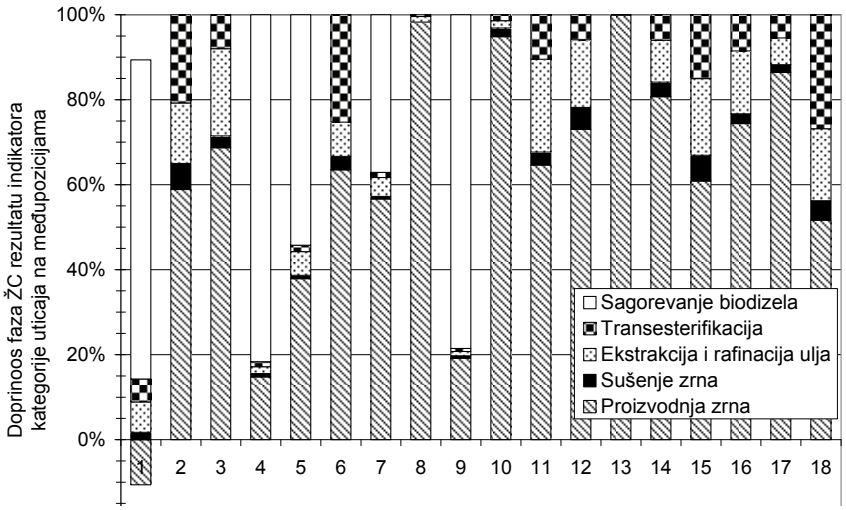

Slika 3. Doprinos pojedinih faza životnog ciklusa rezultatu indikatora na međupozicijama; brojčane oznake na horizontalnoj osi označavaju kategorije uticaja sa istim rednim brojem kao u tabeli 5.
Figure 3. Contribution of life cycle phases to midpoint indicator results.

nog ciklusa i jediničnih procesa rezultatu indikatora kategorija uticaja na krajnjim pozicijama prikazan je u tabeli 6.

Ukupan uticaj životnog ciklusa biodizela (ukupan negativan uticaj životnog ciklusa umanjen za ukupan pozitivan uticaj zbog apsorpcije CO_2 u procesu foto-

Tabela 6. Doprinos pojedinih faza i procesa rezultatu indikatora na krajnjim pozicijama (%)
Table 6. Contribution of life cycle phases and processes to the endpoint indicator results (%)

Faze i procesi	Šteta zbog narušavanja ljudskog zdravlja	Šteta naneta raznolikosti ekosistema	Šteta zbog umanjene raspoloživosti mineralnih resursa
Proizvodnja zrna	9,4	81,6	51,6
Zauzimanje zemljišta	0,0	54,8	0,0
Emisije iz zemljišta	28,5	33,7	0,0
Proizvodnja đubriva	23,5	5,7	34,1
Dizel gorivo	7,2	1,3	15,9
Apsorpcija CO_2	-50,5	-14,4	0,0
Ostalo	0,2	0,3	0,3
Transport	0,5	0,1	1,3
Sušenje zrna	1,6	0,4	4,6
Proizvodnja električne energije	0,2	0,0	0,3
Dobijanja toplotne energije	0,9	0,2	2,8
Transport	0,5	0,1	1,4
Ekstrakcija i rafinacija ulja	7,7	1,6	16,9
Proizvodnja električne energije	4,7	0,7	7,2
Dobijanja toplotne energije	2,9	0,8	9,3
Proizvodnja hemikalija	0,1	0,1	0,4
Transport	0,0	0,0	0,0
Transesterifikacija	4,5	1,2	26,9
Proizvodnja električne energije	0,5	0,1	0,8
Dobijanja toplotne energije	1,7	0,5	7,0
Proizvodnja hemikalija (bez metanola)	0,7	0,2	2,0
Proizvodnja metanola	1,5	0,4	16,6
Transport	0,2	0,0	0,5
Sagorevanje biodizela	76,8	15,3	0,0
Ukupno ŽC	100,0	100,0	100,0

sinteze) je procenjen na 540 Pt (tabela 7). U ukupnom uticaju, šteta zbog narušavanja ljudskog zdravlja, šteta naneta raznolikosti ekosistema i šteta zbog umanjene raspoloživosti mineralnih resursa učestvuju sa 27%, 63% i 10%, redom (tabela 7). Proizvodni lanac biodizela je odgovoran za oko 70% ukupnog uticaja životnog ciklusa, dok preostali deo prouzrokuje faza sagorevanja biodizela. U proizvodnom lancu biodizela faza proizvodnje zrna uljane repice prouzrokuje oko 85% ukupnog uticaja (tabela 7).

Doprinos pojedinih procesa ukupnom negativnom uticaju pojedinih faza proizvodnog lanca biodizela dat je na slici 4. Svega nekoliko procesa prouzrokuje 90% ukupnog negativnog uticaja koji nastaje u proizvodnom lancu biodizela. Uticaji vezani za proizvodni lanac i primenu mineralnih đubriva koji se koriste pri proizvodnji uljane repice su odgovorni za 47% ukupnog negativnog uticaja proizvodnog lanca biodizela. Proizvodni lanac mineralnih đubriva prouzrokuje 15%, dok emisije N_2O i NH_3 iz zemljišta koje nastaju volatizacijom i denitrifikacijom azota iz amonijačno-nitratnog đubriva prouzrokuju 32% negativnog uticaja proizvodnog lanca biodizela. Zauzimanje zemljišta u poljoprivrednoj fazi je odgovorno za 38% negativnog uticaja proizvodnog lanca biodizela (slika 4).

ReCiPe metod omogućuje vrednovanje uticaja na životnu sredinu preko 320 elementarnih tokova iz rezultata inventarisanja životnog ciklusa biodizela. Međutim, rezultati pokazuju da je svega 10 elementarnih tokova odgovorno za 98% ukupnog negativnog uticaja životnog

Tabela 7. Doprinos pojedinih kategorija uticaja i faza životnog ciklusa ukupnom uticaju životnog ciklusa 1000 kg biodizela (u Pt)
Table 7. Contribution of life cycle phases and impact categories to the overall impact of 1000 kg of biodiesel (in Pt)

Kategorije uticaja	Uticaj pojedinih faza ŽC biodizela (Pt)					Ukupno (Pt)
	Proizvodnja zrna	Sušenje zrna	Dobijanje ulja	Transesterifikacija	Sagorevanje biodizela	
Ljudsko zdravlje	13,9	2,4	11,4	6,7	113,7	148,1
Globalno zagrevanje	-11,2	1,8	7,5	5,7	79,2	83,0
Formiranje suspendovanih čestica	24,1	0,5	3,5	1,0	34,5	63,6
Ostalo	1,0	0,0	0,3	0,1	0,0	1,4
Ekosistem	277,1	1,3	5,3	3,9	52,0	339,6
Globalno zagrevanje	-7,3	1,2	4,9	3,7	51,8	54,3
Zauzimanje poljoprivrednog zemljišta	282,1	0,0	0,0	0,0	0,0	282,2
Ostalo	2,2	0,1	0,4	0,2	0,2	3,1
Resursi	27,4	2,4	9,0	14,2	0,0	53,0
Ukupno (Pt)	318,3	6,1	25,6	24,9	165,7	540,7

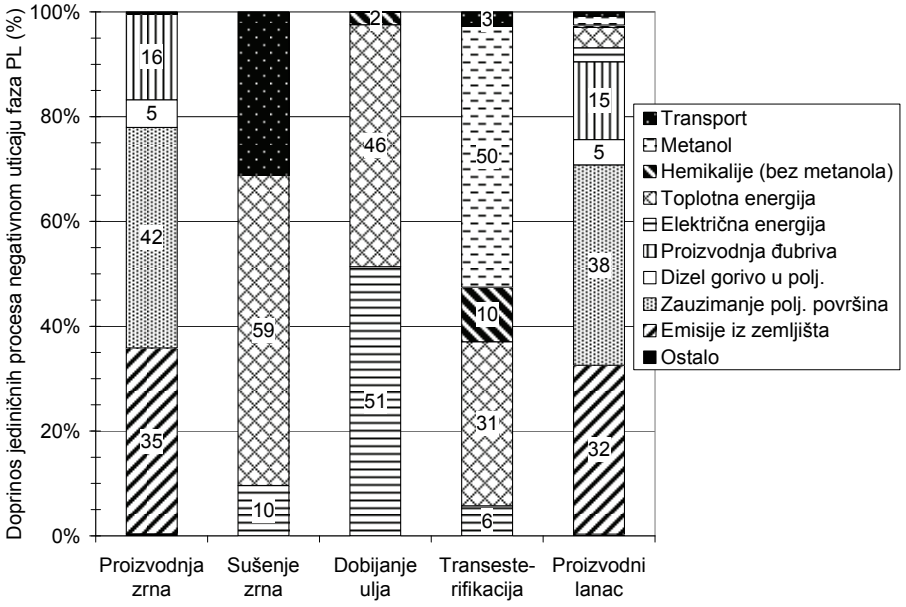

Slika 4. Doprinos jediničnih procesa ukupnom negativnom uticaju pojedinih faza proizvodnog lanca.
Figure 4. Contribution of unit processes to the overall negative impacts caused by the production chain.

ciklusa biodizela (slika 5). Posmatrano na nivou pojedinačnih elementarnih tokova „zauzimanje poljoprivredne površine“ prouzrokuje oko polovine uticaja u životnom ciklusu biodizela. Emisije u vazduh su odgovorne za oko 37%, a eksploatacija rezervi fosilnih goriva za oko 9% uticaja životnog ciklusa biodizela. Emisije u vodu i zemljište imaju mali uticaj na formiranje ukupnog uticaja životnog ciklusa biodizela (<2%) (slika 5).

Zahvalnica

Autori su zahvalni Ministarstvu prosvete, nauke i tehnološkog razvoja Republike Srbije na finansijskoj podršci ovog istraživanja — Projekat OI 172059.

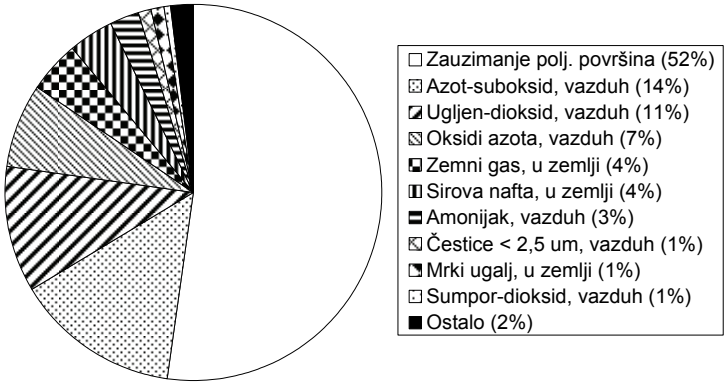

Slika 5. Doprinos pojedinačnih elementarnih tokova ukupnom uticaju životnog ciklusa.
Figure 5. Contribution of specific elementary flows to the overall impact of the life cycle.

ZAKLJUČCI

Prema rezultatima analize najveći izazov održivoj proizvodnji biodizela predstavljaju značajne poljoprivredne površine koju zauzimaju procesi u proizvodnom lancu biodizela. Zauzimanje poljoprivrednih površina je odgovorno za oko 80% štete koju procesi u vezi sa proizvodnim lancem biodizela nanose raznolikosti ekosistema i za 38% ukupnog negativnog uticaja proizvodnog lanca biodizela. Drugi faktor koji ima važan uticaj na formiranje rezultata LCA biodizela je količina i vrsta primenjenih mineralnih đubriva pri gajenju uljane repice. Rezultati analize su pokazali da su tokovi vezani za proizvodni lanac i primenu mineralnih đubriva odgovorni za skoro polovinu ukupnog negativnog uticaja proizvodnog lanca biodizela iz uljane repice. Samo emisije N_2O i NH_3 koje nastaju u procesima denitrifikacije i volatizacije azota iz amonijačno-nitratnog đubriva prouzrokuju skoro trećinu ukupnog negativnog uticaja proizvodnog lanca biodizela.

S obzirom na to da su prinosi uljane repice u Vojvodini znatno ispod prosečnih prinosa u Evropskoj uniji, potrebno je ispitati mogućnost povećanja prinosa uljane repice po jedinici površine uz zadržavanje inputa na postojećem nivou, pre svega racionalnijom upotrebom mineralnih đubriva i blagovremenim izvođenjem agrotehničkih operacija.

LITERATURA

[1] T. Tešić, F. Kiš, V. Janković, Mogućnost proizvodnje i korišćenja biodizela u AP Vojvodini, Monografija, Vojvođanska akademija nauka i umetnosti, Novi Sad, 2008.

[2] D. Skala, S. Glišić, BIODIZEL – I. Istorijat, proizvodnja i standardi, Hem. ind. **58**(2) (2004) 73–78.

[3] I.S. Stamenković, I.B. Banković-Ilić, O.S. Stamenković, V.B. Veljković, D.U. Skala, Kontinualni postupci dobijanja biodizela, Hem. ind. **63**(1) (2009) 1–10.

[4] M. Lapuerta, O. Armas, J. Rodriguez-Fernandez, Effect of biodiesel fuels on diesel engine emissions, Prog. Energy Combust. Sci. **34** (2008) 198–223.

[5] C.M. Gasol, J. Salvia, J. Serra, A. Anton, E. Sevigne, J. Rieradevall, X. Gabarrell, A life cycle assessment of biodiesel production from winter rape grown in Southern Europe, Biomass. Bioenerg. **40** (2012) 71–81.

[6] J. Malca, F. Freire, Life-cycle studies of biodiesel in Europe: A review addressing the variability of results and modeling issues, Renew. Sust. Energ. Rev. **15** (2011) 338–351.

[7] A. Iriarte, J. Rieradevall, X. Gabarrell, Life cycle assessment of sunflower and rapeseed as energy crops under Chilean conditions, J. Clean. Prod. **18** (2010) 336–345.

[8] A. Iriarte, J. Rieradevall, X. Gabarrell, Transition towards a more environmentally sustainable biodiesel in South America: The case of Chile, Appl. Energ. **91** (2012) 263––273.

[9] SRPS ISO 14040: (2008): Upravljanje zaštitom životne sredine – Ocenjivanje životnog ciklusa – Principi i okvir. Institut za standardizaciju Srbije, Beograd, Srbija.

[10] N. Jungbluth, Erdöl. Sachbilanzen von Energiesystemen, Ecoinvent report version 2.0, Vol. 6, Swiss Centre for LCI, Duebendorf and Zurich, 2007.

[11] A.L. Stephenson, J.S. Dennis, S.A. Scott, Improving the sustainability of the production of biodiesel from oilseed rape in the UK. Process. Saf. Environ. **86** (2008) 427––440.

[12] N.D. Mortimer, P. Cormack, M.A. Elsayed, R.E. Horne, Evaluation of the comparative energy, global warming and socio-economic costs and benefits of biodiesel, Final Report, Resources research unit school of environment and development, Sheffield Hallam University, 2003.

[13] S. Bernesson, D. Nilsson, P.A. Hansson, A limited LCA comparing large- and small-scale production of rape methyl ester (RME) under Swedish conditions. Biomass. Bioenerg. **26** (2004) 545–559.

[14] T. Tsoutsos, V. Kouloumpis, T. Zafiris, S. Foteinis, Life Cycle Assessment for biodiesel production under Greek climate conditions, J. Clean. Prod. **18** (2010) 328–335.

[15] F. Kiš, Ekonomsko vrednovanje ekoloških efekata primene biodizela. Doktorska disertacija. Poljoprivredni fakultet, Univerzitet u Novom Sadu, Novi Sad, 2011.

[16] Republički zavod za statistiku, Površine pod uljanom repicom u Republici Srbiji u periodu 2005-2009, http://webrzs.stat.gov.rs/axd/poljoprivreda/index.php?ind=1 (jun, 2012).

[17] K. Refsgaard, N. Halberg, E.S. Kristensen, Energy utilization in crop and dairy production in organic and conventional livestock production systems. Agric. Syst. **57** (1998) 599–630.

[18] Lj. Babić, M. Babić, M. Brkić, Sušenje i skladištenje uljanih kultura, u: T. Furman (Ed.), Biodizel – proizvodnja i korišćenja, Monografija, Institut za poljoprivrednu tehniku, Novi Sad, 1995, str. 73–99.

[19] J. Schmidt, Life assessment of rapeseed oil and palm oil, Part 3: Life cycle inventory of rapeseed oil and palm oil, PhD thesis, Department of Development and Planning, Aalborg University, 2007.

[20] F. Kiss, M. Jovanović, G. Bošković, Economic and ecological aspects of biodiesel production over homogeneous and heterogeneous catalysts, Fuel Process. Technol. **91** (2010) 1316–1320.

[21] T. Nemecek, T. Kägi, S. Blaser, Life Cycle Inventories of Agricultural Production Systems, Ecoinvent report version 2.0, Vol. 15., Swiss Centre for LCI, Dübendorf and Zurich, 2007.

[22] M. Spielmann, R. Dones, C. Bauer, Life Cycle Inventories of Transport Services, Ecoinvent report version 2.0, Vol. 14., Swiss Centre for LCI, PSI, Dübendorf and Villigen, 2007.

[23] R. Frischknecht, M. Faist Emmenegger, Strommix und Stromnetz. Sachbilanzen von Energiesystemen, Ecoinvent report version 2.0, Vol. 6., Swiss Centre for LCI, PSI, Dübendorf and Villigen, 2007.

[24] N. Jungbluth, M. Chudacoff, A. Dauriat, F. Dinkel, G. Doka, M. Faist Emmenegger, E. Gnansounou, N. Kljun, M. Spielmann, C. Stettler, J. Sutter, Life Cycle Inventories of Bioenergy, Ecoinvent report version 2.0, Vol. 17., Swiss Centre for LCI, ESU. Dübendorf and Uster, 2007.

[25] H. J. Althaus, M. Chudacoff, R. Hischier, N. Jungbluth, M. Osses, A. Primas, Life Cycle Inventories of Chemicals, Ecoinvent report version 2.0, Vol. 8., Swiss Centre for LCI, Empa – TSL, Dübendorf, 2007.

[26] D. Kellenberger, H. J. Althaus, N. Jungbluth, T. Künniger, Life Cycle Inventories of Building Products, Ecoinvent report version 2.0, Vol. 7., Swiss Centre for LCI, Empa – TSL, Dübendorf, 2007.

[27] M. Faist Emmenegger, T. Heck, N. Jungbluth, "Erdgas. Sachbilanzen von Energiesystemen", Ecoinvent report version 2.0, Vol. 6., Swiss Centre for LCI, PSI, Dübendorf and Villigen, 2007.

[28] J. Sutter, Life Cycle Inventories of Highly Pure Chemicals, Ecoinvent report version 2.0, Vol. 19, Swiss Centre for LCI, ETHZ, Dübendorf and St. Gallen, 2007.

[29] M. Goedkoop, R. Heijungs, M. Huijbregts, A. De Schryver, J. Struijs, R. van Zelm, ReCiPe 2008. A life cycle impact assessment method which comprises harmonised category indicators at the midpoint and the endpoint level, 1st ed., Ministry of Housing, Spatial Planning and the Environment, Netherlands, 2009.

[30] J.B. Guinée (Ed.), Life Cycle Assessment - An operational guide to the ISO standards, Part 2a, Ministry of Housing, Spatioal Planning and the Environment and Centre of Environmental Science, Leiden University, 2001.

[31] M. Goedkoop, R. Spriensma, The Eco-indicator 99. A damage oriented method for Life Cycle Impact Assessment, 3rd ed., Amersfoort: PRé consultants, 2001.

SUMMARY

LIFE CYCLE IMPACT ASSESSMENT OF BIODIESEL USING THE ReCiPe METHOD

Ferenc E. Kiss, Goran C. Bošković

University of Novi Sad, Faculty of Technology, Novi Sad, Republic of Serbia

(Scientific paper)

This paper presents the life cycle impact assessment (LCIA) results of biodiesel produced from rapeseed oil. The functional unit (FU) is defined as 3750 km of distance traveled by a truck fuelled with biodiesel. The reference flow is 1000 kg of biodiesel. The LCIA method used in the study is the ReCiPe method. At midpoint level the ReCiPe method addresses environmental issues within 18 impact categories. Most of these midpoint impact categories are further converted and aggregated into 3 endpoint categories (damage to human health, damage to ecosystem diversity, damage to mineral resource availability). The total impact of biodiesel's life cycle was estimated at 540 Pt/FU. The damage to ecosystem diversity (1.48×10^{-4} species·year/FU), the damage to human health (7.48×10^{-3} DALY/FU) and the damage to mineral resource availability (8.11×10^{3} US$/FU) are responsible for 63, 27 and 10% of the total negative impact in the life cycle of biodiesel, respectively. The results have revealed that only 4 impact categories are responsible for most of the impacts within the specific endpoint categories. These are impacts associated with global warming (3000 kg $CO_{2,ekv.}$/FU), particulate matter formation (12.4 kg $PM_{ekv.}$/FU), agricultural land occupation (6710 m^2a/FU) and fossil fuel depletion (21168 MJ/FU). Greenhouse gases emitted in the life cycle of biodiesel (mainly N_2O and CO_2) are responsible for 56% of the damage caused to human health and for 16% of the damage caused to ecosystem diversity. Airborne emissions which contribute to particulate matter formation (NO_x, NH_3, PM and SO_2) are responsible for 43% of the damage caused to human health. Agricultural land occupation is responsible for 82% of the damage caused to the ecosystem diversity. Damage to mineral resource availability is almost entirely related to the depletion of fossil energy sources. The production chain of biodiesel and the combustion of biodiesel are responsible for 69% and 31% of the total impact of biodiesel's life cycle, respectively. The negative impact of the production chain is mainly related to biodiversity loss due to agricultural land occupation (38%) and the life cycle impacts of mineral fertilizers used in the production of rapeseed (47%). The environmental impact of biodiesel can be reduced by increasing the yield of rapeseed with more efficient use of fertilizers and optimization of agro-technical processes.

Keywords: Biodiesel • Rapeseed • Life cycle assessment • ReCiPe Method

Characteristics of meat packaging materials and their environmental suitability assessment

Danijela Z. Šuput[1], Vera L. Lazić[1], Ljubinko B. Lević[1], Nevena M. Krkić[1], Vladimir M. Tomović[1], Lato L. Pezo[2]

[1]*University of Novi Sad, Faculty of Technology, Novi Sad, Serbia*
[2]*University of Belgrade, Institute of General and Physical Chemistry, Belgrade, Serbia*

Abstract

After the functional phase, packaging becomes waste that is recycled or disposed of in landfills. Recently, numerous packages have been developed for assessing the packaging risk on the environment. We applied GaBi 4 Education software on polymer product packaging for meat products. The objective of the first part of the paper was characterization of materials used for meat and meat products packaging in terms of mechanical and barrier properties. The results showed that the tested materials were able to keep a protective atmosphere and contribute to the quality and sustainability of the product. Air permeability was 3.60 and 26.60 ml m^{-2}/24 h, and water vapor permeability was 6.90 and 9.50 ml m^{-2}/24 h, respectively, for foils 1 and 2, as a result of different film composition. In the second part, based on real data, GaBi 4 Education software was applied. The obtained results showed that organic compounds emissions had the highest impact on human health and the most damaging environmental impact observed was the emission of CO_2.

Keywords: materials and packaging, environmental impact, meat products.

Available online at the Journal website: http://www.ache.org.rs/HI/

PROFESSIONAL PAPER

UDC 637.5:621.798:54

Hem. Ind. **67** (4) 615–620 (2013)

doi: 10.2298/HEMIND120907104S

One of the main challenges for the European Union is to reach sustainable development [1] because one of the main negative consequences of „plastic revolution“ is the often-emphasised question of plastic waste disposal. This is why packaging has been targeted as one of the most severely polluting activities. As a result, many countries around the world now have measures in place aiming at reduction of packaging waste [2]. A Life Cycle Assessment (LCA) is generally considered the best environmental management tool that can be used to to define designing and operating criteria able to make a programme of recycling and recovery of plastics, economically affordable, and, at the same time, socially acceptable and environmentally effective [3,4]. By a definition LCA is a process „to evaluate environmental burdens related to products, processes or activities, to identify potential impacts on the environment coming from energy or material consumptions, to identify and to evaluate possible product improvements“ [5]. LCA is a methodology for quantifying the potential environmental impacts associated with a product, process or activity. This method has become an important tool for authorities and industries in order to compare alternative products, processes or services [6] and to identify environmental and critical points where the environmental management system should be improved. LCA has a wide-ranging application in decision making, product and process design, research and development, purchasing, information for defining company strategies, identification of areas of improvement, selection of environmental indicators, environmental labeling and ecological product statement [7].

LCA is an ISO standardized method [8–11]. The four steps characterizing a general application of LCA, as defined in the UNI EN ISO 14040 norm, are: definition of goal and scope, inventory analysis, impact assessment and interpretation. Such steps do not describe a static process – they use feedback operation to fine-tune initial objectives and to enable the quality of final results to be improved [12]. The aim of LCA is to provide a picture of an activity and its interaction with the environment at the present level of knowledge; contribute to the understanding of the overall and independent nature of the environmental consequences of human activities; provide decision makers with information about possible environmental improvements [2].

The two most commonly used systems chosen in LCA studies are „cradle-to-factory gate“ and „cradle-to-grave“. A „cradle-to-factory gate“ LCA study includes steps from the extraction of raw materials and fuels, conversion steps up and until the product is delivered at the factory gate (published by material producers). The system „cradle-to-grave“ covers all steps of the system „cradle-to-factory gate“ and in addition, the usage and the disposal phase [13]. Nevertheless, depending on the specific requirements, LCA may also be used in a limited perspective (from „process-to-process“ or from „gate-to-gate“), which can be of par-

Correspondence: D.Z. Šuput, University of Novi Sad, Faculty of Technology, Bulevar Cara Lazara 1, 21000 Novi Sad, Serbia.
E-mail: suput.danijela@gmail.com
Paper received: 7 September, 2012
Paper accepted: 24 October, 2012

ticular interest if the limited part of the whole life cycle should be analysed [12].

In recent years, several LCA studies have focused on food products, such as basic carbohydrate food (bread, potatoes, rice and pasta), fruit and vegetables, dairy products, meat products, fish production and processing [14] as well as canned tuna fish [15], cooked dish [16], ready meals sector [7], but not meat and meat products.

The variables that influence shelf life properties of packaged meat are product type, gas mixture, package and headspace, packaging equipment, storage temperature and additives [17]. Traditionally, the plastic films used for vacuum and modified atmosphere packaging (MAP), techniques that are used in the meat industry to extend the product shelf-life [18], were developed to improve their gas and moisture barriers, shrinking properties, sealing characteristics, cook-in and retort capability and a variety of print and color options. McMillin briefly reviews materials that could be used as packaging [19]. The use of multilayered film including a barrier layer might not be desirable in respect to recycling issues. Any assessment of the environmental impact of food packaging must consider the positive benefits of reduced food waste in the supply chain. Food packaging accounted for almost 2/3 of total packaging waste by volume and food packaging accounted for about 50% by weight of total packaging sales.

In this work, we sampled packaging materials and recorded all necessary data from real system related to packaging process, distribution, sale, meat consumption and packaging disposal, with the aim of applying LCA analysis in order to evaluate damaging system points for the environment.

EXPERIMENTAL

Film samples were provided by a national company that produces meat products and wished to stay anonymous because they import packaging materials. Film samples had different composition: transparent PVC//PE–EVOH-PE, that forms the tray, down foil (foil 1) and PET//PE-EVOH-PE, that forms the closing, upper foil (foil 2).

Film thickness was measured using a micrometer with sensitivity of 0.001 mm. Five thickness measurements were carried out on each film, from which an average was obtained.

Mechanical properties. Prior to the testing of mechanical properties, the films were conditioned for 48 h, at 25±0.5 °C and 50±5% relative humidity (RH). Tensile strength (TS) and elongation to break (EB) of films were measured on the Instron Universal Testing Instrument Model No 4301 (Instron Engineering Corp., Canton, MA), according to ASTM standard method D882-01 [20].

Water vapor permeability (WVP) was determined gravimetrically according to the ASTM E 96-95 desiccant method [21]. The method involves sealing a known open area of an impermeable container with the film being tested. Anhydrous silica gel was used to maintain 0% atmosphere inside the cells. Distilled water was used to maintain 100% RH outside the cells. Test cells were stored under temperature 23±2 °C and weighed periodically until a constant rate of weight gain was reached. Obtained weighting values were used for calculation of the amount of moisture transferred through the film.

Permeability of gasses was measured using method by Lyssy, according to DIN 53 380 on the device Lyssy GPM-200 with an appropriate gas chromatograph Gasukuro Kogyo GC-320 and HP 3396 integrator.

Life cycle analysis (LCA) was conducted by using GaBi 4 Education software that allows life cycle assessment.

Statistical analysis. Descriptive statistical analyses for calculating the means and the standard error of the mean, analysis of variance (ANOVA) and post-hoc Tukey's tests were performed using StatSoft Statistica for Windows ver. 10. All obtained results were expressed as the mean±standard deviation (*SD*).

RESULTS AND DISCUSSION

Thickness determines the mechanical characteristics and essential is for the regular formation of packaging units. The film thickness for layers 1 and 2 samples were 302.50±4.00 and 61.90±0.60 μm, respectively. The obtained results point to the good uniformity of thickness at all positions.

The mechanical properties of packaging materials and packaging are tensile strength (TS) and elongation at break (EAB). These characteristics are important because they show the benefits of a material for proper application, as well as resistance during transport, handling and storage. Tensile strength and elongation at break of specimens cut longitudinally have twice the value of transversally cut specimens (Table 1). The results of tensile strength and elongation at break confirmed the good mechanical properties of tested materials.

Table 1. Tensile strength and elongation at break (mean±SD from N = 5 measurements) for longitudinally and transversally cut foils 1 and 2; different letters printed within the same raw show significantly different means of observed data (p < 0.05), 95% confidence limit, according to post-hoc Tukey's test

Mechanical properties	Sample foil	*TS*, N/15mm	*EAB* / %
Longitudinal	1	0.31 ± 0.01^{d}	44.90 ± 13.70^{d}
	2	0.21 ± 0.01^{c}	6.60 ± 2.10^{c}
Transversal	1	0.15 ± 0.01^{b}	23.10 ± 5.90^{b}
	2	0.12 ± 0.01^{a}	3.20 ± 1.00^{a}

Results related to water vapour permeability (WVP) ml m^{-2}/24 h were 6.90±0.19 and 9.50±0.06 ml m^{-2}/24 h, respectively, for foils 1 and 2 (mean±*SD* from 5 measurements). According to composition of foil 1 it is obvious that PVC contributes to excellent barrier property (WVP for PVC is 1.5-5 ml m^{-2}/24 h). In case of layer 2, WVP of PET and PE are similar [5]. There is a gas permeability through all polymer packaging materials to a lesser or greater extent which determines their usage for packaging of certain food products. Since these materials will be used for modified atmosphere packaging, special attention should be taken to CO_2 and N_2 permeability. Compared to results obtained by Lazić *et al.* [22], who analysed similar packed meat products, our results show better properties regarding CO_2 and N_2 permeabilities.

Results for the permeability of gases are shown in Table 2.

Table 2. Gas permeability (ml m^{-2}/24 h) for foils 1 and 2 samples (mean±SD from N = 5 measurements); different letters printed within the same raw show significantly different means of observed data (p < 0.05), 95% confidence limit, according to post-hoc Tukey's test

Foil	CO_2	O_2	N_2	Air permeability
1	23.80±6.90[a]	15.50±7.60[a]	0[a]	3.60±2.10[a]
2	23.90±4.00[a]	26.00±0.60[b]	26.90±3.50[b]	26.60±2.60[b]

We collected all necessary data related to the packaging process (capacity of packing machine, machine power, working hours, water and electricity consumption, transport packaging, etc.), distribution, sale, consumption and packaging disposal. Our packaging machine takes both layers to form the packaging, and packs 100 g of meat product. Afterwards, 12 packs are put into cardboard boxes and form transport packaging. We took into account distribution, sale and meat consumption. The plan considered plastic materials as waste and cardboard boxes as recyclables.

GaBi 4 Education software demands a functional unit to be defined. The functional unit is a quantified unit of the system's function by some physical unit. We declared one packaging as a functional unit so the scaling factor was set to 15000 because of the plant capacity, which was 500 kg packed meat per day (30 days×500 kg = 15000 kg per month).

System boundaries were set as gate-to-gate. This approach of an LCA involves the assessment of the environmental impact of each phase of working life and end of life (EoL) treatment (including recycling and disposal). After connecting individual processes are recorded in the system, the software runs a balance calculation that provides the results.

The first LCA phase consists of calculating the amount of energy and raw materials during the life cycle, and this process gives an inventory of all inputs and outputs (Table 3). The second LCA stage involves the evaluation of the effects of the elements that have impact on the environment, and this is how becomes an environmental load factor (Figures 1 and 2).

Table 3 indicates that among all system flows, air emission has the greatest impact: organic emission (4407.90), followed by emission of heavy metals (2902.30) and inorganic emission (2768.30). Emissions in fresh and sea water and soil are insignificant compared to the emissions into the air. Table 3 shows that power has the largest effect, which actually means the packaging process, because that is the point where the most power is used. An emission reduction proposal would be a modification of the packaging process.

Between many of the parameters that originally belong to the GaBi 4 Education software, we could choose the units we want to represent our results. We chose Human Toxicity Potential and Global Warming Potential as quantities of our process of packaging negative influence on humans and nature. Emissions

Table 3. Total and particular emissions

Process		Flows	Board boxes	Landfill of plastic	Drinking water	Power
Emissions to air	Heavy metals to air	2902.36	0.15	0.010	101.10	2801.10
	Inorganic emissions to air	2768.29	0.17	0.010	12.60	2755.51
	Organic emissions to air (group VOC)	4407.88	0.02	0.010	2.80	4405.05
	Particles to air	20.80	0	0.001	2.50	18.30
Emissions to air (total)		10099.33	0.34	0.031	119.00	9979.96
Emissions to water	Emissions to fresh water	88.13	0.02	0.006	2.00	86.10
	Emissions to sea water	8.41	0	0.001	0.41	8.00
Emissions to water (total)		96.54	0.02	0.007	2.41	94.10
Emissions to industrial soil		18.62	0.01	0.001	0.01	18.60
Flows - total		10214.49	0.37	0.039	121.42	10092.66

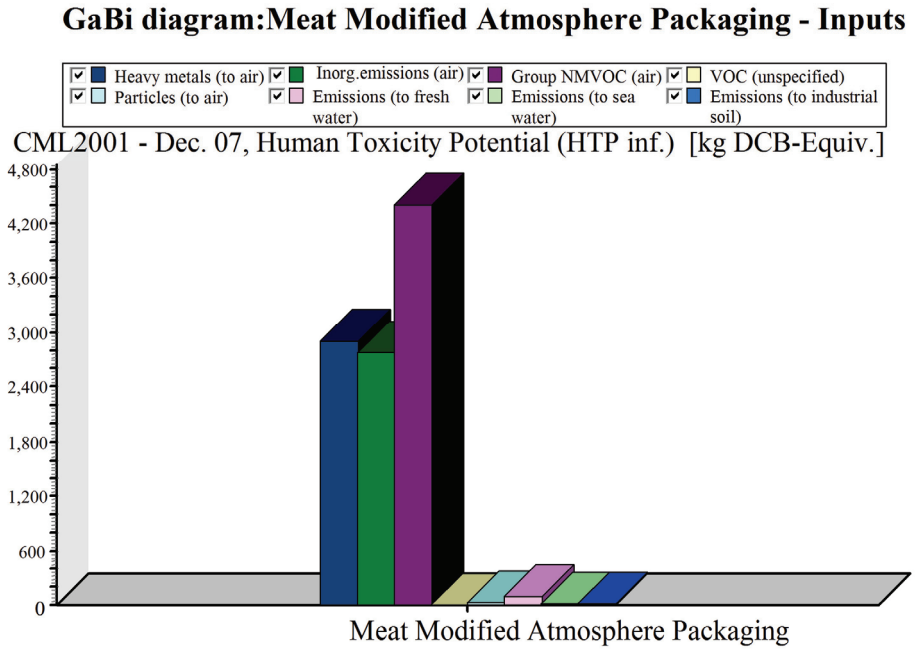

Figure 1. Impact of emissions by using Human Toxicity Potential.

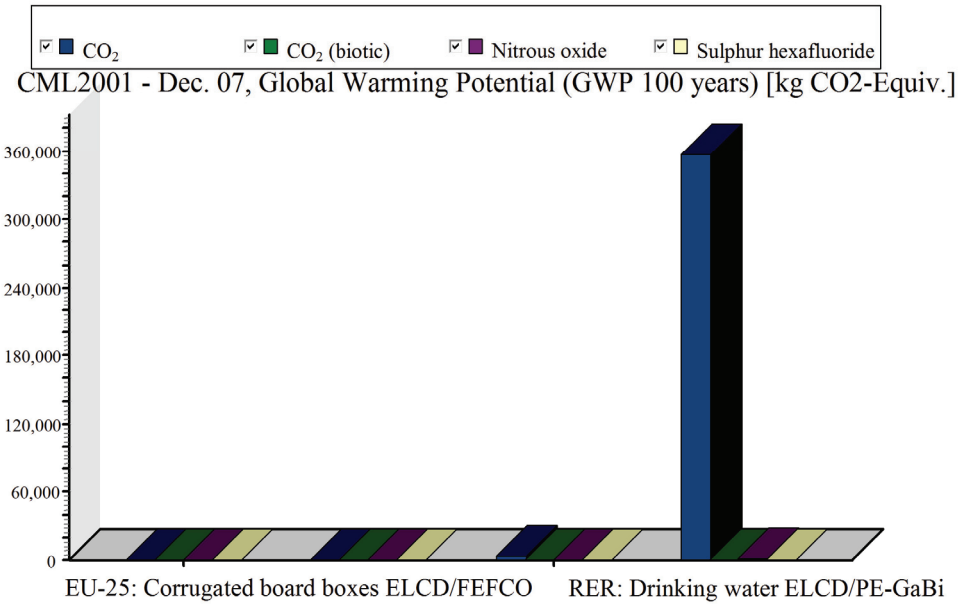

Figure 2. Impact of emissions by using Global Warming Potential.

and impact of emissions are presented in the coming tables and figures.

Result characterization allows us to convert the results in reference units (for example kg DCB-Equiv or kg CO_2/Equiv.) so that each unit is multiplied by a factor and then all function members summarized and unit of the sum is expresses as kg DCB-Equiv. or kg CO_2-Equiv.

We used CML2001 – Dec. 07, Human Toxicity Potential (HTP inf., kg DCB-Equiv.) as a quantity in the plan Meat Modified Atmosphere Packaging. By using weak point analysis, the highest impact on human health came from emission to air, especially organic emission to air, which can be seen in Table 3 and Figure 1.

By using CML 2001 – Dec 07, Global Warming Potential (GWP 100 years, kg CO_2/Equiv.) as a quantity in the plan Meat Modified Atmosphere Packaging, we got further results (Figure 2), which pointed out to CO_2 as a main pollutant.

CONCLUSION

The examined packaging materials can be successfully used on packaging lines of different meat products

in vacuum or modified atmosphere, which was proven by good mechanical and barrier characteristics. Good mechanical properties are important for good material resistance and proper application. Low values of water vapour (6.90±0.19 and 9.50±0.06 ml m^{-2}/24 h, respectively, for foils 1 and 2) and gas permeabilities (less than 30 ml m^{-2}/24 h for O_2 and air) can guarantee that these materials will keep product quality during the declared shelf-life.

Since LCA has been proven to be a useful tool to identify the aspects critical to improve a sustainable production in food industry sector, providing information that can be applied to decision making, we used GaBi 4 Education software, to obtain results related to environmental pollution for our specific case study of meat packaging. It can be concluded that emission to air had the highest impact on human health, especially organic emission to air and CO_2 is indicated as a main pollutant in the field of global warming.

Acknowledgement

This work is part of the project "Osmotic dehydration of food – energy and environmental aspects of sustainable production", project number TR-31055, financed by the Ministry of Education, Science and Technological Development of the Republic of Serbia.

REFERENCES

[1] A. Dobon, P. Cordero, F. Kreft, S.R. Østergaard, M. Robertsson, M. Smolander, M. Hortal, The sustainability of communicative packaging concepts in the food supply chain. A case study: part 1. Life cycle assessment, Int. J. Life Cycle Assess. **16** (2011) 168–177.

[2] K. Sonneveld, The Role of Life Cycle Assessment as a Decision Support Tool for Packaging, Packag. Tech. Sci. **13** (2000) 55–61.

[3] R. Cliff, A. Doig, G. Finnveden, The Application of Life Cycle Assessment to Integrated Waste Management. Part 1 – Methodology, Trans. IchemE. **78(B)** (2000) 279–287.

[4] F.R. McDougall, P. White, M. Franke, P. Hindle, Integrated Solid Waste Management: a Life cycle Inventory, 2nd ed., Blackwell Science, Oxford, 2001.

[5] SETAC, A Conceptual framework for life cycle impact assessment. Pensacola, USA: SETAC (Society of Environmental Toxicology and Chemistry), 1993.

[6] G. Pardo, J. Zufía, Environmental impact of packaging and food losses, J. Clean. Prod. **28** (2012) 198–207.

[7] L.A. Calderón, L. Iglesias, A. Laca, M. Herrero, M. Díaz, The utility of Life Cycle Assessment in the ready meal food industry, Resour. Conserv. Recyc. **54** (2010) 1196–1207.

[8] ISO 14040, Environmental Management e Life Cycle Assessment e Principles and framework. International Organization for Standardization, Geneva, 1997.

[9] ISO 14041, Environmental management e Life cycle assessment e Goal and scope definition and life cycle inventory analysis. International Organization for Standardization, Geneva, 1998.

[10] ISO 14042, a. Environmental management e Life cycle assessment e Life cycle impact assessment. International Organization for Standardization, Geneva, 2000.

[11] ISO 14043, b. Environmental management e Life cycle assessment e Life cycle interpretation. International Organization for Standardization, Geneva, 2000.

[12] M. de Monte, E. Padoano, D. Pozzetto, Alternative coffee packaging: an analysis from a life cycle point of view, J. Food Eng. **66** (2005) 405–411.

[13] L. Shen, M.K. Patel, Life Cycle Assessment of Polysaccharide Materials: A Review, J. Polym. Environ. **16** (2008) 154–167.

[14] P. Roy, D. Nei, T. Orikasa, Q. Xu, H. Okadome, N. Nakamura, A review of life cycle assessment (LCA) on some food products, J. Food Eng. **90** (2009) 1–10.

[15] A. Hospido, M.E. Vazquez, A. Cuevas, G. Feijoo, M.T. Moreira, Environmental assessment of canned tuna manufacture with a life-cycle perspective, Resour. Conserv. Recyc. **47** (2006) 56–72.

[16] J. Zufia, L. Arana, Life cycle assessment to eco-design food products: industrial cooked dish case study, J. Clean. Prod. **16** (2008) 1915–1921.

[17] G.H. Zhou, X.L. Xu, Y. Liu, Preservation technologies for fresh meat – A review, Meat Sci. **86** (2010) 119–128.

[18] A.C. Seydim, J.C. Acton, M.A. Hall, P.L. Dawson, Effects of packaging atmospheres on shelf-life quality of ground ostrich meat, Meat Sci. **73** (2006) 503–510.

[19] K.W. McMillin, Review: Where is MAP Going? A review and future potential of modified atmosphere packaging for meat, Meat Sci. **80** (2008) 43–65.

[20] ASTM D 882-01, Standard test method for tensile properties of thin plastic sheeting. Annual Book of ASTM Standards, Designation D882-01, American Society for Testing Materials, Philadelphia, PA, 2001.

[21] ASTM E 96-95, Standard test methods for water vapor transmission of materials. Annual Book of ASTM Standards, No. E96-95, American Society for Testing and Materials, Philadelphia, PA, 1994.

[22] V. Lazic, N. Krkić, Lj. Petrović, T. Tasić, P. Ikonić, S. Savatić, B. Šojić, Svojstva ambalažnih materijala za pakovanje fermentisanih kobasica pod vakuumom i u modifikovanoj atmosfer, Tehnologija mesa **51** (2010) 95–102 (in Serbian).

IZVOD

KARAKTERISTIKE AMBALAŽNIH MATERIJALA ZA PAKOVANJE MESA I PROCENA NJIHOVE EKOLOŠKE PODOBNOSTI

Danijela Z. Šuput[1], Vera L. Lazić[1], Ljubinko B. Lević[1], Nevena M. Krkić[1], Vladimir M. Tomović[1], Lato L. Pezo[2]

[1]*Univerzitet u Novom Sadu, Tehnološki fakultet, Novi Sad, Srbija*
[2]*Univerzitet u Beogradu, Institut za opštu i fizičku hemiju, Beograd, Srbija*

(Stručni rad)

Upotrebljena ambalaža za pakovanje hrane postaje ambalažni otpad koji se gomila i predstavlja ozbiljan problem današnjice, pa je potrebno obratiti pažnju na celokupan životni ciklus ambalaže. Nakon funkcionalne faze (faze upotrebe), ambalaža postaje otpad koji se ili reciklira ili odlaže na deponije. U skorije vreme razvijeni su brojni softveri za procenu rizika ambalaže na životnu sredinu. U ovom radu korišćen je GaBi 4 Education. Kao primer, odabrani su ambalažni materijali koji se koriste u industriji mesa. S obzirom na to da meso i proizvodi od mesa predstavljaju supstrat osetljiv na delovanje spoljašnjih faktora, neophodno ih je tretirati adekvatnim metodama konzervisanja, ali i upakovati u barijerne materijale pod specifičnim uslovima (vakum, MAP). U prvom delu rada je data karakterizacija odabranih ambalažnih materijala u pogledu mehaničkih i barijernih karakteristika. S Obzirom na dobijene niske vrednosti propustljivosti vodene pare, 6,90±0,19 i 9,50±0,06 ml m^{-2}/24 h, redom za folije 1 i 2, kao i za propustljivosti gasova (vrednosti niže od 30 ml m^{-2}/24 h za O_2 i vazduh), može se zaključiti da su materijali barijerni i da omogućavaju očuvanje vakuma ili zaštitne atmosfere i time doprinose kvalitetu i održivosti proizvoda. U drugom delu rada na odabrane materijale primenjen je GaBi 4 Education softver na osnovu realnih podataka procesa pakovanja, distribucije, prodaje i odlaganja ambalažnog otpada. Softver omogućuje odabir prikaza rezultata kako bi se prikazale kritične tačke životnog ciklusa. Odabran je *Human Toxicity Potential* i *Global Warming Potential* kako bi ukazali na to koji parametri najviše utiču na zdravlje ljudi i zagađenje životne sredine. Rezultati su pokazali da na ljudsko zdravlje najviše utiče emisija organskih jedinjenja u vazduh, a da najštetniji uticaj na životnu sredinu ima emisija CO_2.

Ključne reči: Ambalaža i pakovanje • Uticaj na životnu sredinu • Proizvodi od mesa

Električna, mehanička i temperaturna karakterizacija komercijalno dostupnih LTCC dielektričnih materijala

Goran Radosavljević[1], Andrea Marić[2], Michael Unger[1], Nelu Blaž[2], Walter Smetana[1], Ljiljana Živanov[2]

[1]*Vienna University of Techology, Insitute for Sensor and Actuator Systems, Department of Applied Electronic Materials, Vienna, Austria*
[2]*Univerzitet u Novom Sadu, Fakultet tehničkih nauka, Departman za energetiku, elektroniku i telekomunikacije, Katedra za Elektroniku, Novi Sad, Srbija*

Izvod

U ovom radu su prikazane mehaničke, električne i temperaturne karakteristike nekih komercijalno dostupnih materijala koji se koriste za izradu komponenti, senzorskih sistema, itd., u LTCC (*Low Temperature Co-fired Techology*) tehnologiji. Poznavanje sastava materijala, kao i njegovih električnih i mehaničkih karakteristika predstavlja veoma bitnu informaciju koja je neophodna kako bi se na uspešan način mogle projektovati različite komponente. Obično, proizvođači materijala u tehničkoj dokumentaciji ne prikazuju sve relevantne karakteristike materijala i zbog toga je praktično nemoguće predvideti ponašanje sistema ili komponenti u realnom okruženju. Analizirana su tri materijala koja se koriste za izradu komponenti i sistema u LTCC tehnologiji, firme Heraeus (Heraeus CT700, Heraeus CT707 i Heraeus CT800) i urađena je njihova električna, mehanička i temperaturna karakterizacija. Prikazan je njihov hemijski sastav, zavisnost permitivnosti i modula elastičnosti od temperature i kao i relativno termalno širenje.

Ključne reči: LTCC tehnologija, dielektrični materijali, električna, mehanička i temperaturna karakterizacija.

Dostupno na Internetu sa adrese časopisa: http://www.ache.org.rs/HI/

STRUČNI RAD

UDK 620.1/.2:54:621.38

Hem. Ind. **67** (4) 621–628 (2013)

doi: 10.2298/HEMIND120713105R

LTCC tehnologija predstavlja tehnologiju pomoću koje se mogu praviti jednoslojne i višeslojne komponente i kola. Ona se može definisati kao postupak laminacije više keramičkih traka, pri relativno niskoj temperaturi [1]. Na trake se nanose provodni, dielektrični ili otporni materijali i zatim se radi njihovo istovremeno pečenje. Vreme potrebno za proizvodnju većeg broja komponenti je smanjeno njihovim integrisanjem u više slojeva, u okviru jednog procesa proizvodnje. Projektovanjem višeslojnih komponenti smanjuje se površina koju one zauzimaju na pločici, a time se smanjuje i njihova cena. Velika prednost je i mogućnost pojedinačnog ispitivanja slojeva, i u slučaju greške ili neispravnosti, njegova zamena pre spajanja sa ostalim slojevima komponente. Na taj način se izbegava ponovna proizvodnja cele komponente. U LTCC tehnologiji postoji veliki izbor materijala (traka) različite debljine i karakteristika, pa samim tim postoje veće slobode i mogućnosti prilikom projektovanja.

LTCC tehnologija ima veliku primenu. Glavne oblasti u kojima se primenjuje su: rad na visokim frekvencijama (mikro- i mili-talasi), rad u zahtevnim okruženjima (visoka temperatura i visoka vlažnost), moduli za bežičnu komunikaciju, RF pasivne komponente (induktori, kondenzatori, rezonatori, filtri), senzori, diplekseri, antene, visoko precizni moduli sa više čipova, upravljački uređaji u avionskoj navigaciji, medicinski implanti, itd. [2–21], slika 1.

Slika 1. Primena LTCC tehnologije.
Figure 1. LTCC technology application.

Poznavanje sastava materijala, kao i njegovih električnih i mehaničkih karakteristika predstavlja veoma bitnu informaciju koja je neophodna kako bi se na uspešan način mogle projektovati različite komponente. Obično proizvođači materijala u tehničkoj dokumentaciji ne prikazuju sve relevantne karakteristike materijala i zbog toga je rađena električna, mehanička i

Prepiska: G. Radosavljević, Vienna University of Techology, Insitute for Sensor and Actuator Systems, Department of Applied Electronic Materials, Gusshausstrasse 27–29/366-AEM, A-1040 Vienna, Austria.
E-pošta: goran.radosavljevic@tuwien.ac.at
Rad primljen: 13. jul, 2012
Rad prihvaćen: 7. novembar, 2012

temperaturna karakterizacija korišćenih materijala. U nastavku će biti prikazani rezultati karakterizacije za tri različita dielektrična materijala (Heraeus CT700, Heraeus CT707, Heraeus CT800), [22–24]. Prvo će biti prikazan hemijski sastav korišćenih materijala, nakon toga zavisnost permitivnosti i modula elastičnosti od temperature i dok će na kraju biti prikazano relativno termalno širenje.

EKSPERIMENTI, REZULTATI I DISKUSIJA

Za izradu uzoraka, koji su korišćeni za ispitivanja karakteristika materijala, korišćen je standardni proces izrade u LTCC tehnologiji, koji se zasniva na laserskom sečenju materijala, postupku sitoštampe, laminaciji LTCC traka i istovremenom pečenju svih slojeva. Za sva tri ispitivana materijala korišćeni su isti optimalni parametri izrade koji su prikazani u tabeli 1.

Tabela 1. Optimalni parametri laserskog sečenja. laminacije i pečenja za Heraeus CT700, CT707 i CT800 trake
Table 1. Optimal laser cutting, lamination and sintering parameters for Heraeus CT700, CT707and CT800 tapes

Parametar			Vrednost		
Lasersko sečenje					
Struja diode, A			29		
Broj sečenja			2		
Frekvencija, Hz			10000		
Brzina, mm/s			9		
Laminacija					
Temperatura laminacije, °C			75		
Pritisak, bar			70		
Trajanje laminacije, min			3		
Pečenje					
Temperaturne zone, °C					
1	2	3	4	5	6
350	580	880	880	876	873
Brzina trake, mm/min			≈340		

Hemijski sastav

Ispitivanje hemijskog sastava (kompozicije) materijala rađeno je pomoću EDS (*Energy Dispersive X-ray*) analize. Uzorci koji su bili pripremljeni za EDS analizu napravljeni su primenom nekih od standardnih postupaka LTCC tehnološkog procesa. Trake su prvo sečene pomoću lasera, nakon čega je sledilo njihovo sinterovanje. Posle toga, na test uzorke nanet je tanak sloj zlata (15 nm), a zatim su uzorci podvrgnuti ispitivanjima sa X-zracima. Ova analiza se zasniva na identifikaciji kompozicije materijala na osnovu energije emitovanog X-zraka koji nastaje prilikom sudara elektrona iz snopa elektronskog mikroskopa (SEM – *Scanning Electron Microscope*) i elektrona koji se nalaze na površini uzorka. U tabeli 2 prikazani su hemijski sastavi za Heraeus CT700, CT707 i CT800 dielektrične trake, dok su na slici 2 prikazani njihovi SEM izgledi.

Tabela 2. Hemijski sastav (mas.%) Heraeus CT700, Heraeus CT707 i Heraeus CT800 dielektričnih traka
Table 2. Chemical composition of Heraeus CT700, CT707 and CT800 dielectric tapes

Hemijski element	Heraeus dielektrična traka		
	CT700	CT707	CT800
O	40.50	48.53	45.30
Mg	1.88	1.82	1.42
Al	13.14	3.27	18.70
Si	19.01	28.28	14.04
K	1.17	1.01	1.16
Ca	2.26	1.93	1.90
Ti	1.88	1.71	1.55
Co	1.94	0.67	0.84
Zn	4.03	–	1.82
Ba	14.19	12.77	13.25

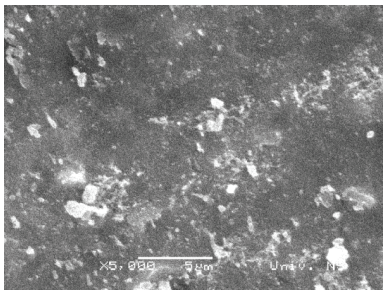

(a)

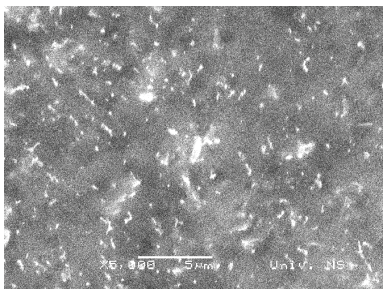

(b)

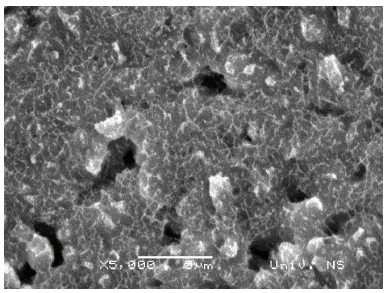

(c)

Slika 2. SEM izgledi Heraeus dielektričnih traka, a) CT700, b) CT707 i c) CT800.
Figure 2. SEM Micrographs of a) CT700, b) CT707 and c) CT800 Heraeus dielectric tape.

Sa slike 2 se može videti da se implementacijom predloženog temperaturnog profila materijali u potpunosti sinteruju, što se može zaključiti na osnovu ne postojanja uočljivih granica između susednih zrna.

Merenje permitivnosti

Merenje permitivnosti materijala rađeno je na posebno pripremljenim uzorcima LTCC traka. Uzorci su izrađeni u obliku diska prečnika 10 mm koji su sinterovani u peći sa pokretnom trakom, koristeći dvočasovni profil pečenja sa desetominutnim zadržavanjem na maksimalnoj temperaturi od 850 °C. Nakon pečenja je urađena obostrana metalizacija i ovako pripremljeni uzorci su ponovo sinterovani. Kako bi se sprečila pojava deformacija usled neujednačenog termalnog širenja trake i sloja paste koja se nanosi, za metalizaciju je korišćen 200 nm sloj AuPd paste kompanije Heraeus (RP26001/59). Permitivnost je zatim posredno određena, preko merene vrednosti kapacitivnosti uzoraka i njihovih geometrijskih parametara. Prilikom proračuna kapacitivnosti smatrano je da su elektrode veoma tanke (mnogo tanje od dielektrične trake) i da zbog toga ne utiču na termalno širenje trake i ne dovode do pojave deformacija. Takođe, ivični efekti polja su zanemareni. Kapacitivnost je merena na frekvenciji od 1 kHz pomoću LCR131 (LCR131 Compenent tester, Megger) uređaja za ispitivanje komponenti, u temperaturnom opsegu od 25 do 500 °C. Uzorci su zagrevani u peći sa komorom, a promena temperature je praćena pomoću termopara tipa K, koji je postavljen u blizini uzorka. Veza između uzorka i uređaja za ispitivanje ostvarena je preko spojnih žica, koje su uvedene u komoru peći kroz keramičke cevi. U tabeli 3 prikazane su vrednosti permitivnosti na sobnoj temperaturi za analizirane materijale, a na slikama 3–5 zavisnost njihove permitivnosti od temperature.

Tabela 3. Vrednosti permitivnosti za Heraeus CT700, CT707 i CT800 trake na sobnoj temperaturi na frekvenciji od 1 kHz
Table 3. Permittivity values of Heraeus CT700, CT707 and CT800 tapes at room temperature and frequency of 1 kHz

Heraeus traka	Debljina uzorka μm	Permitivnost (ε_r) na 25 °C
CT700	170	7.22
CT707	110	6.39
CT800	180	7.54

Na osnovu prethodno prikazanih rezultata može se videti da se najmanja vrednost za dielektričnu konstantu dobija za Heraeus CT707 dielektrične trake, dok se najveća vrednost dobija za Heraeus CT800 dielektrične trake. Takođe, može se primetiti da kod sve tri analizirane trake vrednosti dielektričnih konstanti raste sa temperaturom, međutim ta promena nije posebno izražena. To dovodi do zaključka da se sve tri trake mogu smatrati stabilnim u odnosu na promenu relativne dielektrične konstante u temperaturnom opsegu od 25 do 500 °C.

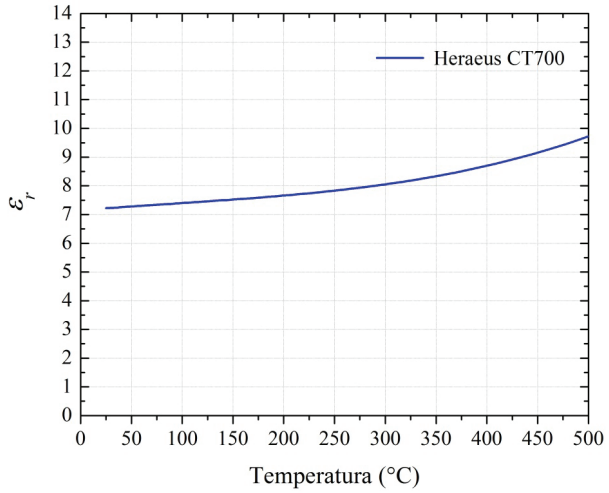

Slika 3. Zavisnost permitivnosti od temperature za Heraeus CT700 traku.
Figure 3. Permittivity–temperature dependence for Heraeus CT700 tape.

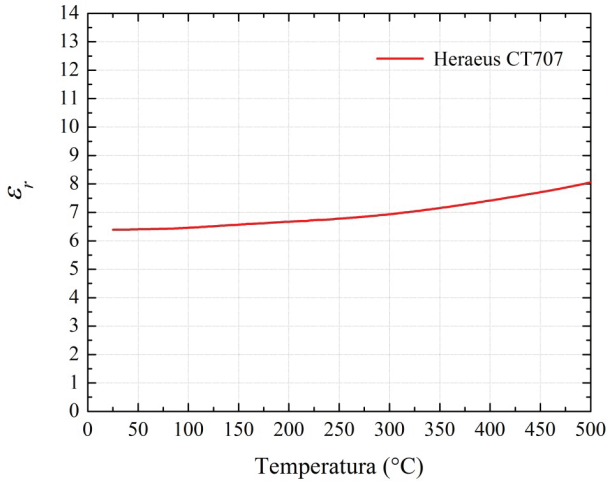

Slika 4. Zavisnost permitivnosti od temperature za Heraeus CT707 traku.
Figure 4. Permittivity–temperature dependence for Heraeus CT707 tape.

Na slici 6 prikazana je relativna promena permitivnosti sa temperaturom za sve tri analizirane trake.

Sa slike 6 se može videti da se najveća promena permitivnosti dobija za Heraeus CT700 dielektričnu traku. Najmanja relativna promena permitivnosti se dobija za Heraeus CT800. Relativna promena permitivnosti za Heraeus CT707 i CT800 trake je uporediva do temperature od 100 °C. Na osnovu toga se može zaključiti da, ukoliko se želi napraviti komponenta ili sistem, od analiziranih dielektričnih traka, za koji je potrebno ostvariti malu promenu permitivnosti sa temperaturom

za temperaturni opseg od 25 °C do 500 °C treba izabrati Heraeus CT800 dielektričnu traku.

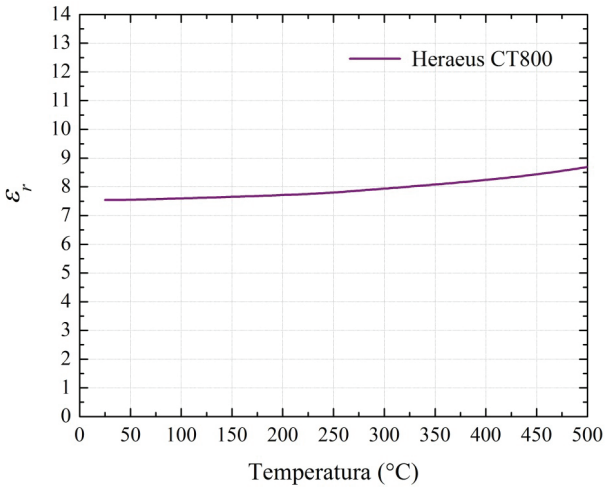

Slika 5. Zavisnost permitivnosti od temperature za Heraeus CT800 traku.
Figure 5. Permittivity–temperature dependence for Heraeus CT800 tape.

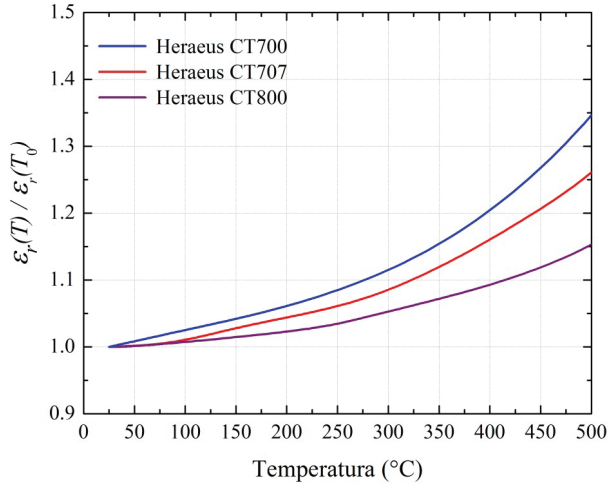

Slika 6. Realtivna promena permitivnosti sa temperaturom za Heraeus CT700, CT707 i CT800.
Picture 6. Relative changes of permittivity with temperature increasing for Heraeus CT700, CT707 and CT800.

Merenje modula elastičnosti

Pored električnih karakteristika, za projektovanje odgovarajućih sistema nekada je veoma bitno poznavati i mehaničke karakteristika materijala [19]. Vrednost modula elastičnosti za materijale je obično teško naći u tehničkoj dokumentaciji koje daje proizvođač materijala i zbog toga je u nastavku prikazan sistem koji je korišćen za određivanje vrednosti modula elastičnosti u odnosu na savijanje. Takođe, prikazana je i promena modula elastičnosti sa temperaturom, za sve tri dielektrične trake. Za merenje modula elastičnosti pripremljeni su uzorci veličine 5×50 mm^2. Primenjen je dinamički test savijanja u tri tačke po standardu SRPS EN ISO 7438 (EN ISO 7438:2005), na mernoj dužini od 20 mm, sa amplitudom ugibanja od 100 µm. Merenje je vršeno u temperaturnom opsegu od 25 do 500 °C, a korišćen je TA Instruments DMA2980 automatizovani ispitni uređaj. Na slici 7 prikazan je šematski izgled principa merenja modula elastičnosti, a u tabeli 4 dati su korišćeni parametri merenja.

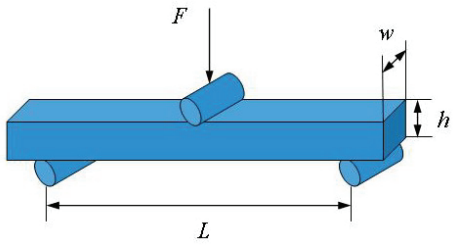

Slika 7. Šematski izgled merenja modula elastičnosti metodom savijanja u tri tačke.
Figure 7. Measurement of elastic modulus using three-point bending method – schematic view.

Tabela 4. Vrednost parametara koji su korišćeni za merenje modula elastičnosti
Table 6. Parameters values which was used for measurement of elastic modulus

Parametri merenja	Vrednost
Frekvencija, Hz	1
Amplituda, µm	100
Temperaturna promena, K/min	3
Merna dužina (*L*), mm	20
Širina uzorka (*w*), mm	5
Debljina uzorka (*h*)	Različita

U tabeli 5 prikazane su vrednosti modula elastičnosti za analizirane dielektrične trake na sobnoj temperaturi, dok je na slikama 8–10 prikazane promene njegove vrednosti sa temperaturom.

Tabela 5. Vrednost modula elastičnosti za Heraeus CT700, CT707 i CT800 trake na sobnoj temperaturi, na frekvenciji od 1Hz
Table 5. Values of elastic modulus for Heraeus CT700, CT707 and CT800 tapes at room temperature and frequency of 1 kHz

Heraeus traka	Debljina uzorka µm	Modul elastičnosti (*E*) na 25 °C, GPa
CT700	121	72.98
CT707	95	53.49
CT800	92.5	91.26

Na osnovu prikazanih rezultata merenja za modul elastičnosti može se videti da se najmanja vrednost dobije za Heraeus CT707 dielektrične trake, dok se najveća vrednost dobije za Heraeus CT800 dielektričnu traku. Na osnovu toga se može zaključiti da, ukoliko je

potrebno ostvariti veću osetljivost u odnosu na mehaničku deformaciju nekog sistema, za njegovu izradu bi trebalo izabrati Heraeus CT707 dielektričnu traku, dok u obrnutom slučaju Heraeus CT800 dielektrična traka predstavljaju bolje rešenje. Analiziranjem temperaturne zavisnosti modula elastičnosti za testirane materijale može se videti da modul elastičnosti opada sa temperaturom. Na slici 11 prikazana je relativna promena modula elastičnosti sa temperaturom za analizirane materijale. Najveća relativna promena modula elastičnosti sa temperaturom do 350 °C se dobija za Heraeus CT700 trake, dok u intervalima od 350 °C do 500 °C se dobija za Heraeus CT800 traku.

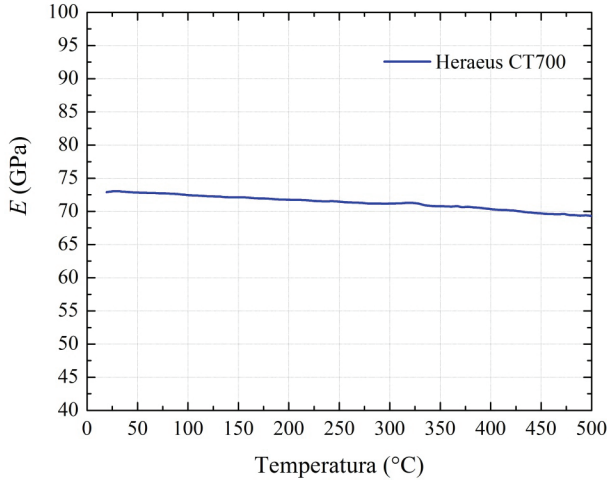

Slika 8. Zavisnost modula elastičnosti od temperature za Heraeus CT700 traku.
Figure 8. Elastic modulus - temperature dependence for Heraeus CT700 tape.

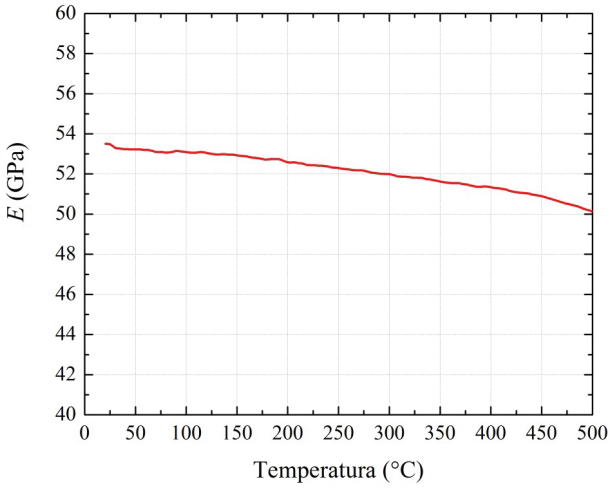

Slika 9. Zavisnost modula elastičnosti od temperature za Heraeus CT707 traku.
Figure 9. Elastic modulus - temperature dependence for Heraeus CT707 tape.

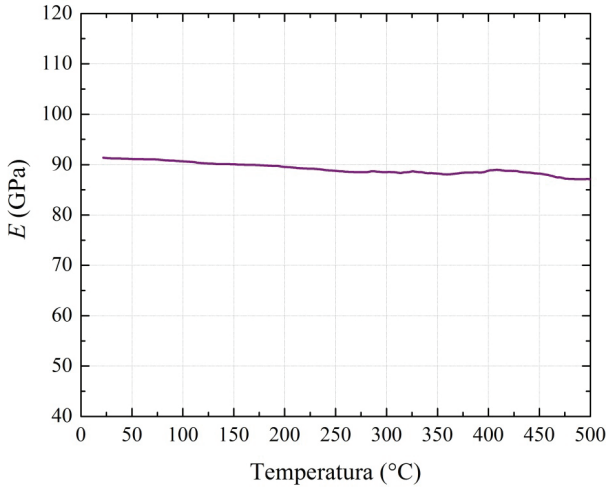

Slika 10. Zavisnost modula elastičnosti od temperature za Heraeus CT800 traku.
Figure10. Elastic modulus - temperature dependence for Heraeus CT800 tape.

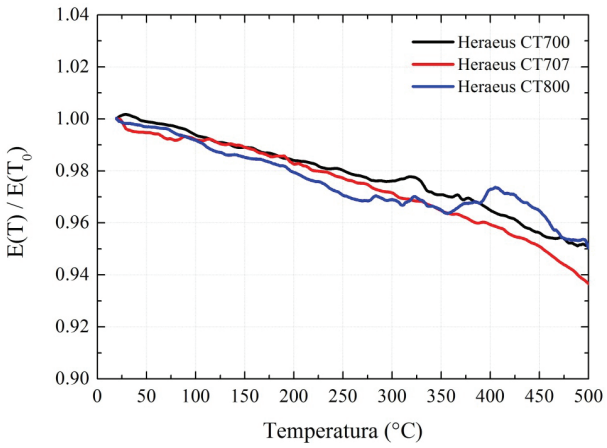

Slika 11. Relativna promena modula elastičnosti sa temperaturom za Heraeus CT700, CT707 i CT800 trake.
Figure 11. Relative changes of elastic modulus with temperature increasing for Heraeus CT700, CT707 and CT800 tapes.

Merenje relativnog termalnog širenja

Pored ispitivanja promene permitivnosti i modula elastičnosti sa temperaturom, za projektovanje određenog sistema koji bi imao primenu u ispitivanom temperaturnom opsegu potrebno je znati i njegovo relativno termalno širenje kao i koeficijent termalnog širenja (TCE, *Thermal Coeficient of Expansion*). Ispitivanje relativnog termalnog širenja rađeno je na posebno pripremljenim blok uzorcima, veličine 5×5×20 mm^3. Za izradu uzoraka korišćene su laserski obrađene trake u nepečenom stanju, koje su zatim naslagane, laminirane i sinterovane u peći sa komorom. Iz ovako obrađenih traka isečeni su uzorci potrebne veličine, urađena je njihova metalizacija i na kraju je izvršeno finalno poliranje. Određivanje relativnog termalnog širenja je vrše-

no pomoću TMA2940 termomehaničkog analizatora kompanije TA Instruments, u temperaturnom opsegu od 100 do 500 °C. Na slici 12 prikazani su rezultati merenja za relativno termalno širenje analiziranih materijala.

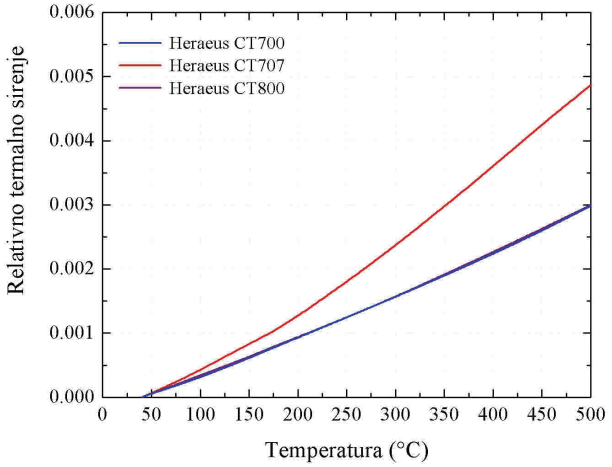

Slika 12. Relativno termalno širenje za Heraeus CT700, CT707 i CT800 trake.
Picture 12. Relative thermal expansion for Heraeus CT700, CT707 and CT800 tapes.

Sa slike se može videti da najveće termalno širenje ima Heraeus CT707 dielektrična traka, dok je termalno širenje za Heraeus CT700 i Heraeus CT800 uporedivo.

Vrednosti koeficijenata termalnog širenja (TCE) su izvedeni iz fitovanih kriva merenih rezultata, zbog toga što su na taj način obezbeđeni bolji rezultati nego da je njihova vrednost izvedena direktno iz merenih rezultata. Rezultati merenja za TCE su prikazani u tabeli 6.

ZAKLJUČAK

Glavni cilj koji je bio postavljen u toku sprovedenog istraživanja koje je prikazano u ovom radu je bio da se izvrši karakterizacija nekih komercijano dostupnih materijala koji se često koriste u LTCC tehnologiji. Razlog zbog čega je ovo istraživanja urađeno je taj što proizvođači materijala ne prikazuju sve relevantne karakteristike materijala u tehničkoj dokumentaciji i zbog toga je praktično nemoguće predvideti ponašanje realizovanih sistema ili komponenti u realnom okruženju. Izvršena je analiza tri materijala koja se koriste za izradu komponenti i sistema u LTCC tehnologiji, firme Heraeus (Heraeus CT700, CT707 i CT800), a urađena je njihova električna, mehanička i temperaturna karakterizacija. Pored toga, prikazan je njihov hemijski sastav, zavisnost relativne permitivnosti i modula elastičnosti od temperature, kao i vrednost koeficijenta njihovog relativnog termalnog širenja. Na osnovu detaljno prikazane analize pokazano je koji od navedena tri materijala je pogodan za različite aplikacije u realizaciji kompleksnih sistema u LTCC tehnologiji, gledano u odnosu na vrednosti parametara dobijenih navedenim ispitivanjima.

Zahvalnost

Ovaj rad je delom podržan od strane Ministarstva prosvete i nauke vlade Republike Srbije, u okviru projekta III 45021 i uključen u EUREKA E!4570 IPCTECH projekat.

LITERATURA

[1] L.J. Golonka, New application of LTCC technology, 28th International Spring Seminar on Electronics Technology (2005) 148–152.

[2] S.O' Reilly, F. John, D.O' Terence, M. Andrew, H. Gerard, B. Michael, M.S. Cian, A comparative analysis of interconnection technologies for integrated multilayer inductors, Microelectronic International **15** (1998) 6–10.

[3] H. Birol, T. Maeder, C. Jacq, P. Ryser, Investigation of interactions between co-fired LTCC components, J. Eur. Ceram. Soc. **25** (2005) 2065–2069.

[4] T. Thelemann, H. Thust, M. Hintz, Using LTCC for microsystems, Microelec. Int. **19** (2002) 19–23.

[5] J. Müller, High-quality RF inductors in LTCC, ISHM Conference **43** (1997) 59–63.

Tabela 6. Koeficijenti termalnog širenja, TCE / ppm, za Heraeus CT700, CT707 i CT800 dielektrične trake
Table 6. Coefficient of thermal expansion, TCE / ppm, for Heraeus CT700, CT707 and CT800 dielectric tapes

t / °C	Heraeus traka		
	CT700	CT707	CT800
	debljina uzorka, µm		
	121	95	92.5
100	5.27	7.35	5.92
200	6.19	9.62	5.90
300	6.42	11.44	6.42
400	6.81	12.42	7.01
500	7.75	12.13	7.36

[6] A. Pietrikova, Potentiality of LTCC for sensor applications, 24th International Spring Seminar on Electronics Technology, Calimanesti-Caciulata, Romania, 2001, pp. 112–116.

[7] H. Birol, Fabrication of Low Temperature Co-fired Ceramic (LTCC)-based sensor and micro-fluid structures, PhD Thesis, EPFL, Switzerland, 2007.

[8] L. Devlin, G. Pearson, J. Pittock, RF and microwave component development in LTCC, http://www.seaceramics.com/Download/Papers/Plexteknordic.pdf (jul, 2013).

[9] R. Kulke, M. Rittweger, P. Uhlig, C. Günner, LTCC – multilayer ceramic for wireless and sensor applications, http://www.ltcc.de/downloads/rd/pub/10-doc-plus--engl-2001.pdf (jul, 2013).

[10] R. Li, G. DeJean, M. Moonkyun, L. Kyutae, S. Pinel, M.M. Tentzeris, J. Laskar, Design of compact stacked-patch antennas in LTCC multilayer packaging modules for wireless applications, IEEE Transactions Comp. Packaging Technol. **27** (2004) 581–589.

[11] C. Kim, H. Kim, J. Kim, An integrated LTCC inductor, IEEE Transactions Magnetics **41** (2005) 3556–3558.

[12] A. Boutz, Inductors in LTCC utilizing full tape thickness features, MSc Thesis, Kansas State University, Manhattan, KS, 2009.

[13] J. Müller, G. Kahmen, R. Schumann, N. Sinnadura, LTCC - a promising technology for high-frequency system-in-packages, http://www.mse-microelectronics.de/research/download/PaperMicrotech2005.pdf (jul, 2013).

[14] S. Scrantom, G. Gravier, T. Valentine, D. Pehlke, B. Schiffer, Manufacture of embedded integrated passive components into low temperature co-fired ceramic systems, http://www.scrantom.com/Outgoing/papers/ /seiipc98.pdf (jul, 2013).

[15] W. Smetana, B. Balluch, G. Stangl, E. Gaubitzer, M. Edetsberger, G. Köhler, A multi-sensor biological monitoring module built up in LTCC-technology, Microelec. Eng. **84** (2007) 1240–1243.

[16] W. Smetana, M. Unger, Design and characterization of a humidity sensor realized in LTCC-technology, Microsys. Technol. **14** (2008) 979–987.

[17] W. Smetana, B. Balluch, G. Stangl, S. Lüftl, S. Seidler, Processing procedures for the realization of fine structured channel arrays and bridging elements by LTCC-technology, Microelectronics Reliability **49** (2009) 592––599.

[18] W. Smetana, Low temperature ceramic processing for microsystem application, Ceramics Processing in Microtechnology, Whittles Publishing, Dunbeath Mill, Dunbeath, Caithness, 2009, pp. 208–225.

[19] G. Radosavljević, W. Smetana, A. Marić, Lj. Živanov, M. Unger, G. Stangl, Parameters affecting the sensitivity of LTCC Pressure Sensors, Microelec. Int. **27** (2010) 159––165.

[20] G. Radosavljević, Lj. Živanov, W. Smetana, A. Marić, M. Unger, L. Nađ, A wireless embedded resonant pressure sensor fabricated in the standard LTCC technology, IEEE Sensor J. **9** (2009) 1956–1962.

[21] G. Radosavljević, A. Marić, W. Smetana, Lj. Živanov, Benefits of the LTCC substrate configuration with an air-gap for realization of RF inductor with high Q-factor and SRF, Int. J. Appl. Ceram. Technol. (2011) 1–10.

[22] http://www.heraeusthickfilm.com/media/webmedia_local/media/datasheets/ltccmaterials/ct_700_en_3.pdf (jun, 2012).

[23] http://heraeusthickfilm.com/media/webmedia_local/ /media/datasheets/ltccmaterials/CT_707_en.pdf (jun, 2012).

[24] http://www.heraeusthickfilm.com/media/webmedia_local/media/datasheets/ltccmaterials/CT_800_en.pdf (jun, 2012).

SUMMARY

ELECTRICAL, MECHANICAL AND THEMPERATURE CHARACTERIZATION OF COMMERCIALY AVAILABLE LTCC DIELECTRIC MATERIALS

Goran Radosavljević[1], Andrea Marić[2], Michael Unger[1], Nelu Blaž[2], Walter Smetana[1], Ljiljana Živanov[2]

[1]*Vienna University of Techology, Insitute for Sensor and Actuator Systems, Department of Applied Electronic Materials, Vienna, Austria*
[2]*University of Novi Sad, Faculty of Technical Sciences, Departmant of Electronics, Novi Sad, Serbia*

(Professional paper)

The present paper deals with the mechanical, electrical and thermal properties of several commercially available materials that are widely used for fabrication of electronic components, sensor systems, etc., in Low Temperature Co-fired Technology (LTCC). Having complete and accurate information of the material's chemical composition, its electrical and mechanical properties are essential for successful design of various components and/or systems. In many cases, the available technical documentation provided by the manufacturers contains less information than designers require for complete pre-design analysis of system behaviour in real time environment. Three frequently exploited commercially available dielectric materials provided by the Heraeus company (Heraeus CT700, Heraeus CT707 and Heraeus CT800) were investigated. Electrical, mechanical and thermal properties analyses were conducted in order to determine some of the important material properties. A full chemical composition analysis was performed resulting in the determination of the materials' chemical composition, followed by the determination of the relative permittivity, elasticity modulus and relative thermal coefficient values.

Keywords: LTCC Technology • Dielectric materials • Electrical, mechanical and temperature characterization

Biodiesel from rapeseed variety "Banaćanka" using KOH catalyst

Radoslav D. Mićić[1], Milan D. Tomić[2], Mirko Đ. Simikić[2], Aleksandra R. Zarubica[3]

[1]*NIS Gasprom, Refinery Novi Sad, Novi Sad, Serbia*
[2]*University of Novi Sad, Faculty of Agriculture, Novi Sad, Serbia*
[3]*University of Niš, Faculty of Natural Sciences and Mathematics, Niš, Serbia*

Abstract

This paper presents a complete characterization of rapeseed oil, of Banaćanka variety, as well as the potential use of oil generated after filtering, in order to obtain biodiesel. The research interest was based on the fact that Banaćanka is the oldest domestic rapeseed variety, a so-called "double-zero" or 00-rapeseed (low in erucic acid, below 5%, and glucosinolates below 30 mmol g^{-1}), suitable for use in the region, since it is low-temperature tolerant, posseses high genetic potential for seed yield of about 5.2 t/ha and high oil content of around 45%. Transesterification was carried out in a Parr 4520 batch reactor, with KOH as a catalyst. Cold pressed oil without prior treatment was used as feedstock for transesterificataion. The paper analyses the effects of temperature, reaction duration, catalyst amount and rate of agitation on the synthesis of biodiesel at constant pressure and molar methanol/oil ratio.

Keywords: transesterification; domestic rapeseed oil, homogeneous alkali catalyst KOH, fatty acid methyl esters (FAME).

Available online at the Journal website: http://www.ache.org.rs/HI/

PROFESSIONAL PAPER

UDC 662.756.3(497.113): 665.334.9:66.095.13

Hem. Ind. **67** (4) 629–637 (2013)

doi: 10.2298/HEMIND120716106M

Biodiesel is a non-toxic, biodegradable fuel prepared from vegetable oil or animal fat originated triglycerides, *via* transesterfication using metanol. It represents an environmentally friendly and renewable fuel [1,2]. From an environmental point of view, the use of biodiesel globally contributes to the reduction of the emission of greenhouse gases (CO, CO_2 and SO_2), particles (soot) and aromatics (benzene, toluene, etc.), while the emission of NO_x is slightly higher than the corresponding emission from diesel of fossil origin [3]. The advantages of biodiesel use over classical diesel fuel are based on the increased oxygen content which provides better engine combustion, as well as the absence of certain contaminants that are inevitably contained by the diesel of fossil origin.

Bearing in mind the engineering aspects, biodiesel produced in line with the EN 14214 standard represents a high quality fuel for diesel engines, which is according to certain properties even better than standard diesel based on fossil origin. Certain properties, such as good lubricity reduces the potential engine damage, and thus contributes to its higher efficiency and durability. In terms of use, particularly interesting features are its high cetane number, high flashpoint and acceptable low temperature properties, such as the cold filter plug point (CFFP), making it an even more acceptable alternative fuel [4]. Being environmentally friendly, and based on all its benefiting properties, biodiesel provides better storage utilization and handling in comparison to diesel of fossil origin. These factors partially compensate for the lack of energy content. The main disadvantage, constraining its wider use is still the high cost of the raw material (comparing to classical fuel), as well as relatively high costs of catalytic transesterification refining.

The transesterfication reaction of raw rapeseed oil to biodiesel (fatty acid methyl ester (FAME), Figure 1, may be catalysed by an alkali, acid or enzyme [5,6]. The alkaline catalysis includes homogeneous and/or heterogeneous alkaline catalysts usage [1]. In alkaline catalytic route as homogeneous catalysts NaOH, KOH and their alkoxides are mostly used. Homogeneous alkaline-catalyst reaction is much faster than acid-catalyst transesterification [7]. Although chemical transesterification by an alkaline catalyst provides a higher level of conversion of triglycerides into methilesters and short reaction run, this reaction has a series of disadvantages. The reaction is intensive in terms of energy, even traces of water content strongly hinder the reaction, glycerol as a by-product is difficult to remove, it is necessary to remove alkaline catalysts from products, and an additional treatment of alkaline waste water as well as from free fatty acids is required. Common problems occurring in biodiesel technologies using homogeneous catalysts (NaOH or KOH) is that they require complete series of relatively expensive and complex steps of neutralization, flushing and separation [1,8–10]. In addition, purification procedures are not ecologically acceptable since they require the use of a large quantity of water and the production takes place with the aid of strong alkali or acids [1,2]. Fur-

Correspondence: R. Mićić, Bulevar Oslobođenja 17, Novi Sad.
E-mail: rmicic@beotel.rs
Paper received: 16 July, 2012
Paper accepted: 29 October, 2012

thermore, there is an issue of an expensive procedure of catalyst separation from the product [11–13].

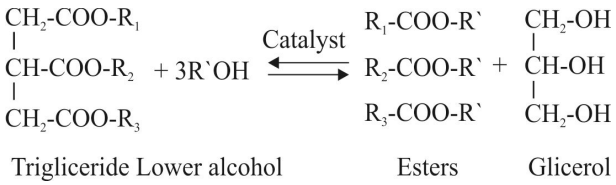

Figure 1. Transesterification reaction.

Despite the evident failings in the use of alkaline catalysts for homogenous catalysis, these processes are still the major ones, due to economic reasons, as well as due to availability. In the processes of alkaline transeserification using methanol, the catalyst dosage used is in the range from of 0.4 to 2% w/w to the feedstock, and the oil to methanol molar ratio is within stoichiometric relation from 1:3 to 1:12.

In this paper, a raw rapeseed oil of "Banaćanka" variety was used as the basic feedstock for the synthesis of biodiesel. The most important characteristic of this variety lies in the fact that this rapeseed oil contains very small quantities of erucic acid (below 5%), so the mixture obtained after pressing may be used as livestock feed. This paper is directed to test the behaviour of such feedstock in the conventional biodiesel production. KOH was selected as the catalyst, which, despite higher prices and greater quantity applied, in comparison to NaOH has one significant advantage – namely, by neutralization of excess KOH, after reaction with phosphoric acid, K_3PO_4 (potassium phosphate) is obtained that may be used as a quite successfully applicable fertilizer, which from the agricultural point of view represents a significant by-product.

EXPERIMENTAL

Materials

As a feedstock, cold pressed rapeseed oil was used. The oil was used in transesterification reaction without prior treatment.

Methanol of 99.5% purity (Lach-Ner, max. 0.1% moisture, 50433 0403) was used in the transesterification process and KOH (≥85%, Sigma-Aldrich) was used as catalyst in the form of pellets with total impurities of ≤2.0% K_2CO_3.

In order to perform the post-treatment of biodiesel sample, a micronized natural zeolite clinoptilolite of fraction 60–100 μm was used, as well as a zeolite sample from the Belgrade Geoinstitute (originated from the Brus municipality, locality "Igroš-Vidojevići") with min. 90% purity $(Na,K,Ca)_{2–3}Al_3(Al,Si)_2Si_{13}O_{36}·12H_2O$ in granulation 1–2 mm.

Feedstock and product characterization

Feedstock was subjected to gas chromatography analysis by GC Chromatograph Clarus 500, according to the instructions given by standard of EN 14214. Analysis findings and literature data were used for the calculation of the molecular mass of the product as well as for the calculation of the iodine number. The separation was performed over a 14 m MET-Biodiesel column with a 0.53 mm internal diameter, 0.16 μm film thickness, and integrated package 2 m×0.53 mm (28668-U). The initial temperature during GC analysis was 150 °C. The column was heated at a rate of 30 °C/min up to a temperature of 350 °C, and this temperature was maintained for an additional 15 min. The analysis was performed using the gas chromatograph equipped with FID detector operating at a temperature of 400 °C. The carrier gas was helium at a flow rate of 15 mL/min. A sample of 1 μL was injected into a cold injector.

Results of the detailed analyses of raw rapeseed oil are presented in Table 1. The results have shown that the obtained values of characteristic physical and chemical values are within the range of internationally declared values.

Biodiesel samples were analysed by a PE Autosystem XL gas chromatograph with a flame ionization detector according to the standard SRPS EN 14103. A 60 m polyethylene glycol capillary column with a 0.32 mm internal diameter and 0.3 μm film thickness were used. Analysis of the standard mixture of methyl esters RM-1 was carried out using a reference probe sample of 0.6 μL at split ratio 30:1. The injector and detector temperatures were 240 °C, and the analysis was performed in isothermal conditions at 210 °C. Helium was applied as the carrier gas with a flow rate of 1.8 mL/min. Methyl heptadecanoate (purity > 99%, Fluka) was used as an internal standard. The only modification of the method employed was the reduction of the quantity of the internal standard solution from 5 mL to 2 mL, due to the limited quantity of the internal standard available. In the same ratio, the sample weighed amount was reduced (from 250 to 100 mg) according to the standard procedure. Experimental results showed that this reduction did not affect the accuracy of results.

The physical and chemical characterization of the raw rapeseed oil and the obtained biodiesel was performed in compliance with EN 14214. Raw rapeseed oil (Banaćanka variety) represented the basic feedstock for the synthesis of biodiesel.

Complete analysis of the content of fatty acids in cold pressed oil "Banaćanka" was performed and the results are given in Table 2, which is also in compliance with analyses given in literature. The obtained raw oil belongs to the group of highly olefin rapeseed oils, with low content of erucic acids. Feedstock analysis was performed by GC, according to the method EN 14214 and

Table 1. Physical and chemical properties of raw rapeseed oil

Property	Unit	Method	Measured value	Standard values acc.	
				Min.	Max.
Density	kg/m^3	EN ISO 3675	–	900	930
Cetane number	–	ASTM D613	37.6	–	–
Caloric value	kJ/kg	DIN 51900-3	39709	35000	–
Cinematic viscosity at 40 °C	mm^2/s	SRPS ISO 3104	37.0	–	38.0
Cloud point	°C	SRPS ISO 3015	–3.9	–	–
Freezing point	°C	–	–31.7	–	–
Flash point	°C	SRPS B.H8.047	246	220	–
Carbon	mass%	EN ISO 10370	0.12	–	0.4
Sulphur content	mg/kg	ASTM D5453-93	6.7	–	20.0
Ash content	mass%	DIN EN ISO 6245	< 0.01	–	0.01
Water content	mass%	EN ISO 12937	0.01	–	0.075

based on the performed analysis and literature data molar mass of the product and iodine number were calculated (Table 2).

The calculated iodine number of 107.1792 matches the literature data (94–120). In addition to the content of fatty acids, the physical properties of refined rapeseed oil were also determined by GC analysis [8]. The results of GC analyses of rapeseed oil were corresponding with the results of analyses of similar rapeseed variety previously published [14].

Table 2. Calculation of molar mass and iodine number based on GC analysis EN 14214, feedstock – refined rapeseed oil of "Banaćanka" variety

Fatty acid	Oil mass%	Acid molar mass	Triglyceride factor (*F*)	*F** mass%	Rapeseed oil, molar shares: Number of moles and *i*-th components in 100 g of mixture g_i/M_i	Multiplication of quantity (2) and acid molar mass $(g_i/M_i)/(g_i/M_i)\times M_i$
Myristic acid (tetradecanoic acid) $CH_3(CH_2)_{12}COOH$ or C14:0	0.071	228.4	–	–	0.000310858	0.199791192
Palmitic acid (hexadecanoic acid) $CH_3(CH_2)_{14}COOH$ or C16:0	4.553	256.4	–	–	0.01775741	12.81196193
Stearic acid (octadecanoic acid) $CH_3(CH_2)_{16}COOH$ or C18:0	1.648	284.4	–	–	0.005794655	4.637406821
Oleic acid $CH_3(CH_2)_7CH=CH(CH_2)_7COOH$ or C18:1	66.19	282.4	0.8599	56.88152	0.234238669	186.1406698
Linoleic acid $CH_3(CH_2)_4CH=CHCH_2CH=CH(CH_2)_7COOH$ or C18:2	17.82	280.4	1.7315	30.97998	0.063808845	50.34738037
Linolenic acid $CH_3CH_2CH=CHCH_2CH=CHCH_2CH=CH(CH_2)_7COOH$ or C18:3	6.905	278.4	2.6151	18.05726	0.024802443	19.43039691
Arachidic acid (eicosanoic acid) $CH_3(CH_2)_{18}COOH$ or C20:0	0.524	312.5	–	–	0.0016768	1.474515276
Eicosenoic $C_{20}H_{38}O_2$ $CH_3(CH_2)_7CH=CH(CH_2)_9COOH$ or C20:1	1.373	310.5	0.7853	1.078216	0.0044219	3.863567698
Behenic acid (docosanoic acid) $CH_3(CH_2)_{20}COOH$ or C22:0	0.413	340.5	–	–	0.001212922	1.162165666
Erucic acid $CH_3(CH_2)_7CH=CH(CH_2)_{11}COOH$ or C22:1	0.252	338.6	0.723	0.182196	0.000744241	0.709118033
Lignoceric acid $CH_3(CH_2)_{22}COOH$ or C24:0	0.222	368.6	–	–	0.000602279	0.62469922
	100	–	–	–	0.355371022	281.4016729
			JB = sum(F*mas%)		M = M_{glic} + 3(sum(x_iM_i)– –Mol mas H_2O)	
			JB =107.1792015		M =882.26	

Measurements of feedstock and product densities were measured using a Parr digital density meter DMA 35, obtaining densities of 0.882 g/cm^3 for cold pressed rapeseed oil and 0.791 g/cm^3 for methanol.

In order to confirm the accuracy of the results, water content was determined by ASTM D-6304 method, coulometer Metro HM, which is used for determination of water content in petroleum products, lubricants and additives by coulometric method based on Karl Fischer titration.

FAME Yield calculation

The experimental results were obtained by variation of transesterification conditions. In all experiments the yield was calculated by the following correlation:

$$\text{FAME Yield (\%)} = \frac{\text{Average amount of ME layer (g)} \times \text{Purity of ME layer (\%)}}{\text{Amount of edible oil, feedstock (g)}} \quad (1)$$

After decanting, all product samples were weighed and it was identified that the average amount of ME was 892.2 g. By involving the values of the average ME amount and the amount of edible oil in Eq. (1), yield is obtained as a function of purity of ME layer:

$$\text{FAME Yield (\%)} = \frac{892.2\ \text{g} \times \text{Purity of ME layer (\%)}}{882.26\ \text{g}} = 1.0163 \times \text{Purity of ME layer (\%)} \quad (2)$$

Apparatus and reaction procedure

Transesterification was performed in a batch reactor Parr 4520, of 2 L volume, at 350 °C as the maximum operating temperature and pressure of 150 bar. The reactor was equipped with a catalyst basket of 150 cm^3 volume (Ø 70 mm×80 mm and Ø 50 mm×80 mm, working volume was in the space between two coverage surfaces with 1 mm openings) and an agitator with a variable number of rotations and impeller in annular area. The reactor was equipped with a transducer, a J type thermocouple and manometer. Temperature and rotation per minute (rpm) control were performed by a Parr 4842 microprocessor controller, with triple regulation and adjustable parameters.

If the experiment was conducted at ambient pressure in an open system, it would be impossible to test the effect of temperatures above the methanol boiling point (64.7 °C), since the effect of decreased methanol in liquid phase could not be eliminated due to evaporation. For this reason it was decided to conduct the experiment at 10 bar, with the assumption that all of the methanol is in liquid phase over the entire observed temperature range.

At the start of experiments, the same amount of pressed oil without pre-treatment was measured and added to the Parr 4520 reactor. The oil was heated up to the reaction temperature, at a heating rate of 2 °C min^{-1}. During the heating process the reactants were mixed with a magnetic agitator at a pre-set number of rpm.

Pastelles of commercial KOH catalyst (Sigma-Aldrich, ≥85% purity) were dissolved in the same quantity of methanol, in the container for decanting and added to the Parr 4520 reactor, after reaching the reaction temperature. The procedure was conducted in such a manner in order to determine the zero reaction time.

In experiments, the same quantity of Banaćanka variety (882.26 g) rapeseed oil was repeteadely used, as well as the same quantity of methanol 192.24 g (Lach-Ner, 99.5%, max. 0.1% of water). These quantities were selected in order to obtain the desired 6:1 methanol to oil molar ratio. The catalyst quantity was varied from 4.6–5.4 g (calculated for the total mass of input feedstock, this is equal to 0.381–0.5 mass%). All experiments were performed with 10 bar over-pressure of inert gas (N_2) in order to eliminate the impact of temperature on the content of liquid phase methanol.

This paper presents 4 series of experiments (a–d) conducted by varying different parameters and by a blind experiment, in order to determine the temperature effect and net gain of activity due to the presence of catalyst.

Series a of experiments were conducted with a closed reactor without external pressure impact, with a 6:1 methanol/oil molar ratio, constant catalyst content 5.4 g (0.5 mass%) and by varying the transesterification duration (from 15 to 60 min). This experiment was conducted in order to identify the yield as a function of reaction time. KOH catalyst previously dissolved in methanol was used, and the agitator was maintained at 665 rpm during the entire experiment.

Series b of experiments were conducted at a temperature of 65 °C, with a 6:1 methanol to oil molar ratio. The quantity of catalyst was varied (4.6, 5.0 and 5.4 g; which is 0.428, 0.465 and 0.5 mass%), with the maximum number of agitator rotations of 665 rpm. This experiment was conducted at two reaction times of 45 and 60 min in order to establish the change of yield as a function of the catalyst quantity for different reaction durations.

Series c of experiments were conducted within a temperature range (from 50 to 75 °C), at maximum number of agitator rpm (665 rpm), with a 6:1 methanol to oil molar ratio. The experiment was conducted for two different reaction durations of 30 and 60 min. This experiment was aimed to determine the activity as a

function of reaction temperature for different reaction times.

Series d of experiments were conducted at a temperature of 65 °C, with a 6:1 methanol to oil molar ratio, in duration of 60 min, with a varying number of agitator rpm (from 100 to 665 rpm). This experiment was aimed to determine the change in activity based on the variation of number of agitator rotations.

Separation procedures

After the transesterification reaction was carried out, the separation process was performed in two phases: first, to remove the remaining methanol, flash evaporation was conducted, for 3 h duration, at the temperature of 100 °C, and subsequently, the remaining triglycerides and glycerine were removed by different separation methods. Products separation was conducted in 3 ways in order to determine the efficiency of different methods and their effects on the purity of the product.

Ordinary procedures of decanting were performed in a decanter. All samples were left in the decanting vessel for 24 h and subsequently, a careful decanting procedure of methanol/glycerine mixture was performed.

The next procedures of separation includes decanting and subsequent soaking in a zeolite layer of micro granulation (60–100 μm). After the first product of transesterification was decanted, the glycerine layer was separated, and the biodiesel layer was soaked in the layer of zeolite of microgranulation for 24 h, after which decanting was repeated.

The third procedures of separation included decanting and subsequent filtering through zeolite layer of certain granulation (1–2 mm).

RESULT AND DISCUSSION

Effect of reaction duration on the level of transesterification

In the first series of experiments, as the reaction time was extended, the level of transesterification increased over the entire observed range (Figure 2). After 15 min of the reaction run, the level of trancesterification is low (85.2%). It is characteristic that over the entire observed range the increase of level of transesterification is not linear. After 40 min of the reaction, the level of transesterification increased by approximately 3.5%, and after 45 min the increase of transesterification level dropped to approximately 1.8%. This can be explained by slowing down of the reaction rate due to dilution of reagents by the final product, methyl esters and by-product glycerine, by which the contact surface of reagents and catalyst is reduced. This suggests that by decreasing the amount of biodiesel during reaction, much better results could be obtained and the reaction time might be reduced.

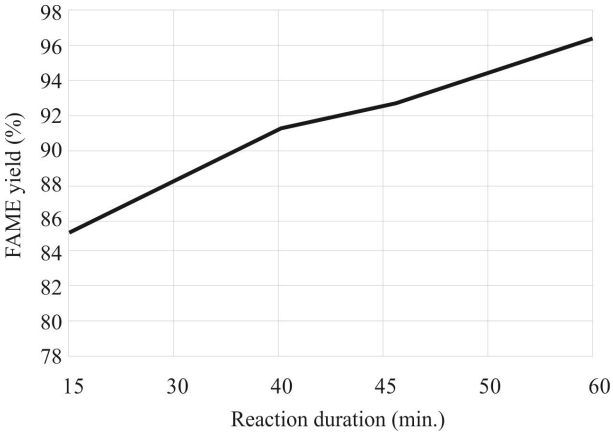

Figure 2. Effect of reaction time on the level of transesterification (FAME yield); constant methanol/oil molar ratio, 6:1; catalyst content, 5.4 g (0.5 mass%); 665 rpm.

Effect of catalyst amount/mass (g) to the level of transesterification

The second series of experiments performed comprised test of the effect of catalyst amount to the level of transesterification. Two series of reactor tests were conducted (Figure 3):

Series I: maximum number of rpm (655 rpm), reactor temperature of 65 °C and the reaction lasted 60 min.

Series II: maximum number of rpm (655 rpm), reactor temperature of 65 °C and the reaction lasted 45 min.

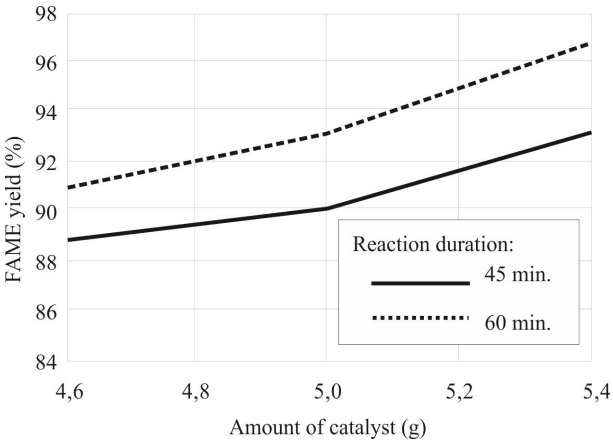

Figure 3. Effect of catalyst amount/mass to the level of transesterification (FAME yield); constant methanol/oil molar ratio, 6:1; temperature 45 and 65 °C; 665 rpm.

This experiment was conducted at two different durations in order to try to eliminate the effect of reaction time and to identify exclusively the trend of transesterification increase with the catalyst amount. As the amount of the catalyst increased, the level of transesterification also increased. The highest level of

esterification was obtained at maximum amount of catalyst used (5.4 g, which is 0.5 mass%) and at the longest reaction time. Considering the effect of catalyst amount and the reaction time on the level of transesterification, it becomes evident that the amount of catalyst has smaller effect on the level of transesterification than the treatment time (11.2% is the increase achieved based on the treatment time, while only 5.7% increase was obtained based on the increase of catalyst amount). Furthermore, it can be concluded that sufficient amounts of catalyst for transesterification were used in the experiments, and that the increase of catalyst amount above the minimum value (taken from literature), does not contribute to the proportional increase of transesterification level. Both curves show the same trend, with the break-point at 5 g of catalyst. A possible explanation would be that by increasing the catalyst amount the effect of transesterification reaction reversibility is proportionally decreased. The experiment was not followed up to the value when the increase of catalyst amount does not affect the level of transesterification, so it can be assumed that by further increase of the catalyst amount the level of transesterification would be further increased.

Effect of reaction temperature upon the level of transesterification

The third series of experiments was conducted to determine the impact of the reaction temperature on the level of transesterification. In order to separate the effect of the reaction time and temperature, the experiment was conducted in two parts at different reaction times (Figure 4).

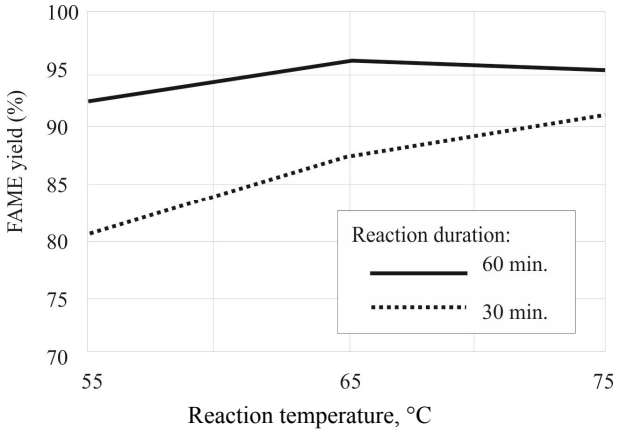

Figure 4. Effect of reaction temperature on the level of transesterification (FAME yield); constant methanol/oil molar ratio, 6:1; time, 30 and 60 min; 665 rpm.

As it can be seen in Figure 4, in both temperature modes there is a curve point at 65 °C. When the reaction lasted only 30 min, the reaction product yield within the temperature range of 55–65 °C increased by 6.8%, and within the range of 65–75 °C this increase was only 3.5%. When the reaction was carried out for 60 min, the reaction yield within the temperature range of 55–65 °C shows an increase of 3.6% and within the range of 65–75 °C there is a reduction of 0.7%. The maximum obtained after 30 min was reached at 75 °C and was 91.6% methylesters. For the reaction duration of 60 min, the maximum was obtained at 65 °C and was equal to 96.4%. This can be explained by the reversibility of the transesterification reaction, which was favoured by temperature and by the increase of the concentration of esters and glycerine along with the duration of the reaction run. In case of shorter reaction durations, reversibility is manifested by a decrease of yield dynamic growth, while for longer reaction durations by yield decrease. The general conclusion of this experiment is that at constant velocity of the agitator and at constant catalyst amount, the optimal reaction duration is 60 min at a temperature of 65 °C.

Effect of agitator rpm to the level of transesterification

The fourth series of experiments was conducted in order to determine the optimal rate of agitation rotation and the impact of agitation rate to the transesterification reaction. The amount of catalyst was 5.4 g (0.5 mass%), reaction time was 60 min, and the temperature was 65 °C. After changing the number of rotations, two trends became evident: 100–300 rpm and 300–665 rpm (Figure 5). Within the first range, there is a clear increase of transesterification level of 34.8%, and within the second range there was an increase of only 4.3%. This could be explained by the fact that a certain number of rotations actually improve the contact of the reactant and catalyst by turbulence, while being heavier and concentrated in the lower part of the reactor only partially contributes to the decrease of the contact between the reactant and catalyst. By further increase of the number of agitator rotations the mixture of reactants, the catalyst and product become approximately equally mixed throughout the entire reactor, which leads to the fact that the positive effect of better contact between reactants by mixing is partially annulled by the increase of the concentration of products in the mixture of reactants. Moreover, it can be concluded that higher level of transesterification might be obtained by decreasing the number of agitator rotations during the reaction. At the lowest product concentration the highest number of agitator rotations is required; then, as the product concentration increases during the course of the reaction, the concentration of the product in the bottom part of the reactor is enabled and the contact area of the remaining reactants in the mixture is undisturbed. The second way to eliminate the effect of "dissolution" by the product of reaction mixture is to conduct the transesterification

procedure in two phases with a separation between 2 reactions.

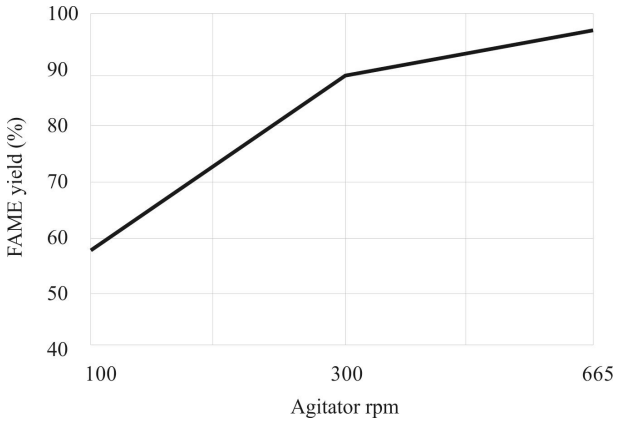

Figure 5. Effect of agitator rpm on the level of transesterification (FAME yield); constant methanol/oil molar ratio, 6:1; temperature, 65 °C; time 60 min; catalyst content, 5.4 g (0.5 mass%.

Separation

The first stage of separation was conducted by product evaporation. This operation produced good results and good repeatability. After the evaporation process, and previously decanted biodiesel, it was identified that the purity of biodiesel obtained was increased by approximately 1% in all samples, which confirms that this method of separation of methanol from the product is sufficiently effective and that it is not necessary to apply vacuum evaporation, as stated in the literature [15].

In both methods applying the natural zeolite clinoptilolite (micronized from 60–100 μm and granulation of 1–2 mm), regularity in the increase of biodiesel purity was not identified, so it can be concluded that its application for such purpose is not adequate, since the adsorption is unselective. The impact of separation procedures upon the level of transesterification is presented in Figure 6.

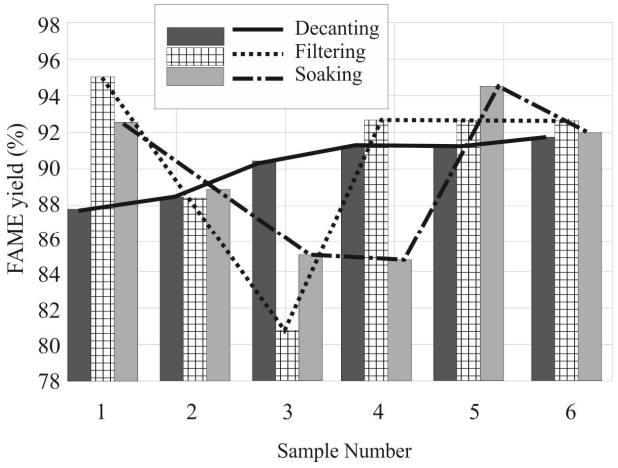

Figure 6. Impact of separation procedures on the level of transesterification.

Characterization of the biodiesel

After the completion of the transesterification procedure and separation of the product from the by-product and impurities, a complete analysis of the finished product was conducted and the results are presented in Table 3.

Regarding the properties of the finished product, one can notice that the largest discrepancy was in the case of kinematic viscosity, flash point and water content. Namely, kinematic viscosity can not be influenced since it is a consequence of the type of the feed; however, the flash point, which is a result of the content of unseparated methanol and the water content, can be affected. The authors underline that methanol evaporation under atmospheric pressure and at 120 °C is not sufficient.

After passing the product through the layer of zeolite, analyses of water and flash point were repeated. It was determined that the flash point was increased from 25 to 132 °C, and water content decreased from 1400 to 275 mg/kg. The obtained values of flash point and water content are consistent with the standard EN 14214.

CONCLUSION

It has been concluded, based on the results of transesterification of raw rapeseed oil of domestic rapeseed „Banaćanka", that methyl esters of fatty acid are obtained with regular yield and an adequate purity under the reaction conditions applied. Production of biodiesel from this rapeseed oil variety is highly recommendable, since the obtained residual mixture can be used as livestock feed due to the low content of erucic acid.

The duration of transesterification in the presence of homogenous alkali catalyst KOH up to a certain level positively affects the level of transesterification, and after that moment the reaction is slowed down. The same conclusion can be made for the study of the impact of the reaction temperature. This may be explained by reversibility of the transesterification reaction, which suggests the advantages of two-phase transesterification procedure, with the separation of the product as an inter-phase. The impact of the amount of the catalyst is evident and the reaction increases over the entire range of catalyst dosage. Since the minimal amount of catalyst was used in this paper (according to the listed literature data), further research could be conducted with the increase of the catalyst amount. The rate of agitation drastically increased the level of transesterification up to the middle of the range observed, after which it declined when the number of agitator rotations was increased. It can be concluded that it is recommendable to set up the

Table 3. Results of the analysis of the finished product

No.	Property, unit	Measured value	Values acc. to Standard (EN 14214)		Method
			Min.	Max.	
1.	Density at 15 °C, kg/m^3	878.4	860	900	SRPS ISO 12185
2.	Distillation, start , °C	296	–	–	SRPS EN ISO 3405
	10 vol.%, °C	340	–	–	
	20 vol.%, °C	343	–	–	
	30 vol.%, °C	345	–	–	
	40 vol.%, °C	346	–	–	
	50 vol.%, °C	347	–	–	
	60 vol.%, °C	349	–	–	
	70 vol.%, °C	350.5	–	–	
	80 vol.%, °C	352	–	–	
	90 vol.%, °C	359, cracking	–	–	
	Residue, vol.%	9.5	–	–	
	Loss, vol.%	0.5	–	–	
3.	Cinematic viscosity at 40 °C , mm^2/s	6.359	3.5	4	SRPS ISO 3104
4.	Flash point, °C	25	120	–	SRPS B.H8.047
5.	Cloud point, °C	-2	–	–	SRPS ISO 3015
6.	Filterability point, °C	-8	–	–	EN 116
7.	Iodine number	107.3 g/100 g	–	120	SRPS ISO 3961
8.	Sulphur content, mg/kg	0,6	–	10	ISO 20846
9.	Water content, mg/kg	1400	–	500	SRPS ISO 12937
10.	Cetane index	54.0	51	–	SRPS ISO 4264
11.	Corros. Cu band, 3 h/50 °C	1a	–	1	SRPS ISO 2160
12.	Lubricity at 60 °C, µm	323	–	–	SRPS ISO 12156-1
13.	Transparency	Clear, transp.	–	–	Visually
14.	Colour	L 0.5	–	–	SRPS ISO 2049
15.	Coke content, mass%	1.85	–	0.03	SRPS ISO 10370
16.	Caloric value, kJ/kg	40449	–	–	DIN 51900-3

reaction with the maximal number of rotations at start time, and after that it is necessary to reduce the number of rotations, for the purpose of better separation of the product and reactant.

Neutralization of alkali waste solution was successfully conducted with phosphoric acid. The by-product obtained can be successfully applied as mineral fertilizer in agriculture.

Based on the results mentioned above, it can be concluded that the application of zeolite clinoptilolite, for the purpose of additional treatment of biodiesel and separation of water and methanol is highly desirable and efficient.

Acknowledgement

This work was supported by the Ministry of Education and Science, the Republic of Serbia (project: Improvement of the quality of tractors and mobile systems with the aim of increasing competitiveness and preserving soil and environment, No. TR-31046).

REFERENCES

[1] F. Ma, M.A. Hanna, Biodiesel production: a review, Bioresour. Technol. **70** (1999) 1–5.

[2] A. Srivastava, R. Prasad, Triglycerides-based diesel fuels, Renewable Sustainable Energy Rev. **4** (2000) 111–133.

[3] C. Carraretto, A. Macor, A. Mirandola, A. Stoppato, S. Tonon, Biodiesel as alternative fuel: experimental analysis and energetic evaluations, Energy **29** (2004) 195––211.

[4] M.S. Graboski, R.L. McCormick, Combustion of fat and vegetable oil derived fuels in diesel engines, Prog. Energy Combust. Sci. **24** (1998) 125–164.

[5] W. Du, Y.Y. Xu, D.H. Liu, J. Zhang, Comparative study on lipase catalyzed transesterification of soybean oil for biodiesel production with different acyl acceptors. J. Mol. Catal., B **30** (2004) 125–129.

[6] G. Vicent, A. Coteron, M. Martinez, J. Aracil, Application of the factorial design of experiments and response surface methodology to optimize biodiesel production. Indus Crop Prod. **8** (1998) 29–35.

[7] G. Vicente, M. Martinez, J. Aracil, Integrated biodiesel production: a comparison of different homogeneous catalysts systems, Bioresour Technol. **92** (2004) 297––305.

[8] J. Van Gerpen, Biodiesel processing and production, Fuel Process. Technol. **86** (2005) 1097–1107.

[9] Y. Zhang, M.A. Dube, D.D. McLean, M. Kates, Biodiesel production from waste cooking oil: economic assessment and sensitivity analysis, Bioresour. Technol. **90** (2003) 229–240.

[10] Y. Zhang, M.A. Dube, D.D. McLean, M. Kates, Biodiesel production from waste cooking oil: process design and technological assessment, Bioresour. Technol. **89** (2003) 1–16.

[11] T. Ebiura, T. Echizen, A. Ishikawa, K. Murai, T. Baba, Selective transesterification of triolein with methanol to methyl oleate and glycerol using alumina loaded with alkali metal salt as a solid-base catalyst, Appl. Catal., A **283** (2005) 111–116.

[12] J.K. Hak, S.K. Bo, J.K. Min, M.P. Young, Transesterification of vegetable oil to biodiesel using heterogeneous base catalysts, Catal. Today **93** (2004) 315–320.

[13] M.P. Dorado, E. Ballesteros, F.J. Lopez, M. Mittelbach, Optimization of alkali-catalyzed transesterification of *Brassica carinata* oil for biodiesel production, Energy Fuels **18** (2004) 77–83.

[14] M. Kachel-Jakubowska, M.Szpryngiel, Influence on drying condition on quality properties of rapeseed. Int. Agrophysics **22** (2008) 327–331.

[15] J. Van Gerpen, Biodiesel processing and production, Fuel Process. Technol. **86** (2005) 1097–1107.

IZVOD

DOBIJANJE BIODIZELA OD ULJANE REPICE SORTE „BANAĆANKA“ KORIŠĆENJEM KOH KATALIZATORA

Radoslav D.Mićić[1], Milan D.Tomić[2], Mirko Đ.Simikić[2], Aleksandra .R. Zarubica[3]

[1]*NIS Gasprom, Rafinerija Novi Sad, Novi Sad, Srbija*
[2]*Univerzitet u Novom Sadu, Poljoprivredni fakultet, Novi Sad, , Srbija*
[3]*Univerzitet u Nišu, Prirodno–matematički fakultet, Niš, Srbija*

(Stručni rad)

U ovom radu je ispitivana mogućnost korišćenja ulja dobijenog ceđenjem uljane repice sorte “Banaćanka” za proizvodnju biodizela. Korišćeno ulje, kao i zaostala uljana sačma su potpuno okarakterisani. Sorta “Banaćanka”, najstarija domaća sorta uljane repice, je interesantna zbog niskog sadržaja eruka kiseline i glikozinolata, zbog čega je svrstna u sorte “00”. Transesterifikacija neobrađenog, sirovog repičinog ulja je vršena u šaržnom reaktoru u prisustvu KOH kao katalizatora. Ispitivan je uticaj temperature, vremena tretmana, količine katalizatora, brzine mešanja i molarnog odnosa metanol/ulje na sintezu biodizela. Optimizovana je metoda prečišćavanja sintetisanog biodizela. Sadržaj metil-estra u prečišćenom proizvodu je određen GC u skladu sa metodom SRPS EN 14103. U analizi rezultata naglašen je pojedinačni uticaj ispitivanih parametara kao i njihov odnos, pri čemu je konstatovan poseban značaj brzine mešanja, zbog prirode sirovina koje su nemešljive. Finalni proizvod, biodizel, je prečišćen zeolitom i utvrđen je njegov uticaj na sadržaj vlage i tačku paljenja.

Ključne reči: Transesterifikacija • Banaćanka • Uljana repica • Homogeni bazni katalizator KOH • Metil-estri masnih kiselina (FAME) • Procesni parametri

Gljive i mikotoksini – kontaminenti hrane

Sunčica D. Kocić-Tanackov, Gordana R. Dimić

Univerzitet u Novom Sadu, Tehnološki fakultet, Novi Sad, Srbija

Izvod

Rast gljiva na/u hrani prouzrokuje fizičke i hemijske promene, koje negativno utiču na senzorni i nutritivni kvalitet. Vrste iz rodova *Aspergillus, Penicillium, Fusarium, Alternaria, Cladosporium, Mucor, Rhizopus, Eurotium* i *Emericella* su najčešće utvrđene na/u hrani. Neke od njih predstavljaju potencijalnu opasnost za ljude i životinje jer biosintetišu i izlučuju toksičnine sekundarne metabolite – mikotoksine (aflatoksine, ohratoksina A, sterigmatocistin, zearalenon, fumonizin, deoksinivalenol, i dr.). Toksični efekti mikotoksina ispoljavaju se u vidu različitih sindroma kod ljudi i životinja, poznati kao mikotoksikoze, a manifestuju se kao citotoksičnost, hepatotoksičnost, neurotoksičnost, teratogenost, mutagenost i kancerogenost prema ciljnom tkivu, organu ili sistemu organa. Ovaj rad daje pregled najznačajnijih mikotoksina, njihove biološke efekte, pod kojim uslovima se sintetišu, rasprostranjenost u hrani, dozvoljeni tolerantni unos, kao i mogućnost njihove razgradnje.

Ključne reči: gljive, mikotoksini, hrana.

Dostupno na Internetu sa adrese časopisa: http://www.ache.org.rs/HI/

PREGLEDNI RAD

UDK 579.67:543:616

Hem. Ind. **67** (4) 639–653 (2013)

doi: 10.2298/HEMIND120927108K

GLJIVE U HRANI

Najčešće izolovane vrste gljiva iz hrane pripadaju rodovima *Aspergillus, Penicillium, Fusarium, Alternaria, Cladosporium, Mucor, Rhizopus, Eurotium* i *Emericella* (Tabela 1) [1–3].

Vrste rodova *Aspergillus, Penicillium* i *Eurotium* su „skladišne“ gljive koje se razvijaju pri aktivnosti vode (a_w vrednosti) 0,85 i nižim, tako da se mogu izolovati iz začina [2–11], sušenog voća, povrća [12–15], semena tikve golice, suncokreta [16] i sličnih proizvoda. Vrste iz rodova *Fusarium* i *Alternaria* su „poljske“ gljive i za njihov razvoj je potreban veći sadržaj vlage u supstratu i niže temperature. Ove vrste se najčešće mogu naći u/na zrnima žita i proizvodima od žita [15–24]. Takođe, navode se kao česti uzročnici oboljenja voća i povrća još u polju, pored vrsta iz rodova *Sclerotina, Botrytis, Monillia, Rhizopus, Mucor* i *Penicillium* [25]. Gljive su česti kontaminenti i proizvoda od mesa i mleka tokom skladištenja. Vrste iz rodova *Penicillium, Aspergillus, Cladosporium, Geotrichum, Mucor, Sporotrichum, Trichoderma* su najčešće izolovane iz ovih grupa namirnica [1–3,22,26].

Tokom rasta filamentozne gljive mogu proizvoditi veliki broj enzima (lipaza, proteaza, karbohidrogenaza). U hrani ovi enzimi mogu nastaviti svoje aktivnosti nezavisno od uništenja ili uklanjanja micelije gljiva. Enzimske aktivnosti mogu uticati na promene ukusa i mirisa hrane, kao što su miris na buđ kod vina i suvog voća ili netipična aroma (”rioy”) kafe [1,27,28]. Navedene promene mogu prouzrokovati *Penicillium brevicompactum, P. crustosum* i *Aspergillus flavus* transformacijom 2,4,6-trihlorofenola u trihloroanisol (TCA). Neki od ovih mirisa mogu nastati već pri malim količinama TCA (8 ng/L u kafi) ili trans-1,3-pentadiona nastalog transformacijom sorbinske kiseline usled aktivnosti *Penicillium* spp., *Trichoderma* spp. i *Paecilomyces variotii* [1,29,30]. Rezultat enzimske aktivnosti gljiva može biti potpuna dezintegracija strukture hrane, npr. kod pasterizovanih plodova jagode usled rasta *Byssochlamys fulva* i *B. nivea* koje su otporne na toplotu. Vrste iz rodova *Penicillium*, *Aspergillus* i *Fusarium* mogu proizvoditi isparljiva jedinjenja, kao što su dimetil-disulfid, geosmin i 2-metilisoborneol, koja u veoma malim količinama negativno utiču na kvalitet hrane i pića [31,32].

U poslednjih 50 godina gljive u hrani su privukle posebnu pažnju zbog sposobnosti da proizvode mikotoksine. Prisustvo toksigenih gljiva i mikotoksina u namirnicama biljnog i životinjskog porekla, kao i u hrani za životinje, dokumentovano je od strane mnogih autora kod nas u i svetu [4,5,7,10,14,15,19,21,33–46].

MIKOTOKSINI U HRANI

Mikotoksini, kao sekundarni produkti metabolizma nekih vrsta filamentoznih gljiva, sintetišu se od velikog broja biohemijski jednostavnih međuprodukata primarnog metabolizma (acetata, malonata, mavalonata i nekih aminokiselina – fenilalanina, serina, triptofana, alanina) usled aktivnosti različitih enzima. Glavne biosintetske reakcije uključuju kondenzaciju, oksido-redukciju, alkiliranje i halogeniranje, u kojima nastaje veliki broj različitih jedinjenja.

Glavni biohemijski putevi uključeni u nastajanje mikotoksina su poliketidni (aflatoksini, sterigmatocistin, ohratoksini, zearalenoni, citrinin, patulin), terpenski

Prepiska: S. Kocić-Tanackov, Univerzitet u Novom Sadu, Tehnološki fakultet, Bulevar cara Lazara 1, 21000 Novi Sad, Srbija.
E-pošta: suncicat@uns.ac.rs
Rad primljen: 27. septembar, 2012
Rad prihvaćen: 6. novembar, 2012

Tabela 1. Najčešće vrste gljiva izolovane iz hrane (modifikovano prema Filtenborg i sar. [1])
Table 1. The most common species of fungi isolated from foods (modified by Filtenborg et al. [1])

Vrsta hrane	Vrste gljiva
Citrusno voće	*Alternaria citri, A. tangelonis, A. turkisafria, A. colombiana, A. perangusta, A. interrupta, A. dumosa, Penicillium digitatum, P. italicum, P. ulaiense*
Kaša od jabuke i koštičavo voće	*Penicillium expansum, P. crustosum, P. solitum, Alternaria gaisen, A. mali, A. tenuissima* group*, A. arborescens* group*, A. infectoria* group*, Cladosporium* spp.
Beli i crni luk	*Penicillium allii, P. albocoremium, P. glabrum, Petromyces alliaceus, Botrytis aclada*
Krtola krompira	*Fusarium sambucinum, F. coeruleum*
Paradajz	*Alternaria arborescens, Stemphylium* spp., *Penicillium olsonii*
Pšenica i raž u polju	*Fusarium culmorum, F. graminearum, F. avenaceum, F. equiseti, F. poae, F. tricinctum, Alternaria triticimaculans, A. infectoria, A. oregonensis, A. triticina, A. triticicola, A. tenuissima* group*, Cladosporium herbarum, Epicoccum nigrum, Stemphylium* spp., *Ulocladium* spp., *Drechslera* spp., *Botrytis* spp., *Penicillium* spp., *Claviceps purpurea*
Pšenica i raž u skladištu	*Penicillium aurantiocandidum, P. cyclopium, P. freii, P. hordei, P. melanoconidium, P. polonicum, P. verrucosum, P. aurantiogriseum, P. viridicatum, Aspergillus flavus, A. niger, A. candidus, Eurotium* spp., *Alternaria infectoria* group
Žita u skladištu	*Paecilomyces variotii, Scopulariopsis candida, Penicillium roqueforti, Candida* spp., *Byssochlamys fulva, B. nivea, Fusarium* spp., *Alternaria* spp., *Cladosporium* spp.
Začini	*A. flavus, A. tamarii, A. niger, A. ochraceus, A. candidus, A. versicolor, Eurotium* spp., *Wallemia sebi, P. islandicum, P. neopurpurogenum, P. citrinum, P. aurantiogriseum*
Orašasto voće	*P. commune, P. crustosum, P. discolor, P. solitum, P. funiculosum, P. oxalicum, P. citrinum, A. flavus, A. wentii, A. versicolor., Eurotium* spp., *Alternaria infectoria* group
Raženi hleb	*Penicillium roqueforti, P. paneum, P. carneum, P. corylophilum, Eurotium repens, E. rubrum, Paecilomyces variotii, Monascus ruber*
Sir	*Penicillium commune, P. nalgiovense, P. atramentosum, P. nordicum, Aspergillus versicolor, Scopulariopsis fusca, S. candida, S. brevicaulis*
Masti, margarin i slčni proizvodi	*P. echinulatum, P. commune, P. solitum, P. spinulosum, Cladosporium herbarum*
Fermentisane kobasice	*Penicillium nalgiovense, P. olsonii, P. chrysogenum, P. nordicum, P. solitum, P. oxalicum, P. commune, P. expansum, P. miczynskii, P. brasilianum, P. aurantiogriseum*
Pasterizovana hrana	*Byssochlamys fulva, B. nivea, Hamigera reticulata, Neosartorya fischeri, N. glabra, N. spinosa, Eupenicillium lapidosum, Talaromyces macrosporus, T. bacillisporus, Paecilomyces variotii*
Hrana sa niskim sadržajem a_w	*Eurotium chevalieri, E. herbariorum, E. amstelodami, Wallemia sebi, Aspergillus penicillioides, A. restrictus, Eremascus albus, E. fertilis, Xeromyces bisporus, Scopulariopsis halophilica, Chrysosporium inops (sensu* Pitt), *C. farinicola, C. fastidium, C. xerophilum, Polypaecilum pisce*

(trihoteceni), aminokiselinski (gliotoksini, ergotamin, sporidezmin, malformin C, ciklohlorotin, ksantocilin, ksantoascin) i put trikarbonskih kiselina (rubratoksini) [47–50]. Neki mikotoksini (npr. ciklopiazonična kiselina, alfatrem, rokfortin) nastaju iz dva ili više prekursora poreklom iz različitih puteva biosinteze. Postoji nekoliko hipoteza o fiziološkoj funkciji sekundarnih metabolita kod gljiva koje ih produkuju. Najverovatnija je da ovi metaboliti poseduju zaštitnu i regulatornu ulogu. Pretpostavlja se da sekundarni metabolizam predstavlja neku vrstu „sigurnosnog ventila“ kojim se međuproizvodi, nastali primarnim metabolizmom, uklanjuju iz ćelije u momentu kada se prekida faza optimalnog rasta gljiva [50].

Vrste iz rodova *Aspergillus, Penicillium*, *Fusarium* i *Alternaria*, kao i teleomorfi klase *Ascomycetes* (*Petromyces alliaceus, Emericella nidulans*, i dr.) najčešće se navode kao potencijalni proizvođači mikotoksina [51].

Biogenetski i strukturno, mikotoksini pripadaju različitim vrstama prirodnih jedinjenja. Njihova biološka aktivnost na ljude i životinje obuhvata akutnu i hroničnu toksičnost (citoksičnost, hepatotoksičnost, neurotoksičnost, teratogenost, mutagenost i kancerogenost), poznata kao mikotoksikoza. Prema stepenu toksičnosti mikotoksini se dele na tri grupe. Prvu grupu čine izrazito toksični kao što su ciklohlorotin i rubratoksin B, sa letalnim efektom u količinima manjim od 1 mg/kg TM. Drugu grupu čine vrlo toksični mikotoksini (aflatoksin B_1, trihoteceni i citreoviridin) koji su letalni pri koncentracijama od 1 do 10 mg/kg TM. Treću grupu čine svi ostali toksični metaboliti sa letalnim efektom pri koncentracijama većim od 10 mg/ kg TM [48,49].

Na ćelijskom nivou neki mikotoksini reaguju sa nukleinskim kiselinama i inhibiraju biosintezu makromolekula DNK i RNK ili proteina. Drugi deluju na strukture i funkcije bioloških membrana ili na nivou energetskog metabolizma [24,52–54]. Stepen osetljivosti organizma

zavisi od pola, starosti, ishrane, stanja organizma, količine i vrste, kao i dužine perioda njihovog unošenja.

U istoriji se nailazi, ne retko, na podatke o masovnim trovanjima ljudi i životinja koja se povezuju sa konzumiranjem hrane kontaminirane gljivama i mikotoksinima. Jedna od prvih poznatih mikotoksikoza je ergotizam, prouzrokovana ergot alkaloidima koje biosintetišu vrste roda *Claviceps.* Ergotizam je bio odgovoran za smrt hiljada ljudi srednjovekovne Evrope [48,54]. U 20. veku opisana je pojava nekoliko mikotoksikoza životinja i ljudi: bolest konja i svinja u SAD, povezana sa uzimanjem raži koja je bila kontaminirana sa *Fusarium graminearum*; stahibotrikoza konja u bivšem SSSR-u i ovaca u Slovačkoj i Mađarskoj; facijalni ekcem ovaca na Novom Zelandu; tumori jetre indukovani „žutim pirinčanim toksinom" u Japanu nakon II svetskog rata; alimentarna toksična aleukija (ATA) u Sibiru 1913. godine; balkanska endemska nefropatija, i dr. Međutim, mikotoksinima i mikotoksikozama se nije pridavala velika pažnja sve do 1960. godine, kada je „X"-bolest ćurana, pačića i fazana prouzrokovala velike ekonomske štete u Engleskoj i dovela do otkrića uzročnika – aflatoksina. Ovaj mikotoksin je dobio ime po vrsti koja ga je sintetisala, *Aspergillus flavus*, izolovanoj iz kikirikijevog brašna kojim su hranjene živine [51,52,54].

Danas je poznato više od 400 vrsta mikotoksina, ali njihov broj se stalno povećava. Međutim, svega nekoliko mikotoksina je veoma dobro opisano u toksikologiji. Aflatoksini su najviše istraživani.

S obzirom na značaj, u ovom radu posebna pažnja biće posvećena aflatoksinima, sterigmatocistinu, ohratoksinima, fuzariotoksinima, Alternaria toksinima i patulinu.

Aflatoksini

Aflatoksini su veoma toksični kumarinski derivati koje uglavnom biosintetišu *A. flavus* i *A. parasiticus*. Najvažniji mikotoksini iz ove grupe su aflatoksini B_1 (AB_1) (Slika 1), B_2 (AB_2), G_1 (AG_1), G_2 (AG_2), M_1 (AM_1) i M_2 (AM_2). Aflatoksini B_2 i G_2 su dihidroderivati aflatoksina B_1 i G_1. Aflatoksini M_1 i M_2 su dihidroderivati aflatoksina B_1 i B_2 i izlučuju se mlekom, urinom i fecesom [51,55].

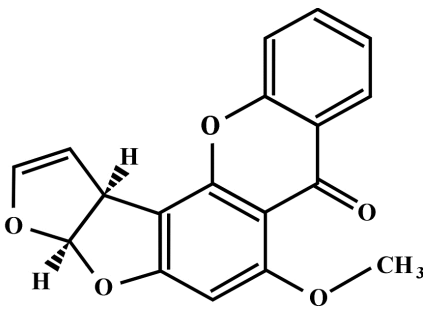

Slika 1. Strukturna formula aflatoksina B_1.
Fig. 1. The structural formula of aflatoxin B_1.

Ove mikotoksine gljive biosintetišu u/na velikom broju supstrata, kao što su semena uljarica, žita i njihovi proizvodi, koštičavo voće, suptropsko voće, začini [56]. Najčešće se nalaze u proizvodima koji nisu dovoljno osušeni posle žetve ili tokom skladištenja pri relativno visokim temperaturama. Iz ove grupe mikotoksina AB_1 je najjači kancerogen, slede AG_1, AM_1 i AB_2. Kod sisara aflatoksini prouzrokuju akutne aflatoksikoze, koje se manifestuju pre svega oštećenjem jetre, mada mogu biti oštećeni i bubrezi, pluća i slezina. AB_1 opisan je kao najsnažniji potencijalni hepatokancerogen [57]. Da bi izazvali reakciju u živom organizmu moraju se biotransformisati u visokoreaktivne metabolite. Tako, specifične monooksigenaze u mitohondrijama prevode AB_1 u AB_1--2,3-epoksid koji reaguje sa nukleofilnim mestima u makromolekulama i na taj način inhibira replikaciju DNK i RNK i sintezu proteina [48,49]. Takođe su dokazana i delovanja ovog mikotoksina na citoplazmatičnu membranu i na put oksidativne fosforilacije [54].

Letalna doza (LD_{50}) za životinje varira od 0,3 do 10 mg/kg telesne mase (TM) [48]. U Indiji je kod 647 pacijenata iz 150 gradova, koji su konzumirali plesnivi kukuruz, utvrđen AB_1 u koncentracijama od 0,25 do 5,6 mg/kg [52].

Za biosintezu aflatoksina optimalna temperatura je 30 °C i relativna vlažnost između 88 i 95% [58,59]. Pokazuju veliku stabilnost na uticaj visokih temperatura (razgrađuju se na temperaturi višoj od 250 °C), na promene koncentracije vodonikovih jona, na UV i gama zračenje. Zagrevanjem na 100 °C u kiseloj sredini oko 90% AB_1 prelazi u AB_2, dok se na 160 °C razgrađuje samo 20% AB_1. Mogu se razgraditi pod dejstvom hromsumporne kiseline, natrijumhipohlorita, koncentrovanog natrijumhidroksida, dužim izlaganjem svetlosti, pri temperaturama od 268 do 269 °C, kao i pod uticajem bakterija mlečne kiseline (*Lactobacillus rhamnosus*, *L. delbrueckii*, *L. plantarum, L. lactis* i *L. casei*), bifidobakterija (*Bifidobacterium bifidum* i *B. longum*), *Flavobacterium aurantiacum* i *Saccharomyces cerevisiae* [48,49,54].

Kuiper-Gudman [60] je ustanovio tolerantni dnevni unos od 0,15 ng/kg TM za AB_1 i 0,20 ng/kg TM za AM_1.

Sterigmatocistin

Sterigmatocistin (STC) je sekundarni metabolit nekih vrsta iz rodova *Aspergillus* (*A. versicolor, A. ustus, A. rugulosus, A. bipolaris, A. aurantio-brunens, A. quadrilineatus*), *Eurotium* (*E. herbariorum*), *Emericella* (*E. nidulans*), *Drechslera, Bipolaris* i *Penicillium* [45,61]. Kao najvažniji proizvođač ovog toksičnog metabolita navodi se *A. versicolor* [45]. U hemijskoj strukturi ima difurometoksibenzenski prsten (Slika 2), kao i AB_1, te se smatra da bi ova dva mikotoksina mogla imati zajednički itermedijer (norsolorinična kiselina) u njihovoj biosintezi [62,63].

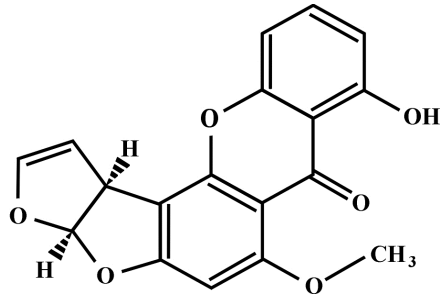

Slka 2. Strukturna formula sterigmatocistina.
Fig. 2. The structural formula of sterigmatocystin.

Iako je STC oko 100 puta slabiji kancerogen od AB_1, njegova široka rasprostranjenost i znatno veće količine u namirnicama [56] i stočnoj hrani, navode na zaključak da bi on mogao biti štetniji od AB_1 [64]. U prilog ovoj tvrdnji govori i činjenica da je iz 100 g suvog *A. versicolor* izolovano čak 1,3 g STC. Istraživanja ukazuju da se u određenim uslovima STC može transformisati u AB_1. Internacionalna agencija za istraživanje kancera (International Agency for Research on Cancer, IARC) svrstala je STC u 2B grupu kancerogena, na osnovu komparacije njegove akutne toksičnosti, kancerogenosti i metabolizma sa AB_1 i drugim hepatotoksičnim mikotoksinima [65–67].

Dovodi do oštećenje jetre i renalne nekroze kod pacova. Smatra se da je uključen u etiologiji hronične bolesti jetre kod ljudi u Africi [52,68]. Zabeleženi su i slučajevi miokardijalne nekroze srca i pulmonalnih tumora kod eksperimentalnih životinja [69].

Opisana je toksičnost i derivata STC. Istraživanja ukazuju da je dimetilsterigmatocistin kancerogen, a da dihidrosterigmatocistin inhibira mitozu i spajanje markiranih timidina i uridina, što upućuje na inhibiciju sinteze DNK i RNK. Suprotno tome, dihidro-*O*-metilsterigmatocistin ispoljava slab inhibitorni uticaj na mitozu i sintezu DNK i RNK [54,70]. Lipidna peroksidacija se javlja kao sekundarni mehanizam toksičnosti STC [71].

Optimalni uslovi za biosintezu STC od strane *A. versicolor* i *Bipolaris sorokiniana* su temperatura između 23 i 29,1 °C, a_w 0,76 i sadržaj vlage 5% [45].

STC je detektovan u žitima, hlebu, siru, začinima, kafi, pasulju, soji, pistaćima, koštičavom voću, pivu, povrću, stočnoj hrani i silaži [45,46,56,72].

Stabilan je 60 min na temperaturi od 115 °C. Nakon pečenja hleba, pripremljenog od pšenice kontaminirane sa 83 μg/kg STC, sadržaj ovog mikotoksina je bio 48 μg/kg, što je ekvivalentno 78 μg/kg u pšenici [45].

Republika Češka i Slovačka jedine propisuju zakon o maksimalno dozvoljenim koncentracijama STC u hrani [45]. Maksimalno dozvoljena koncentracija ovog mikotoksina je 5 μg/kg za pirinač, žita, brašno, krompir, povrće, meso i mlečne proizvode, a 20 μg/kg za ostale proizvode.

Ohratoksini

Glavni proizvođači ohratoksina su vrste *A. ochraceus* (*A. ochraceus, A. melleus, A. ostianus, A. sulphurues*) i *Penicillium verrucosum*. Međutim, mnogi autori navode da ove metabolite mogu biosintetisati i crne gljive roda *Aspergillus* (*A. niger* i *A. carbonarius*) [73––76], kao i *A. albertensis, A. auricomus* i *A. wentii* [75]. Vrste *P. nordicum*, *P. viridicatum* [77] i *P. aurantiogriseum* [78] se takođe, navode kao potencijalni proizvođači ohratoksina.

Prema hemijskoj strukturi su dihidroizokumarini, povezani sa L-α-fenilalaninom (Slika 3) [55]. Ohratoksine čine ohratoksin A (OA), ohratoksin B (OB), ohratoksin C (OC), 4-hidroohratoksin A i ohratoksin α. Osim ovih metabolita, u ovu grupu su uključene još dve grupe dihidroizokumarina. Jedna obuhvata mikotoksine grupe viomeleina (viriditoksin, ksantomegnin, ksantoviridikatin A i G), dok predstavnici druge grupe (kladosporin, melein i njegovi derivati, monocerin i 7-*o*-dimetilmonocerin) nemaju potvrđena svojstva mikotoksina, ali ispoljavaju druge biološke efekte [48].

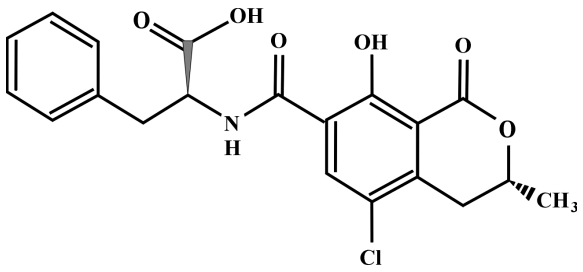

Slika 3. Strukturna formula ohratoksina A.
Fig. 3. The structural formula of ochratoxin A.

Iz ove grupe najrasprostranjeniji i najtoksičniji je OA. Smatra se da je potencijalni nefrotoksin i da je uključen u etiologiju balkanske endemske nefropatije, teške hronične bolesti bubrega zabeležene kod ljudi u ruralnim sredinama u nekim područjima Bosne i Hercegovine, Hrvatske, Srbije, Bugarske i Rumunije [52]. Isto tako, smatra se mogućim uzročnikom tumora urinarnog trakta kod ljudi i životinja.

Embriotoksičnost i teratogenost ovog mikotoksina je utvrđena kod velikog broja eksperimentalnih životinja. Opisani su i imunosupresivni efekti [57]. OA inhibira sintezu proteina kod prokariota i eukariota, utiče na glukoneogenezu, transportni lanac u mitohondrijama i respiraciju [79]. Od mikotoksina grupe viomeleina, ksantomegnin pokazuje efekat na mitohondrijsku fosforilaciju – povećava prelazak elektrona od NADH dehidrogenaze do citohroma C u mitohondrijskom transportnom lancu [80].

U 50% uzoraka humane krvi u zemljama zapadne Evrope OA je utvrđen u koncentracijama od 1 do 2 μg/kg. Detektovan je i u majčinom mleku u niskim koncetracijama [52].

Dokazano je da fenilalanin može neutralisati njegove toksične efekte u kulturi ćelija hepatoma i kod miševa. Ovaj efekat može biti povezan s konkurencijom u sintezi proteina između ovog mikotoksina i fenilalanina [48].

Produkcija OA zavisi od uslova okruženja. Tako, *A. ochraceus* sintetiše ovaj mikotoksin pri temperaturama od 12 do 37 °C i a_w 0,80 [81], dok psihrofilne *Penicillium* spp. (npr. *P. verrucosum*) mogu produkovati OA pri temperaturama od 4 do 31 °C [51].

Detektovan je u kukuruzu, ječmu, pasulju, kikirikiju, voću, povrću, vinu i pivu [56]. Glavni put unosa kod ljudi je preko kontaminiranih žita, lešnika, pirinča, kafe, vina, piva, maslina, ali i preko proizvoda od mesa. S obzirom da se svinjska krv i plazma, kao i različite vrste začina koriste u pripremi kobasica, i ovi proizvodi mogu sadržavati OA [51].

FAO/WHO (*Food and Agriculture Organization*/ /*World Health Organization*) ekspertski komitet za dodatke u hrani su ustanovili nedeljni toleranti nivo unosa OA od 100 ng/kg TM. Radna grupa nordijskih zemalja i Naučnog komiteta za hranu propisali su znatno manji dnevni unos ovog mikotoksina od 5 ng/kg TM [51].

Fuzariotoksini

Fuzariotoksini su sekundarni metaboliti vrsta roda *Fusarium*. Poznato je da 35 od 61 vrsta ovog roda biosintetišu 137 mikotoksina, od kojih 79 pripada grupi trihotecena [24, 82]. Marasas [83] izdvaja tri najznačajnije toksigene vrste roda *Fusarium*: *F. sporotrichioides* (T-2 toksin, deoksinivalenon), *F. graminearum* (zearalenon i deoksinivalenon) i *F. verticillioides* (sin. *F. moniliforme*) (fumonizini).

Na osnovu biogenetskog porekla Desjardins i Proctor [84] su fuzariotoksine klasifikovali u nekoliko grupa:

- poliketide (fumonizini, fuzarinska kiselina, fuzarini, moniliformin, naftazarini, sambutoksin i zearalenoni),
- terpenoide (fuzaproliferin, trihoteceni),
- derivati aminokiselina (enijatini, bovorecin) i
- derivati šikimske kiseline (fuzarohromanon).

Najučestaliji i najtoksičniji fuzariotoksini su iz grupe fumonizina, trihotecena i zearalenona.

Fumonizini

Glavni proizvođači fumonizina su *F. verticillioides* (sin. *F. moniliforme*) i *F. proliferatum*. Po hemijskoj prirodi su derivati poliketida (Slika 4). Njihovo otkriće povezuje se sa pojavom leukoencefalomalacije (ELEM) kod konja (1970. godine), koja se manifestovala nekrozom bele kičmene mase, a prouzrokovana je hranjenjem životinja hranom koja je bila zaražena gljivom *F. verticillioides*. U prirodi preovlađuje B serija fumonizina (B_1, B_2, B_3 i B_4) od kojih je FB_1 zastupljen do 70% od ukupnog nivoa fumonizina [24]. Ovi mikotoksini su rasprostranjeni kao kontaminenti zrna žita, pre svega kukuruza, kao i hrane za ljude i životinje bazirane na žitima [24,56,85].

Kod ljudi i životinja mogu prouzrokovati hepatotoksične, nefrotoksične i neurotoksične efekte. Takođe, dovode do degeneracije koštane srži i neuromišićnih veza [24,57]. Karcinom jednjaka kod ljudi u Kini i Južnoj Africi povezuje se sa visokim koncentracijama fumonizina B_1, B_2 i B_3 u kukuruzu [86,87].

Utiču na prekid biosinteze sfingolipida, na akumulaciju masnih kiselina i proliferaciju ćelija, na oksidativni stres i peroksidaciju lipida, na proliferaciju peroksizoma [24,57,88].

Najbolja sinteza FB_1 utvrđena je na zrnima kukuruza koji je sadržavao od 27 do 32% vlage i pri temperaturi od 20 °C [89].

Postupkom amonizacije u kombinaciji sa visokom temperaturom moguća je uspešna detoksikacija fumonizina [24]. Tretmanom kukuruza kombinacijom H_2O_2 i $NaHCO_3$ ili $(NH_4)_3PO_4$ smanjuje se njihova količina i do 100% [24,90]. U rastvoru metanola nakon šest nedelja čuvanja pri temperaturama 4, 25 i 40 °C dolazi do razgradnje FB_1 i FB_2 od 5,35 do 60,0% [24,91].

Naučni komitet za hranu Evropske unije ustanovio je dnevno tolerantno unošenje fumonizina kod ljudi do 2,0 μg/kg TM [92].

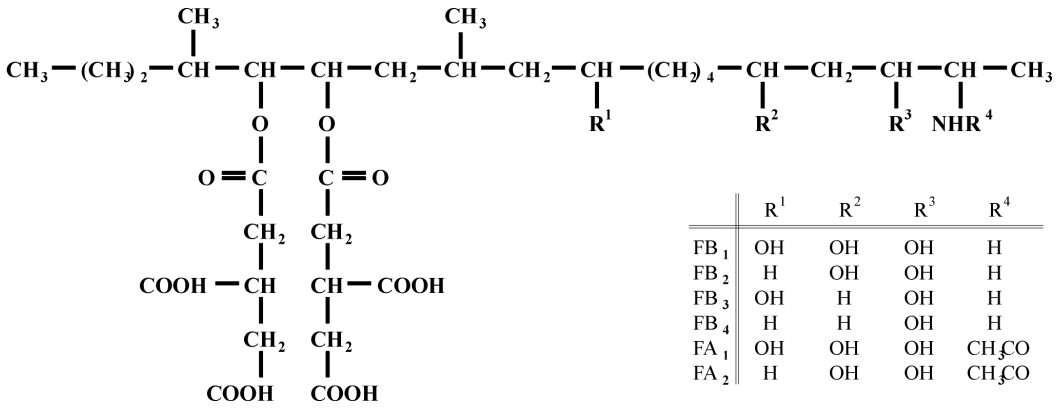

	R^1	R^2	R^3	R^4
FB_1	OH	OH	OH	H
FB_2	H	OH	OH	H
FB_3	OH	H	OH	H
FB_4	H	H	OH	H
FA_1	OH	OH	OH	CH_3CO
FA_2	H	OH	OH	CH_3CO

Slika 4. Strukturne formule fumonizina A i B serije.
Fig. 4. The structural formulas of fumonisins A and B series.

Trihoteceni

Trihoteceni su velika grupa hemijski sličnih jedinjenja koji su produkti gljiva (*Fusarium, Stachybotrys, Myrothecium, Verticimonosporium, Cylindrocarpon, Trichoderma, Trichothecium, Calonectria* i *Cephalosporium*), ali i nekih biljnih vrsta (*Asteraceae* i *Baccharis megapotamica*) [24,51,82,93].

Derivati su seskviterpena (Slika 5) i prirodni kontaminenti žita i njihovih proizvoda [24,56]. Na osnovu prisustva makrocikličnog prstena (Slika 5), koji je u C-4 i C-15 položaju vezan diestrom i triestrom, trihoteceni se dele na nemakrociklične (podgrupe A-C) i makrociklične (podgrupe D-F) [24,48].

Fusarium vrste biosintetišu trihotecene tipa A i B. Prema Thraneu [94] *F. poae, F. sporotrichioides, F. acuminatum* i *F. equiseti* su glavni proizvođači trihotecena tipa A, a *F. crookwellense, F. culmorum, F. graminearum* i *F. sambucinum* tipa B.

T-2 toksin i njegovi derivati, deoksinivalenol ili vomitoksin (DON), 3-acetildeoksinivalenol (3-AcDON), 15-acetildeoksinivalenol (15-AcDON), nivalenol (NIV), diacetoksisciprenol i fuzarenon-X (Fus-X) su najčešći mikotoksini iz grupe trihotecena koji su određeni u hrani. Odgovorni su uzročnici alimentarne toksične aleukije (ATA) u Sibiru 1913. godine i tokom II svetskog rata. Ova bolest se manifestovala leukopenijom, granulopenijom i limfocitozom, a uzrokovana je konzumiranjem prezimljenih plesnivih žita i njihovih proizvoda koji su bili kontaminirani toksigenim vrstama iz roda *Fusarium* (*F. sporotrichioides* i *F. poae*) [24,55]. Toksikološki, ovi mikotoksini kod sisara uzrokuju i povraćanje, odbijanje hrane, dijareju, neurološke promene, iritaciju kože, hemoragije i poteškoće u razmnožavanju. Deluju na degeneraciju ćelija i ćelijskog jedra timusa, koštane srži, tankog creva, testisa, jajnika i drugih ćelija tokom deobe. Na ćelijskom nivou utiču na proces metabolizma ugljenih hidrata, masti, steroida, funkciju mitohondrija i sprečavanje biosinteze proteina i nukleinskih kiselina. Snažni su inhibitori sinteze proteina na eukariotskim 60S ribozomima i dovode do inaktivacije početka (T-2 toksin, HT-2 toksin, DAS, NIV, Fus-X) ili završetka (DON) procesa sinteze proteina [24,48,54].

Za rast *Fusarium* spp. i biosintezu trihotecena pogoduju visoka vlažnost i niže temperature (21 °C).

Nivo trihotecena se može smanjiti tokom tehnoloških postupaka dobijanja prehrambenih proizvoda, kao

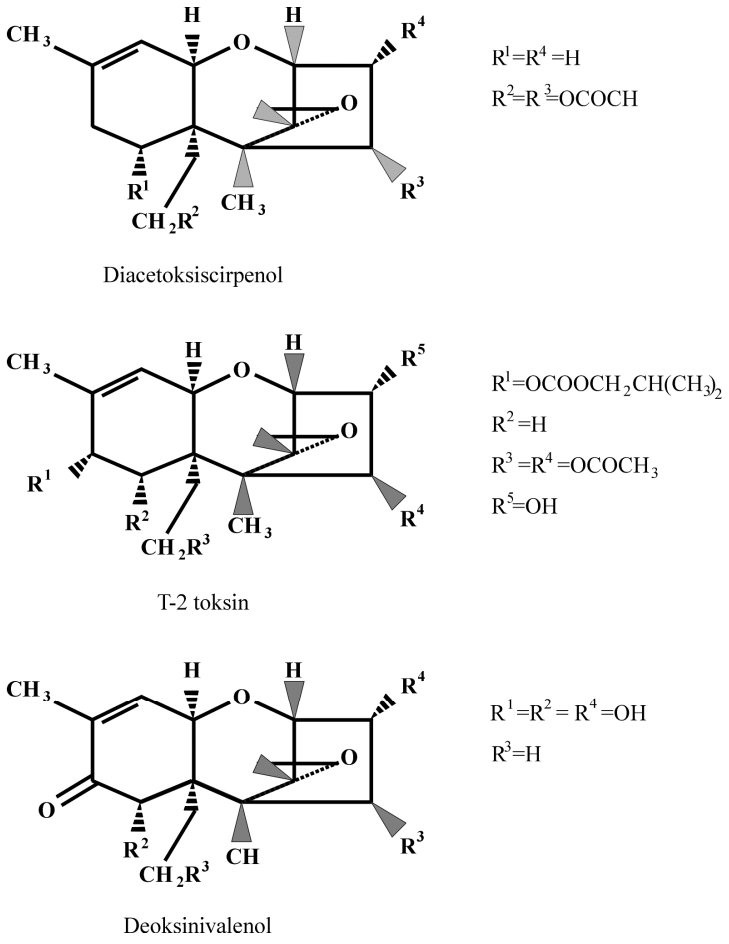

Slika 5. Strukturne formule nekih trihotecena.
Fig. 5. The structural formulas of some trichothecenes.

što su prečišćavanje zrna, suva i mokra meljava, fermentacija u proizvodnji piva, pečenje ili kuvanje. Dodatkom preparata na bazi zeolita takođe se smanjuje koncentracija ili eliminišu trihoteceni tipa A [95,96]. Antihistaminici (triazolam, diltazem, ketotifen) i antioksidansi (lutein i likopen) mogu smanjiti toksične efekte T-2 toksina [97,98].

Dnevno tolerantno unošenje pojedinih trihotecena za ljude ustanovio je Naučni komitet za hranu Evropske unije [92] i iznosi:

- 1 μg DON/kg TM,
- 0,7 μg povremeno NIV/kg TM i
- 0,06 μg T-2 i HT-2 toksina kombinovano/kg TM.

Zearalenoni

Zearalenoni su kao i fumonizini derivati poliketida (Slika 6). Prirodni su kontaminenti požnjevenih i uskladištenih žita i njihovih proizvoda širom sveta [19,24,40,56,99], voća, povrća [56,100,101], a mogu biti prenešeni i u mleko, meso i jaja [56,101]. Metaboliti su 18 vrsta roda *Fusarium* (*F. graminearum, F. sporotrichioides, F. semitectum, F. equiseti, F. crookwellense*, *F. culmorum* i dr.) i obuhvataju 15 derivata zearalenona sa estrogenim dejstvom (zearalenol, dihidrozearalenol, zearalan, dideoksizearalan, O-metilzearalen, p-metilzearalen, dideoksizearalanon, 2-deoksizearalenon, i dr.) i još 100 derivata koji nemaju svojstva mikotoksina, ali pokazuju druge biološke aktivnosti [24,54,55,102]. Najznajčajniji derivati zearalenona (ZON) su α- i β-zearalenoli koji uzrokuju jače toksične efekte od ZON-a. Ovi mikotoksini su poznati po estrogenim i anaboličkim efektima na ljude i životinje [55].

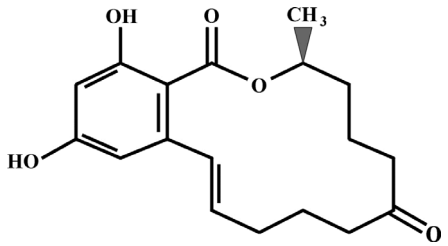

Slika 6. Strukturna formula zearalenona.
Fig. 6. The structural formula of zearalenone.

Pri konzumiranju velikih doza u hrani, s obzirom da se ZON, pogotovu njegov derivat α-zearalanol brzo resorbuju preko crevnog trakta, njihovo dejstvo može izazvati odbijanje hrane, seksualnu apatiju, pobačaje [104,105] i kancerogene efekte (karcinom prostate muškaraca i cervikalni kancer kod žena) [102,106,107]. Zabeležena je i pojava zearalenona u krvnoj plazmi dece Portorika i Mađarske u koncentraciji od 18,9 do 103,5 μg/mL, koja je izazvala sindrom preranog puberteta [101,108–110].

U istraživanjima na velikom broju životinjskih vrsta dokazano je da su za dobijanje toksičnih efekata ZON-a potrebne visoke koncentracije (i do 20000000 ppb LD_{50}), pa ga neki autori češće navode kao mikoestrogen nego mikotoksin [102]. U prilog ovoj tvrdnji ukazuju i činjenice da se ZON i njegovi derivati koriste kao anabolički agensi za podsticanje rasta i bolje iskorišćenje stočne hrane kod ovaca i goveda [48] i u humanoj medicini kao hemoterapeutici u cilju ublažavanja tegoba u periodu menopauze kod žena [49,111].

Mehanizam delovanja na ćelije sličan je delovanju estrogenih hormona. Prvo se vezuju za estrogene receptore cistola, zatim se translociraju u jedro ćelije i vezuju na lanac DNK i RNK menjajući sintezu proteina [24,102]. Koncentracija ZON-a od 60 μM u toku 72 h inhibira za preko 80% rast ćelija, sintezu DNA i proteina [112].

Koncentracija ovih mikotoksina se može smanjiti suvom i mokrom meljavom zrna žita, upotrebom vitamina E, dodavanjem 0,2 i 0,4% preparata Emagala i 0,4% Iprogala u smešama za svinje [24].

Naučni komitet za hranu Evropske unije [92] ustanovio je dozvoljeni dnevni unos ZON-a kod ljudi do 0,2 μg/kg TM.

Alternaria toksini

Alternaria toksine biosintetišu različite vrste roda Aternaria, čestih prouzrokovača bolesti biljaka. Ove vrste gljiva su glavni kontaminenti pšenice, sirka, ječma, suncokreta, uljane repice, paradajza, jabuke, citrusnog voća, maslina [113]. Zbog rasta i razmnožavanja na niskim temperaturama odgovorne su i za kvarenje proizvoda tokom transporta i skladištenja. Alternaria vrste proizvode više od 70 sekundarnih metabolita, od kojih su samo neki svrstani u mikotoksine zbog štetnog delovanja na ljude i životinje, kao što su: alternariol (AOH), alternariol monometil etar (AME), tentoksin (TEN), tenuazonična kiselina (TeA), altertoksini (ATX-I i II), *Alternaria alternata* f. sp. *lycopersici* toksini (AAL-toksini), stemfiltoksin III, altenuen (ALT) i dr. (Tabela 2, Slika 7) [114].

Vrsta *Alternaria alternata* se navodi kao najvažniji proizvođač ovih sekundarnih metabolita. Optimalni uslovi za biosintezu nekih toksina od strane ove vrste u podlozi od paradajza su: a_w 0,954 i temperatura 21 °C za AOH, a_w 0,982 i temperatura 21 °C za TeA, a_w 0,954 i temperatura 21 °C za AME [118].

Toksičnost TeA je utvrđena kod biljaka, embriona pileta, nekoliko životinjskih vrsta, uključujući zamorce, miševe, zečeve, pse i majmune [119]. Kod pasa je ovaj metabolit prouzrokovao krvarenja na nekoliko organa i subakutnu toksičnost kod pilića. Prekancerozne promene su uočene na sluznici jednjaka miševa [120]. AOH i AME su uzrokovali mutagene promene na sistemu mamalnih ćelija [121,122]. Takođe, postoje dokazi i o njihovoj kancerogenosti kao što je planocelularni karcinom indukovan kod miševa koji su tretirani sa AOH i subkutani karcinom kod tretiranih miševa sa AME

Tabela 2. Najčešće Alternaria vrste i njihovi toksini produkovani u hrani [114,115–117]
Table 2. The most common Alternaria species and their toxins produced in food [114,115–117]

Mikotoksini	Vrste gljiva
Alternariol (AOH)	*Alternaria alternata, A. brassicae, A. brassicicola, A. capsici-annui, A. cheiranthi, A. citri, A. cucumerina, A. dauci, A. infectoria, A. japonica, A. longipes, A. porri, A. solani, A. tenuissima, A. tomato*
Alternariol monometil etar (AME)	*A. alternata, A. solani, A. brassicae, A. brassicicola, A. capsici-annui, A. cheiranthi, A. citri, A. cucumerina, A. dauci, A. infectoria, A. japonica, A. solani, A. tenuissima, A. tomato*
Tentoksin (TEN)	*A. alternata, A. porri*
Tenuazonična kiselina (TeA)	*A. alternata, A. brassicae, A. brassicicola, A. capsici-annui, A. cheiranthi, A. citri, A. infectoria, A. japonica, A. longipes, A. porri, A. radicina, A. tenuissima, A. tomato*
Altertoksini (ATX-I i II)	*A. alternata, A. capsici-annui, A. radicina, A. tenuissima, A. tomato*
Alternaria alternata f. sp. *lycopersici* toksini (AAL-toksini)	*Alternaria alternata* f. sp *lycopersici*
Stemfiltoksin III	*A. alternata*
Altenuen (ALT)	*A. alternata, A. capsici-annui, A. citri, A. porri, A. radicina, A. tenuissima, A. tomato*

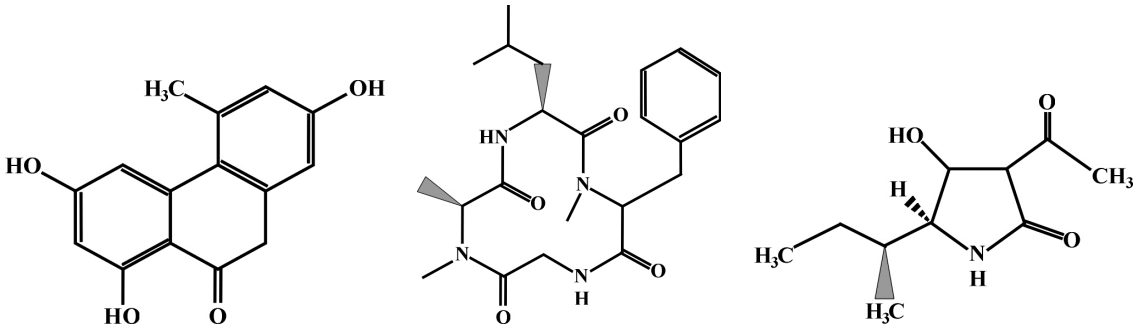

(a) (b) (c)

Slika 7. Strukturne formule nekih Alternaria toksina; a) AOH, b) TEN i c) TeA.
Fig. 7. The structural formulas of some Alternaria toxins; a) AOH, b) TEN and c) TeA.

[123]. Lehmann i sar. [124] su ukazali na estrogeni potencijal AOH, inhibitorni efekat na proliferaciju ćelija, i na genotoksične posledice u kulturama ćelija sisara. ATX i može dovesti do akutne toksičnosti kod miševa i smatra se potentnijim mutagenom od AOH i AME [125].

Pretpostavlja se da je TeA uključena u etiologiju hematoloških poremećaja kod ljudi u Africi [123]. Takođe, smatra se da su ovi toksini odgovorni za kancer jednjaka kod ljudi koji su konzumirali zrna žita kontaminirana *A. alternata* u nekim oblastima Kine [126].

Nekoliko studija ukazuje na stabilnost Alternaria mikotoksina. AOH, AME i ATX I su bili stabilni u voćnim sokovima i vinu tokom 20 dana, kao i na 80 °C u toku 20 min [127]. Veliki procenat toksina ostao je nepromenjen nakon pasterizacije paradajza prilikom proizvodnje paradajz paste.

Trenutno ne postoje propisi za Alternaria toksine u hrani i hrani za životinje u Evropi i drugim regionima sveta, međutim njihov nalaz u sirovinama i proizvodima ukazuje da bi mogli predstavljati opasnost po zdravlje ljudi.

Ovi toksini su utvrđeni u voću (uključujući mandarine, dinje, jabuke, maline, paradajz, masline), paprikama, žitima, semenkama suncokreta i uljane repice. Utvrđena je i pojava niskog sadržaja AOH i AME u prerađevinama od voća: proizvodi od jabuka i paradajza, soku od grožđa, brusnica i malina, kao i u crvenom vinu [123,128]. Visoke koncentracije AOH, AME, TeA i TEN su određene u mahunarkama, orasima i uljaricama, a posebno u semenkama suncokreta. Srednja koncentracija AOH za ovu grupu proizvoda iznosila je od 22 do 26 μg/kg, a maksimalna od 1200 μg/kg. Srednja vrednost koncentracije AME je varirala od 11 do 12 μg/kg, sa maksimalnom vrednošću od 440 μg/kg. TeA je određen u znatno većim koncentracijama u odnosu na AOH, AME i TEN sa srednjim vrednostima od 333 do 349 μg/kg i maksimalnom vrednošću od 5400 μg/kg. Srednje vrednosti koncentracije TEN varirale su od 47 do 50 μg/kg sa maksimalnom vrednošću od 880 μg/kg [114].

Na osnovu dostupnih podataka Komisija za kontaminente u lancu ishrane (CONTAM Panel) izvršila je procenu izloženosti ljudi od 18 do 65 godina starosti na

uticaj Alternaria mikotoksina unošenjem preko hrane. Procenjena dnevna izloženost stanovništva bila je u opsezima od 1,9 do 39 ng/kg TM za AOH, od 0,8 do 4,7 ng/kg TM za AME, od 36 do 141 ng/kg TM za TeA i od 0,01 do 7 ng/kg za TEN. Najčešće vrste hrane preko kojih se unose ovi mikotoksini u organizam čoveka su: zrnasta hrana, voće i njihovi proizvodi, povrće i njihovi proizvodi (pre svega poroizvodi od paradjza), uljarice (uglavnom seme suncokreta), biljna ulja (pre svega suncokretovo ulje) i alkoholna pića (vino i pivo) [114].

Patulin

Patulin (4-hidroksi-4*H*-furol-[3,2-*c*]-piran-2(6*H*)-on) (Slika 8) je sekundarni metabolit nekih vrsta iz rodova *Penicillium* (*P. expansum, P. griseofulvum, P. carneum, P. glandicola, P. coprobium, P. vulpinum, P. clavigerum, P. concentricum*), *Aspergillius* (*A. clavatus, A. giganteus, A. terreus*), *Paecilomyces* (*P. variotii*), *Bissochlamys* [51], kao i drugih gljiva koje poseduju IDH (izopoksidon dehidrogenaza) gen, neophodan za njegovu biosintezu [129]. *P. expansum* i *P. griseofulvum* navode se kao najznačajniji proizvođači patulina u hrani. Proizvodnja patulina od strane *P. expansum* je utvrđena u temperaturnom opsegu od 0 do 25 °C, pri pH od 3,2 do 3,8 u soku od jabuke [130].

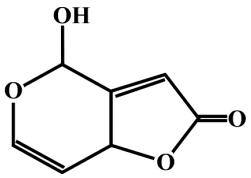

Slika 8. Strukturne formule patulina.
Fig. 8. The structural formula of patulin.

Stabilan je pri niskim pH vrednostima i otporan je na visoke temperature, tako da se ne razgrađuje na temperaturi pasterizacije od 90 °C u trajanju od 10 s [130].

Međutim, neke studije pokazuju da se značajno smanjuje sadržaj patulina tokom proizvodnje soka od jabuke ukoliko se koriste centrifugiranje (89%), bentonit filtracija (77%), filtracija filter papirom (70%) i enzimski tretman (73%) [131]. Istraživanja Altmaier i sar. [132] ukazuju na potpunu eliminaciju patulina tokom procesa fermentacije. Utvrđeno je da se dodatakom SO_2 [133], tiamina, piridoksina, kalcijum-pantotenata [134], askorbinske kiseline [135], folne i pantotenske kiseline [136] može takođe smanjiti nivo ovog toksičnog metabolita u soku ili koncentratu od jabuke. Baert i sar. [137] navode smanjenje koncentracije patulina u soku od jabuke kao posledicu interakcije sa čvrstim delovima sokova, koji sadrže više proteina.

Prvobitno je opisan kao antibiotik širokog dejstva zbog izraženog antimikrobnog delovanja na gram-pozitivne i gram-negativne bakterije, uključujući *Micobacterium tuberculosis* [138]. Međutim, nakon utvrđivanja njegove toksičnosti prema eksperimentalnim životinjama svrstan je u treću grupu kancerogena od strane IARC [139–143], ali njegov mehanizam delovanja na organizam ljudi i životinja nije još uvek u potpunosti objašnjen. Opisani su akutni simptomi nakon unošenja visokih koncentracija praćeni sa uznemirenošću, konvulzijama, ulceracijama, edemom, crevnim upalama i povraćanjem [144]. Mahfoud i sar. [145] su utvrdili da koncentracija od 1 μM patulina oštećuje epitelne ćelije creva ljudi. Na ćelijskom nivou deluje na raskidanje jednostrukih i dvostrukih veza u molekulu DNK, inhibiciju sinteze RNK i proteina [141].

Zbog učestale pojave patulina u jabukama i u proizvodima od jabuka, tokom posledenjih nekoliko godina poraslo je interesovanje za ovaj mikotoksin u hrani. Veliki broj zemalja su propisale maksimalno dozvoljene nivoe ovog toksičnog metabolita za neke vrste proizvoda. Evropska Unija utvrdila je maksimalno dozvoljene koncentracije patulina od 50 μg/kg za voćne sokove i pića koja sadrže sok od jabuke. Za plodove jabuka i pirea od jabuke maksimalno dozvoljena koncentracija ovog mikotoksina je 25 μg/kg. Donja granica od 10 μg/kg je određena za namirnice namenjene odojčadima i maloj deci. FDA je postavila gornju granicu od 50 μg/kg za patulin u soku od jabuke. Komisija Codex Alimentarius je, takođe, postavila gornju granicu od 50 μg/kg za jabuke, sok od jabuke i druga pića koja sadrže jabuke.

Svetska zdravstvena organizacija – Stručna komisija za aditive u hrani (*World Health Organization Expert Committee on Food Additives*) i FAO su ustanovile dnevni tolerantni unos patulina kod ljudi do 0,4 μg/kg TM [142].

Ovaj mikotoksin je osim u jabukama i njihovim proizvodima, često nađen i u kruškama, njihovim sokovima i džemovima, kao i drugim proizvodima dobijenim od ovih plodova [146]. Detektovan je i u drugom voću, kao što su grožđe, višnje, šljive, borovnice, pomorandže, jagode, lubenice, banane, ananas, breskve i kajsije, kao i u nekim žitaricama (ječmu, pšenici, kukuruzu) [147––149]. Rast gljiva i proizvodnja patulina su uobičajeni na oštećenom voću, međutim, patulin je detektovan i kod vizuelno zdravog voća [150].

Zahvalnica

Istraživanja su finansirana od strane Ministarstva prosvete, nauke i tehnološkog razvoja Republike Srbije (TR 31017).

LITERATURA

[1] O. Filtenborg, J.C. Frisvad, A.R. Samson, in: R.A. Samson, E.S. van Reen-Hoekstra (Eds.), Introduction to Foodborne Fungi: Specific Association of Fungal to Foods and Influence of Physical Environmental Factors, Centra-

albureau voor Shimmelcultures, Baarn-Delft, 2004, pp. 306–320.

[2] J. Jay, M. Loessner, D. Golden, in: D.R. Heldman (Ed.), Modern Food Microbiology, Springer Science-Business Media, Inc., New York, 2005, pp. 61–210.

[3] T. Montville, K. Matthews, Food Microbiology: An Introduction, 7th ed., ASM Press, Washington, 2005, pp. 241–261.

[4] G. Dimić, Mikološki i mikotoksikološki aspekti pojave plesni u začinima, Doktorska disertacija, Tehnološki fakultet, Univerzitet u Novom Sad, 1999.

[5] V. Krasić, Određivanje mikotoksina u začinima primenom ELISA testa, Specijalistički rad, Tehnološki fakultet, Univerzitet u Novom Sadu, 2003.

[6] G. Dimić, S. Kocić-Tanackov, D. Karalić, Occurence of toxigenic *Penicillium* spp. in spices, I International Congress on Food Technology, Quality and Safety, Novi Sad, Proceedings, 2007, pp. 87–93.

[7] S. Kocić-Tanackov, D. Dimić, D. Karalić, Contamination of spices with moulds potential producers of sterigmatocystine, Apteff **38** (2007) 29–35.

[8] B. Romagnoli, V. Menna, N. Gruppioni, C. Bergamini, Aflatoxins in spices, aromatic herbs, herbs – teas and medicinal plants marketed in Italy, Food Contr. **18** (2007) 697–701.

[9] D. Dimić, S. Kocić-Tanackov, A. Tepić, B. Vujučić, Z. Šumić, Mycopopulation of spices, Apteff 39 (2008) 1–9.

[10] J. Vukojević, M. Ljaljević-Grbić, D. Karan, V. Janković, Moulds and mycotoxins in spices, 6th Congress of Medical Microbiologists, MIKROMED, Belgrade, Proceedings, 2008, pp. 333–334.

[11] M. Hashem, S. Alamri, Contamination of common spices in Saudi Arabia markets with potential mycotoxin-producing fungi, Saudi J. Biol. Sci. **17** (2010) 167–175.

[12] M. Škrinjar, M. Govedarica, G. Dimić, M. Jarak, M. Milošović, Mikrobiologija voća i proizvoda od voća, Univerzitet u Novom Sadu, Tehnološki fakultet-Poljoprivredni fakultet, 1996.

[13] M. Škrinjar, V. Injac, S. Kocić-Tanackov, Da li je "zdrava hrana" zaista zdravstveno bezbedna imajući u vidu njen mikološki i mikotoksikološki kvalitet, III Međunarodna EKO-konferencija, Novi Sad, Tematski zbornik radova (Zdravstveno bezbedna hrana II), 2004, pp. 333–338.

[14] G. Dimić, Ž. Maletić, S. Kocić-Tanackov, Xerotolerant mycopopulations and mycotoxins in muesli components, Proc. Nat. Sci. Matica Srpska **109** (2005) 81–87.

[15] Ž. Maletić, Kserofilne mikopopulacije i proizvođači mikotoksina u musliju i komponentama, Specijalistički rad, Tehnološki fakultet, Univerzitet u Novom Sadu, 2005.

[16] G. Dimić, E. Dimić, S. Kocić-Tanackov, Ž. Maletić, Mikološka ispitivanja semena tikve golice (*Cucurbita pepo* L.) i jezgra suncokreta (*Helianthus annuus* L.) kao komponenata musli proizvoda, Uljarstvo **37**(1-2) (2006) 3–6.

[17] A. Ackerman, Mycoflora of South Africa barley and malt, J. Am. Soc. Brew. Chem. **56**(4) (1998) 169–176.

[18] K. Kosiak, M. Torp, E. Skjerve, B. Andersen, *Alternaria* and *Fusarium* in Norvegian grains of reduced quality – a matched pair sample study, Int. J. Food Microbiol. **93**(1) (2004) 51–62.

[19] S. Kocić-Tanackov, Rast toksigenih *Fusarium* vrsta i sinteza zearalenona u ječmu namenjenom proizvodnji pivskog slada, Magistarska teza, Tehnološki fakultet, Univerzitet u Novom Sadu, 2004.

[20] S. Kocić-Tanackov, M. Škrinjar, Udeo toksigenih *Fusarium* vrsta u mikopopulacijama izolovanim iz ozimog dvoredog ječma, Žito-Hleb **1–2** (2004) 35–41.

[21] M. Škrinjar, S. Kocić-Tanackov, Fungal infection and occurrence of zearalenone in barley harvested 2003. in Serbia, Acta Agriculturae Slovenica **1** (2004) 233–238.

[22] J. Lević, S. Stanković, A. Bočarov-Stančić, M. Škrinjar, Z. Mašić, in: A. Logrieco, A. Visconti (Eds.), An Overview on toxigenic fungi and mycotoxins in Europe: The Overview on Toxigenic Fungi and Mycotoxins in Serbia and Montenegro, Kluwer Academic Publishers, Dordrecht, 2004, pp. 201–218.

[23] M. Škrinjar, A. Vengušt, S. Kocić-Tanackov, Mikotoksini u hrani – uzorkovanje, detekcija, zakonski propisi, Tehnologija mesa **45**(5–6) (2004) 163–169.

[24] J.T. Lević, Vrste roda *Fusarium*, Institut za kukuruz "Zemun Polje" i Društvo genetičara Srbije, Cicero, Beograd, 2008.

[25] B. Jovićević, M. Milošević, Bolesti semena, Dnevnik, Novi Sad, 1990.

[26] S.J. Andersen, Compositional changes in surface mycoflora during ripening of naturally fermented sausages, J. Food Prot. **58** (1995) 426–429.

[27] [C.R. Tindale, F.B. Whitfield, S.D. Levingston, T.H.L. Nguyen, Fungi isolated from packaging materials: their role in the production of 2,4,6-trichloroanisole, J. Sci. Food Agric. **49** (1989) 437–447.

[28] F.B. Whitfield, T.H.L. Nguyer, Last effect of relative humidity and chlorophenol content on the fungal conversion of chlorophenols to chloroanisols in fibreboard cartons containing dried fruit, J. Sci. Food Agricult. **54** (1991) 595–604.

[29] M.B. Liewen, E.H. Marth, Growth and inhibition of micro-organisms in the presence of sorbic acid: a review, J. Food Prot. **48** (1985) 364–375.

[30] J. Kinderlerer, P.V. Hatton, Fungal metabolites of sorbic acid. Food Addit. Contam. **7** (1990) 657–669.

[31] T.O. Larsen, J.C. Frisvad, Characterization of volatile metabolites from 47 *Penicillium* taxa, Mycol. Res. **99** (1995) 1153–1166.

[32] T.O. Larsen, J.C. Frisvad, Chemosystematics of *Penicillium* based on profiles of volatile metabolites, Mycol. Res. **99** (1995) 1167–1174.

[33] T. Horvat-Skenderović, Uticaj ekoloških i drugih faktora na rast mikopopulacija i stvaranje mikotoksina u supstratima od mesa, Doktorska disertacija, Tehnološki fakultet, Novi Sad, 1989.

[34] A. Dalcero, C. Magnoli, S. Chiacchiera, G. Palacios, M. Reynoso, Mycoflora and incidence of aflatoxin B1, zearalenone and deoxynivalenol in poultry feeds in Argentina, Mycopathologia **137** (1997) 179–184.

[35] P. Zöllner, D. Berner, J. Jodlbauer, W. Lindner, Determination of zearalenone and its metabolites α- and β-zearalenol in beer samples by high-performance liquid

chromatography-tandem mass spectrometry, J. Chromatogr., B **738** (2000) 233–241.

[36] L. Legzduna, H. Buerstmayr, Comparision of infection with *Fusarium* head blight and accumulation of mycotoxins in grain of hulless and covered barley, J. Cereal Sci. 40 (2004) 61–67.

[37] F. Galvano, A. Ritieni, G. Piva, A. Pietri, in: D. Diaz (Ed.), The Mycotoxin Blue Book: Mycotoxins in the Human Food Chain, Nottingham University Press, Nottingham, 2005, pp. 187–225.

[38] D. Karan, J. Vukojević, D. Milićević, M. Ljajević-Grbić, V. Janković, Presence of moulds and mycotoxins in spices, Proc. Nat. Sci. Matica Srpska **108** (2005) 77–85.

[39] S. Kocić-Tanackov, M. Škrinjar, O. Grujić, J. Lević, J. Pejin, Capacity of *Fusarium* species isolated from brewer's barley to synthesise zearalenone, Proc. Nat. Sci. Matica Srpska **108** (2005) 157–165.

[40] A. Zinedine, J.M. Soriano, J.C. Molto, J. Manes, Review on the toxicity, occurrence, metabolism, detoxification, regulations and intake of zearalenone: an oestrogenic mycotoxin, Food Chem. Toxicol. **45** (2007) 1–18.

[41] I.Y. Sengun, D.B. Yaman, S.A. Gonul, Mycotoxins and moulds contamination in cheese: a review, World Myc. J. **3** (2008) 291–298.

[42] R. Coffey, E.Cummins, S. Ward, Exposure assessment of mycotoxins in dairy milk, Food Contr. **20** (2009) 239––249.

[43] D. Garcia, J.A. Ramos, V. Sanchis, S. Marin, Predicting mycotoxins in foods: A review, Food Microbiol. **26** (2009) 757–769.

[44] S. Kocić-Tanackov, G. Dimić, J. Lević, D. Pejin, J. Pejin, I. Jajić, Occurrence of potentially toxigenic mould species in fresh salads of different kinds of ready-for-use vegetables, Apteff **41** (2010) 33–45.

[45] A. Veršilovskis, S. De Saeger, Sterigmatocystin: Occurrence in foodstuffs and analytical methods – An overview, Mol. Nutr. Food Res. **54** (2010) 136–147.

[46] S. Kocić-Tanackov, Uticaj ekstrakata začina na rast plesni i biosintezu mikotoksina, Doktorska disertacija, Tehnološki fakultet, Univerzitet u Novom Sadu, 2012.

[47] S. Steyn, The biosynthesis of mycotoxins, RMV **149** (1998) 496–478.

[48] S. Duraković, L. Duraković, Mikologija u biotehnologiji, Kugler, Zagreb, 2003.

[49] Z.J. Sinovec, R.M. Resanović, S.M. Sinovec, Mikotoksini: pojava, efekti i prevencija, Univerzitet u Beogradu, Fakultet veterinarske medicine, 2006.

[50] M.E. Fox, J.B. Howlett, Secondary metabolism: regulation and role in fungal biology, Curr. Opin. Microbiol. **11** (2008) 481–487.

[51] A.R. Samson, S.E. Hoekstra, C.J. Frisvad, Introduction to Food-and Airborne Fungi, Centraalbureau vor Schimmelcultures, Utrecht, 2004.

[52] D.R. Wyatt, in: D.E. Diaz, (Ed.), The Mycotoxin Blue Book: Mycotoxin Interactions, Nottingham University Press, Nottingham, 2005, pp. 269–278.

[53] S. Mayer, S. Engelhart, A. Kolk, H. Blome, The significance of mycotoxins in the framework of assessing workplace related risks, Mycol. Res. **24**(3) (2008) 151––164.

[54] D. Diaz, The Mycotoxin Blue Book, Nottingham University Press, Nottingham, 2005.

[55] L.D. Park, E.C. Ayala, S.E. Guzman-Perez, R. Lopez-Garcia, S. Trujillo, in: K.C. Winter (Ed.), Food Toxicology: Microbial Toxins in Foods: Algal, Fungal and Bacterial, CRC Pres, Boca Raton- London- Washington, 2000, pp. 15–20.

[56] M. Weidenbörner, Mycotoxins in Foodstuffs, Springer Science+Business Media, LLC, New York, 2008.

[57] J. Fink-Gremmels, The role of mycotoxins in the health and performance of dairy cows, Vet. J. **176** (2008) 84––92.

[58] C. Finoli, A. Galli, A. Vecchio, A. Villani, Aflatoxin-producing strain of *Aspergillus flavus* from spices, Industrie Alimentari **34**(342) (1995) 1147–1151.

[59] N. Gqaleni, J.E. Smith, J. Lasey, G. Gettinby, Effect of temperature, water activity and incubation time on production of aflatoxin and cyclopiazonic acid by an isolate of *Aspergillus flavus* in surface agar culture, Appl. Environ. Microbiol. **63**(3) (1997) 1048–1053.

[60] T. Kuiper-Goodman, Mycotoxins: risk assessment and legislation, Toxicol. Lett. **82**/**83** (1995) 853–859.

[61] J.C. Frisvad, in: R.A. Samson, E.S. van Reen-Hoekstra (Eds.), Introduction to Food-borne Fungi: Fungal Species and Their Specific Production of Mycotoxins, Centraalbureau voor Shimmelcultures, Baarn-Delft, 1988, pp. 321–331.

[62] N.P. Keller, C. Nesbitt, B. Sarr, T.D. Phillips, G.B. Burow, pH regulation of sterigmatocystin and aflatoxin biosynthesis in *Aspergillus* spp, Phytopathology **87** (1997) 643––648.

[63] J.K. Hicks, K. Shimizu, N.P. Keller, in: F. Kempken (Ed.), The Mycota XI – Agricultural Applications: Genetics and Biosynthesis of Aflatoxins and Sterigmatocystin, Springer-Verlag, Berlin, 2002, pp. 55–69.

[64] J. Domagala, A. Bluthgen, W. Heeschen, Methods of determination of aflatoxins precursors in dairy cows' feed. 1. Determination of sterigmatocystin level in mixed feed and corn silage, Milk Sci. Int. **52** (1997) 452––455.

[65] International Agency for Research on Cancer (IARC), Some Naturally Occurring Substances, Monographs 10, Lyon, 1976, pp. 245–251.

[66] International Agency for Research on Cancer (IARC), Some Naturally Occurring Substances: IARC Monographs on the Evaluation of Carcinogenic Risks to Humans. Summaries and Evaluations, Sterigmatocystin, Monographs 10, Lyon, 1987, p. 72.

[67] International Agency for Research on Cancer (IARC), Some Naturally Occurring Substances: Food Items and Constituents, Heterocyclic Aromatic Amines and Mycotoxins, IARC Monographs Evaluation of Cancorogenic Risks to Human 56, Lyon, 1993, pp. 245–540.

[68] H.F.I. Purchase, J.J. van der Watt, Carcinogenicity of sterigmatocystin, Food Chem. Toxicol. **8**(3) (1970) 289––290.

[69] H.P. van Egmond, G.J.A. Speijers, R.B.M. Wouters, Naturally occurring toxicants in foodstuffs 1, Mycotoxins, Voeding **51**(4) (1990) 82–86.

[70] J.S. Wang, J.D. Groopman, DNA damage by mycotoxins, Mutat.Res. **424**(1/2) (1999) 167–181.

[71] V. Sivakumar, J. Thanislass, S. Niranjlai, H. Devaraj, Lipid peroxidation as a possible secondary mechanism of sterigmatocystin toxicity, Hum. Exp. Toxicol. **20**(8) (2001) 398–403.

[72] M.M. Metwally, A.M. El-Sayed, A. Alia, A.M. Mehriz, Y.H. Abu Sree, Sterigmatocystin - incidence, fate and production by *A. versicolor* in Ras cheese, Myc. Res. **13** (1997) 61–66.

[73] M.L. Abarca, M.R. Bragulat, G. Castella, F.J. Cabanes, Ochratoxin production by strains of *Aspergillus niger* var. *niger*, Appl. Environ. Microbiol. **60** (1994) 2650––2652.

[74] D.T. Wicklow, P.F. Dowd, A.A. Alftafta, J.B. Gloer, Ochratoxin A: an antiinsectan metabolite from the sclerotia of *Aspergillus carbonarius* NRRL 369, Cand. J. Microbiol. **42** (1996) 1100–1103.

[75] J. Varga, E. Kevei, E. Rinyu, J. Teren, Z. Kozakiewicz, Ochratoxin production by *Aspergillus* species, Appl. Environ. Microbiol. **62**(4) (1996) 4461–4464.

[76] C.N. Heenan, K.J. Shaw, J.I. Pitt, Ochratoxin A production by *Aspergillus carbonarius* and *Aspergillus niger* isolates and detection using coconut cream agar, J. Food Microbiol. **1** (1998) 67–72.

[77] Y. Ueno, in: K. Miller (Ed.), Mycotoxins: Toxicological Aspects of Food, Elsevier Applaid Science LTD, New York, 1987.

[78] M. Škrinjar, R.D. Stubblefield, I.F. Vujičić, Ochratoxigenic moulds and ochratoxin A in forages and grain feeds, Acta Vet. Hung. **40**(3) (1992) 185–190.

[79] A. Pfohl-Leszkowitza, K. Chajkor, E.E. Creppy, G. Dirheimer, in: M. Castegnaro, R. Pleština, G. Dirheimer, I.N. Chernozemsky, H. Bartsch (Eds.), Mycotoxins, Endemic Nephropthy and Urinary Tract Tumors: Biological activity of ochratoxin A, IARC, Lyon, 1991, p. 245.

[80] K. Kawai, M.L. Cowger, Y. Nozawa, The redox reaction of xanthomegnin and a bypass to the electron transport system in mitochondria, Proc. Jap. Assoc. Mycotoxicol. **15** (1982) 22–24.

[81] J.I. Pitt, A.D. Hocking, Fungi and Food Spoilage, 2nd ed, Blackie Academic & Academic Professional, London, 1997.

[82] M. De Nijs, H.P. van Egmond, F.M. Rombouts, S.H.W. Notermans, Identification of hazardous *Fusarium* secondary metabolites occurring in food raw materials, J. Food Saf. **17** (1997) 161–191.

[83] W.F.O. Marasas, J.D. Miller, R.T. Riley, A. Visconti, Environmental Health Criteria 219: Fumonisin B1, World Health Organization, Vammala, 2000, p. 9.

[84] A.E. Desjardins, R.H. Proctor, Biochemistry and genetics of *Fusarium* toxins, See Ref. **81** (2001) 50–69.

[85] S.C. Nayaka, A.C.U. Shankar, S.R. Niranjana, E.G. Wulff, C.N. Mortensen, H.S. Prakash, Detection and quantification of fumonisins from *Fusarium verticillioides* in maize grown in southern India, World J. Microbiol. Biotechnol. **26**(1) (2010) 71–78.

[86] T. Yoshizawa, A. Yamashita, Y. Luo, Fumonisin occurrence in corn from high- and lowrisk areas for human esophageal cancer in China, Appl. Environ. Microbiol. **60** (1994) 1626–1629.

[87] H.P. Gao, T. Yoshizawa, Further study on *Fusarium* mycotoxins in corn and wheat from a high-risk area for human esophageal cancer in China, Mycotoxins **45** (1997) 51-55.

[88] P.C. Turner, P. Nikiema, C.P. Wild, Fumonisin contamination of food: Progress in development of biomarkers to better assess human health risks, Mutat. Res. **443** (1999) 81–93.

[89] J. Le Bars, P. Le Bars, J. Dupuy, H. Boudra, R. Cassini, Biotic and abiotic factors in fumonisin B1 production and stability, J. Assoc. Offic. Anal. Chem. **77** (1994) 517––521.

[90] W-B. Shim, C.P. Woloshuk, Nitrogen repression of fumonisin B1 biosynthesis in *Gibberella fujikuroi*, FEMS Microbiol. Lett. **177** (1999) 109–116.

[91] A. Visconti, M.B. Doko, C. Bottalico, B. Schurer, A. Boenke, Stability of fumonisins (FB1 and FB2) in solution, Food Addit. Contam. **11** (1994) 427–431.

[92] Commission Regulation (EC) No 856/2005 of 6 June 2005 amending Regulation (EC) No 466/2001 as regards *Fusarium* toxins, Official Journal of the European Union L143/3, 2005.

[93] Y. Ueno,Trichothecenes – Chemical, Biological and Toxicological Aspects, Kodsnsha LTD., Tokyo and Elsevier, Amsterdam-Oxford-New York, 1983, p. 316.

[94] U. Thrane, in: J. Chelkowski (Ed.), *Fusarium* Mycotoxins, Taxonomy and Pathogenicity: *Fusarium* species and their specific profiles of secondary metabolites, Elsevier, Amsterdam, 1989, pp. 199–225.

[95] B. Živković, A. Bočarov-Stančić, M. Vlahović, M. Gluhović, S. Kovčin, M. Fabjan, N. Nedić, Harmful effects of mycotoxins in weaned pig nutrition (2), Biotehnol. stoč. **13**(1-2) (1997) 25–31.

[96] A. Bočarov-Stančić, M. Tomašević-Čanović, A. Daković, Mogućnost upotrebe preparata klinoptilolita (Minazel) za prevenciju mikotoksikoza prouzrokovanih trihotecenima tipa A, Ecologica **7**(2) (2000) 162–164.

[97] H. Yazdanpanah, H.R. Rasekh, F. Roshanzamir, B. Shafaghi, N. Naderi, K.H. Abbas, Possible roles of diphenhydramine, triazolam, diltiazem, and ketotrifen in protection against T-2 toxin toxicity, Cereal Res. Commun. **25**(3/1) (1997) 397–398.

[98] M. Leal, E.G. Demejia, F. Ruiz, A. Shimada, Effect of carotenoides on cytotoxicity of T-2 toxin on chicken hepatocytes *in vitro*, Toxicol. *In vitro* **12** (1998) 133–139.

[99] P. Rhyn, P. Zoller, Zearalenone in cereals for human nutrition: relevant data for the Swiss population, Eur. Food Res. Technol. **216** (2003) 316–322.

[100] N.H. Aziz, E.S. Attia, S.A. Farag, Effect of gamma-irradiation on the natural occurrence of *Fusarium* mycotoxins in wheat, flour and bread, Nahrung-Food **41** (1997) 34––37.

[101] A. Yiannikouris, J. François, L. poughon, C.G. Dussap, G. Bertin, G. Jeminet, J.P. Jouany, Adsorption of zearalenone by beta-D-glucans in the *Saccharomyces cerevisiae* cell wall, J. Food Prot. **67**(6) (2004) 1195–2000.

[102] W.M. Hagler, N.R. Towers, C.J. Mirocha, R.M. Eppley, W.L. Bryden, in: B.A. Summerell, J.F. Leslie, D. Backhouse, W.L. Bryden, LW. Burgess (Eds.), *Fusarium* – Paul E. Nelson Memorial Symposium: Zearalenone - Mycotoxin or mycoestrogen?, APS Press, St. Paul, MN, 2001, pp. 321–331.

[103] D.G. Kennedy, J.D. McEvoy, W.J. Blanchflower, S.A. Hewitt, A. Cannavan, W.J. McCaughey, C.T. Elliott, Possible naturally occurring zeranol in bovine bile in Northern Ireland, J. Vet. Med., B **42** (1995) 509–512.

[104] F.M. Launay, P.B. Young, S.S. Sterk, M.H. Blokland, D.G. Kennedy, Confirmatory assay for zeranol, taleranol and the *Fusarium* spp. toxins in bovine urine using liquid chromatography-tandem massspectrometry, Food Addit. Contam. **21** (2004) 52–62.

[105] M.H. Blokland, S.S. Sterk, R.W. Stephany, F.M. Launay, D.G. Kennedy, L.A. van Ginkel, Determination of resorcylic acid lactones in biological samples by GC-MS, Discrimination between illegal use and contamination with *Fusarium* toxins, Anal. Bioanal. Chem. **384** (2006) 1221––1227.

[106] Codex Committee on food additives and contaminants, 32nd session, Beijing, China, 2000.

[107] E.E. Creppy, Update and survey, regulation and toxic effects of mycotoxins in Europe, Toxicol. Lett. **127** (2002) 19–27.

[108] C.A. Saens de Rodruguez, Enviromental hormone contamination in Puerto Rico, New Engl. J. Med. **310** (1984) 1742–1743.

[109] J.D. Miller, Fungi and mycotoxins in grain: Implications for stored product research, J. Stored Prod. Res. **31**(1) (1995) 1–16.

[110] P. Szuets, A. Mesterhazy, G.Y. Falkay, T. Bartok, Early telarche symptoms in children and their relation to zearalenone contamination in foodstuffs, Cereal Res. Commun. **25** (1997) 429–436.

[111] M. Muñtanola-Cvetković, Opšta mikologija, Književne novine, Beograd, 1990.

[112] S. Abid-Esefi, Z. Ouanes, W. Hassen, I. Baudrimont, E. Creppy, H. Bacha, Cytotoxicity inhibition of DNA and protein synthese and oxidative damage in cultured cells exposed to zearalenone, Toxicol. *Vitro* **18** (2004) 467––474.

[113] S.S. Desphande, in: Handbook of Food Toxicology: Fungal Toxins, Marcel Dekker Inc., New York, 2002, pp. 387––456.

[114] EFSA, Scientific Opinion on the risks for animal and public health related to the presence of *Alternaria* toxins in feed and food, EFSA J. **9**(10) (2011) 2407–2504.

[115] N. Montemurro, A. Visconti, in: J. Chełkowski, A. Visconti (Eds.), *Alternaria*: biology, plant diseases and metabolites: *Alternaria* metabolites – Chemical and biological data, Elsevier, Amsterdam, 1992, pp. 449–557.

[116] A. Bottalico, A. Logrieco, in: K.K. Sinha, D. Bhatnager (Eds.), Mycotoxins in Agriculture and Food Safety: Toxigenic *Alternaria* species of Economic Importance, Marcel Dekker, New York, 1998, pp. 65–108.

[117] B.P.H.J. Thomma, *Alternaria* spp.: from general saprophyte to specific parasite, Molecul. Plant Pathol. **4** (2003) 225–236.

[118] G. Pose, A. Patriarca, V. Kyanko, A. Pardo, V. Fernández Pinto, Water activity and temperature effects on mycotoxin production by *Alternaria alternata* on a synthetic tomato medium, Int. J. Food Microbiol. **142** (2010) 348––353.

[119] M. Solfrizzo, A. De Girolamo, C.Vitti, K.Tylkowska, J. Grabarkiewicz-Szczesna, D. Szopinska, H. Dorna, Toxigenic profile of *Alternaria alternata* and A*lternaria radicina* occurring on umbelliferous plants, Food Addit. Contam. **22**(4) (2005) 302–308.

[120] G.T. Liu, Y.Z., P. Qian Zhang, W.H. Dong, Y.M. Qi, H.T. Guo, Etiologic role of *Alternaria alternata* in human esophageal cancer, Chin. Med. J. **105** (1992) 394–400.

[121] P.M. Scott, D.R. Stoltz, Mutagens produced by *Alternaria alternata*, Mutat. Res. **78** (1980) 33–40.

[122] Y.H. An, T.Z. Zhao, J. Miao, G.T. Liu, Y.Z. Zheng, Y.M. Xu, R. van Etten, Isolation, identification and mutagenicity of alternariol monomethyl ether, J. Agr. Food Chem. **37** (1989) 1341–1343.

[123] P.M. Scott, in: N. Magan, M. Olsen (Eds.), Mycotoxins in Food - Detection and Control: Other Mycotoxins, Woodhead Publishing Ltd., Cambridge, 2004, pp. 406–440.

[124] L. Lehmann, J. Wagner, M. Metzler, Estrogenic and clastogenic potential of the mycotoxin alternariol in cultured mammalian cells, Food Chem. Toxicol. **44** (2006) 398–408.

[125] V. Ostry, *Alternaria* mycotoxins: an overview of chemical characterization, producers, toxicity, analysis and occurrence in foodstuffs, World Mycotoxin J. **1** (2008) 175––188.

[126] G.T. Liu, Y.Z. Qian, P. Zhang, Z.M. Dong, Z.Y. Shi, Y.Z. Zhen, J. Miao, Y.M. Xu, in: I.K. O'Neill, J. Chen, H. Bartsch (Eds.), Relevance to Human Cancer of N-Nitroso Compounds, Tobacco Smoke and Mycotoxins: Relationships between *Alternaria alternata* and Oesophageal Cancer, International Agency for Research on Cancer, Lyon, France, 1991, pp. 258–262.

[127] R. Lawley, *Alternaria*, Factsheet, European Mycotoxin Awareness Network (EMAN) http://www.mycotoxins.org, 2010.

[128] L. Terminiello, A. Patriarca, G. Pose, V. Fernández Pinto, Occurrence of alternariol, alternariol monomethyl ether and tenuazonic acid in Argentinean tomato puree, Mycotoxin Res. **22** (2006) 236–240.

[129] R. Russell, M. Paterson, Primers from the isoepoxydon dehydrogenase gene of the patulin biosynthetic pathway to indicate critical control points for patulin contamination of apples, Food Contr.**17**(9) (2006) 741–744.

[130] J.S. Silva, Z.P. Schuch, R.C. Bernardi, H.M. Vainstein, A. André Jablonski, J.R. Bender, Patulin in food: state-of-the-art and analytical trends, Rev. Bras. Frutic. **29**(2) (2007) 406–413.

[131] J. Bissessur, K. Permau,l B. Odhav, Reduction of patulin during apple juice clarification, J. Food Protect. **64**(8) (2001) 1216–1219.

[132] B. Altmayer, K.W. Eichhorn, R. Plapp, Untersuchungen über den Patulingehalt von Traubenmosten und Wein, ZFL: Intern. Forschung, A **175**(3) (1982) 172–174.

[133] J.O. Roland, L.R. Beuchat, Biomass and patulin production by *Byssochlamys nivea* in apple juice as affected by sorbate, benzoate, SO_2 and temperature, J. Food Sci. **49**(2) (1984) 402–406.

[134] S. Yazici, Y.S. Velioglu, Effect of thiamine hydrochloride, pyridoxine dydrochloride and calcium-d-pantothenate on the patulin content of apple juice concentrate, Nahrung-Food **46**(4) (2002) 256–257.

[135] S. Drusch, S. Kopka, J. Kaeding, Stability of patulin in a juice-like aqueous model system in the presence of ascorbic acid, Food Chem. **100**(1) (2007) 192–197.

[136] N. Asefi, M. Rahgoy, Feasibility of patulin reduction in apple juice concentrates, 23rd International ICFMH Symposium FoodMicro 2012, Instanbul, Abstract Book, 2012, p. 426.

[137] K. Baert, B.D. Meulenaer, C. Kasase, A. Huyghebaert, W. Ooghe, F. Devlieghere, Free and bound patulin in cloudy apple juice, Food Chem. **100**(3) (2007) 1278–1282.

[138] R. Russell, M. Paterson, A. Venâncio, N. Lima, Solutions to *Penicillium* taxonomy crucial to mycotoxin research and health, Res. Microbiol. **55**(7) (2004) 507–513.

[139] I. Alves, N.G. Oliveira, A. Laires, A.S. Rodrigues, J. Rueff, Induction of micronuclei and chromosomal aberrations by the mycotoxin patulin in mammalian cells: role of ascorbic acid as a modulator of patulin clastogenicity, Mutagenesis **15**(3) (2000) 229–234.

[140] T.S. Wu, F.Y. Yu, C.C. Su, J.C. Kan, C.P. Chung, B.H. Liu, Activation of ERK mitogen-activated protein kinase in human cells by the mycotoxin patulin, Toxicol. Appl. Pharmacol. **207**(2) (2005) 103–111.

[141] D.M. Schumacher, C, Müller, M. Metzler L. Lehmann, DNADNA cross-links contribute to the mutagenic potential of the mycotoxin patulin, Toxicol. Lett. **166**(3) (2006) 268–275.

[142] J.W. Bennett, M. Klich, Mycotoxins, Clin. Microbiol. Rev.**16**(3) (2003) 497–516.

[143] G. Selmanoglu, Evaluation of the reproductive toxicity of patulin in growing male rats, Food Chem. Toxicol. **44**(12) (2006) 2019–2024.

[144] G.J.A. Speijers, in: N. Magan, M. Olsen (Eds.), Mycotoxins in Food-detection and Control: Patulin, Woodhead Publishing, Cambridge, 2004, pp. 339–352.

[145] R. Mahfoud, M. Maresca, N. Garmy, J. Fantini, The mycotoxin patulin alters the barrier function of the intestinal epithelium: mechanism of action of the toxin and protective effects of glutathione, Toxicol. Appl. Pharmacol. 181 (3) (2002) 209–218.

[146] L.M. Kawashima, L.M.V. Soares, P.R. Massaguer, The development of an analytical method for two mycotoxins, patulin and verruculogen, and survey of their presence in commercial tomato pulp, Braz. J. Microbiol. **33** (2002) 269–273.

[147] H.K. Frank, Occurrence of patulin in fruit and vegetables, Annal. Nutrit. Aliment. **31** (1977) 459–465.

[148] B. Bartolomè, M.L. Bengoechea, F.J. Pérez-Ilzarbe, T. Hernández, I. Estrella, C. Gómez-Cordovés, Determination of patulin in apple juice by high-performance liquid chromatography with diode-array detection, J. Chromatogr., A **664**(1) (1994) 39-43.

[149] J. Li, R. Wu, Q. Hu, J. Wang, Solid-phase extraction and HPLC determination of patulin in apple juice concentrate, Food Contr. **18**(5) (2007) 530–534.

[150] L.S. Jackson, M. Hoeltz, H.A. Dottori, I.B. Noll, Apple quality, storage, and washing treatments affect patulin levels in apple cider, J. Food Protect. **66**(4) (2003) 618––624.

SUMMARY

FUNGI AND MYCOTOXINS – FOOD CONTAMINANTS

Sunčica D. Kocić-Tanackov, Gordana R. Dimić

University of Novi Sad, Faculty of Technology, Food Microbiology, Novi Sad, Serbia

(Review paper)

The growth of fungi on food causes physical and chemical changes, which further negatively affect the sensory and nutritive quality of food. Species from genera: *Aspergillus, Penicillium, Fusarium, Alternaria, Cladosporium, Mucor, Rhizopus, Eurotium* and *Emericella* are commonly found in food. Some of them are potentially dangerous for humans and animals, due to possible synthesis and excretion of toxic secondary metabolites – mycotoxins into the food. Their toxic syndromes in animals and humans are known as mycotoxicoses. The pathological changes can be observed in parenchymatous organs, and in bones and central nervous system also. Specific conditions are necessary for mycotoxin producing fungi to synthetize sufficient quantities of these compounds for demonstration of biological effects. The main biochemical paths in the formation of mycotoxins include the polyketide (aflatoxins, sterigmatocystin, zearalenone, citrinine, patulin), terpenic (trichothecenes), aminoacid (glicotoxins, ergotamines, sporidesmin, malformin C), and carbonic acids path (rubratoxins). Aflatoxins are the most toxigenic metabolites of fungi, produced mostly by *Aspergillus flavus* and *A. parasiticus* species. Aflatoxins appear more frequently in food in the tropic and subtropic regions, while the food in Europe is more exposed to also very toxic ochratoxin A producing fungi (*A. ochraceus* and some *Penicillium* species). The agricultural products can be contaminated by fungi both before and after the harvest. The primary mycotoxicoses in humans are the result of direct intake of vegetable products contaminated by mycotoxins, while the secondary mycotoxicoses are caused by products of animal origin. The risk of the presence of fungi and mycotoxin in food is increasing, having in mind that some of them are highly thermoresistant, and the temperatures of usual food sterilization is not sufficient for their termination. The paper presents the review of most important mycotoxins, their biologic effects, the condition of their synthesis, occurrence in food, permitted tolerant intake, as well as the possibility of their degradation.

Keywords: Fungi • Mycotoxins • Food

Uniaxial tension of drying sieves

Nada V. Bojić[1], Ružica R. Nikolić[2,3], Branimir Z. Jugović[4], Zvonimir S. Jugović[5], Milica M. Gvozdenović[6]

[1]*Fabrika sita i ležaja "FASIL" A.D., Arilje, Serbia*
[2]*Faculty of Engineering, Kragujevac, Serbia*
[3]*Faculty of Civil Engineering, University of Žilina, Žilina, Slovakia*
[4]*Institute of Technical Science Serbian Academy of Science and Arts, Belgrade, Serbia*
[5]*Technical Faculty Čačak, University of Kragujevac, Čačak, Serbia*
[6]*Faculty of Technology and Metallurgy, University of Belgrade, Belgrade, Serbia*

Abstract

Although the literature contains numerous studies that have been developed to describe the nonlinear behavior of drying sieves operation, there are no papers that report deeper investigation of the drying sieve behavior when exposed to tension and thermo-stabilization. The aim of this paper is to provide insight into the elastoplastic behavior of the thermo-stabilized and non-stabilized sieves subjected to tensile force. Within this work both theoretical and experimental investigations were performed. The sieves were joined by using a spiral. In separate experiments, tests of wire base and weft of the weave mesh were performed, both for thermo-stabilized and non-thermo-stabilized sieves, sieves joining and the sieve thermo-stabilization itself. It was established that the thermo-stabilization of sieves provides for stability of sieves dimensions and that open thermo-stabilized drying sieve exhibits better mechanical properties and exploitation characteristics than the sieves joining.

Keywords: drying sieve, thermo-stabilization, joining spiral, tensile forces.

Available online at the Journal website: http://www.ache.org.rs/HI/

SCIENTIFIC PAPER

UDC 676.8:676.015.8

Hem. Ind. **67** (4) 655–662 (2013)

doi: 10.2298/HEMIND120824109B

Drying sieves are widely applied in all groups of paper drying machines and they are used for the production of all kinds of paper and cardboard [1–4]. Since the operation of complete plants depends on proper operation of the drying sieves, special attention has been devoted to their reliable operation [5–8]. Exploitation of sieves leads to their elongation, wear, reduction in the wire cross-section and ultimately to breaking [9–15]. For this reason, joining of sieves is a very important process for ensuring their smooth exploitation. Drying sieves are exploited at a temperature of 120 °C. The polyester that the sieves are made of is prone to contraction at elevated temperatures. In order for a sieve not to be exposed to shrinking forces, due to shrinkage at high temperatures in exploitation, a thermo-stabilization is performed at temperatures higher than the exploitation one [16–17]. Thanks to technical progress over time it became possible to influence cer–tain properties of the material [18].

The main field of composite materials properties research are the tensile properties, where the indicators of the material behavior in tension are being determined, such as tensile strength, Poisson's ratio, deformations, etc. The objective of tensile testing of was not only to determine the strength and deformation properties of the sieves material, but the tests performed had an objective to improve those properties of drying sieves as well, in order to obtain new fields for their application [19].

The closed (joined) sieve plays a role of a transporter (conveyer belt), which, while realizing the elastic connection also powers all the driven machine cylinders and as such is subjected to multifold straining of uneven intensity. As for the belt in operation of sieves exists the pre-loading in the stationary state (S), loading of the "pulling" portion of the belt – sieve (S_1) and loading of the "free" portion of the belt – sieve (S_2), for which the following relations hold:

$$S = K\frac{P}{2}\frac{e^{m\alpha}+1}{e^{m\alpha}-1}+\frac{\gamma v^2}{g} \quad (1)$$

$$S_1 = KP\frac{1}{e^{m\alpha}-1}+\frac{\gamma v^2}{g} \quad (2)$$

$$S_2 = KP\frac{e^{m\alpha}}{e^{m\alpha}}+\frac{\gamma v^2}{g} \quad (3)$$

where P (N) is the perimeter force which the sieve is transmitting, K (m) is the tolerance coefficient – in order to avoid the sieve's slipping it is always $K > 1$, m is the friction coefficient between the sieve and the cylinder, α, °, is the enhancing angle of the sieve on the leading cylinder, γ, kg/m, is the sieve's weight per unit length,

Correspondence: B.Z. Jugović, Institute of Technical Science Serbian Academy of Science and Arts, Knez Mihailova 35, Belgrade, Serbia.
E-mail: branimir.jugovic@itn.sanu.ac.rs
Paper received: 24 August, 2012
Paper accepted: 19 November, 2012

v, m/s, is the sieve's rotational velocity and g, m/s^2, is the gravity acceleration.

The sieve's stress due to folding over the cylinder can be expressed as:

$$\sigma_s = E\frac{d_0}{D} \tag{4}$$

where E, N/m^2, is the Young's elasticity modulus and D, m, is the cylinder diameter.

Due to loading during operation, the sieve elongation can be expressed as:

$$\Delta L = \frac{SL}{EA} \tag{5}$$

where: ΔL, m, is the stretching (elongation) of the sieve, S is the sieve load, L, m, is the base length, E, N/m^2, is the elasticity modulus, and A, m^2, is the base cross-sectional area.

The nominal length is always smaller than the base length, due to wear of the base wire the cross-sectional area is reduced, and thus the sieve elongation due to mechanical load is calculated according to the following equation:

$$\Delta L_{\mathrm{m}} = \frac{S'L}{E'} \tag{6}$$

where S' is the stress per 1 cm of the drying sieve width, L, m, is the nominal length of the dry sieve, and E', N/m^2, is the elasticity modulus per 1 cm of the drying sieve width, which depends on degree of the sieve's wear.

Additionaly, the thermal elongation of the drying sieve is:

$$\Delta L_t = \alpha \Delta t L \tag{7}$$

where α, 1/°C, is the linear thermal expansion coefficient and Δt, °C, is the temperature increase.

The tensile strength of the non-thermo-stabilized sieve is calculated because the sieves that were not thermally stabilized have the worst mechanical properties:

$$R_{\mathrm{m}} = \frac{F_{\mathrm{break}}}{bd} \tag{8}$$

where R_{m}, MPa, is the tensile strength, F_{break}, N, is the breaking force, d, mm, is the drying sieve's sample thickness and b, mm, is the drying sieve's sample width.

The contribution of this paper represents an investigation of the drying sieve behavior, with and without temperature influence, and combined temperature and joining influence. Based on the appearance of the broken samples, micromechanical analysis of appearance and development of damages due to tensile loading was performed [20–26].

EXPERIMENTAL

The material the drying sieve is made of is a polyester wire (polybutylene terephthalate, PBT). In this work, a two weft sieve was used, with the base wire of rectangular cross-section of dimensions 0.36 mm×0.67 mm and the weft wire of circular cross section with diameter of 1.6 mm. The appearance of those wires is presented in Figures 1 and 2, respectively.

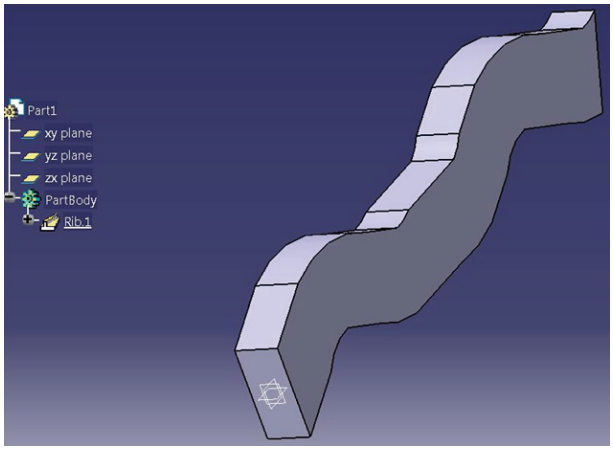

Figure1. Sieve base wire.

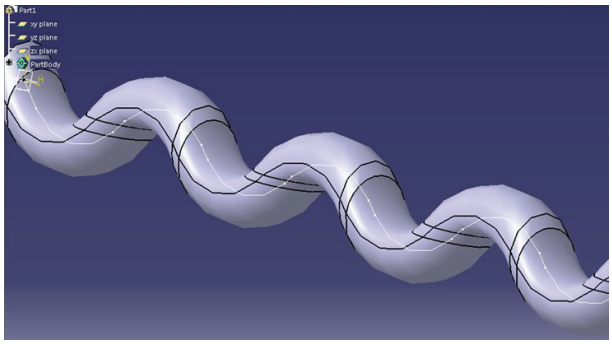

Figure 2. Sieve weft wire.

Prior to investigation, the specimen width and thickness (dry sieve) were controlled, with accuracy of 1%. The static tensile test experiments were performed on testing machine ZWICK Roell Z010, Fmax 10000 N; the maximum distance between the testing machine hydraulic jaws is 590 mm. For the tensile tests, the maximum distance between the jaws was 200 mm. The test speed was 400 mm/min. The limit force to stop the test was 60% of F_{max}. The force upper limit is 500 N. The length measure (standard path) was 50 mm.

In the first part of the experiment the base wire elongation was investigated on 3 samples. The wire material base was polyester (PBT) of a rectangular cross section, a_0 = 0.36 mm, b_0 = 0.67 mm, the sample length was L_0 = 200 mm, the area weight was 80 g/m^2.

For the weft wire test, only one sample was used. The weft wire material is polyester (PBT). The weft wire

was of a circular cross-section with diameter of 0.7 mm, the sample length was L_0 = 200 mm.

Then the non-thermally stabilized (virgin) sieve and the thermally stabilized sieve were tested and their mechanical properties were determined. The material was polyester mesh (PBT). The sample dimensions were a_0 = 1.6 mm and b_0 = 20 mm and the length was L_0 = 200 mm.

Finally, the mechanical properties of the thermally stabilized open sieve were compared to properties of the sieve's joints. The joint itself was a woven unmarked one, where the thickness of the joining spiral was approximately equal to the thickness of the sieve (the experimental procedure was the same as described in the previous section).

The joining of the sieves was performed in the following way:

The wefts were were pulled out from the sieve for about 10 to 15 cm, leaving the bases free. Then, one end was clamped between the two sieves clamp, where the free ends were ripped. The strip was then prepared from which the base was pulled out and the weft remained, about 10 to 15 cm wide. Every single weft was threaded through the joining device, to realize the weaving as in the real sieve. Then the joining spiral was prepared. The size of the spiral depends on the sieve's thickness and on the weaving. The ripped wires were then, one after another, bent over the spiral and weft into the ripped weft wires; the same procedure was applied at the other end of the sieve, where the spiral was weft. Afterwards, the two ends were joined into an endless strip in the way that the two spirals are zipped together. A wire was pulled through the holes to perform the joining. After this, the neutral ends of the base were cut off, and the tips were treated by special sandpaper, in order to obtain a fine surface of the sieve. Then, the second thermal stabilizing was performed in order to fasten the joint. The edges of the sieve were finally processed by let-lamp, *i.e*., they are molten together and a polyurethane two-component glue, which is stable at elevated temperatures, was applied as an about 40 mm wide layer.

RESULTS AND DISCUSSION

Uniaxial tensile test of a virgin base wire from the coil

The test of the base wire elongation is shown in Figure 3, while the results of the test are shown in Tables 1 and 2.

Table 1. Results of the virgin base wire tension test (F_{break} – breaking force, ε_{break} – extension at break)

Sample no.	F_{break} / N	ε_{break} / %
1	114.47	33.89
2	107.42	29.76
3	111.96	32.20

Table 2. The virgin base wire test statistics (F_{break} – breaking force, ε_{break} – extension at break, x_{sr} – arithmetic mean of measurements, σ_x – quadratic mean of measurements, δx – relative error of measurements)

Parameter	F_{break} / N	ε_{break} / %
x_{sr}	111.28	31.95
σ_x	3.57	2.08
δx / %	3.21	6.50

Zwick Roell software was used to obtain values of F_{break} and ε_{break} and perform statistical analysis of the results. Tests of the three base wire samples showed that wires of rectangular cross-section have a slight initial elongation of 2% at the force of 28 N, because the force did not reach the value prescribed by the manufacturer. The further force increase up to 106 N

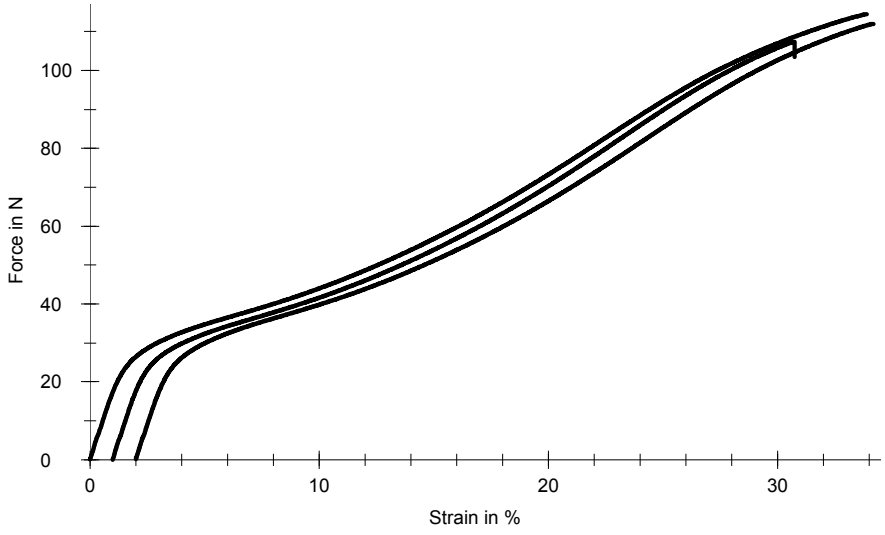

Figure 3. Force–strain diagram for tension test of the virgin base wire.

caused maximum elongation of the wire, though it was not equal for all the three samples. The reason for this difference lies in fact that the wire was not thermally stabilized and the cross section is approximated as rectangular. The maximum breaking force, obtained by static calculation, for all the three samples was 455.91 N and the corresponding elongation was 31.95%. Comparison of mechanical properties of the base and weft wires (of the rectangular and circular cross-sections, respectively) can be seen that the base wire elongation is higher for about 3 to 8%, which is in accordance with the way the sieves are manufactured. The weft wire deformation arises due to forces of the base wires; the weft wire shrinks during the sieve's extension, while the base wire is elongated, both as a function of the tensile force per unit area (cm^2).

Uniaxial tensile test of a virgin weft wire from the coil

In uniaxial tension of the weft wire, as the test progresses, the increment of wire length elongation becomes larger for the same increment of force, thus the curve bends towards the abscissa axis. The linear force-extension dependence (Figure 4), which is normal for metals, here practically does not exist, *i.e*., the deformation is plastic, almost from the very beginning of the test. The property of the wire to significantly deform plastically, without breaking, is the most useful property in sieves manufacturing. Within the force interval 0 to 45 N the small elongation of the wire occurs, and the force-deformation curve is exponential function. In the next interval, 45 to 169 N, the wire is maximally extended; where in the narrow range of 23 to 24% of elongation, the more prominent change of the curve slope occurs as well as the bend towards the abscissa. With further increase of force, the ability of material to deform further is exhausted and the breaking of the wire occurs at the maximum tensile force of 426.89 N, with the maximum achieved elongation of 24.68%.

Uniaxial tensile test of a virgin thermally non-stabilized sieve

The obtained force deformation diagram is shown in Figure 5, while the results of the test are shown in Tables 3–5.

As can be seen from Table 6, the tensile strength of the sieve exhibits small dispersion around the average value of $R_{m,av}$ = 641.2 MPa. This is explained by the manufacturing technology of manually weaving threading the sieve on the weaving machine. To get the real picture about the virgin non thermo-stabilized sieve, a micromechanical analysis was performed, which showed that this sieve's wires were exposed to bending stress.

Uniaxial tensile test of a virgin thermally stabilized sieve

The obtained force deformation diagram is shown in Figure 6, while the results of the test are shown in Tables 6 and 7.

Since the non-thermo-stabilized sieves are obtained by weaving the base and weft wires, which do not have the same mechanical properties, thermal stabilization of the sieve was performed. This results in the two kinds of wires having the same mechanical properties, so that they can be compared to each other.

Thermal stabilization was performed by exposing the sieve to elevated temperatures, gradually, in several passes. The temperature was increased in each pass for 10 °C, until the final temperature was reached. The sieve was kept at that temperature for 15 min. During the entire heating process, the sieve was subjected to tensile forces in both directions (base and weft wires) and the sieve was moved through the machine at a constant speed of 2 m/min. The pulling force was pre-

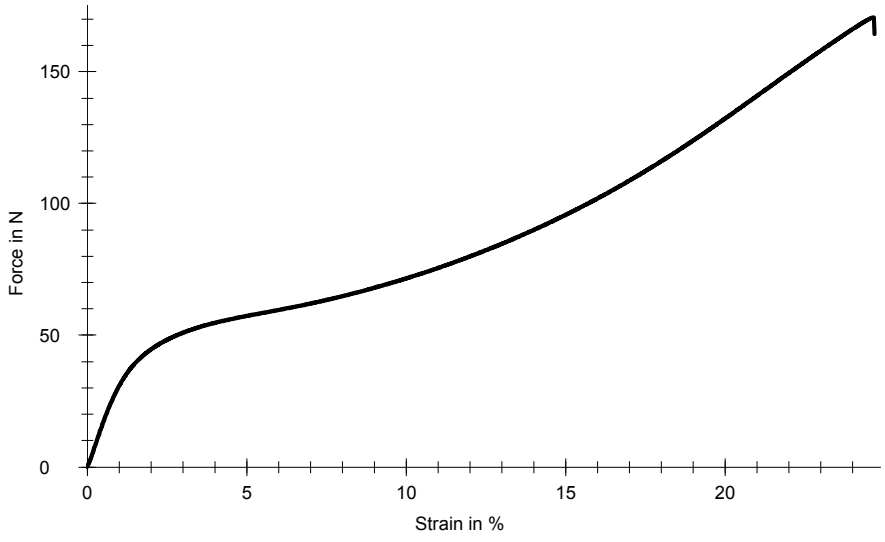

Figure 4. Force–strain diagram for tension test of the weft wire.

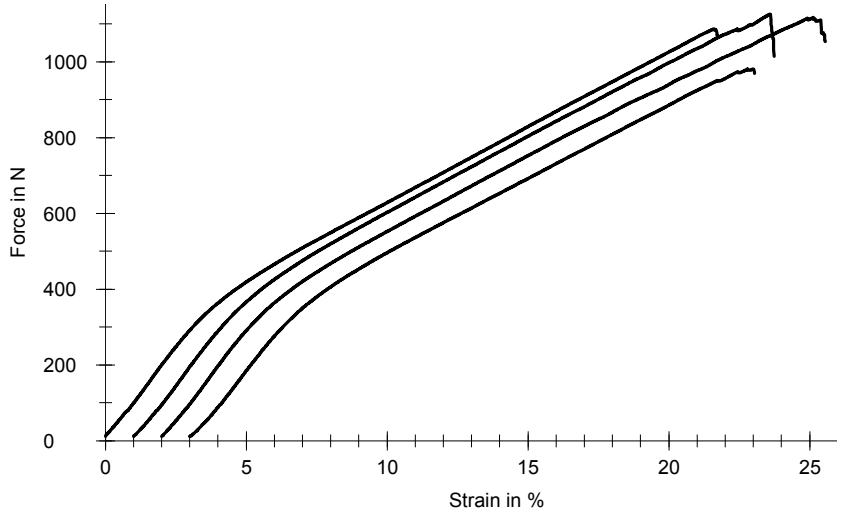

Figure 5. Force–strain diagram of the non thermo-stabilized sieve.

scribed for each type of wire forming the sieve. The sieve is considered as thermally stable if no cracks appear on it after the described process. A thermally stabilized sieve shrinks with respect to a non-stabilized sieve such that the decrease in width is less than decrease in its length, which actually is the objective of thermal stabilization – for the sieve to become homogeneous.

Table 3. Results of the not thermo-stabilized sieve tension test (F_{break} – breaking force, ε_{break} – extension at break)

Sample No.	F_{break} / N	ε_{break} / %
1	1068.68	21.72
2	1013.73	22.73
4	1052.62	23.55
5	968.39	20.05

By comparing the mechanical properties of the two sieves, non-thermo-stabilized and thermo-stabilized, one could conclude that the former sieve has worse mechanical properties; its elongation average value at break was ε_{break} = 22.01%, while for the latter sieve, this value was ε_{break} = 225.50%. The obtained experimental results support this conclusion.

Table 4. The non-thermo-stabilized sieve tension test statistics (F_{break} – breaking force, ε_{break} – extension at break %, x_{sr} – arithmetic mean of measurements, σ_x – quadratic mean of measurements, δx – relative error of measurements)

Parameter	F_{break} / N	ε_{break} / %
x_{sr}	1025.86	22.01
σ_x	44.72	1.51
δx / %	4.36	6.86

Table 5. The tensile strength of non-thermo-stabilized sieve

Sample No.	1	2	3	4
R_m / MPa	667.9	633.58	657.88	605.24

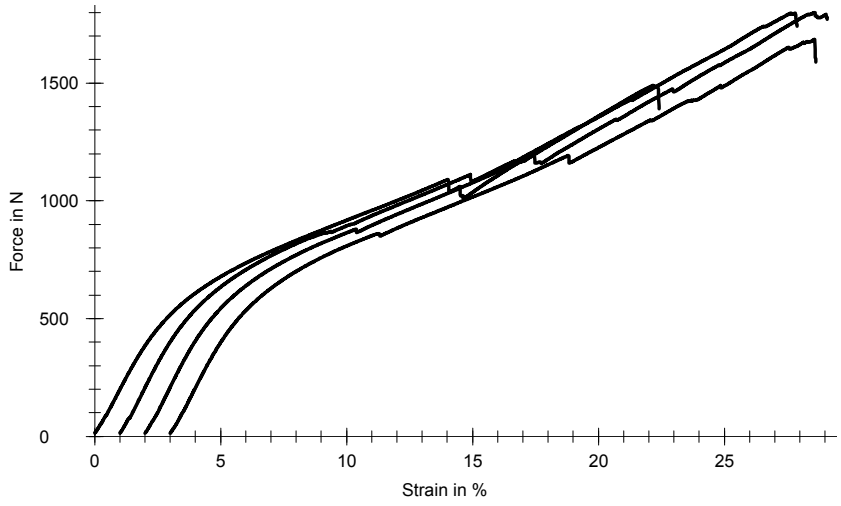

Figure 6. Force–strain diagram of the thermo-stabilized sieve.

Table 6. Results of thermo-stabilized sieve tension test (F_{break} – breaking force, ε_{break} – extension at break, σ_{break} – tension at break)

Sample No.	F_{break} / N	σ_{break} / N mm^{-2}	ε_{break} / %
1	1490.70	43.42	22.40
2	1797.32	54.45	26.88
3	1800.66	55.29	27.08
4	1685.29	49.64	25.64

Table 7. The thermo-stabilized sieve tension test statistics (F_{break} – breaking force, ε_{break} – extension at break, σ_{break} – tension at break)

Parameter	F_{break} / N	σ_{break} / N mm^{-2}	ε_{break} / %
x_{sr}	1693.49	50.70	25.50
σ_x	145.44	5.46	2.16
δx / %	8.59	10.76	8.48

Uniaxial tensile test of the thermally stabilized sieve's joint

The obtained force deformation diagram is shown in Figure 7, while the results of the test are shown in Tables 8 and 9.

Table 8. Results of tension test of the thermally stabilized sieve's joint (F_{break} – breaking force, ε_{break} – extension at break, σ_{break} – tension at break)

Sample No.	F_{break} / N	σ_{break} / N mm^{-2}	ε_{break} / %
1	1191.64	37.01	20.37
2	871.56	13.02	11.43
3	1125.28	34.99	19.38
4	1125.59	33.17	21.84

The closed (welded or soldered) sieve plays the role of the belt transmitter, which, by realizing the elastic connection and transmitting the power, drives all the cylinders of the machine and thus it is exposed to multifold loading of uneven intensity. As with the belt in operation, here also exists the pre loading in the stationary state, loading of the pulling portion of the belt–sieve and loading of the led ("free") portion of the belt-sieve. For these reasons, the sieve is first thermally stabilized and then joined. From the results of tensile tests of all the sieves, one can see that the joined sieve had a carrying capacity (average breaking force) of 29.55 N/mm^2, which is 1.7 times lower than the average breaking force of the thermally stabilized sieve, which was 50.70 N/mm^2. The thermally stabilized sieve's joint is the weakest point, with respect to the thermally stabilized sieve itself. It was noticed that in tensile tests the joined sieve was breaking either in the immediate vicinity of the joining spiral or at the spiral. Due to the uneven stress distribution the exterior ("surface") threads are being pulled out from the sample first and it breaks at the angle of 45°, which is caused by appearance of shear stresses. In further extension of the sample, the neighboring threads break, and the crack that appeared due to breaking of the external threads propagates through the middle threads and causes appearance of a macro-crack, *i.e.*, the breaking of the whole sample. Software Zwik Roell moves the notch for each new sample (curves in Figures 3 to 7).

Table 9. Tension test of the thermally stabilized sieve's joint statistics (F_{break} – breaking force, ε_{break} – extension at break, σ_{break} – tension at break)

Parameter	F_{break} / N	σ_{break} / N mm^{-2}	ε_{break} / %
x_{sr}	1078.52	29.55	18.26
σ_x	141.46	11.13	4.66
δx / %	13.12	37.67	25.52

CONCLUSION

Proper operation of drying sieves affects the work of complete plants, therefore special attention should

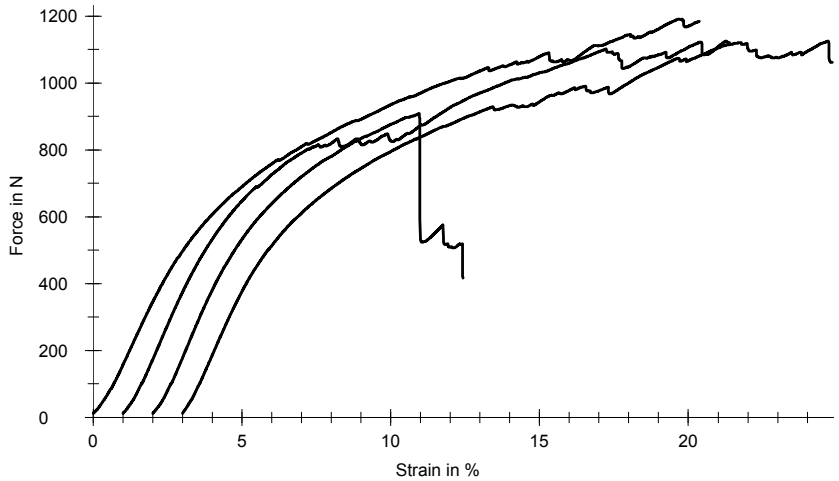

Figure 7. Force–strain diagram of the thermally stabilized sieve's joint.

be paid to their reliable operation. Exploitation of the sieves results in their elongation, wear, reduction in cross-section of wire and ultimately breaking. The objective is to produce a drying sieve with low air flow and high resistance to soiling.

The sieve joint is the weakest point of the sieve and its mechanical properties should not be below 30% of mechanical properties of the sieve itself. Anything below that is not considered a good joint. Due to the load during operation the sieves are elongated. Stresses are the highest for sieves that operate on rollers of the smallest diameter. Wear of the base wires causes increase of the sieve stress. Additional sieve elongation is caused by increased operating temperature, which causes shrinkage of materials. To avoid this shrinkage, thermal stabilization of the sieves is performed, thus the stability of the sieve's dimensions is ensured, as well as its homogeneity. Another reason for thermal stabilizing is that it strengthens molecular bonds in the polymer, thus securing sieve strength. Based on the performed experiments, all the aforementioned conclusions were confirmed, since the best mechanical properties were obtained for the thermally stabilized sieve, while the worst properties were obtained for the non-stabilized one. The mechanical properties of thermally stabilized sieves are better because they can withstand a higher force before the sieve breaks.

Acknowledgement

Parts of this research were supported by the Ministry of Education, Science and Technological Development of Republic of Serbia through Grants ON174004, “Micromechanics criteria of damage and fracture”, and TR 32036, “Development of software for solving the coupled multi-physical problems”, and realized while Mrs. Ružica R. Nikolić was on the SAIA grant of the Slovak Republic government at University of Žilina, Slovakia.

REFERENCES

[1] A. Golubović, Tehnologija izrade i svojstva papira, Grafički fakultet, Zagreb, 1984 (in Croatian).

[2] F. Ćorlukić, Tehnologija papira, Školska knjiga, Zagreb, 1987(in Croatian).

[3] M. Križan, Savremena proizvodnja papira, Mrlješ, Beograd, 1997(in Serbian).

[4] W. Kufferath, Plastic sieves for dehydration of paper, Das Papier, 1972.

[5] H.G. Merkus, Sieves and Sieving, Particle Size Measurements, in: Particle Size Measurements: Fundamentals, Practice, Quality, Springer, 2009, pp. 219–240.

[6] M. Krgovic, Determining parameters for a rate of heat transmission during paper drying, Cell. Chem. Technol. **38** (2004) 277–287.

[7] M.V. Krgović, V.J. Valent, M.M. Kršikapa, M.B. Milojević, B.S. Rašeta, D.V. Ošap, Increasing of energy efficiency in paper industry, Hem. Ind. **62** (2008) 233–246.

[8] J. Schlegel, Erfahrungen von verchiedenen Schuhpressen-Anwendungen, Wochenbl. Papierfabr. **136** (2008) 670–680.

[9] WS. Chow, Tensile and thermal properties of poly-butyleneterephtalate)/organo-montmorillonite nano composites, Malays. Polym. J. **3** (2008) 1–13.

[10] R. Srinivasan, K. Young, N. Ricci, J. Sawka, Engineering polymers in non-wovens, fibers and other extruded substrates – processing and applications for polyphenylene sulfide and thermoplastic polyesters, INTC – TAPPI, 2001.

[11] S. Hashemi, Temperature dependence of work of fracture parameters in polybutylene-terephthalate (PBT), Pol. Eng. Sci. **40** (2000) 1435–1446.

[12] A. Pegoretti, A. Gorigato, A. Penati, Tensile mechanical response of polyethylene-clay nano composites, Express Polym. Lett. **1** (2007) 123–132.

[13] I.M. Ward, An introduction to the mechanical properties of solid polymers, John Wiley and sons, Chichester, 1993.

[14] S. Qin, J. Yu, Q. Zheng, M. He, H. Zhu, Morphology and mechanical properties of nylon 6/PBT blends compatibilized with styrene/maleic anhydride copolymer, Chem. Res. Chinese U. **23** (2007) 726–732.

[15] Z.A. Mohd Ishak, Y. W. Leong, M. Steeg, J. Karger-Kocsis, Mechanical properties of woven glass fabric reinforced *in situ* polymerized poly-butylene terephthalate) composites, Mater. Sci. **67** (2007) 390–399.

[16] D.F. Wu, C.X. Zhou, X. Fan, D.L. Mao, Z. Bian, Linear rheological behavior and thermal stability of poly(butylene terephthalate)/epoxy/clay ternary nano composites, Polym. Degrad. Stab. **87** (2005) 511–520.

[17] D.R. Kelsey, K.S. Kiibler, N. Tutunjian, Thermal stability of poly(trimethylene terephthalate), Polymer **46** (2005) 8937–8947.

[18] M.Krgović, O. Perviz, Grafički materijali, Tehnološko-metalurški fakultet, Beograd, 2005 (in Serbian).

[19] N. Bojić, Z. Jugović, R. Nikolić, V. Lazić, R. Čukić, Determination of optimal way for the diagonal sieves joining, IRMES, Zlatibor, Serbia, 2011.

[20] J. Wu, Y.W. Mai, B. Cotterell, Fracture toughness and fracture mechanisms of PBT/PC/IM blend Part I – Fracture properties, J. Mater. Sci. **28** (1993) 3373–3384.

[21] S. Hashemi, Determination of the fracture toughness of polybutylene terephthalate (PBT) film by the essential work method: Effect of specimen size and geometry, Pol. Eng. Sci. **40** (2000) 798–809.

[22] S. Hashemi, Temperature dependence of work of fracture parameters in polybutylene terephthalate (PBT), Pol. Eng. Sci. **40** (2000) 1435–1447.

[23] P. Du, B. Xue, Y. Song, S. Lu, J. Yu, Q. Zheng, Fracture surface characteristics and impact properties of poly-(butylene terephthalate), Polym. Bull. **64** (2012) 185––196.

[24] W. Grellmann, S. Seidler, Deformation and fracture behavior of polymers, Springer, 2001.

[25] W. Grellmann, S. Seidler, K Jung, K. Kotter, Crack resistance behavior of polypropylene copolymers, J. Appl. Polym. Sci. **64** (2001) 1079–1091.

[26] A. Pavan, Fracture of polymers, composites and adhesives II, Elsevier, Ampsterdam, 2003.

IZVOD

JEDNOOSNO ZATEZANJE SUŠNIH SITA

Nada V. Bojić[1] , Ružica R. Nikolić[2,3], Branimir Z. Jugović[4], Zvonimir S. Jugović[5], Milica M. Gvozdenović[6]

[1]*Fabrika sita i ležaja "FASIL" A.D., Arilje, Srbija*
[2]*Fakultet inženjerskih nauka, Univerzitet u Kragujevcu, Kragujevac, Srbija*
[3]*Faculty of Civil Engineering, University of Žilina, Žilina, Slovakia*
[4]*Institut tehničkih nauka Srpske akademije nauka i umetnosti, Beograd, Srbija*
[5]*Tehnički fakultet Čačak, Univerzitet u Kragujevcu, Čačak, Srbija*
[6]*Tehnološko–metalurški fakultet, Univerzitet u Beogradu, Beograd, Srbija*

(Naučni rad)

Iako literatura sadrži brojne studije koje su razvijene da bi opisale nelinearna ponašanja sušnih sita, radovi iz ove oblasti nisu dublje istražili ponašanje sušnih sita pri zatezanju i termostabilizaciji. Cilj ovog rada je da pruži uvid u elastoplastično ponašanje termostabilizovanih i netermostabilizovanih sita pod dejstvom sile zatezanja. U okviru ovog rada izvršena su teorijska i eksperimentalna ispitivanja. Spajanje sita je izvršeno pomoću spirale. U odvojenim eksperimentima je radjeno ispitivanje žica osnove i potke od kojih se tkaju sita, netermostabilizovana sita, termostabilizovana sita, spojevi sita, kao i eksperiment termostabilizacije sita. Ispitivanjem se došlo do zaključka da termostabilizovana sita obezbeđuju stabilnost dužine i širine sita, kao i da otvoreno termostabilizovano sušno sito ima bolje mehaničke osobine i eksploatacione karakterisike nego spoj sita.

Ključne reči: Sušna sita • Spoj spiralom • Termostabilizacija

Kvalitet zeolita iz ležišta Vranjska Banja po klasama krupnoće

Živko T. Sekulić[1], Aleksandra S. Daković[1], Milan M.Kragović[1], Marija A. Marković[1], Branislav B.Ivošević[1], Božo M. Kolonja[2]

[1]*Institut za tehnologiju nuklearnih i drugih mineralnih sirovina, Beograd, Srbija*
[2]*Univerzitet u Beogradu, Rudarsko-geološki fakultet, Beograd, Srbija*

Izvod

Obavljena su ispitivanja kvaliteta polaznog uzorka i kvaliteta pojedinih klasa krupnoće na uzorku prirodnog zeolita iz ležišta Zlatokop (okolina Vranjske Banje, Srbija). Cilj ispitivanja je bio da se utvrdi homogenost kvaliteta zeolita u pogledu klasa krupnoće i da li se odvajanjem neke klase lošijeg kvaliteta može izdvojiti klasa sa višim sadržajem osnovnog minerala – klinoptilolita. Krakterizacija polaznog zeolita, kao i određenih klasa krupnoće je urađena određivanjem hemijskog sastava, sadržaja oksida $CaO+MgO+Na_2O+K_2O$ kao i kapaciteta katjonske izmene (KKI) kao i korišćenjem XRD analize. Dobijeni rezultati su ukazali da sve analizirane klase krupnoće (–2+0,8; –0,8+0,6; –0,6+0,4; –0,4+0,1; –0,1+0; –0,3+0,63; –0,63+0 i –0,43+0 mm) imaju dobar kvalitet. Najveće vrednosti kapaciteta katjonske izmene (KKI) imaju klase –0,043+0mm (166,5 meq/100 g) i –0,063+0 mm (158,8 meq/100 g). Rezultati su ukazali da nešto bolji kvalitet zeolita se može postići kada se ove klase izdvajaju prosejavanjem iz polaznog uzorka nego kada se iste dobiju mlevenjem polaznog uzorka na tu finoću.

Ključne reči: prirodni zeolit, klase krupnoće prirodnog zeolita, mlevenje, prosejavanje, kapacitet katjonske izmene.

Dostupno na Internetu sa adrese časopisa: http://www.ache.org.rs/HI/

STRUČNI RAD

UDK 549.67(497.11Vranjska Banja):54:543.218

Hem. Ind. **67** (4) 663–669 (2013)

doi: 10.2298/HEMIND120724107S

U oblasti pripreme mineralnih sirovina, da bi se utvrdio sadržaj ili raspodela minerala po klasama krupnoće rade se hemijske analize po klasama krupnoće. Dobijene klase krupnoće se usitnjavaju na 100% –0,074 mm i u njima se određuje hemijski sastav. Na primer, podaci o kretanju sadržaja Cu u klasam krupnoće su od značaja za izbor postupka i načina odstranjivanja nečistoća iz sirovine u cilju dobijanja koncentrata sa što većim sadržajem bakra [1]. O uticaju finoće mlevenja na iskorišćenje bakra u osnovnom koncentratu govore Magdalinović i saradnici [2].

Kad je reč o nemetaličnim mineralnim sirovinama, na primer kvarcni šljunak ili kvarcni pesak, obično se prati sadržaj nečistoća (Fe_2O_3) da bi se definisalo koja klasa ima najviše primesa pa se onda ta klasa ne koristi za najkvalitetnije asortimane proizvoda [3].

Postoji veliki broj radova koje su istraživači objavili na osnovu istraživanja na prirodnom zeolitu. Ta istraživanja su iz različitih aspekata, a najčešće se prirodni zeolit razmatra kao sirovina za dobijanje materijala za uklanjanje toksičnih metala, amonijaka, i drugih neorganskih i/ili organskih zagađivača. U radovima istraživači obično imaju poglavlje u kome se govori o polaznom uzorku koji je korišćen u eksperimentima. Tu se obično kaže da je prirodni zeolit uzet iz određenog ležišta i da je od njega napravljena određena klasa krupnoće koja je korišćena za realizaciju cilja ispitivanja. Na primer, za modifikovanje površine prirodnog zeolita koriste se klase –0,1+0, –0,063+0 i –0,043+0 mm [4–9].

Za eksperimente remedijacije koristi prirodni zolitni tuf bogat klinoptilolitom iz St. Cloud ležišta kod Vinston, Novi Meksiko, krupnoće –0,4; –1,4+0,4 ili –2,4+1,4 mm. Kvantitavnom XRD analizom je određeno da polazni uzorak zeolita sadrži 74% klinoptilolita, 5% smektita 10% kvarca i kristobalita, 10% feldspata i 1% ilita. Spoljašnja specifična površina, određena adsorpcijom azota, neznatno je varirala za tri klase krupnoće (od 13.3 do 15.2 m^2/g) [10]. Na prirodnom zeolitu modifikovanom sa organskim katjonima (surfaktanti) je ispitivana adosrpcija neorganskih oksi anjona, kao i organskih zagađivača i patogenih mikroorganizama.

Orha i saradnici u svom radu [11] za eksperimente antibakterijskih osobina zeolita koji u sebi sadrži jone srebra i bakra koriste rumunski zeolitni mineral iz ležišta Mirsida koji isporučuje Cemacon kompanija. Mineral je u prahu i prosejan sa multilab sito šejkeru, prečnik veličine zrna izabran za obavljanje eksperimenata je bio između –0,50+0,315 mm.

Tarasevich i saradnici [12] su određivali poziciju katjona u Na-zeolitu izmenjim sa Cs^+ i Co^{2+}. Za eksperimente katjonske izmene koristili su zeolit – klinoptilolit veličine čestica 0,5+0,25 mm.

Trgo i Perić [13] su u eskperimentima adsorpcije cinka koristili zeolit iz ležišta Donje Jesenje, Republika Hrvatska, koji je mleven i prosejan da se odvoji frakcija

Prepiska: Ž.T. Sekulić, Institut za tehnologiju nuklearnih i drugih mineralnih sirovina, Franše d' Eperea 86, Beograd, Srbija.
E-pošta: z.sekulic@itnms.ac.rs
Rad primljen: 24. jul, 2012
Rad prihvaćen: 9. oktobar, 2012

–0.5+0,1 mm. U sastavu ovaj zeolit ima do 50% klinoptilolita, a feldspat, kalcit i kvarc su glavne nečistoće.

Ćurković i saradnici [14] u eksperimentima adsorpcije bakra koriste prirodni klinoptilolitski zeolit iz ležišta Donje Jesenje, Republika Hrvatska, tri klase krupnoće: –0,5; –2+0,5 i –5+2 mm. Eksperimenti su rađeni u cilju izučavanja kinetike i termodinamike procesa adsorpcije Cu katjona iz vode. Određeno je da adsorpcija bakra raste sa porastom temperatore i smanjenjem veličine čestica prirodnog zeolita.

Li i Hong [15] su ispitivali adsorpciju hromata na prirodnom zeolitu modifikovanom surfaktantima. Korišćene su sledeće frakcije zeolita: 3,6–4,8 mm, 1,4–2,4 mm i <0,4 mm. Potvrđeno je da adsorpcija hromata raste sa smanjem veličine čestica zeolita. Ukazano je i na činjenicu da je neophodna veća krupnoća čestica da bi se postigla veća hidraulična provodljivost, i da je zbog toga značajno da se ispita uticaj veličine čestice na adsorpciju specifičnog zagađivača.

Na osnovu pregleda literature se može videti da se eksperimenti adsorpcije neorganskih, kao i organskih zagađivača na modifikovanim zeolitima najčešće rade u stacionarnim uslovima („*batch*“ eksperimenti) i u dinamičkim uslovima (eksperimenti sa kolonom). Za eksperimente u stacionarnim uslovina, obično se koristi zeolit granulacije ispod 100 μm, dok je za eksperimente u koloni neophodno da granulacija zeolite bude iznad 100 μm. Filtrabilnost zeolita kao adsorbenta je značajan parametar koji ukazuje na mogućnost njegovog korišćenja kao reakcionog filtra u jednom ili više slojeva. Adsorpciona sposobnost zeolita u ovom slučaju jeste sposobnost zadržavanja zagađivača pri prolasku kontaminirane vode. Za razliku od glinenih minerala smektita i njihove osobine bubrenja u vodi, zeoliti imaju čvršću trodimenzionu kristalnu strukturu, a samim tim i hidrauličke osobine koje im omogućavaju širi spektar primene pri prečišćavanju kontaminiranih voda [9]. Zbog obrnute proporcionalnosti između veličine zrna i specifične površine, u eksperimentima adsorpcije različitih zagađivača na prirodnim zeolitimaa je neophodno da se ispita i uticaj veličine čestica na adsorpciju specifičnog zagađivača.

Prema tome, veoma važno koja krupnoća zeolita se koristi u određene svrhe. Isto tako, veoma je važno kako je pripremljena neka klasa krupnoće zeolita i u kojoj klasi krupnoće je najviši sadržaj osnovnog minerala, odnosno da li su neke klase krupnoće boljeg kvaliteta nego polazni uzorak? U ovom radu urađeni su eksperimenti dobijanja pojedinih klasa krupnoće prirodnog zeolita a zatim je na svim klasama kao i na polaznom uzorku određena hemijski sastav, kapacitet katjonske izmene i urađena XRPD analiza. U esperimentima je korišćen uzorak prirodnog zeolita iz ležišta Zlatokop (okolina Vranjske Banje, Srbija).

EKSPERIMENTALNI DEO

Materijal i plan eksperimenta

Za eksperimentalni rad korišćen je uzorak prirodnog zeolita iz firme „MineraliCO”, Vranjska Banja, koji je dobijen postupkom usitnjavanja na postrojenju u Vranjskoj Banji na krupnoću 100%–2 mm. Hemijski i mineraloški sastav polaznog uzorka se daje u sklopu rezultata ispitivanja.

Eksperimentalni rad se sastojao u dobijanju određenih klasa krupnoće iz polaznog uzorka, a zatim je na tim klasama urađena hemijska analiza, mineraloška analiza, XRD analiza i određivnje kapaciteta katjonske izmene (KKI). Šematski prikaz eksperimenta je dat na slici 1.

Uzorak br. 1 je uzet iz polaznog uzorka i njegovim prosejavanjem na laboratorijskim sitima otvora 0,8, 0,6, 0,4 i 0,1 mm, dobijene su klase –2+0,8; –0,8+0,6; –0,6+0,4; –0,4+0,1 i –0,1+0 mm.

Uzorak br. 2 uzet iz polaznog uzorka, a zatim je samleven u laboratorijskom mlinu sa prstenovima na krupnoću 100%–0,3 mm. Nakon toga, mokrim postupkom prosejavanja na laboratorijskim sitima otvora 0,1 i 0,063 mm su dobijene klase –0,3+0,1 mm; –0,1+0,063 i –0,063+0 mm, a prosejavanjem na situ situ otvora 0,043 mm dobijene su klase –0,1+0,043 i –0,043+0 mm.

Uzorak br. 3 jeste polazni uzorak zeolita na kome je urađena hemijska i XRPD analiza i određeđen je KKI.

Metode

Određivanje hemijskog sastava

Kvantitativna hemijska analiza polaznog uzorka zeolita urađena je na atomskom adsorpcionom spektrofotometru Aanalysis 300.

Određivanje ukupnog kapaciteta katjonske izmene

Kapacitet katjonske izmene – KKI – je određen metodom jonske izmene sa amonijum-hloridom na sledeći način: 1 g uzorka ostavi se da stoji 24 h u 100 ml amonijačnog rastvora, na pH 7, uz povremeno mućkanje. Nakon završene jonske izmene, suspenzija se filtrira i u filtratu se određuju koncentracije izmenjivih katjona Ca, Mg, K i Na, koja preračunata na meq/100g uzorka predstavlja ukupni KKI. Koncentracije izmenljivih jona su određivane na atomskom spektrofotometru Analytic Jena Spekol 300.

Metoda rendgenske difrakcije (XRPD)

Za određivanje i praćenje faznog sastava polaznog uzorka zeolita, kao i izdvojenih klasa korišćen je rendgenski difraktometar marke “PHILIPS”, model PW-1710, sa zakrivljenim grafitnim monohromatorom i scintilacionim brojačem. Uzorci su prethodno pripremljeni u obliku praha.

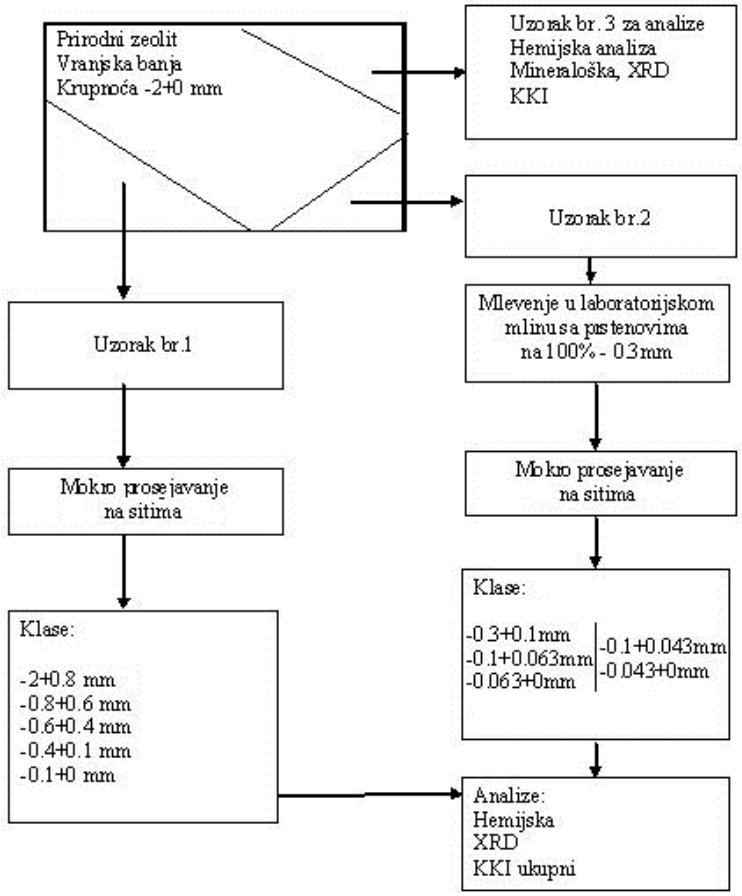

Slika 1. Šematski prikaz eksperimenta.
Figure 1. Experiment scheme.

REZULTATI I DISKUSIJA

Hemijski sastav uzoraka pojedinih klasa krupnoće prirodnog zeolita kao i polaznog uzorka zeolita je dat u tabeli 1.

Na osnovu rezultata hemijske analize datih u tabeli 1 vidi se da su najveće vrednosti sadržaja oksida $CaO+MgO+Na_2O+K_2O$ za uzorak klase –0,8+0,6 mm (10,38%) i –0,043+0 mm (10,14%), s tim što je u uzorku –0,8+0,6 mm nešto povišen sadržaj kalcijum-oksida. Isto tako se može oučiti da je odnos Si/Al > 4,5 što ukazuje da se radi o klinoptilolitskom zeolitu [11].

Rendgenska difrakciona analiza je urađena na uzorku polaznog prirodnog zeolita iz lokaliteta Vranjska Banja, a zatim na nekoliko uzoraka po klasama krupnoće. Difraktogrami rendgenskih analiza su dati na slici 2.

Iz difraktograma datih na slici 1 se vidi da su u svim klasama zastupljeni sledeći minerali: dominantan zeolitski mineral je klinoptilolit, dok su kao prateći minerali u uzorcima prisutni kvarc, feldspati, karbonati (kalcit), smektitski minerali. Takođe, intenziteti difrakcionih pikova osnovnog minerala klinoptilolita su nešto viši u sitnijim klasama krupnoće.

Uporedni prikaz sadržaja oksida $CaO+MgO+Na_2O+K_2O$ i vrednosti kapaciteta katjonske izmene (KKI) dobijenih analiziranjem klasa krupnoće zeolita i polaznog uzorka je dat u tabeli 2.

U tabeli 3 je dato kretanje ili distribucija sadržaja oksida $CaO+MgO+Na_2O+K_2O$ i KKI po klasama krupnoće dobijenih prosejavanjem, a u tabelama 4 i 5 distribucija oksida $CaO+MgO+Na_2O+K_2O$ i KKI po klasama krupnoće koje su dobijene mlevenjem i prosejavanjem. Distribucija po klasama krupnoće se dobija računskim putem preko bilanasa raspodele uvažavajući maseno učešće pojedinih klasa u polaznom uzorku (–2+0mm).

Iz literature je poznato da vrednost za teorijski kapacitet katjonske izmene KKI iznosi preko 200 meq/100g zeolita [14]. Isto tako nije zadata minimalna granica vrednosti KKI, ona zavisi od oblasti primene. Na osnovu datih vrednosti za kapacitet katjonske izmene (tabela 2) vidimo da je najveća vrednost za kapacitet katjonske izmene (KKI) za klasu –0,043+0 mm (166,5 meq/100g) i onda za klasu –0,063+0 mm (158,8 meq/100g).

Raspodela sadržaja oksida $CaO+MgO+Na_2O+K_2O$ (tabela 3) po klasama krupnoće ukazuje da je 54,22% ovih oksida u klasi –2+0,8 mm, a da je 45,78% u klasama

Tabela 1. Hemijski sastav analiziranih klasa zeolita i polaznog uzorka tog prirodnog zeolita iz Vranjske Banje
Table 1. Chemical composition of zeolite classes and starting natural zeolite from Zlatokop deposit

Klasa, mm	Sadržaj komponente, %							
	SiO_2	Al_2O_3	Fe_2O_3	CaO	MgO	Na_2O	K_2O	G.Ž.
Polazni uzorak (–2+0 mm)	64,72	13,12	3,42	5,15	0,79	1,19	1,06	9,76
Klase dobijene prosejavanjem polaznog uzorka								
–2+0,8	65,81	12,91	3,04	4,88	0,76	1,17	0,60	9,99
–0,8+0,6	63,79	12,33	3,12	6,65	0,77	1,30	1,66	9,70
–0,6+0,4	64,24	13,47	3,37	4,55	0,97	1,38	1,60	9,74
–0,4+0,1	66,47	12,85	2,52	4,90	0,65	1,77	1,31	9,02
–0,1+0	62,50	13,61	4,36	5,60	0,85	1,04	1,66	9,53
Klase dobijene mlevenjem polaznog uzorka (100%–0,3mm) i prosejavanjem na situ 0,1 mm i 0,063 mm								
–0,3+0,1	65,55	14,04	2,83	4,88	0,682	1,15	0,406	9,62
–0.1+0.063	66,72	12,57	2,26	5,25	0,670	1,62	0,548	9,52
–0.063+0	63,24	12,66	2,75	6,30	1,09	1,34	0,84	11,26
Klase dobijene mlevenjem polaznog uzorka (100% –0,3mm) i prosejavanjem na situ 0,1 mm i 0,043mm								
–0,1+0,043	65,27	13,42	2,28	5,60	0,87	0,97	1,38	9,86
–0,043+0	62,28	12,33	3,20	6,65	1,18	1,46	0,85	11,84

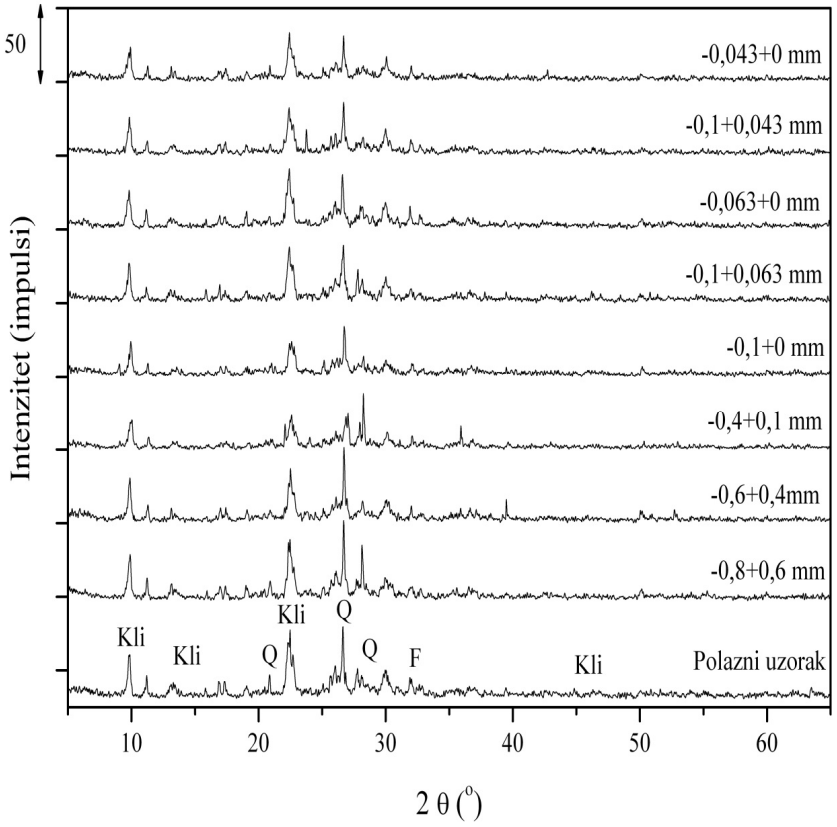

Slika 2. Difraktogrami praha ispitivanih uzoraka zeolita Vranjska Banja.
Figure 2. XRPD Patterns of zeolite samples.

ispod 0,8 mm, od čega 29,56% u klasi –0,1+0 mm. Ovo ukazuje da je veća koncentracija klinoptilolita u najsitnijoj klasi krupnoće.

Iz rezultata datih u u tabelama 4 i 5, koji se odnose na klase –0,063 i –0,043 mm vidimo da je sadržaj oksida $CaO+MgO+Na_2O+K_2O$ u sitnijim klasama veći nego u krupnijim. Naime, u klasi –0,063+0 mm taj sadržaj je 9,57%, a u klasi –0,1+0,063 mm 8,09%. U klasi –0,043+0 mm sadržaj ovih oksida je 10,14%, a u klasi –0,1+0,043 mm 8,82%. Ovaj trend prati i raspodela KKI po klasama. Tako je za klasu –0,063+0 mm sadržaj KKI 62,5%, a za klasu –0,043+0 mm 56,0 %.

Tabela 2. Uporedni prikaz sadržaja oksida CaO+MgO+Na_2O+K_2O i vrednosti kapaciteta katjonske izmene (KKI) u različitim klasama
Table 2. Content of of CaO+MgO+Na_2O+K_2O oxides and cation exchange capacity (CEC) in different classes

Klasa, mm	Prema KKI, meq/100g	Prema sadržaju CaO+MgO+Na_2O+K_2O, %	Prema XRD
Polazni (–2+0 mm)	145,6	8,19	Najviše: klinoptilolit, manje: kvarc, feldspat; zanemarljivo: kalcit i smektit
Klase dobijene prosejavanjem			
–2+0,8	146,3	7,41	–
0,8+0,6	148,27	10.38	Kao polazni
–0,6+0,4	149,1	8,50	Ima više kvarca nego u polaznom
–0,4+0,1	146,2	8.63	Ima više feldspata nego u polaznom
–0,1+0	141,7	9.15	Kao klasa -0,6+0,4mm
Klase dobijene mlevenjem polaznog uzorka na 100% – 0,3 mm i prosejavanjem na situ 0,1 i 0,063 mm			
–0,3+0,1	110,5	7,12	–
–0,1+0,063	143,2	8,09	Kao polazni
–0,063+0	158,8	9,57	Kao polazni
Klase dobijene mlevenjem polaznog uzorka na 100% – 0,3 mm i prosejavanjem na situ otvora 0,1 i 0,043 mm			
–0,1+0,043	141,5	8,82	Kao polazni
–0,043+0	166,5	10,14	Kao polazni

Tabela 3 Distribucija oksida CaO+MgO+Na_2O+K_2O i KKI po klasama krupnoće dobijenih prosejavanjem
Table 3. Distribution of CaO+MgO+Na_2O+K_2O oxides and CEC in different classes

Klasa, mm	Maseni udeo, mas.%	Sadržaj oksida, mas.%		KKI, meg/100g		Distribucija po klasama	
1	2	3	4	2×3	2×4	Oxid, %	KKI, %
–2,0+0,8	53,96	7,41	146,3	399,8436	7894,35	48,84	54,22
–0,8+0,6	3,73	10,38	148,27	38,7174	553,05	4,73	3,80
–0,6+0,4	4,71	8,50	149,1	40,035	702,26	4,89	4,82
–0,4+0,1	7,56	8,63	146,2	65,2428	1105,27	7,97	7,60
–0,1+0	30,04	9,15	141,7	274,866	4307,70	33,57	29,56
Ulaz, –2+0 (računski)	100,00	8,19	145,6	818,7048	14562,63	100,00	100,00

Tabela 4. Distribucija oksida CaO+MgO+Na_2O+K_2O i KKI po klasama krupnoće: –0,3+0,1; –0,1+0,063 i –0,063+0 mm
Table 4. Distribution of CaO+MgO+Na_2O+K_2O oxides and CEC in classes: –0.3+0.1, –0.1+0.0063 and –0.63+0 mm

Klasa, mm	Maseni udeo, mas.%	Sadržaj oksida, mas.%		KKI, meg/100g		Distribucija po klasama	
1	2	3	4	2×3	2×4	Oxidi, %	KKI, %
–0,3+0,1	17,00	7,12	105,1	121,04	1878,5	13,78	12,90
–0,1+0,063	25,00	8,09	143,2	202,25	3580,0	23,03	24,60
–0,063+0	58,00	9,57	158,8	555,06	9210,4	63,19	62,5
Ulaz, –0,3+0 (računski)	100,00	8,78	145,6	878,35	14560,0	100,00	100,00

Tabela 5. Distribucija oksida CaO+MgO+Na_2O+K_2O i KKI po klasama krupnoće: –0,3+0,1; –0,1+0,043 and –0,043+0 mm
Table 5. Distribution of CaO+MgO+Na_2O+K_2O oxides and CEC in classes:-0.3+0.1, -0.1+0.043 and -0.043+0 mm

Klasa, mm	Maseni udeo, mas.%	Sadržaj oksida, mas.%		KKI, meg/100g		Distribucija po klasama	
1	2	3	4	2×3	2×4	Oxida,%	KKI,%
–0,3+0,1	17,00	7,12	91	121,04	1878,5	13,15	12,90
–0,10+0,043	32,00	8,82	141,5	282,24	4528,0	30,66	31,10
–0,043+0	51,00	10,14	166,5	517,14	8491,5	56,19	56,00
Ulaz, –0,3+0 (računski)	100,00	9,20	145,6	920,42	14560,0	100,00	100,00

Sve ovo ukazuje da je sadržaj minerala klinoptilolta rasopoređen po klasama krupnoće tako što je njegov sadržaj nešto veći u najsitnijim klasam (–0,063+0 i –0,043+0 mm). U prilog ovome idu i rezultati mineraloške analize dati u tabeli 2 i na difraktogramima na slici 2.

ZAKLJUČAK

Ispitivanja na polaznom uzorku zeolita kao i na klasama krupnoće: –2+0,8; –0,8+0,6; –0,6+0,4; –0,4+0,1; –0,1+0; –0,3+0,63; –0,63+0 i –0,43+0 mm pokazala su da je kvalitet pojedinih klasa krupnoće ispitivanog zeolita iz ležišta Zlatokop (okolina Vranjske Banje) veoma dobar. Na ovakav zaključak upućuju rezultati sadržaja oksida CaO+MgO+Na_2O+K_2O i vrednosti kapaciteta katjonske izmene kao i kvalitativna XRD analiza. Veći kapacitet katjonske izmene (KKI), kao bitan parametar kvaliteta, je dobijen u sitnijim klasama krupnoće: –0,063+0 i –0,043+0 mm. Naime, vrednosti kapaciteta katjonske izmene u ostalim klasam se kreću od 141,5 do 149,1 meq/100 g, dok u slučaju klase –0,063+0 i –0,043+0mm te su vrednosti 158,8, odnosno 166,5 meq/100 g. Ovo ukazuje na to da je prosejavanjem usitnjenog uzorka, na primer na –0,043 mm, moguće dobiti nešto bolji kvalitet nego mlevenjem kompletnog polaznog uzorak na tu klasu. Sadržaj klinoptilolita je veći u sitnijim klasama krupnoće.

Zahvalnica

Ovaj rad je rezultat projekata koje finansira Ministarstvo prosvete, nauke i tehnološkog razvoja Republike Srbije, TR 34013 i ON 172018 u periodu 2011-2014. godine.

LITERATURA

[1] R. Milosavljević, Metode ispitivanja mineralnih sirovina u pripremi mineralnih sirovina, Rudarsko–greološki fakultet Beograd, 1974.

[2] S. Magdalinović, D. Urošević, S. Petković, Uticaj finoće mlevenja na iskorišćenje bakra u osnovnom koncentratu, Rudarski radovi **1** (2010) 103–114.

[3] Z. Bartulović, M. Petrov, D. Todorović, Lj. Andrić, I. Jovanović, J. Stojanović, Possibility of High Grade SiO_2 Concentrate Production From Raw Quartz Gravel, XIV Balkan Mineral Processing Congress, 2011, pp. 314–317.

[4] T. Stanić, A. Daković, A. Živanović, M. Tomašević-Čanović, V. Dondur, S. Milićević, Adsorption of arsenic (V) by iron (III)-modified natural zeolitic tuff, Environ. Chem. Lett. **7** (2009) 161–166.

[5] M. Tomašević-Čanović, A. Daković, G. Rottinghaus, S. Matijašević, M. Đuričić, Surfactant modified zeolites – new efficient adsorbents for mycotoxins, Microporous Mesoporous Mater. **61** (2003) 173–180.

[6] A. Vujaković, M. Tomašević-Čanović, A. Daković, V. Dondur, The adsorption of sulphate, hydrogenchromate and dihydrogenphosphate anions on surfactant-modified clinoptilolite, Appl. Clay Sci. **17** (2000) 265–277.

[7] A. Daković, M. Tomašević-Čanović, G.Rottinghaus, V. Dondur, Z. Mašić, Adsorption of ochratoxin A on octadecyldimethyl benzyl ammonium exchanged-clinoptilolite-heulandite tuff, Colloids Surf., B **30** (2003) 157–165.

[8] D. Krajišnik, A. Daković, M. Milojević, A. Malenović, M. Kragović, D. Bajuk Bogdanović, V. Dondur, J. Milić, Properties of diclofenac sodium sorption onto natural zeolite modified with cetylpyridinium chloride, Colloids Surf., B **83**(2011) 165–172.

[9] J. Lemić, Modifikovani alumosilikatni minerali kao adsorbenti u tretiranju kontaminiranih voda, doktorska disertacija, Institut za tehnologiju nuklearnih i drugih mineralnih siroivina, Beograd, 2006, str. 99.

[10] R.S. Bowman, Applications of surfactant-modified zeolites to environmental remediation, Microporous Mesoporous Mater. **61** (2003) 43–56

[11] C. Orha, F. Manea, A. Popi, G. Burtica, I. Fazakas Todea, Obtaining and Characterization of Zeolitic Materials with Antibacterial Properties, Rev. Chim. (Bucuresti) **59** (2008) 173–177.

[12] Yu.I. Tarasevich, I.G. Polyakova, V.E. Polyakov, Microcalorimetric Study of the Interaction between Water and Cation-Substituted Clinoptilolites, Colloid J. **65** (2003) 493–499.

[13] M. Trgo, J. Perić, Interaction of the zeolitic tuff with Zn-containing simulated pollutant solutions, J. Colloid Interface Sci. **260** (2003) 166–175.

[14] L. Ćurković, M. Trgo, M. Rožić, N. Vukojević Medvidović, Kinetics and thermodynamics study of copper ions removal by natural clinoptilolite, Indian J. Chem. Technol. **18** (2011) 137–144.

[15] Z. Li, H. Honga, Retardation of chromate through packed columns of surfactant-modified zeolite, J. Hazard. Mater. **162** (2009) 1487–1493.

SUMMARY

QUALITY OF ZEOLIT FROM VRANJSKA BANJA DEPOSIT ACCORDING TO SIZE CLASSES

Živko T. Sekulić[1], Aleksandra S. Daković[1], Milan M.Kragović[1], Marija A. Marković[1], Branislav B.Ivošević[1], Božo M. Kolonja[2]

[1]*Institute for Technology of Nuclear and Other Mineral Raw Materials, Belgrade, Serbia*
[2]*Faculty of Mining and Geology, Belgrade, Serbia*

(Professional paper)

This paper presents the results of investigations of the quality of the natural zeolite as well as the quality of specific particle size classes of the natural zeolite. The aim of the investigations was to determine if the different classes possess different qualities. The starting material used in experiments was the natural zeolite from the Zlatokop deposit (Vranjska Banja, Serbia). The classes –0.2+0.8 mm; –0.8+0.6 mm; –0.6+0.4 mm; –0.4+0.1 mm were obtained by wet sieving of the natural zeolite. Grinding processes of the natural zeolite gave classes –0.3+0.63 mm; –0.63+0 mm; –0,43+0 mm. Chemical composition, mineralogical XRPD and cation exchange capacities (CEC) were analyzed for the starting sample and the obtained particle size classes. It was determined that all particle size classes possess similar qualities. The highest cation exchange capacity was observed in classes –0.043+0 mm (166.5 meq/100 g) and –0.063+0 mm (158.8 meq/100 g).

Keywords: Natural zeolite • Size classes of natural zeolite • Grinding • Screening • Cationic exchange capacity

Content of capsaicin extracted from hot pepper (*Capsicum annuum* ssp. *microcarpum* L.) and its use as an ecopesticide

Liljana Koleva Gudeva[1], Sasa Mitrev[1], Viktorija Maksimova[2], Dusan Spasov[1]

[1]*Goce Delcev University, Faculty of Agricultural Sciences, Stip, Macedonia*
[2]*Goce Delcev University, Faculty of Medical Sciences, Stip, Macedonia*

Abstract

The latest world trends in scientific research are directed towards the production of secondary metabolites, their use and application. Capsaicin, the pungent principle of hot peppers is one of the best-known natural compounds. Nowadays, research has been focusing the influence of capsaicin on physiological and biochemical processes of humans, animals, and recently plants as a biopesticide. Phytochemical studies of *Capsicum annuum* L. increase the application of secondary metabolites in pharmacy, food technology and medicine. In this paper, the possibilities of utilization of *Capsicum annuum* ssp. *microcarpum* L. for extracting capsaicin and its use as a biopesticide against the green peach aphid *Myzus persicae* Sulz. in pepper culture are summarized. The content of capsaicin was evaluated spectrophotometrically, and the ability of capsaicin for acting as biopesticide was calculated according to Abbott. Results showed that oleoresin from *Capsicum annuum* ssp. *microcarpum* L. and its dilution 1:20 are the most efficient as a biopesticide. From these results we can say that this kind of peppers can be used as a raw material for extraction of capsaicin, because of its high concentration and efficiency.

Keywords: capsaicinoids, ethanol extraction, oleoresin, biopesticides.

Available online at the Journal website: http://www.ache.org.rs/HI/

PROFESSIONAL PAPER

UDC 664.521:615.322:66

Hem. Ind. **67** (4) 671–675 (2013)

doi: 10.2298/HEMIND120921110K

Secondary plant metabolites represent a significant economic group used in different areas such as production of food additives, pigments, pharmacuticals and biopesticides [1]. The most important components in the group of secondary metabolites, derived from the biologically active components of the species *Capsicum annum* L. are the group of alkaloids-capsaicinoids.

Capsaicinoids are derivates of benzylamin. Differences within their structure depend mainly on their acyl moieties, and three structural elements are involved: first, the length of the acyl chain (C8-C13), then the way it terminates (linear, iso or anteiso-series), and the presence or absence of unsaturation at the ω-3(capsaicin type) or ω-4 carbon atom (homocapsaicin type I and II) [2,3].

Capsaicin, a homovanillic acid derivative (8-methyl--*N*-vanillyl-6-nonenamide, Figure 1), is an active component of the red pepper. The level of the capsaicin in the seasonal pepper is around 0.025%, and in the hot pepper around 0.25% [4,5].

It is an extraordinarily versatile agent, and its use in a variety of fields ranges from pharmacology and nutrition to chemical weapons and shark repellence. Capsaicin is represented with 69% in the group of capsacinoids; dihydrocapsacinoids with 22%; nordihydrocapsacinoids with 7%; homocapsaicin and homohydrocapsaicin takes only 1% in the group of capsaicinoids. Capsaicin and dihydrocapsaicin being approximately twice as pungent as nordihydrocapsaicin and homocapsaicin and they are responsible for the hotness of the pepper. The pungency of capsaicinoids and pepper containing preparations can be expressed in Scoville Heat Units (SHU) and the human palate can detect it even diluted in 1:17 000 000 ratio [2,3,6].

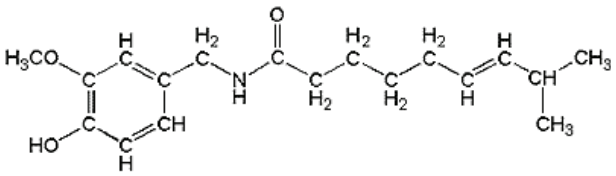

Figure 1. Structural formula of capsaicin.

Because of the antimicrobial capacity of the capsaicin, Walter (1995), for the first time, suggested a protective medium that contains capsaicin, as a base component in the product that belongs to the group of biochemical pesticides. From 1995 onwards, a lot of products have been registered in the EPA (Environmental Protection Agency, USA), insecticides and rodenticides based on capsaicin. In the end of 2001, the EPA registered around 195 active materials as biopesticides and 780 products [7].

Correspondence: V. Maksimova, Goce Delcev University, Faculty of medical sciences, Krste Misirkov str. bb, P.O. Box 201, 2000 Stip, Macedonia.
E-mail: viktorija.maksimova@ugd.edu.mk
Paper received: 21 September, 2012
Paper accepted: 26 November, 2012

Because of great interest and the complex nature of the research aimed to examine the character of the biopesticides, they are categorized into three major classes: microbial pesticides, protective elements, and biochemical pesticides. Biopesticides are natural substances made from herbal extracts or from pheromones from insects, which in the control of the pests have no toxic effect. Capsaicin belongs to the third class of biopesticides [8–10].

It is important to note that capsaicin-containing products have primarily been used to repel insects since ancient times. Literature survey has revealed that capsaicin has lethal and antifeedant effects on various invertebrates, which is another reason why organic farming is directed toward the production of biopesticides [9,11]. The aim of this experiment is to examine the relationship between the concentration of capsaicin and its activity as a biopesticide.

EXPERIMENTAL

Plant material for extraction of capsaicin

Dried fruits of hot pepper *Capsicum annuum* ssp. *microcarpum* L. were used for extraction of capsaicin (Figure 2).

Figure 2. Habitus of hot pepper, Capsicum annuum ssp. microcarpum, in the phase of fruiting.

The seed of the hot peppers from the breed "Bonbona" was taken from the gene bank at the Faculty of Agricultural Sciences, Strumica, Macedonia. The peppers were grown in an open field area, which was situated in the region of Strumica (41°26'15'' NGW and 22°38'35" EGL). They were collected in late September, in the phase of botanical maturity [12]. The fruits were dried in a Binder dryer at a temperature of 50 °C until constant weight. The dried material was powdered in a blender (Gorenje SIC400B).

Plant material for testing the efficiency of capsaicin extraction

The examinations for determining the efficiency of capsaicin as biopesticide were made in closed conditions on another type of pepper culture from the breed Inferno, which was infected with the plant louse of *Myzus persicae* Sulz (Figure 3).

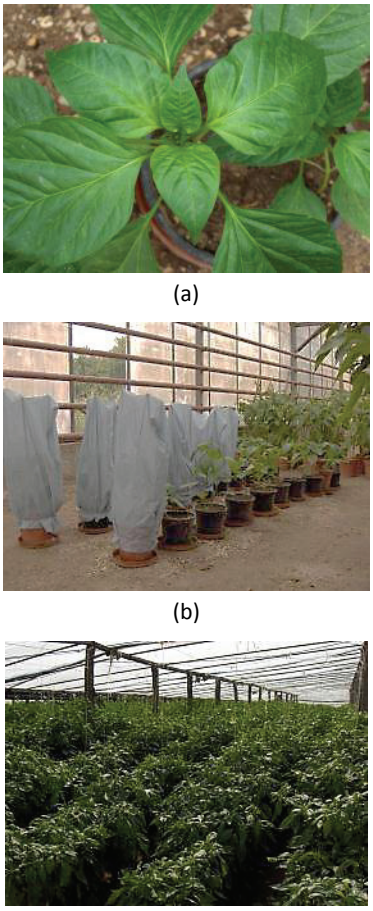

Figure 3. Pepper Capsisum annuum L. breed Inferno grown in a greenhouse under controlled conditions. a) Apical bud of pepper host plant infected with Myzus persicae Sulz.; b) Infected host plants covered with trap bag; c) Pepper production breed Inferno.

The infection was formed on the apical buds of the host plant right before the phase of initial flowering. The initial infection on the hosting plant is given in Figure 3a. In order to enable better and faster development of the plant louse, and also to prevent the spreading of the infection to the other plants, the infected samples were covered with trap bags (Figure 3b). The procedure for controlling the efficiency of the extract of capsaicin was repeated three times on the same infected plants. Infected plants were treated in the period of 14 days after the initial infections. Treated plants were in the phenological phase of full flowering, when the eggs of the plant louse and adult forms of the parasite were noted on the leafs.

In the other case of growing peppers, the presence of plant-louse of *Myzus persicae* Sulz. was also noticed in the early fruiting phase on pepper fruits. These plants were infected without any artificial infection.

The same treatment was used in this case, where capsicum oleoresin and variant 1 and 2 (Table 1) were used as the treatment solution.

Table 1. Capsaicin concentration in oleoresin and its dilutions

Variant	Rate of dilution	Capsaicin concentration, mg/ml
Oleorasin	–	12.2375
1	1:2	6.1187
2	1:10	1.2237
3	1:20	0.6118
4	1:50	0.2447
5	1:125	0.0998
6	1:625	0.0167

Methods of work

Capsicum oleoresin can be prepared from hot peppers using a variety of organic solvents, but ethanol is the only one suitable for obtaining pharmaceutical grade material [3]. The dried and smashed material from hot pepper *Capsicum annuum* ssp. *microcarpum* L. was kept into desiccators and this material was used for obtaining the capsicum oleoresin. Extraction was performed with 96% (v/v) ethanol from dry plant material (0.1–0.5 g of powdered plant material was taken for extraction), in a water bath using a temperature of 40 °C, within a period of 5 h. Then, water vacuum filtration was included in the experiment for obtaining an ethanol extract of capsaicin. The obtained oleoresin had a concentration of 12.712 mg capsaicin/ml extract.

After obtaining the basic oleoresin, six dilutions were made for treatment of the plants (Table 1) with the aim of determining the effects of different concentration of capsaicin in the diluted samples. Dilutions were made ex tempore, before the treatment of infected plants, and sterile distillated water was used as a control.

Capsaicin and analogs were detected at 100 ng level by UV monitoring at 279 nm [8]. The absorbance of capsaicin, in the proper dilutions of the ethanol extract, was measured spectrophotometrically (UV/Vis Varian 50) at a wave length of 281 nm [13].

The standard curve (Figure 4) was made with standard dilution (0.02–0.1 mg/ml) of capsaicin (Sigma), and the coefficient of the linear correlation (Figure 5) was $R^2 = 0.998$ ($y = 9.7734x + 0.1409$).

Testing of the effectiveness of capsaicin as an ecopesticide

The second part of this study, aimed to determine the relationship between content of capsaicin and it use as a biopesticide, was conducted on pepper from the breed Inferno, which was infected with aphis *Myzus persicae* Sulz. Three replicates of the infection were maintained for each concentration along with the control. The evaluation of the efficiency of the active material was based on the number of infected leaves with aphis. The results of the efficiency of the capsaicin as biopesticide were measured in 24 hours, and calculated according to Abbott's formula [14]:

$$\text{Efficiency by Abbott (\%)} = \frac{\text{Test mortality (\%)} - \text{Control mortality (\%)}}{100 - \text{Control mortality (\%)}}$$

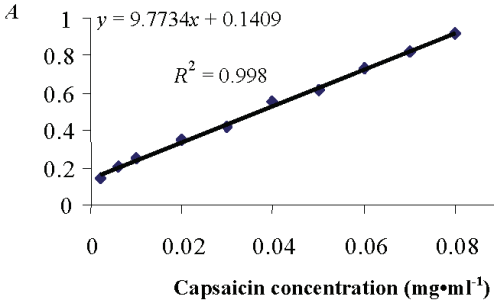

Figure 4. Capsaicin standard curve at 281 nm.

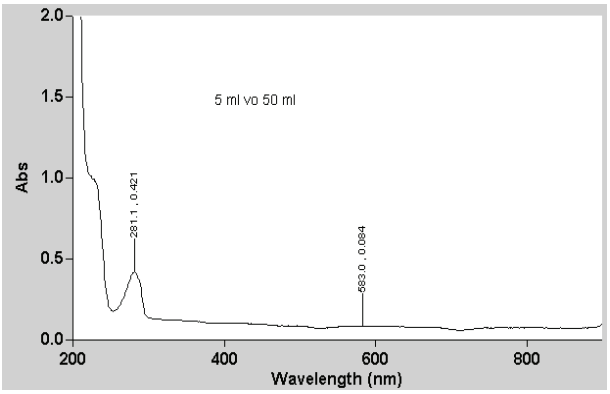

Figure 5. UV/Vis spectra of capsaicin standard (Sigma) with typical peak at 281 nm.

The efficiency of capsicum oleoresin and variant 1 and 2 on the accidentally infected plants in the phase of fruiting was also evaluated as a demonstration of their activity as biopesticides.

RESULTS AND DISCUSSION

The content of capsaicin in the oleoresin dilutions is given in Table 1. As expected, the results confirmed the highest concentration of capsaicin in the oleoresin, and a 700 times lower concentration in the last diluted sample.

The intensity of the aphis attack on the pepper was high, with a large number colonies formed. The treatment of the pepper, with all the research variants, depending on the concentration of the capsaicin in the dilution, gave a different effect (Table 2).

Table 2. Efficiency of the capsaicin in appropriate dilutions according to Abbott after 24 hours of the treatment on the pepper

Variant	No. of leaves infected with Aphids	No. of Aphids before treatment	No. of Aphids after treatment	Control	Efficiency by Abbott, %
Oleorasin	3	132	2	78	97.4
1	3	118	6	66	90.9
2	3	76	5	51	90.1
3	3	77	13	48	72.9
4	3	38	21	36	41.7
5	3	49	13	21	38.1
6	3	37	20	21	4.8

The results obtained in this experiment, once again confirmed concentration/dose dependent increase in larvicidal activity, according to the literature [15]. The largest efficiency in the repression of the aphis on the pepper is observed at oleoresin with 97.4%, where the capsaicin concentration is 12.2374 mg/mL. Its activity drops gradually until the last dilution.

LC_{50} = 0.2934 mg/mL is concentration that is achieved with dilution of 1:50. This means that the concentration of capsaicin in oleoresin and first two dilutions (variants 1 and 2 with efficiency from 97.4–90.1%) is high enough to kill 90% of the insects, and in third variant the concentration is enough to kill 50% of parasites. In the next three variants, dilution is very high and the concentration of the capsaicin is in the range of 0.2447 to 0.0167 mg/mL, so the smallest effect of this dilution is completely understandable. The highest concentration, in contrast with the smallest, is 20.3 times more efficient. From the results it is obviously that capsaicin showed high efficiency with larvicide and adulticide capacity, but only if it is in proper concentration. We can say that the dose and efficiency are linearly dependent (Figure 6) for the first three concentration of capsaicin.

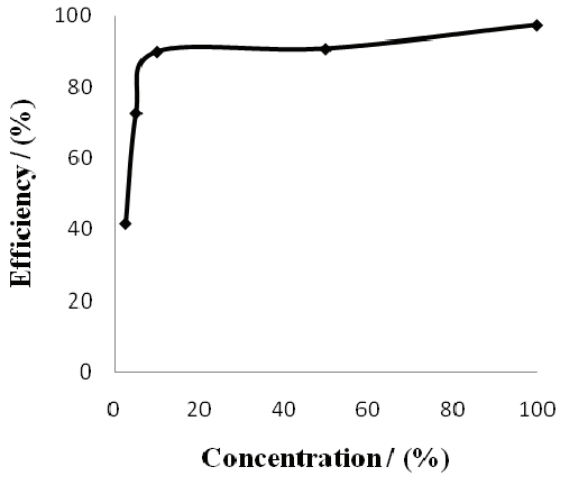

Figure 6. Concentration dependent efficiency of capsaicin against Mayzus persicae Sulz.

CONCLUSION

The everyday use of different types of pesticides makes the aphis *Myzus persicae* Sulz. more resistant to today's products. On the other hand, the written records point to the use of new products as biopesticides in control and repression of pests, especially popular in organic production. This resulted in efforts to find a new natural and safety way to protect plants from insects and parasites.

The experimental results confirmed that the examined pepper contains a high concentration of capsaicin. It can be widely used as material for extracting capsaicin. Its oleoresin can be used as an effective biopesticide along with its dilutions even to the rate of 1:20.

The aim of this study was to make a chemical and insecticide characterization of oleoresin extracted from *Capsicum annuum* ssp. *microcarpum*, giving an emphasis on quantitative information about the concentration of capsaicin in different variants, and correlation with its activity as a biopesticide.

REFERENCES

[1] A. Sasson, Production of useful biochemicals by higher-plant cell cultures: biotechnological and economic aspects, CHIEAM, Options Mediterraneennes **14** (1991) 59–74.

[2] A. Brossi, The alkaloids, Chemistry and pharmacology, Academic Press, Orlando, FL, 1984, pp. 228–286.

[3] E. Fattorusso, O.Taglialatela-Scafati, Modern alkaloids: structure, isolation, synthesis and biology, Wiley, Weinheim, 2008, pp. 73–104.

[4] B. Lazić, Povrtarstvo, Paprika (*Capsicum annuum* L.), Poljoprivredni fakultet, Univerzitet u Novom Sadu, Jugoslavija, 1995 (in Serbian).

[5] P. Holzer, Capsaicin: cellular targets, mechanisms of action, and selectivity for thin sensory neurons. Pharmacol. Rev. **43** (1994) 143–201.

[6] D. De Witt, The nature of capsaicin, The Chile Pepper Encyclopedia, HarperCollins Publishers, New York, 1999.

[7] Environmental Protection Agency, USA, http:// //www.epa.gov/

[8] T. Aniszewski, Alkaloids-secrets of life: Alkaloid Chemistry, Biological Significance, Applications and Ecological Role, Elsevier, Amsterdam, 2007, pp. 205–214.

[9] R.K. Sinha, G. Hahn, P.K. Singh, R.K. Suhane, A. Anthonyreddy, Organic Farming by Vermiculture: Producing Safe, Nutritive and Protective Foods by Earthworms, Am. J. Exp. Agric. **1**(4) (2011) 363–399.

[10] W.R. Walter, Wax and Capsaicin based pesticide, Wilder Agricultural Product Co Inc., New Wilmington, PA, 1995.

[11] A.P. Madhumathy, A.-A. Aivazi, V.A. Vijayan, Larvicidal efficacy of *Capsicum annum* against *Anopheles stephensi* and *Culex quinquefasciatus*, J. Vect. Borne Dis. **44** (2007) 223–226.

[12] V.S. Govindarajan,. Capsicum – production, technology, chemistry and quality – Part I. Botany, cultivation and primary processing, CRC Cr. Rev. Food Sci. **22**(2) (1985) 109–176.

[13] V.S. Govindarajan, Capsicum- production, technology, chemistry and quality – Part II. Processed products, standards world production and trade, CRC Cr. Rev. Food Sci. **23**(3) (1985) 207–288.

[14] W.S. Abbott, A method of computing the effectiveness of an insecticide, J. Econ. Entomol. **18** (1925) 265–267.

[15] P.M.E. Ubulom, N.G. Imandeh, C.E. Udobi, I. Ilya, Larvicidal and Antifungal Properties of *Picralima nitida* (Apocynaceae) Leaf Extracts, Eur. J. Med. Plants **2**(2) (2012) 132–139.

IZVOD

SADRŽAJ KAPSAICINA U LJUTOJ PAPRICI (*Capsicum annuum* ssp. *microcarpum* L.) I NJEGOVA PRIMENA KAO BIOPESTICIDA

Liljana Koleva Gudeva[1], Sasa Mitrev[1], Viktorija Maksimova[2], Dusan Spasov[1]

[1]*Goce Delcev University, Faculty of Agricultural Sciences, Stip, Macedonia*
[2]*Goce Delcev University, Faculty of Medical Sciences, Stip, Macedonia*

(Stručni rad)

Alkaloidi dugo vremena predstavljaju predmet istraživanja u organskoj hemiji i farmakologiji, zbog svoje biološke i fiziološke aktivnosti uslovljene hemijskom strukturom. Kapsaicinoidi su grupa alkaloida, koji se javljaju kao kompleksne mešavine acil konjugata na vanilamin u rodu *Capsicum*. U ovom eksperimentu je korišćena vrsta paprike *Capsicum annuum* ssp. *microcarpum* koja predstavlja jednu od najljućih sorti koje se proizvode u Makedoniji. Iz paprike je izolovan kapsaicin, čija je koncentracija određivanja spektrofotometrijski. Uzimajući u obzir da je u poslednje vreme malo podataka o kapsaicinu kao biopesticidu, u radu je ispitan uticaj kapsaicina, kao i njegove koncentracije, na larve i adultne parazitske organizme *Myzus periceae* Sulz. Rezultati istraživanja su pokazali da je capsaicin efikasan biopesticid protiv *Myzus periceae* Sulz., jer je LC_{50} = 0,2934 mg/ml, i da je njegova aktivnost direktno zavisna od koncentracije. Najveća aktivnost kapsaicina kao biopesticida je u opsegu koncentracija od 1,2237 do 12,2375 mg/ml, pri kojima se postiže efikasnost od 90,1-97,0%. Dobijeni rezultati opravdavaju upotrebu ove vrste paprike kao sirovine za ekstrakciju kapsaicina, kao i upotrebu kapsaicina kao biopesticida za navedenu vrstu organizama.

Ključne reči: Kapsaicinoidi • Ekstrakcija etanolom • Oleoresin • Biopesticidi

Rhamnolipid and lipase production by *Pseudomonas aeruginosa* san-ai: The process comparison analysis by statistical approach

Sonja M. Jakovetić[1], Zorica D. Knežević-Jugović[1], Sanja Ž. Grbavčić[2], Dejan I. Bezbradica[1], Nataša S. Avramović[3], Ivanka M. Karadžić[3]

[1]*University of Belgrade, Faculty of Technology and Metallurgy, Belgrade, Serbia*
[2]*University of Belgrade, Faculty of Technology and Metallurgy, Innovation Center, Belgrade, Serbia*
[3]*University of Belgrade, School of Medicine, Belgrade, Serbia*

Abstract

Pseudomonas aeruginosa has been repeatedly reported as a powerful producer of rhamnolipid biosurfactants as well as hydrolytic enzymes. In this study, the effects of four fermentation factors were evaluated using response surface methodology and experiments were performed in accordance with a four-factor and five-level central composite experimental design. The investigated factors were: fermentation temperature, time of fermentation, concentration of sunflower oil and concentration of Tween® 80. The most important finding was that regression coefficients of the highest values were those that describe interactions between factors and that they differ for lipase and rhamnolipid production, which were both investigated in this study. Production of both metabolites was optimized and response equations were obtained, making it possible to predict rhamnolipid concentration or lipase activity from known values of the four factors. The highest achieved rhamnolipid concentration and lipase activity were 138 mg dm^{-3} (sunflower oil concentration: 0.8%, Tween® 80 concentration: 0.05%, temperature: 30 °C and fermentation time: 72 h) and 11111 IU dm^{-3} (sunflower concentration: of 0.4%, Tween® 80 concentration: 0.05%, temperature: 30 °C and fermentation time: 120 h), respectively.

Keywords: *Pseudomonas aeruginosa*, rhamnolipid, lipase, response surface methodology.

Available online at the Journal website: http://www.ache.org.rs/HI/

SCIENTIFIC PAPER

UDC 579:577.115:66

Hem. Ind. **67** (4) 677–685 (2013)

doi: 10.2298/HEMIND121008114J

Pseudomonas aeruginosa is a gram-negative opportunistic pathogen, known for its ability to survive in a wide range of habitats such are water, plants, oil, etc. This ubiquitous environmental bacterium produces and secrets numerous virulence factors which conduce to its high environmental adaptability [1,2]. Humans, animals, plants, nematodes, amoebae are all prone to infections with *P. aeruginosa*, and all virulence factors take place in processes of infection initiation or establishment [3–5].

Pseudomonas aeruginosa san-ai strain was isolated from water-soluble, rancid mineral cutting oil utilized as an aid for cooling and lubrication in metalworking processes [6–9]. This water-soluble cutting oil is mixture of surfactants and mineral oils with high alkaline pH (pH 10), which makes it unaccommodating for bacterial growth [8]. Nevertheless, *P. aeruginosa* san-ai strain has the ability to survive in these extreme conditions owing to its potential to product enzymes with very distinct properties [8]. Extracellular hydrolytic enzymes produced by this strain have been proven to have exceptional properties suitable for several biotechnological applications. These enzymes are especially interesting for application in detergent formulations and, therefore, have been tested for stability in presence of several oxidizing agents and commercial surfactants [6,7]. These enzymes have already been characterized and it has been known that protease exhibits optimal behavior in alkaline environment, pH 9, and at 60 °C, while lipase shows optimal behavior at pH 11 and 70 °C [8,9].

In addition, other than highly applicable hydrolytic enzymes, *Pseudomonas aeruginosa* strains also produce surface-active compounds known as rhamnolipids. This was firstly reported by Jarvis *et al.* more than sixty years ago, but the chemical nature of these biosurfactants was not elucidated [10]. Nowadays, it is known that *P. aeruginosa* strains produce primarily two forms of rhamnose containing glycolipids: mono-rhamnolipid (rhamnosyl-β-hydroxydecanoyl-β-hydroxydecanoate) and di-rhamnolipid (rhamnosyl-rhamnosyl-β--hydroxydecanoyl-β-hydroxydecanoate) [11–13].

During the last twenty years, numerous efforts have been made with purpose of increasing yield of rhamnolipid production by *Pseudomonas* species, since various areas of their application emerged. Predominantly, rhamnolipids and modified rhamnolipids are applied instead of chemical surfactants due to biodegradability and non-toxicity of rhamnolipids. Additionally, the pos-

Correspondence: Z.D. Knežević-Jugović, Faculty of Technology and Metallurgy, University of Belgrade, Karnegijeva 4, 11000 Belgrade, Serbia.
E-mail: zknez@tmf.bg.ac.rs
Paper received: 8 October, 2012
Paper accepted: 16 November, 2012

sibility of their application in bioremediation, food industry, and in the production of fine chemicals has been reported [11,14,15]. Recently, rhamnolipids were proved to have antimicrobial, anti-adhesive and immunomodulating properties making them worth for further research in biomedical area [15].

The main obstacles for substitution of synthetic surfactants by biosurfactants are high production costs of biosurfactants, related with complex process control due to foam formation during fermentation and expensive downstream processing [16]. Therefore, the main goal of majority of studies focused on rhamnolipid production is selection of appropriate carbon and nitrogen source, which allows high yields and reduction of a number of downstream processing steps. Literature data reveal the most diverse list of carbon sources tested in rhamnolipid production by *P. aeruginosa* strains including different vegetable oils (soybean, olive, sunflower and corn) as well as petrochemicals, such as diesel and kerosene [17–21]. In order to decrease production costs, several authors have proposed an alternative strategy, featuring the development of technologies based on cheap waste carbon sources, which are usually a significant environmental problem. A waste fraction from soybean oil refining process, frying oil waste, molasses from sugarcane refining, soap stock from oil refining, whey from dairy industry, spent wash as distillery waste, crude glycerol from vegetable oil industries were all successfully employed in rhamnolipid production as carbon sources [17,22-28]. Rhamnolipid production is also very dependent on carbon/nitrogen ratio in growth medium, and it could be significantly improved by optimization of these factors [22].

The aim of this study was the optimization of process factors for production of two principal metabolites, namely rhamnolipid and lipase, using multifactorial experimental design and response surface methodology (RSM). The effects of several fermentation factors on rhamnolipid and lipase production were investigated including temperature, fermentation time, concentration of sunflower oil and concentration of Tween® 80. Application of experimental design facilitates optimization process and on the other hand, it provides information regarding effects of each experimental factor as well as their interactions. Another aim of this research was to understand the interaction of rhamnolipid production with lipase production and to find a correlation between these outputs.

EXPERIMENTAL

Chemicals and bacterial strain

Growth medium components were purchased from Torlak, Institute of Immunology and Virology, Serbia. Surfactant Tween® 80, *p*-nitrophenyl palmitate (*p*-NPP), and orcinol were obtained from Sigma, St. Luis, CA. *P. aeruginosa* san-ai strain was isolated from mineral oil used in metalworking processes. This strain was originally isolated in San-ai Oil (Tokyo) and it was provided to us by the courtesy of Dr. N. Fujiwara (Technology Research Institute of Osaka Prefecture, Osaka, Japan). Agar slant used for microorganism maintenance consisted of peptone I (10 g dm^{-3}), yeast extract (5 g dm^{-3}), NaCl (5 g dm^{-3}) and agar (15 g dm^{-3}) at it was kept at 4 °C.

Fermentation

P. aeruginosa san-ai was cultivated at 30 °C for 24 h with shaking (250 rpm) in tryptic soy broth, which was prepared in accordance with the instructions provided by the manufacturer.

Growth medium used for *P.aeruginosa* san-ai cultivation was LB medium comprising peptone (10 g dm^{-3}), NaCl (5 g dm^{-3}), and yeast extract (5 g dm^{-3}). Fermentations were carried out in Erlenmeyer flasks on a horizontal shaker (Kühner, Switzerland), set at 250 rpm and temperature predetermined by the experimental plan. During the fermentation, samples were taken, in sterile conditions, from the liquid culture to monitor rhamnolipid concentration, and lipase activity.

Lipase activity assay

Determination of lipase activity was conducted using *p*-nitrophenyl palmitate method (*p*-NPP), which is based on spectrophotometric measurement of *p*-nitrophenol released in enzymatic hydrolysis of *p*-NPP. The substrate was prepared by dissolving 30 mg of *p*-NPP in 10 cm^3 of isopropanol and 90 cm^3 of 50 mmol dm^{-3} phosphate buffer (pH 8). Prior to spectrophotometric measurement both substrate and enzyme were incubated at 37 °C. Lipase solution, 0.1 and 0.9 cm^3 of substrate were mixed directly in spectrophotometric cuvette and absorbance was measured at 410 nm during the first 3 min of reaction. One unit of lipase activity (IU) was defined as the amount of lipase that released 1 μmol of *p*-nitrophenol per minute (ε = 1500 $dm^3\ mol^{-1}\ cm^{-1}$) under the conditions defined in the assay [6,9].

Determination of rhamnolipid concentration

The concentration of rhamnolipids, glycolipids secreted by *P. aeruginosa* san-ai, in the bacterial culture supernatant was evaluated by measuring the concentration of hydrolysis-released rhamnose by the orcinol method, which has been previously described [5,29].

Experimental design

The effects of four fermentation parameters on lipase activity and rhamnolipid production by *P. aeruginosa* san-ai were investigated using a five-level-four-factor central composite rotatable experimental design.

The experimental design included 30 experimental points, which consisted of 16 factorial points, 8 axial points and 6 central points [30]. Based on the preliminary study and literature survey, four experimental factors were analyzed in given ranges: sunflower oil concentration (0.2–1% (w/v)); Tween® 80 concentration (0–0.2% (w/v)); temperature (20–60 °C), and incubation time (48–144 h). The relation between actual values and coded values are given in Table 1.

Experimentally obtained data were fitted using the following equation:

$$Y = \beta_{k0} + \sum_{i=1}^{4} \beta_{ki} X_i + \sum_{i=1}^{4} \beta_{kii} X_i^2 + \sum_{i=1}^{3} \sum_{j=i+1}^{4} \beta_{kij} X_i X_j \quad (1)$$

where Y is the response variable, in our case rhamnolipid concentration (mg dm^{-3}) or lipase activity (IU dm^{-3}), β_{k0}, β_{ki}, β_{kii} and β_{kij} are the regression coefficients variables, for the intercept, linear, quadratic and interaction terms, respectively, and X_i and X_j are independent variables. The least square method was used both for the response function coefficients calculation and evaluation of their statistical significance. Fisher test was used to evaluate adequacy of model, and Student distribution was used to evaluate the significance of the coefficients.

RESULTS AND DISSCUSSION

Pseudomonas aeruginosa san-ai strain has already been established as an efficient producer of extracellular hydrolytic enzymes [6–9]. Nevertheless, *Pseudomonas aeruginosa* strains have been known as producers of rhamnolipids, microbial surfactants that deserve at least equal attention due to increasing areas for their utilization.

RSM Analysis: Influence of fermentation factors on rhamnolipid production

The main goal of this study was to ameliorate the lipase production as well as rhamnolipid production by *P. aeruginosa* san-ai and to establish the most influential fermentation factors and their correlations. The data showing the lipase activity and rhamnolipid concentration for the 30 experiments conducted according to the experimental design are presented in Table 2.

Among the various treatments, the highest rhamnolipid concentration (138 mg dm^{-3}) was achieved in experiment no. 2 (sunflower oil concentration 0.8%, Tween® 80 concentration 0.05%, temperature 30 °C, and fermentation time 72 h), while the highest lipase activity (11111 IU dm^{-3}) was achieved in run no. 12 (sunflower concentration of 0.4%, Tween® 80 concentration of 0.05%, temperature of 30 °C, and fermentation time of 120 h). The experimental results were fitted with a second order regression model which included interaction of factors. The regression coefficients were determined using least square method and following regression model was obtained:

$$\begin{aligned} Y = {} & 11.42 + 4.66X_1 - 8.86X_2 - 2.30X_3 + 2.24X_4 - \\ & - 8.07X_1X_2 - 18.2X_1X_3 - 22X_1X_4 + 13.5X_2X_3 + \\ & + 1.86X_2X_4 + 10.9X_3X_4 + 6.66X_1^{\,2} + 5.58X_2^{\,2} + \\ & + 5.82X_3^{\,2} + 5.54X_4^{\,2} \end{aligned} \quad (2)$$

Equation (2) represents quantitative effects of process variables and their interactions on the response, which is in this case rhamnolipid concentration (mg dm^{-3}).

After statistical analysis of experimental results and results obtained by the regression model, the Fischer test of 3.0779 was obtained. Since this value is lower than table values for adequate degree of freedom, obtained regression model can be used for describing obtained experimental results. The analysis of obtained regression coefficients implies that significant interaction between effects of experimental factors occurred. The coefficient of highest value (coefficient –18.24) is the one that describes negative interaction between sunflower oil concentration and temperature. The influence of these factors on rhamnolipid concentration, under fixed values of other factors, is presented in Figure 1.

It can be easily observed that temperature exhibits mild positive effect on rhamnolipid production at lowest oil concentration. On the other hand, at the highest examined oil concentration (1%), a steep decrease of the yield of rhamnolipids occurred with the temperature rise. Hence, maximum rhamnolipid concentration was obtained at maximum sunflower oil concentration and minimum temperature. This is correlated with a higher lipase activity produced at high sunflower concentration and low temperature (Table 2, experiments No. 10 and 12). These results cannot be simply

Table 1. Experimental and coded values of fermentation factors

Experimental factor	Coded values				
	–2	–1	0	1	2
X_1, Sunflower oil conc., % (w/v)	0.2	0.4	0.6	0.8	1
X_2, Tween® 80 conc., % (v/v)	0	0.05	0.1	0.15	0.2
X_3, Temperature, °C	20	30	40	50	60
X_4, Time, h	48	72	96	120	144

Table 2. Experimental design

Run No.	Sunflower oil	Tween® 80	*t* / °C	Time, h	Lipase activity, IU dm^{-3}	Rhamnolipid concentration, mg dm^{-3}
1	–1	–1	–1	–1	533.34	47.17
2	1	–1	–1	–1	155.56	138.06
3	–1	1	–1	–1	544.44	5.46
4	1	1	–1	–1	166.67	40.78
5	–1	–1	1	–1	0	25.39
6	1	–1	1	–1	0	18.00
7	–1	1	1	–1	0	40.72
8	1	1	1	–1	0	17.46
9	–1	–1	–1	1	7377.8	30.65
10	1	–1	–1	1	10844	87.42
11	–1	1	–1	1	7422.2	0
12	1	1	–1	1	11111	40.11
13	–1	–1	1	1	0	44.91
14	1	–1	1	1	0	55.70
15	–1	1	1	1	0	65.70
16	1	1	1	1	0	27.19
17	–2	0	0	0	33.33	20.79
18	2	0	0	0	22.22	0
19	0	–2	0	0	0	12.26
20	0	2	0	0	0	0.53
21	0	0	–2	0	2288.9	1.33
22	0	0	2	0	0	24.25
23	0	0	0	–2	0	0
24	0	0	0	2	111.11	21.99
25	0	0	0	0	19.82	23.59
26	0	0	0	0	22.22	0
27	0	0	0	0	26.73	0
28	0	–1	–1	–1	21.54	0
29	0	–1	–1	–1	28.21	4.66
30	0	1	–1	–1	22.22	37.31

explained since the control of both rhamnolipids and lipase production is complex, influencing by numerous factors at both genetic control and environmental/nutritional levels. It is well known that production of the biosurfactant is subjected to cell density-dependent regulation and limitation of specific nutrients. The rhamnolipid synthesis is positively controlled in a cell-density manner by a cell-to-cell communication system called quorum sensing (QS) [31,32]. It might be plausible that under suboptimal conditions for the cell growth (higher temperature and high oil concentration), the suppressed cell growth had negative effects on QS regulation.

Significant positive interaction between Tween® 80 concentration and temperature (coefficient 13.5) was also observed. The influence of these factors on rhamnolipid concentration, under fixed values of other factors, is presented in Figure 2. At high Tween® 80 concentration the effect of temperature seemed to be negligible. Nevertheless, at low Tween® 80 concentration positive interaction triggered a steep increase of rhamnolipid concentration with decrease of fermentation temperature.

Concentrations of sunflower oil and Tween® 80 have shown a negative interaction (coefficient -8.068) and the influence of these factors is illustrated in Figure 3. At low oil concentrations, as well as at high Tween® 80 concentrations the influence of other factor is very mild. Nevertheless, at highest oil concentrations the effect of surfactant is more intensive, leading to steep increase of rhamnolipid production with the decrease of Tween® 80 concentration.

Model proposed that maximum rhamnolipid concentration of 270 mg dm^{-3}, is achieved when the highest sunflower oil concentration was used. Reports on rhamnolipid production indicate that rhamnolipid concentrations obtained in large scale batch bioreactors (30 dm^3) exceed up to 100 folds those obtained in the

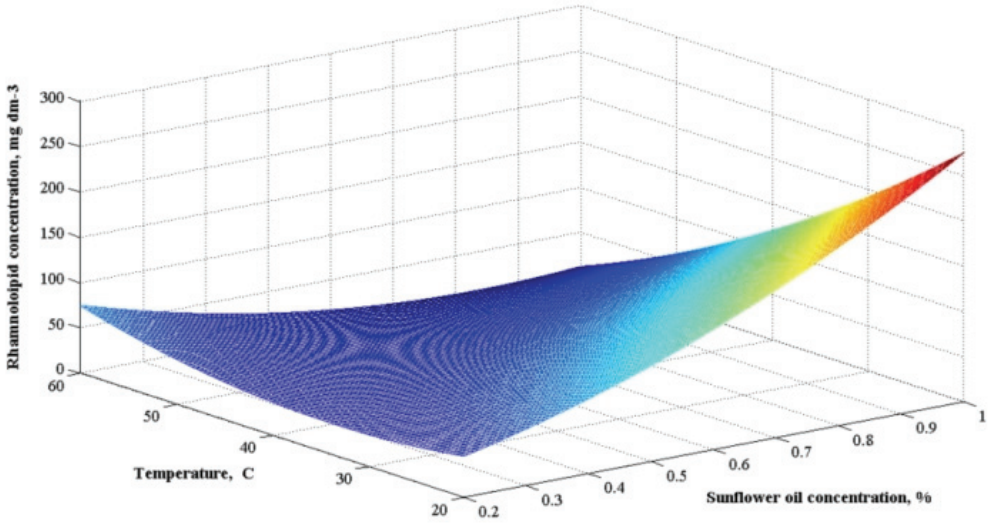

Figure 1. The effect of sunflower oil concentration and fermentation temperature on rhamnolipid production.

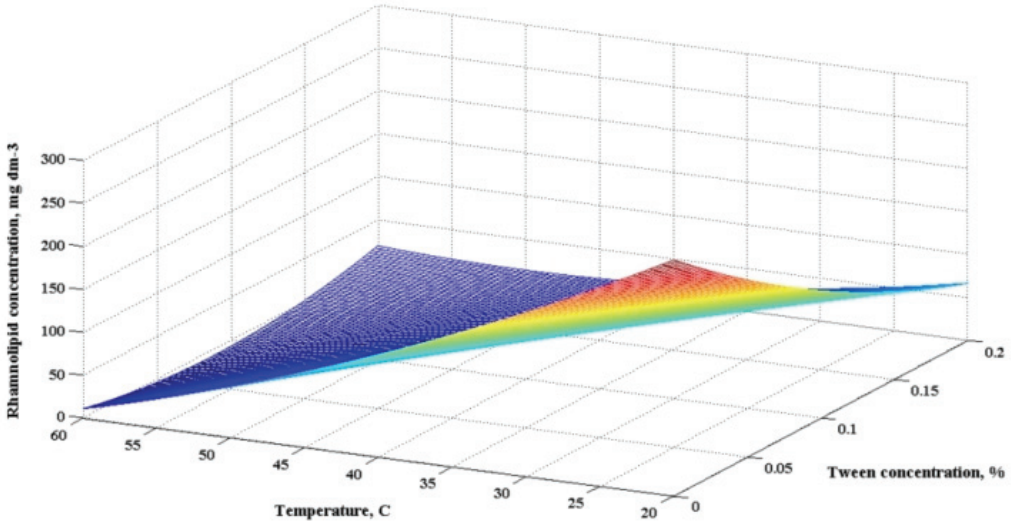

Figure 2. The effect of Tween® 80 concentration and fermentation temperature on rhamnolipid production.

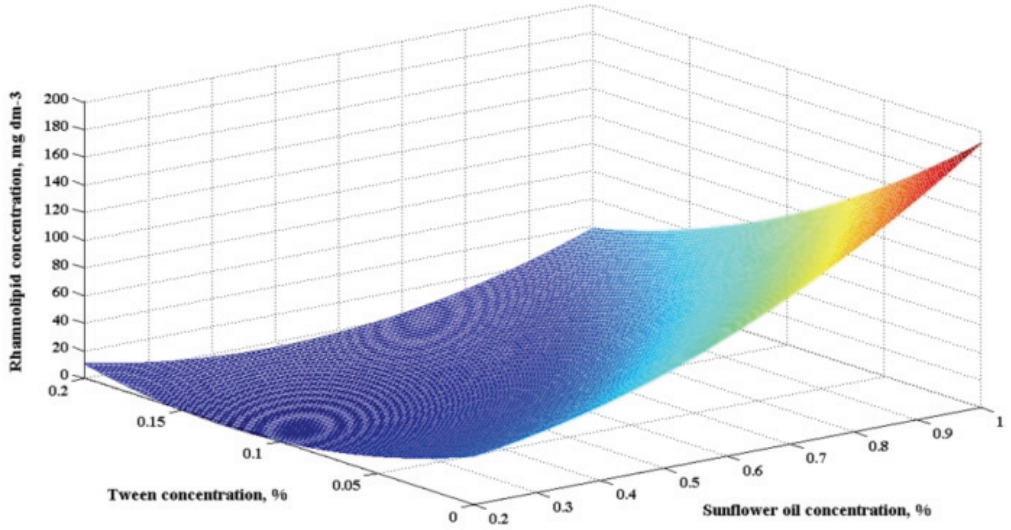

Figure 3. The effect of Tween® 80 concentration and oil concentration on rhamnolipid production.

shake flasks with the same strains [20]. This could be an explanation for relatively low rhamnolipid concentrations obtained in this experiment comparing to literature data. Müller *et al.* [20] reported rhamnolipid concentration of 39 g dm^{-3} after 90 h in bioreactor, while the highest concentration of rhamnolipid obtained with the same strain in shake flask was 2.2 g dm^{-3}. Martínez--Toledo *et al*. [33] recently reported usage of RSM for improving of biosurfactant production by *Pseudomonas putida*. Reported rhamnolipid concentrations were almost 5-fold lower than those obtained in this study.

RSM Analysis: Influence of fermentation factors on lipase activity

Unlike rhamnolipid production, the most relevant variables for the lipase production appear to be temperature and incubation time. The effect of temperature incubation time interaction was the most significant ($p < 0.05$). While incubation time had a positive effect (coefficient 1484), temperature and incubation time-temperature interaction had a significant negative influence on lipase production (coefficients of –1788 and –2220, respectively). The final response equation obtained after eliminating the insignificant terms was as follows:

$$Y = -1782X_3 + 650X_3^2 - 2220X_3X_4 + 1484X_4 + 378X_4^2 \quad (3)$$

where Y presents predicted response (IU dm^{-3}) and other variables have been previously defined.

Proposed model excludes sunflower oil and Tween® 80 concentrations as statistically insignificant although the preliminary study showed their favorable effect on lipase production (unpublished results). Some considerations should be made in the terms of these predictions. This model incorporates a greater number of lipase production curves over an appreciably wide temperature range, including some temperature values highly inimical to the growth of *Pseudomonas* spp. [34]. The inclusion in our model of a considerable amount of data from environmental conditions that adversely affect growth may have the diminishing effect on the importance of medium constituents, sunflower oil and Tween® 80.

Results obtained mathematically confirmed the experimental results regarding an inverse relationship between the influence of temperature and fermentation time on lypolytic activity. The shape of the three-dimensional surface-representing lipase activity *versus* temperature and incubation time is shown in Figure 4.

In addition, contour plot was also generated which delineates predicted response over a range in the design surface (Figure 5). It appears that the surface is smooth, showing increase/decrease in one axis and decrease/increase in the other axis, which reflect that the temperature may affect lipase production in opposite ways. In particular, the lipase activity increased as the temperature increased at initial period. For example, as the temperature increased from 20 to 60 °C, the lipase activity increased from minor to 6460 IU dm^{-3} at 48 h. At intermediate and high levels of incubation period, however, different behavior was observed as the surface decreased when the reaction temperature increased. Such influence could be explained due to the heat sensitivity of lipase-synthesizing reactions or lipase inactivation by the simultaneously produced proteases [6].

CONCLUSION

Pseudomonas aeruginosa san-ai has been proven to be a producer of hydrolytic enzymes with properties

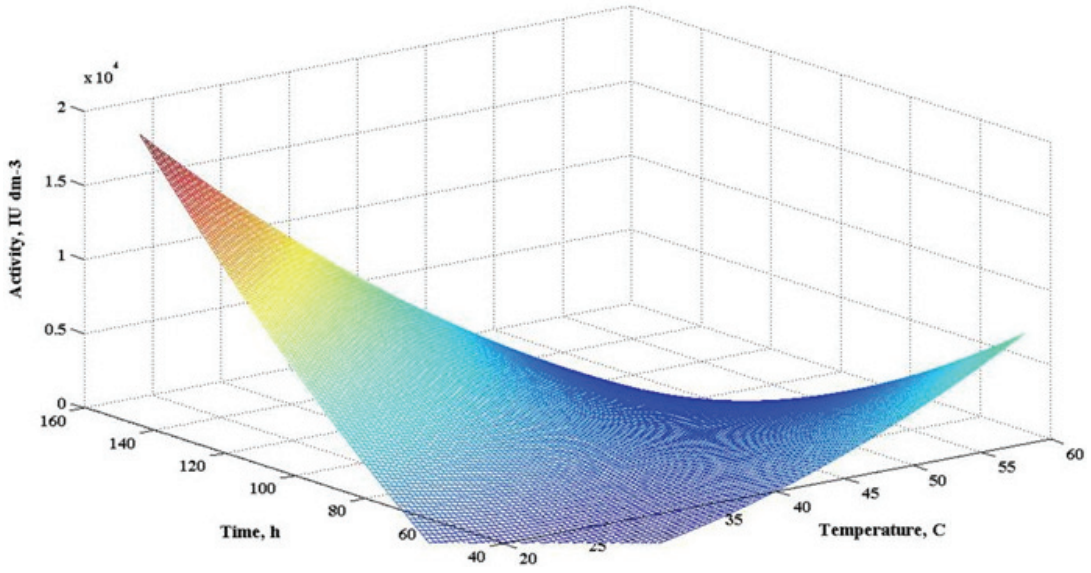

Figure 4. The effect of temperature and fermentation time on lipase activity.

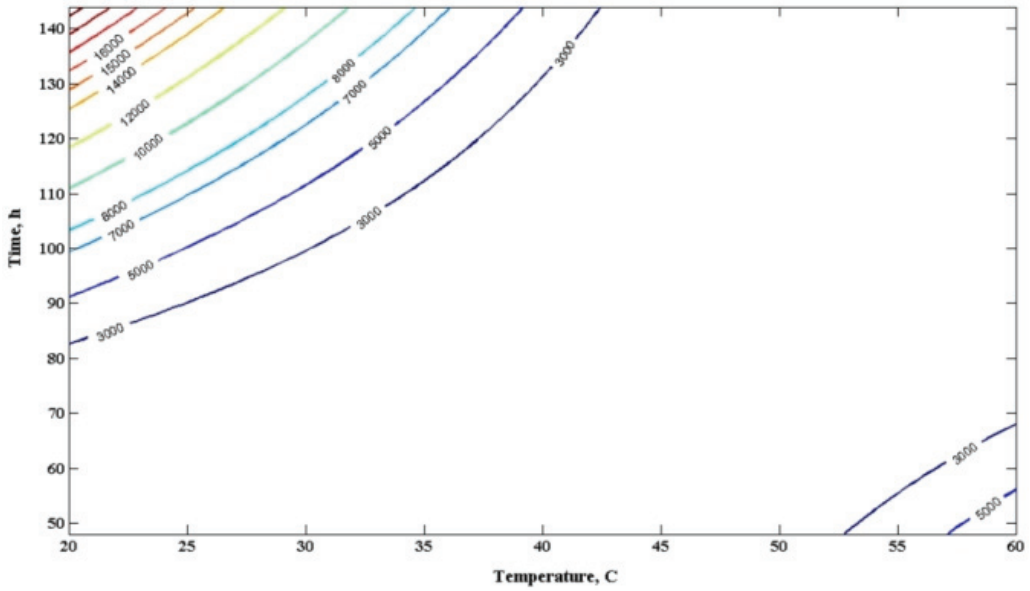

Figure 5. Isoresponse contour plot for lipase activity.

interesting for several biotechnological applications. Although an efficient producer of proteolytic and lypolytic enzymes, this strain was previously poorly understood as a producer of rhamnolipids, microbial surfactants characteristic for *Pseudomonas* spp. [35].

The most important finding of this research related to rhamnolipid production was that regression coefficients of highest values were those that describe interactions between factors.

Negative interaction between sunflower oil concentration and temperature is the most noticeable at high sunflower oil concentrations, when rhamnolipid concentration has steep fall with temperature increasing. On the other hand, temperature and Tween® 80 showed positive interaction, which was most evident in the fermentations with low Tween® 80 concentrations, when the decrease of temperature led to a sudden increase in rhamnolipid concentration. Negative interaction between sunflower oil and Tween® 80 concentrations was obvious at fermentations with high sunflower oil concentrations where the decrease of Tween® 80 concentration caused an increase in rhamnolipid production. Summarizing these findings, rhamnolipid production appeared to be stimulated with high sunflower oil concentrations, and diminished when surfactants were present in the growing medium and at high temperatures.

On the other hand, for lipase production, only temperature and incubation time were shown as significant among four tested fermentation factors.

Acknowledgements

This work was supported by Grant numbers E!6750 and III 46010 from The Ministry of the Education and Science and Technological Development, Republic of Serbia.

REFERENCES

[1] G. Girard, G.V. Bloemberg, Central role of quorum sensing in regulating the production of pathogenicity factors in *Pseudomonas aeruginosa*, Future Microbiol. **3** (2008) 97–106.

[2] R.S. Reis, A.G. Pereira, B.C. Neves, D.M.G. Freire, Gene regulation of rhamnolipid production in *Pseudomonas aeruginosa* – A review, Bioresour. Technol. **102** (2011) 6377–6384.

[3] P. Cosson, L. Zulianello, O. Join-Lambert, F. Faurisson, L. Gebbie, M. Benghezal, C. Van Delden, L.K. Curty, T. Kohler, *Pseudomonas aeruginosa* virulence analyzed in a *Dictyostelium discoideum* host system, J. Bacteriol. **184** (2002) 3027–3033.

[4] E. Potvin, D.E. Lehoux, I. Kukavica-Ibrulj, K.L. Richard, F. Sanschagrin, G.W. Lau, R.C. Levesque, In vivo functional genomics of *Pseudomonas aeruginosa* for high-throughput screening of new virulence factors and antibacterial targets, Environ. Microbiol. **5** (2003) 1294–1308.

[5] S. Wilhelm, A. Gdynia, P. Tielen, F. Rosenau, K. Jaeger, The autotransporter esterase EstA of *Pseudomonas aeruginosa* is required for rhamnolipid production, cell motility and biofilm formation, J. Bacteriol. **189** (2007) 6695–6703.

[6] S. Grbavčić, D. Bezbradica, L. Izrael-Živković, N. Avramović, N. Milosavić, I. Karadžić, Z. Knežević-Jugović, Production of lipase and protease from an indigenous *Pseudomonas aeruginosa* strain and their evaluation as detergent additives: Compatibility study with detergent ingredients and washing performance, Bioresour. Technol. **102** (2011) 11226–11233.

[7] S.Ž. Grbavčić, I.M. Karadžić, Z.D. Knežević-Jugović, Lipaze i proteaze dobijene iz ekstremofilne *Pseudomonas aeruginosa* vrste kao aditivi u formulacijama deterdženata, Hem. Ind. **63** (2009) 331–335 (in Serbian).

[8] I. Karadžić, A. Masui, N. Fujiwara, Purification and characterization of a protease from *Pseudomonas aeruginosa* grown in cutting oil, J. Biosci. Bioeng. **98** (2004) 145–152.

[9] I. Karadžić, A. Masui, L.I. Živković, N. Fujiwara, Purification and characterization of an alkaline lipase from *Pseudomonas aeruginosa* isolated from putrid mineral cutting oil as component of metalworking fluid, J. Biosci. Bioeng. **102** (2006) 82–89.

[10] F.G. Jarvis, M.J. Johnson, A Glyco-lipide Produced by *Pseudomonas aeruginosa*, J. Am. Chem. Soc. **71** (1949) 4124–4126.

[11] R.M. Maier, G. Soberón-Chávez, *Pseudomonas aeruginosa* rhamnolipids: biosynthesis and potential applications, Appl. Microbiol. Biotechnol. **54** (2000) 625–633.

[12] A. Abdel-Mawgoud, F. Lépine, E. Déziel, Rhamnolipids: diversity of structures, microbial origins and roles, Appl. Microbiol. Biotechnol. **86** (2010) 1323–1336.

[13] G. Soberón-Chávez, R. Maier, in: G. Soberón-Chávez (Ed.), Biosurfactants: A General Overview Biosurfactants, Springer, Berlin, 2011, pp. 1–11.

[14] T.T. Nguyen, N.H. Youssef, M.J. McInerney, D.A. Sabatini, Rhamnolipid biosurfactant mixtures for environmental remediation, Water. Res. **42** (2008) 1735–1743.

[15] I. Banat, A. Franzetti, I. Gandolfi, G. Bestetti, M. Martinotti, L. Fracchia, T. Smyth, R. Marchant, Microbial biosurfactants production, applications and future potential, Appl. Microbiol. Biotechnol. **87** (2010) 427–444.

[16] M. Heyd, A. Kohnert, T.H. Tan, M. Nusser, F. Kirschhöfer, G. Brenner-Weiss, M. Franzreb, S. Berensmeier, Development and trends of biosurfactant analysis and purification using rhamnolipids as an example, Anal. Bioanal. Chem. **391** (2008) 1579–1590.

[17] Y.-H. Wei, C.-L. Chou, J.-S. Chang, Rhamnolipid production by indigenous *Pseudomonas aeruginosa* J4, Biochem. Eng. **27** (2005) 146–154.

[18] L.M. Prieto, M. Michelon, J.F.M. Burkert, S.J. Kalil, C.A.V. Burkert, The production of rhamnolipid by a *Pseudomonas aeruginosa* strain isolated from a southern coastal zone in Brazil, Chemosphere **71** (2008) 1781–1785.

[19] M.M. Müller, J.H. Kügler, M. Henkel, M. Gerlitzki, B. Hörmann, M. Pöhnlein, C. Syldatk, R. Hausmann, Rhamnolipids—Next generation surfactants?, J. Biotechnol. **162** (2012) 366–380.

[20] M. Müller, B. Hörmann, C. Syldatk, R. Hausmann, *Pseudomonas aeruginosa*PAO1 as a model for rhamnolipid production in bioreactor systems, Appl. Microbiol. Biotechnol. **87** (2010) 167–174.

[21] T. Hembach, Untersuchungen zur mikrobiellen Umsetzung von Maiskeimöl zu Rhamnolipid, PhD Thesis, University Press Hohenheim, Stuttgart, 1994.

[22] Y. Zhu, J.J. Gan, G.L. Zhang, B. Yao, W.J. Zhu, Q.Meng, Reuse of waste frying oil for production of rhamnolipids using *Pseudomonas aeruginosa* zju.u1M, J. Zhejiang Univ. Sci., A **8** (2007) 1514–1520.

[23] M.E. Mercadé, M.A. Manresa, M. Robert, M.J. Espuny, C. de Andrés, J. Guinea, Olive oil mill effluent (OOME). New substrate for biosurfactant production, Bioresour. Technol. **43** (1993) 1–6.

[24] K. Dubey, A. Juwarkar, Distillery and curd whey wastes as viable alternative sources for biosurfactant production, World J. Microbiol. Biotechnol. **17** (2001) 61–69.

[25] M. Benincasa, J. Contiero, M.A. Manresa, I.O. Moraes, Rhamnolipid production by *Pseudomonas aeruginosa* LBI growing on soapstock as the sole carbon source, J. Food Eng. **54** (2002) 283–288.

[26] A. Abalos, A. Pinazo, M.R. Infante, M. Casals, F. García, A. Manresa, Physicochemical and Antimicrobial Properties of New Rhamnolipids Produced by *Pseudomonas aeruginosa* AT10 from Soybean Oil Refinery Wastes, Langmuir **17** (2001) 1367–1371.

[27] Z.A. Raza, M.S. Khan, Z.M. Khalid, Physicochemical and surface-active properties of biosurfactant produced using molasses by a *Pseudomonas aeruginosa* mutant, J. Environ. Sci. Health. Part A Toxic/Hazard. Subst. Environ. Eng. **42** (2007) 73–80.

[28] M. Henkel, M.M. Müller, J.H. Kügler, R.B. Lovaglio, J. Contiero, C. Syldatk, R. Hausmann, Rhamnolipids as biosurfactants from renewable resources: Concepts for next-generation rhamnolipid production, Process Biochem. **47** (2012) 1207–1219.

[29] U.A Ochsner, A.K. Koch, A. Fiechter, J.Reiser, Isolation and characterization of a regulatory gene affecting rhamnolipid biosurfactant synthesis in *Pseudomonas aeruginosa*, J. Bacteriol. **176** (1994) 2044–2054.

[30] G.E.P. Box, W.G. Hunter, J.S. Hunter, Statistics for Experimenters: An Introduction to Design, Data Analysis and Model Building, 1st ed., John Wiley & Sons, New York, 1978.

[31] U. Ochsner, T. Hembach, A. Fiechter, in: A. Fiechter (Ed.), Downstream Processing Biosurfactants Carotenoids, Springer Berlin Heidelberg, 1995, pp. 89–118.

[32] [32] J.P. Pearson, E.C. Pesci, B.H. Iglewski, Roles of *Pseudomonas aeruginosa* las and rhl quorum-sensing systems in control of elastase and rhamnolipid biosynthesis genes, J. Bacteriol. **197** (1997) 5756–5767.

[33] A. Martínez-Toledo, R. Rodríguez-Vázquez, Response surface methodology (Box-Behnken) to improve a liquid media formulation to produce biosurfactant and phenanthrene removal by *Pseudomonas putida*, Ann. Microbiol. **61** (2011) 605–613.

[34] M. Doudoroff, N.J. Palleroni, in: R.E. Buchanan, N.E. Gibbons (Eds.), Bergey's Manual of Determinative Bacteriology, Williams and Wilkins, Baltimore, 1974, pp. 217–243.

[35] M.G. Rikalović, G. Gojgić-Cvijović, M.M. Vrvić, I. Karadžić, Production and characterization of rhamnolipids from *Pseudomonas aeruginosa* san-ai, J. Serb. Chem. Soc. **77** (2012) 27–42.

IZVOD

PROIZVODNJA RAMNOLIPIDA I LIPAZE IZ *Pseudomonas aeruginosa* san-ai: OPTIMIZACIJA PROCESA PRIMENOM METODE ODZIVNIH POVRŠINA

Sonja M. Jakovetić[1], Zorica D. Knežević-Jugović[1], Sanja Ž. Grbavčić[2], Dejan I. Bezbradica[1], Nataša S. Avramović[3], Ivanka M. Karadžić[3]

[1]*Univerzitet u Beogradu, Tehnološko–metalurški fakultet, Karnegijeva 4, 11000 Beograd, Srbija*
[2]*Univerzitet u Beogradu, Inovacioni centar, Tehnološko–metalurški fakultet, Karnegijeva 4, 11000 Beograd, Srbija*
[3]*Univerzitet u Beogradu, Medicinski fakultet, Višegradska 26, 11000 Beograd, Srbija*

(Naučni rad)

Pseudomonas aeruginosa san-ai, izolovan je iz izrazito alkalne emulzije koja je korišćena kao mazivo u industriji pri obradi metala. Sposobnost da preživi u visoko alkalnoj sredini (pH 10) učinila je ovaj mikroorganizam veoma interesantnim za istraživanje, budući da je za preživljavanje u tako ekstremnim uslovima neophodno da mikroorganizam proizvodi enzime specifičnih karakteristika. Prethodna istraživanja su pokazala da ovaj ekstremofilni mikroorganizam ekstracelularno produkuje hidrolitičke enzime, koji zbog izuzetno atraktivnih karakteristika imaju potencijal za primenu u nizu biotehnoloških postupaka. Ipak, iako je pokazano da ovaj atraktivni soj produkuje industrijski veoma interesantne biomolekule (proteaze i lipaze), produkcija ramnolipida, jedinjenja čija oblast primene svakodnevno raste, pomoću ovog soja je malo ispitana. Ramnolipidi su amfifilna jedinjenja, koja se sastoje iz hidrofilne šećerne komponente i hidrofobne komponente koju čine β-hidroksi masne kiseline. Spadaju u grupu mikrobioloških surfaktanata ili biosurfaktanata, koji bi trebalo u budućnosti da se koriste kao zamena za sintetičke surfaktante koji nisu biodegradabilni i kao takvi predstavljaju opasnost za životnu sredinu. Sve veće interesovanje za industrijsku primenu ramnolipida, dovelo je do potrebe za optimizacijom njihove proizvodnje. Cilj ovog rada bila je optimizacija produkcije ramnolipida kao i lipaze pomoću *Pseudomonas aeruginosa* san-ai. Ispitan je uticaj četri fermentaciona faktora: koncentracije suncokretovog ulja u intervalu: 0,2-1,0 % (w/v), Tween® 80 u intervalu: 0–0,2 % (v/v), temperature: 20––60 °C i vremena trajanja fermentacije: 48–-144 h. Uticaj fermentacionih faktora na prinos navedenih metabolita ispitan je pomoću centralnog kompozitnog rotatabilnog eksperimentalnog plana, na pet nivoa vrednosti ispitivanih faktora. Analizom dobijenih regresionih koeficijenata ustanovljeno je da su vrlo izražena interaktivna dejstva nekoliko parova faktora. Kod produkcije ramnolipida, najveća je vrednost koeficijenta koji opisuje negativnu interakciju između koncentracije suncokretovog ulja i temperature, a kao bitne pokazale su se i pozitivna interakcija između koncentracije Tween® 80 i temperature, kao i negativna interakcija između koncentracija suncokretovog ulja i Tween® 80. Interesantno je da su se kod produkcije lipaze kao značajni faktori pokazali samo temperatura i vreme fermentacije. Najveći prinos ramnolipida, 138 mg dm^{-3}, postignut je pri niskoj koncentraciji Tween® 80 (0,05 %) i visokoj koncentraciji ulja (0,8 %) na 30 °C posle 72 h, dok je najveća lipolitička aktivnost, 11111 IU dm^{-3}, ostvarena pri istoj koncentraciji Tween® 80 (0,05 %) i istoj temperaturi od 30 °C, nešto nižoj koncentraciji suncokretovog ulja (0,4 %) i dužem vremenu fermentacije od 120 h.

Ključne reči: *Pseudomonas aeruginosa* • Ramnolipid • Lipaza • Metoda odzivnih površina

Influence of extraction method on protein profile of soybeans

Milica Ž. Pavlićević, Slađana P. Stanojević, Biljana V. Vucelić-Radović

University of Belgrade, Faculty of Agriculture, Institute for Food technology and biochemistry, Department of Chemistry and Biochemistry, Belgrade, Serbia

Abstract

Comparison between protein profiles of soybean obtained by commonly used methods of extraction (Tris buffer and Tris-urea buffer) with methods used for extraction of plant proteins for 2D PAGE analysis (direct solubilization in IEF buffer, acetone extraction, phenol extraction, extraction with urea solubilization buffer and thiourea-urea extraction) was investigated. 2D profiles of samples extracted directly in IEF buffer, in urea solubilization buffer and in acetone were characterized with low number of spots. Analysis of 2D PAGE profiles of Tris buffer and Tris-urea buffer extracts showed high degree of horizontal and vertical streaking. Thiourea–urea extraction gave a higher number of less intense protein spots than phenol extraction. The method of choice, due to a large number of intense spots, would be phenol extraction.

Keywords: soybean proteins; 2D PAGE analysis; extraction; densitometry; isoelectric focusing.

Available online at the Journal website: http://www.ache.org.rs/HI/

SCIENTIFIC PAPER

UDC 633.34:664:66.061.3

Hem. Ind. **67** (4) 687–694 (2013)

doi: 10.2298/HEMIND120919115P

Soy seed (*Glycine max* L.) contains, on average, 35–40% proteins, 18–22% oils, 5–6% oligosaccharides and 5% of fiber [1]. Because of high protein content (with a high ratio of essential amino acids [2]), as well as high concentration of antioxidants [3] and unsaturated fatty acids [4], soy has been recognized as functional food. Modification in ratio and/or structure of soybean proteins has an important influence on technological functional properties of soybean products [5–8].

There are two major types of soybean proteins: 11S (glycinin) and 7S (β-conglycinin) [8]. Glycinin (MW: 320000–360000) possesses a hexameric structure with three basic polypeptides (MW: 18000–20000, pI 6.5––8.5) and three acidic polypeptides (MW 36000–40000, pI 4.8–5.5) linked by a disulfide bond. Conglycinin (MW: 140000–180000) has a trimeric form consisting of an α subunit (MW: 76000, pI 4.9), α' subunit (MW: 70000, pI 5.2) and β subunit (MW: 53000, pI 6.0) aggregated by non-covalent interaction. It is known that the pH and ionic strength of the extraction solution greatly influence isoforms of proteins [5–8] present in the extract. The influence of isoforms composition on important technological characteristics of soybean proteins, such as protein solubility, gelling properties, the ability to form stable emulsions and foams is well documented [6-9]. Commonly, proteins of soybean seed are extracted either by Tris-HCl buffer as suggested by Than and Shibasaki [10], or by distilled water with subsequent enforcement of ionic strength and addition of denaturant [11]. However, for extraction of plant proteins for 2D PAGE analysis, the typically used methods are phenol extraction and extraction with TCA-acetone [12,13].

Several papers have been published in which comparison between different extraction methods of plant proteins had been conducted [14,15]. Furthermore, compatibility of such extraction methods for subsequent analysis by mass spectrometry has also been examined [16,17].

However, such examinations mainly employed methods of extraction developed specifically for 2D PAGE analysis. So far, no attempt was done to analyze soybean Tris-HCl or Tris-urea buffer protein extracts by two-dimensional electrophoresis.

SDS-PAGE analysis is often used as a screening method for soybean protein samples to be examined by 2D PAGE. The wide application of SDS PAGE analysis as a screening method can be explained by the fact that there is a variety of literature data on main protein fractions and proteins of soybeans analysis employing this method. Thus, the positions of subunits of major storage proteins in the gel are very well characterized. Since extraction with Tris-HCl is a method of choice when soybean extract is analyzed by SDS-PAGE, it would be useful to know whether Tris-HCl extract of soybean proteins could be used for both types of analyses. This could help in avoiding either loss of proteins in steps of precipitation and resolubilization in other buffer or loss of the plant material when two different extractions are needed. In fact, this would allow the analysis of heterogeneous soy protein extracts without previous separation of major protein fractions. These, also, could be potentially beneficial for industry because it would allow the same extract to be analyzed by both SDS-PAGE and 2D electrophoresis. Thus, by analysis of single extract it would be possible to obtain large num-

Correspondence: B.V. Vucelić-Radović, Department of Chemistry and Biochemistry, Institute for Food technology and biochemistry, Faculty of Agriculture, University of Belgrade, Nemanjina 6, 11030 Belgrade, Serbia.

E-mail: bvucelic@agrif.bg.ac.rs

Paper received: 19 September, 2012

Paper accepted: 29 November, 2012

ber of data. Also, such analyses would be faster and less expensive then analysis of extracts obtained by different extraction methods.

Thus, the aim of this work was to examine if Tris-HCl buffer or Tris-urea buffer extraction of soybean proteins could be used for 2D PAGE analysis and to compare protein profiles of these extracts with protein profiles of extracts obtained by usual methods of plant protein extraction for proteomic analysis (phenol extraction, extraction with urea solubilization buffer, direct extraction in IEF buffer, acetone extraction, thiourea–urea extraction).

MATERIALS AND METHODS

Plant materials. Soybean seed (*Glycine max* L.) of cultivar Novosađanka were provided by the Institute for Field and Vegetable Crops (Novi Sad, Serbia).

Chemicals. All chemicals were p.a. grade. Tris, acrylamide, bis-acrylamide, ammonium persulfate, thiourea, urea, EDTA, sucrose, methanol, ammonium acetate, ethanol, phosphoric acid, *n*-hexane, bromophenol blue (BPB), Sodium dodecyl sulfate (SDS), beef serum protein (BSA), Coomassie brilliant blue (CBB) G250 and CBB R250 were purchased from Merck (Germany). Tetramethylethylenediamine (TEMED) and phenol were purchased from Sigma (St. Louis, MO, USA). CHAPS was purchased from Serva (Heidelberg, Germany). Dithiothreitol (DTT), iodoacetamide, ampholytes (pH 3–10) overlaying agarose, immobilized pH gradient (IPG) strips (ReadyStrip) (pH 3–6, pH 3–10) were purchased from Bio-Rad (Hercules, CA, USA).

Determination of proteins: Concentration of proteins was determined according to the method of Bradford [18]. For determination of proteins, a standard curve was made by mixing 100 µl of sample of known protein concentration with 5 ml of dye (Coomassie Brilliant Blue G-250). As a standard for construction of standard curve, BSA was used. Concentration of proteins in samples was determined in the same manner as described for construction of standard curve. Quantification was done by spectroscopic measurement of adsorption maximum of bonded dye at 595 nm.

Isoelectric focusing. Prior to isoelectric focusing, strip was rehydrated with sample for 12 h at room temperature. Isoelectric focusing was performed in a Protean IEF Cell (Bio-Rad) using 7 cm strips (pH 3–6 and 3–10) under the following conditions: S01-250V, 15 min; S02-4000V, rapid; S03-10000Vh, rapid; focusing temperature, 20 °C. Extracts of each extraction method were analyzed using strips of pH range 3-6 and 3-10. Total protein content per strip was 100 µg. Each analysis was performed in duplicate.

Second dimension. Prior to placing strips on top of the gels, strips were equilibrated in equilibration buffer 1 (0,375 M Tris–HCl (pH 8.8), 6 M urea, 20% glycerol, 2% SDS, 0.002% bromophenol blue, 2% (w/v) DTT) for 15 min and equilibration buffer 2 (0,375 M Tris–HCl (pH 8.8), 6 M urea, 20% glycerol, 2% SDS, 0.002% bromophenol blue, 2.5% iodoacetamide) for 20 min. Then, the strips were placed for 5 min in the electrode buffer (0.25 M Tris base, 1.92 M glycine, 1% SDS) and placed on top of the gels. After placing strips on gels, strips were sealed with an overlaying agarose solution (0.25 M Tris base, 1.92 M glycine, 1% SDS, 0.5% agarose, 0.002% bromophenol blue). SDS PAGE was done in Mini Protean Tetra Cell (Bio-Rad) using Laemmli method [19] on 12% acrylamide gels. During the run, the voltage was constant (250 V). Gels were visualized by mixing for 1 h at room temperature in dye solution (0.001% (w/v) CBB G250, 40% ethanol, 10% acetic acid, 10% (w/v) TCA). The gels were destained for 24 h in a solution containing 40% ethanol, 10% acetic acid.

Acetone extraction. Samples were prepared by grinding previously frozen (with liquid nitrogen) seeds with mortar and pestle. 500 mg of sample was vortexed with 2.5 ml of 100% acetone. Extraction was performed at –20 °C for 2 h. The pellet was recovered by centrifugation (10 min, 13500 rpm). Then, the pellet was washed twice by resuspending in 0.5 ml 70% acetone and centrifuged (10 min, 13500 rpm). The pellet was dried at room temperature and dissolved in IEF buffer (8 M urea, 2% (w/v) CHAPS, 50 mM DTT, 0.2% (w/v) ampholytes pH 3-10, 0.01% (w/v) BPB), by vortexing (10 min) and sonication (1 h).

Phenol extraction. Phenol extraction was done by method of Hurkman and Tanaka [20], with modification in content of IEF buffer (higher concentration of urea and CHAPS and absence of thiourea). 1 g of frozen (in liquid nitrogen) soybean seeds were ground using mortar and pestle. The sample was then extracted with 1:1 ratio of buffered phenol and extraction buffer (2.5 ml of phenol buffered with Tris–HCl (pH 8.8) and 2.5 ml of extraction solution (0.1 M Tris–HCl (pH 8.8), 10 mM EDTA, 0.4% 2-mercaptoethanol, 0.9 M sucrose). The extract was vortexed for 5 min and sonicated for 30 min at 4 °C. Then the extract was centrifuged twice for 15 min at 13500 rpm at 4 °C. The upper, phenolic phase was separated and proteins were precipitated by adding ice cold 0.1 M ammonium acetate in 100% methanol in ratio 5:1. The extract was vortexed and left to precipitate overnight at –20 °C. The precipitate was obtained by centrifugation (twice at 14000 rpm, 20 min, 4 °C). Pellet was washed with cold solution of 0.1 M ammonium acetate in methanol (twice), with 80% acetone at –20 °C, and with cold 70% ethanol. The pellet was dissolved in 1.0 ml of IEF buffer, by incubation for 1 h at room temperature.

Thiourea–urea extraction. This extraction was carried out as described by Herman *et al.* [21]. Sample was prepared in similar manner as for acetone and phenol

extraction, with difference that sample for thiourea-urea extraction was further defatted twice with hexane (hexane to sample ratio 20:1, time 1 h, temperature 60 °C) and dried at room temperature. 100 mg of seed powder was vortexed with 1.5 ml of extraction buffer (5 M urea, 2 M thiourea, 4% (w/v) CHAPS, 65 mM DTT, 0.8% (w/v) ampholytes (pH 3–10)) for 5 min at room temperature. The supernatant was collected by centrifugation (13500 rpm, 10 min).

Direct extraction in IEF buffer. Modified method by Gallardo *et al.* [22] was used for this extraction. The modification included difference in content of IEF buffer (lower concentration of CHAPS and ampholytes (pH 3–10), higher concentration of DTT and absence of EDTA and Tris) and usage of sonication for extraction. The sample was prepared as described for acetone and phenol extraction. 100 mg of sample was extracted with 600 µl of IEF buffer at room temperature. Extraction was done by vortexing (15 min) and sonication (45 min). Then, the extract was centrifuged (twice for 15 min at 13500 rpm) and the supernatant was collected.

Extraction with urea solubilization buffer. This procedure was suggested by Berklman *et al.* [22]. The original procedure was modified in the sense that the ratio extraction buffer: sample was twice as high and the sonication time was extended to 45 min. The sample was prepared as described for acetone, phenol and direct IEF extraction. 100 mg of sample was extracted with 600 µl urea solubilization buffer (8 M urea, 4% CHAPS, 2% ampholyte (pH 3–10). Extraction was done by vortexing (5 min) and sonication (45 min) at room temperature. The sample was then centrifuged (15 min, 13500 rpm) and the supernatant was collected.

Tris–HCl buffer extraction. Extraction was preformed according to the method of Than and Shibasaki [10]. Soybean seeds were ground into powder and 100 mg of powder was defatted with 2 ml of hexane for 1 h at 60 °C. The sample was then dried at room temperature and dried sample was extracted with 0.03 M Tris–HCl buffer pH8.0 with 0,01 M β-mercaptoethanol for 1 h at room temperature. Pellet was removed by centrifugation (15 min, 13500 rpm). The supernatant was diluted with IEF buffer, so that the final concentration of proteins was 1 µg/µl.

Tris–urea buffer extraction. Modified procedure of Yagasaki *et al.* [10] was carried out. Time of extraction was prolonged (from 3 to 15 min). Soybean seed was defatted as explained for Tris–HCl buffer extraction. 500 mg of defatted sample was homogenized with 2 ml of distilled water for 15 min at room temperature. Supernatant was obtained by centrifuging (15 min, 13500 rpm). Proteins from 20 µl of supernatant were re-extracted with 160 µl of Tris-urea buffer (0.05 M Tris–HCl pH 8.0, 0.2% SDS, 5 M urea). 1 h before isoelectric focusing, 20 µl of β-mercaptoethanol was added to the extract. The extract was then diluted with IEF buffer to a final protein concentration of 1 µg/µl.

Densitometric analysis and determination of molecular weights. Densitometric analysis of spots in 2D gels, as well as determination of molecular weights of proteins under spots, was done using SigmaGel, version 1.1, software (Jandel Scientific, USA). 2D SDS PAGE standard for determination of molecular weight of spots was purchased from Bio Rad (Hercules, CA, USA) (MW: 76, 66.2, 36, 31, 21.5, 17.5, pI 4.5-8.5).

RESULTS

2D profiles of soybean proteins obtained by different extraction method were each determined in two pH regions: 3–10 (Figure 1) and 3–6 (Figure 2).

Due to the initial charge of reagents used for extraction or produced charge of extracts (as a consequence of either pH range of strips or oxido-reduction reaction) Tris–HCl and Tri–urea buffer extracts were characterized by time-consuming isoelectric focusing step. This effect was prominent in the case of Tris-HCl extracts. Isoelectric focusing of these samples took as long as 12 h in comparison to focusing of phenol extract that took only 3 h. These in turn caused visible horizontal streaking.

In order to show differences in one-dimensional profiles of soybean proteins obtained by different extraction methods, the results of SDS PAGE analysis of these samples are presented in Figure 3.

High concentrations of lipids might have caused the appearance of diffuse bands in electrophoregrams of some extracts (especially evident for acetone extract), making densitometric analysis of such sample unreliable.

The usefulness of different extraction methods in analysis of soybean proteins was also assessed based on the number of spots and spot intensity in particular pH range (Tables 1 and 2). Such analysis could help the determination of amounts of both total proteins and particular protein isoforms present on precise pH. Thus, it would be possible to deduce the influence of ratio of major protein fractions and/or concentration of low abundant proteins on their functional properties.

DISCUSSION

Acetone extraction is a fast method that efficiently removes salts, sugars and some lipids and concentrates proteins [12]. However, the produced pellet was of low solubility, as has been reported by Thiellement *et al*. [13] and many of the lipids of higher polarity, as well as phenolic compounds remained as contaminants (Figure 3, C-2). These lipids interfered with isoelectric focusing, thus causing broadening of bands on strips and subsequent horizontal streaking (Figures 1B and 2B). Also,

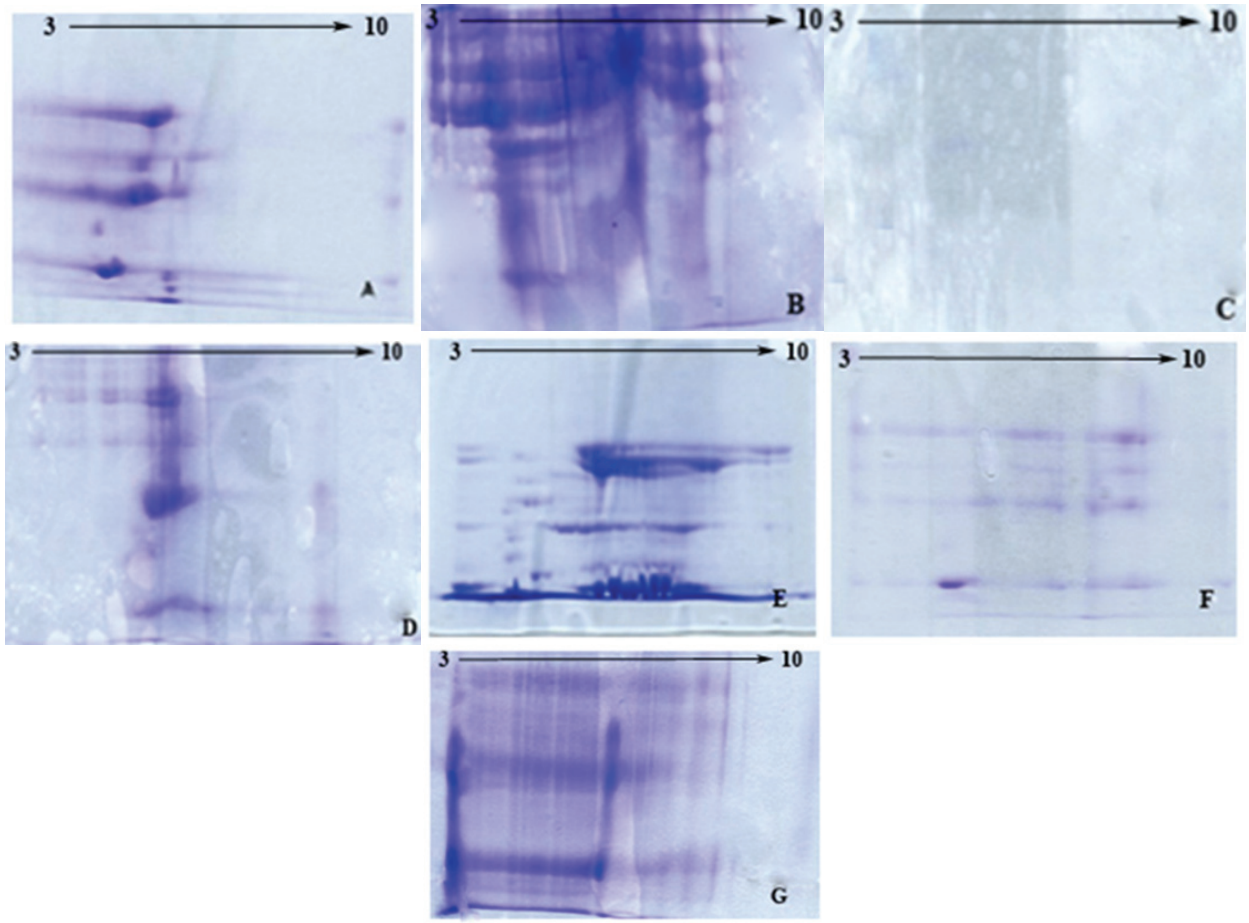

Figure 1. Protein profiles of soybean seed proteins extracted by different extraction methods in pH range 3–10; A) phenol extraction, B) acetone extraction, C) urea solubilization buffer extraction, D) direct extraction in IEF buffer, E) thiourea–urea extraction, F) extraction with Tris–HCl buffer, G) extraction with Tris–urea buffer.

higher rehydratation volumes were necessary because of a low final content of protein (1.5 mg/ml). These could have also led to a loss of less abundant proteins. Vertical streaking could be explained by prolonged time necessary for solubilization of the pellet. Also, it is possible that the room temperature used during the solubilization step favored hydrophobic interactions and formation of complexes, thus leaving sample only partially solubilized. The lack of clearly defined spots affected the quality of densitometric measurements, but it was evident that the intensity of spots (Table 1) was around 20% lower than that of thiourea-urea extraction and for 30% lower than that of phenol extraction. The analysis of molecular weights distribution also proved that, although in the same range as in the other extraction methods, a smaller number of spots per region suggested that the resolution of these proteins was also lower.

It is known that phenol extraction gives intense and sharply defined spots [14–16]. Our results were in agreement with such data (Figures 1A and 2A and Tables 1 and 2).

Densitometric analysis confirmed that phenol extraction produced spots of highest intensity (Table 1). Besides the initial difference in solubility and a large number of steps in phenol extraction method, the final protein content (2.5 mg/ml) was lower compared to extraction with urea solubilization buffer or direct extraction with IEF buffer. Although most of the polar contaminants were removed, some of phenolic compounds remained present [14–16], causing spots to diffuse. This was especially evident in acidic pH, due to their redox reactions, as reported by Cilia *at al*. [15]. Also, the lower number of spots (18) compared to thiourea–urea extraction (Figures 1E and 2E) could be explained by lower detection of low abundant proteins [17].

Extraction by urea solubilization buffer resulted in high horizontal and vertical streaking in pH range 3–6, while in pH range 3–10 spots were less intensive and diffused (Tables 1 and 2).

This was probably due to ionization of urea at acidic pH, which affected isoelectric focusing. Horizontal streaking (Figures 1C and 2C) could be explained by the presence of polar, non-protein (*e.g*., nucleic acids, phenolic compounds, sugars) contaminants that interfere

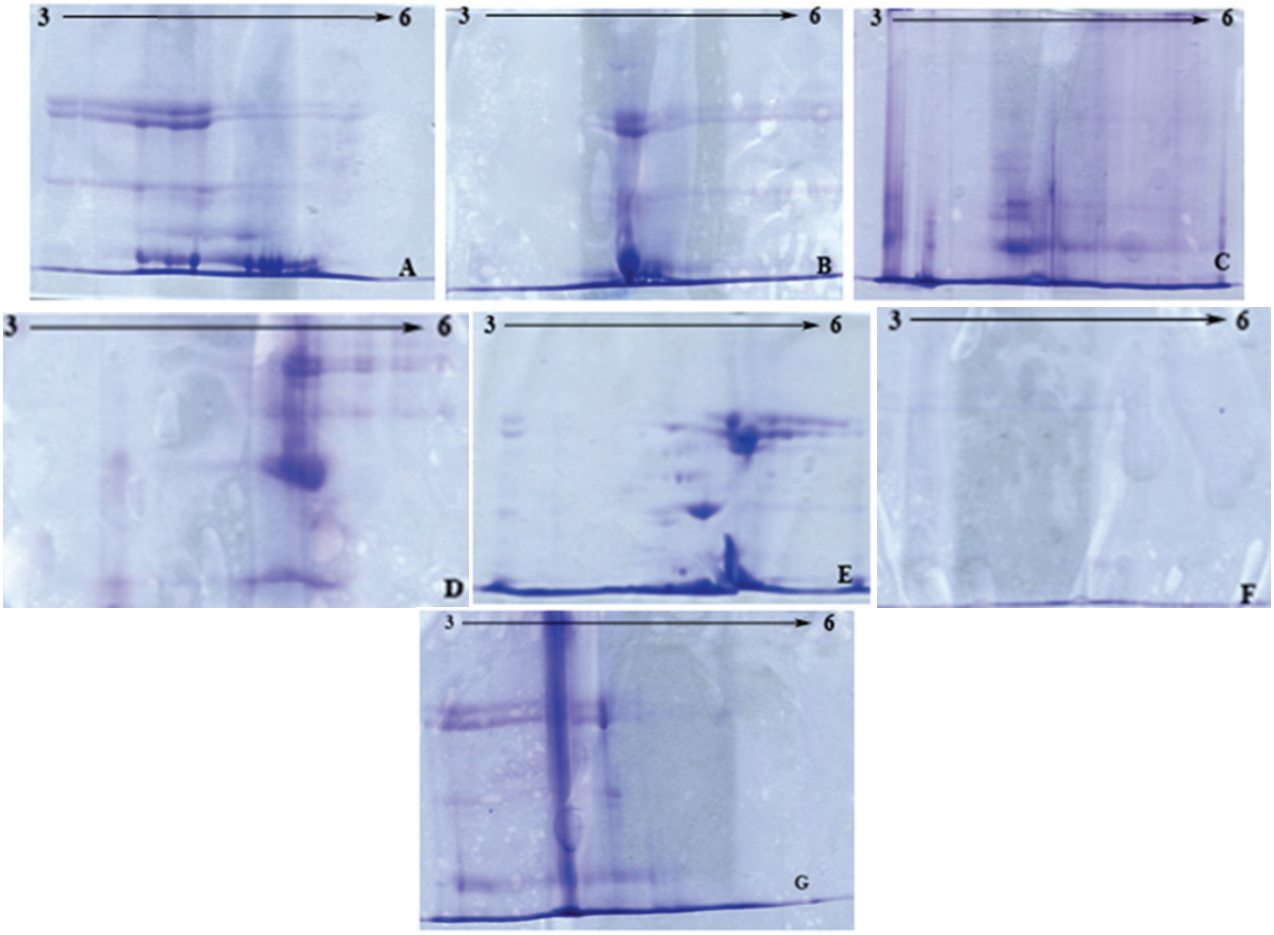

Figure 2. Protein profiles of soybean seed proteins extracted by different extraction methods in pH range 3–6; A) phenol extraction, B) acetone extraction, C) urea solubilization buffer extraction, D) direct extraction in IEF buffer, E) thiourea–urea extraction, F) extraction with Tris–HCl buffer, G) extraction with Tris–urea buffer.

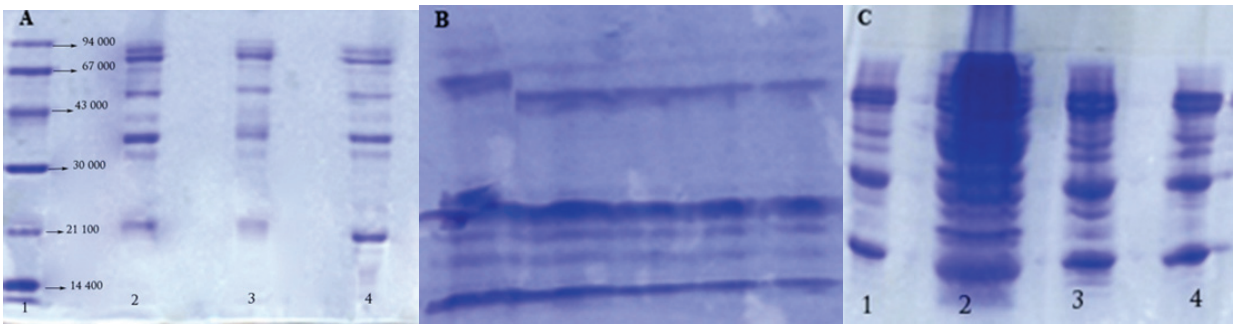

Figure 3. SDS PAGE profiles of soybean proteins obtained by different extraction method. A) Comparison between Tris–HCl and Tris–urea buffer extraction (1 – standards, 2,3 – Tris-HCl buffer extraction, Tris–urea buffer extraction). B) Thiourea–urea extraction. C) 1 – Standards, 2 – acetone extraction, 3 – direct extraction in IEF buffer, 4 – extraction with urea solubilization buffer.

with isoelectric focusing. Vertical streaking might be the result of insufficient focusing or carbamoylated proteins. Protein content in extract was 3.1 mg/ml of sample.

Direct IEF extraction gave similar results as extraction by urea solubilization buffer when number of spots and their intensity were compared (Tables 1 and 2). However, IEF extraction resulted in higher concentration of extracted proteins (3.6 mg/ml), although it might be due to the larger number of contaminants that interfere with the Bradford method, which was used for protein determination. Also, in pH region 3–10 it gave better results visible in higher number of spots, which could be explained by presence of DTT which favors protein dissociation and suppresses ionization of urea (Figures 1D and 2D).

Table 1. Intensity of spots (in pixel units) at particular pI range using different extraction methods

Extraction method	pI Range					
	3–4	4–5	5–6	6–7	7–8	8–9
Phenol extraction	7360	15776	17329	3932	3790	3735
Acetone extraction	6585	12595	17203	9929	8115	6585
Direct extraction in IEF buffer	9287	11633	11414	11799	15854	5112
Urea buffer extraction	10130	14971	11564	3956	3393	2934
Tris–HCl extraction	5688	7499	4940	9928	7752	8020
Tris–urea buffer extraction	8565	17280	10521	7979	6873	3578
Thiourea–urea extraction	10843	16971	11017	9050	4697	4423

Table 2. Range of molecular weights of proteins present in spots (presented as 10^3 folds) at particular pI range using different extraction methods

Extraction method	pI Range					
	3–4	4–5	5–6	6–7	7–8	8–9
Phenol extraction	11–30	32–76	40–72	15–23	11–27	27–32
Acetone extraction	10–32	29–75	42–77	18–25	13–28	28–39
Direct extraction in IEF buffer	16–29	33–78	41–73	16–22	14–25	25–34
Urea buffer extraction	14–31	35–77	43–71	15–25	13–27	22–31
Tris–HCl extraction	12–30	37–78	44–70	17–24	15–28	23–32
Tris–urea buffer extraction	13–32	36–75	45–72	18–27	14–21	24–31
Thiourea–urea extraction	10–35	34–77	46–73	17–24	15–27	25–33

Tris–HCl buffer extraction gave very small number of spots in acidic pH region (Figure 2F) while in pH region 3–10 (Figure 1F) large horizontal streaking was present. Although it was evident from SDS PAGE that Tris extract (Figure 3, A-1) was cleaned from lipid contaminants, the presence of polar contaminants and large concentration of salts prolonged the time of isoelectric focusing. Particularly sensitive to such contamination is the first phase in equilibration of IPG strips that has a role in "cleaning up" strips from salts and other charged molecules. It is possible that by prolonging these steps horizontal streaking would be less prominent, but it could interfere with transferring proteins from strips to gels. Although spots were of low intensity, low-abundant proteins as well as basic subunits could be observed (as confirmed by analysis of molecular weights). Protein content in the extract was 12 mg/ml.

Tris–urea buffer extraction yields higher content of extracted proteins than Tris–HCl buffer extraction (15 mg/ml), but large vertical and horizontal streaking, due to insufficient focusing as consequence of charged molecules, prevents precise densitometric analysis (Figures 1G and 2G). Also, probably due to the presence of charged molecules that interfered with electrostatic interactions, better separated subunits were observed, as confirmed by the presence of two additional spots at acidic pH compared to Tris-HCl buffer extraction (Figure 2G and Table 2).

Thiourea–urea extraction gave the highest number of intense spots (Table 1). Although spots were less intense than those obtained by phenol extraction, it was possible to simultaneously analyze both more and less abundant proteins (Figures 1E and 2E). These results are in agreement with those reported by Natrajan *et al.* [14] and Lee *et al.* [17]. From the analysis of molecular weights, it was evident that proteins were sharply defined, since the number of spots per narrow pI range was the highest (Table 2). However, total protein content in extract (4.6 mg/ml) was lower when compared to Tris–urea buffer extraction and Tris buffer extraction.

CONCLUSION

Based on the presented results, it can be concluded that the application of Tris–HCl buffer and Tris–urea buffer for extraction of soybean proteins to be analyzed by 2D electrophoresis is at least questionable. 2D PAGE profiles of this extracts were characterized by low number of spots and high degree of horizontal and vertical streaking. Also, the time needed for completion of isoelectric focusing step was longer than for extracts produced by other extraction methods. It appears that the application of Tris or Tris–urea extraction is limited only to SDS PAGE analysis of soybean proteins. Therefore, it would not be advisable to use the same extract for both types of analysis. Better results could be achieved by prolonging the time of the isoelectric

focusing step, but this bears the risk of strong incorporation of proteins into the strip, thus causing large horizontal streaking.

Direct extraction in IEF buffer and extraction by urea solubilization buffer gave similar results and were both characterized by low number of diffused spots. Acetone extraction gave low concentration of soluble proteins and high degree of horizontal streaking. Thiourea–urea extraction gave the highest number of less intense protein spots than phenol extraction. Low spot intensity might mean that low abundant proteins could not be analyzed. Phenol extraction consisted of a large number of steps that prolonged the time needed for analysis. However, phenol extraction gave a large number of spots of high intensity. Also, because of a few contaminants present in sample and short time needed for the isoelectric focusing step, there was no horizontal and vertical streaking. Because of its capacity to resolve a high number of intense protein spots, the method of choice would be phenol extraction.

Acknoledgement

The authors are grateful to the Ministry of Education, Science and Technological Development of the Republic of Serbia for the financial support, project No.: TR 31022.

REFERENCES

[1] I. Mateos-Aparicio, A. Redondo Cuenca, M. J. Villanueva-Suárez, M.A. Zapata Revilla, Soybean, a promising health source, Nutr. Hosp. **23** (2008) 305–312.

[2] K. Jayakumar, M.M. Azooz, P. Vijayarengan, C. Abdul Jaleel, Biochemical changes with exogenous cobalt application in soybean, J. Phytology **2** (2010) 7–12.

[3] E.B. Cahoon, Genetic enhancement of soybean oil for industrial uses: Prospects and challenge, Ag. Bio Forum **6** (2003) 11-13.

[4] K.L. McCord, W.R. Fehr, T. Wang, G.A. Welke, S.R. Cianzio, S.R. Schnebly, Tocopherol content of soybean lines with reduced linolenate in the seed oil, Crop Sci. **44** (2004) 772–776.

[5] G. Remondeto, R. Gonzales, M. Anon, Effect of Simultaneous Heat and Reducing Treatments on Some Structural Characteristics of Soy Protein Isolates, Food Sci. Technol. Int. **8** (2002) 223–228.

[6] J.R. Wagner, D.A. Sorgentini, M.C. Anon, Thermal and Electrophoretic behavior, Hidrophobicity and Some Functional properties of Acid Treated Soy Isolates, J. Agric. Food Chem. **44** (1996) 1881–1889.

[7] J.R. Wagner, J. Gueguen, Surface Functional Properties of Native, Acid-Treated and Reduced Soy Glycinin. 2. Emulsifying Properties, J. Agric. Food Chem. **47** (1999) 2181–2187.

[8] M.B. Pešić, B. V. Vucelić-Radović, M.B. Barać, S.P. Stanojević, The influence of genotypic variation in protein composition on emulsifying properties of soy proteins, JAOCS **82** (2005) 667–672.

[9] S. P. Stanojević, M. B. Barać, M. B. Pešić, B. V. Vucelić Radović, Assessment of soy genotype and processing method on quality of soybean tofu, J Agric Food Chem. **59** (2011) 7368–7376.

[10] V.H. Than, K. Shibasaki, Proteins of soybean seeds. A straight forward fractionation and their characterization, J. Agric. Food Chem. **24** (1976) 1117–1121.

[11] K. Yagasaki, T. Takagi, M. Sakai, K. Kitamura, Biochemical Characterization of Soybean protein Consisting of Different Subunits of Glycinin, J. Agric. Food Chem. **45** (1997) 656–660.

[12] F.S. Wu, M.Y. Wang, Extraction of proteins for sodium dodecyl sulfate-polyacrylamide gel electrophoresis from protease-rich plant tissues, Anal. Biochem. **139** (1983) 100–103.

[13] H. Thiellement, M. Zivy, C. Damerval, V. Mechin, Plant proteomics: methods and protocols, Humana Press Inc, Totowa, NJ, 2007, p. 1.

[14] S. Natrajan, C. Xu, T.J. Caperna, W.M. Garret, Comparison of protein solubilization methods suitable for proteomics analysis of soybean seed proteins, Anal. Biochem. **342** (2005) 214–220.

[15] M. Cilia, T. Fish, X. Yang, M. McLaughlin, T.W. Thannhauser, S. Gray,A Comparison of Protein Extraction Methods Suitable for Gel-Based Proteomic Studies of Aphid Proteins, J. Biomol. Tech. **20** (2009) 201–215.

[16] I. S. Sheoran, A. R.S. Ross, D. J. H. Olson, V.K. Sawhney, Compatibility of plant protein extraction methods with mass spectrometry for proteome analysis, Plantsci. **176** (2009) 99–104.

[17] D.G. Lee, N. L. Houston, S.E. Stevenson, G. S. Ladics, S. McClain, L. Privalle, J. J. Thelen, Mass spectrometry analysis of soybean seed proteins: optimization of gel-free quantitative workflow, Anal. Methods **2** (2010) 1577–1583.

[18] M.M. Bradford, A Rapid and Sensitive Method for the Quantitation of Microgram Quantities of Protein Utilizing the Principle of Protein-Dye Binding, Anal.Biochem. **72** (1976) 248–254.

[19] U. Laemmli, Cleavage of Structural Proteins during the Assembly of the Head of Bacteriophage T4, Nature **227** (1970) 680–685.

[20] W.J. Hurkman, C.K. Tanaka, Solubilization of Plant Membrane Proteins for Analysis by Two-Dimensional Gel Electrophoresis, Plant Physiol. **81** (1986) 802–806.

[21] E.M. Herman, R.M. Helm, R. Jung, A.J. Kinney, Genetic modification removes an immunodominant allergen from soybean, Plant Physiol. **132** (2003) 36–43.

[22] K. Gallardo, C. Job, S.P.C. Groot, M. Puype, H. Demol, J. Vanderkerckhove, D. Job, Proteomic Analysis of Arabidopsis Seed Germination and Priming, Plant Physiol. **126** (2001) 835–848.

[23] T. Berkelman, T. Stenstedt, B. Bjellqvist, N. Laird, M. McDowell, I. Olsson, R. Westermeier, 2D Electrophoresis Using Immobilized pH Gradients: Principles and Methods, Amersham Biosciences, Piscataway, NJ, 1998.

IZVOD

UTICAJ METODE EKSTRAKCIJE NA PROTEINSKE PROFILE PROTEINA SOJE

Milica Ž. Pavlićević, Slađana P. Stanojević , Biljana V. Vucelić-Radović

Univerzitet u Beogradu, Poljoprivredni fakultet, Institut za prehrambenu tehnologiju i biohemiju, Katedra za hemiju i biohemiju, Beograd, Srbija

(Naučni rad)

Upoređeni su profili proteina semena soje dobijeni tradicionalnim metodama ekstrakcije (Tris–HCl puffer i Tris–urea pufer) sa profilima proteina soje ekstrahovanim metodama koje se obično koriste za ekstrakciju biljnih proteina za 2D PAGE analizu (direktno rastvaranje u IEF puferu, acetonska ekstrakcija, fenolna ekstrakcija, ekstrakcija puferom sa ureom i tiourea/urea ekstrakcija). Cilj rada je bio utvrditi primenljivost ekstrakcije Tris–HCl i Tris–urea puferom u 2D PAGE analizi. Raširena primena ove dve metode ekstrakcije zasnovana je na dobijanju visoke koncentracije proteina koji se karakterišu dobrom rastvorljivošću, kao i na već dobro poznatim Rf vrednostima pojedinih proteinskih podjedinica na SDS PAGE elektroforegramima visoke rezolucije. Tako bi njihova eventualna primena u proteomiks analizama, omogućila kako brzu analizu uzoraka, tako i prikupljanje većeg broja podataka, jer bi se izbegla potreba za resolubilizacijom i gubitak proteina. Poređenje ekstrakcionih metoda vršeno je na osnovu broja rastvornih proteina u ekstraktu, kao i denzitometrijskih merenja broja, intenziteta i oštrine tačaka na 2D profilima u okviru dva različita pH opsega. Premda ekstrakcije sa Tris–HCl i Tris––urea puferom daju najveću koncentraciju proteina u ekstraktu, ove metode daju manji broj tačaka u poredjenju sa ostalim ispitivanim metodama. Takođe, izraženo vertikalno i horizontalno “razvlačenje” onemogućavaju preciznu denzitometrijsku analizu. Dodatni nedostatak ovih metoda (pogotovu ekstrakcije sa Tris–HCl puferom) jeste produženo vreme potrebno za korak izoelektričnog fokusiranja u poredjenju sa ostalim metodama. Direktna ekstrakcija u IEF puferu i ekstrakcija puferom sa ureom daju slične rezultate i karakterišu se malim brojem difuznih tačaka. Acetonskom ekstrakcijom dobija se mala koncentracija rastvorljivih proteina, a na 2D PAGE profilima uočava se visok stepen horizontalnog razvlacenja. Tiourea––urea ekstrakcija daje veći broj manje intenzivnih tačaka u poređenju sa fenolnom ekstrakcijom. Manji intenzitet tačaka može značiti gubitak manje zastupljenih proteina. U slučaju fenolne ekstrakcije, veliki broj koraka tokom pripreme uzorka produžava vreme analize, ali su tačke najintenziivnije. Na osnovu dobijenih rezultata, zaključeno je da je fenolna ekstrakcija metoda izbora za ekstrakciju proteina iz semena soje za analizu 2D PAGE metodom.

Ključne reči: Sojini proteini • 2D PAGE analiza • Ekstrakcija • Denzitometrija • Izoelektrično fokusiranje

Raman study of surface optical phonons in ZnO(Co) nanoparticles prepared by hydrothermal method

Branka Hadžić[1], Nebojša Romčević[1], Maja Romčević[1], Izabela Kuryliszyn-Kudelska[2], Witold D. Dobrowolski[2], Ursula Narkiewicz[3], Daniel Sibera[3]

[1]*Institute of Physics, University of Belgrade, Belgrade, Serbia*
[2]*Institute of Physics, Polish Academy of Science, Warsaw, Poland*
[3]*Institute of Chemical and Environment Engineering, Szczecin University of Technology, Szczecin, Poland*

Abstract

Raman scattering spectra of nanocrystalline samples of ZnO(Co) prepared by microwave-assisted hydrothermal synthesis were obtained and surface optical phonons (SOP) where observed in the range of 519–572 cm^{-1}. The mean crystalline size (33–300 nm) as well as the phase composition of obtained samples (ZnO and $ZnCo_2O_4$) were determined by X-ray diffraction measurements. These measurements allowed us to study the change of SOP modes position with crystalline size and how the change in concentration of doping component CoO affects the change of SOP modes intensity.

Keywords: nanostructured materials; optical properties; light absorption and reflection, surface optical phonon modes.

Available online at the Journal website: http://www.ache.org.rs/HI/

SCIENTIFIC PAPER

UDC 66.017/.018:54:543.424.2:53

Hem. Ind. **67** (4) 695–701 (2013)

doi: 10.2298/HEMIND121022119H

Diluted magnetic semiconductors (DMS) have attracted great interest recently due to their properties combining both spin and charge transport. With these characteristics, DMS are one of the most promising materials for spintronics [1,2]. Increasing attention has been devoted to nanostructures made of ZnO doped with transition metals such as Co, Ni, Cr, Fe and V after theoretical prediction of room temperature ferromagnetism in such systems [3–5]. Nanoparticles induce ferromagnetism in the host semiconductor material, if they contain inclusions of nanoscale oxides of transition metals [6] and/or a large concentration of magnetic ions [7].

Among other techniques, Raman spectroscopy is a convenient, non-destructive tool for gaining information about vibrational properties of ZnO, because of its ability to probe the local atomic arrangement around foreign elements, sample quality, information about phonon life times, isotopic effects and electron–––phonon coupling [8,9]. For this reason, it is used with for bulk crystals, nanocrystals and thin films, of both the pure host material and the crystal containing impurities. Besides the local atomic arrangement and dopant incorporation, in ZnO and ZnO-related compounds Raman scattering has also been used to study phonon processes, temperature dependence of Raman active modes, influence of annealing process, electron-phonon coupling, etc.[10–15].

Correspondence: N. Romčević, Institute of Physics, University of Belgrade, Pregrevica 118, 11080 Belgrade, Serbia.
E-mail: romcevi@ipb.ac.rs
Paper received: 22 October, 2012
Paper accepted: 21 November, 2012

In samples with large surface-to-volume ratios, the appearance of surface optical phonons (SOP) is expected in their Raman spectra, such as in the case of ZnO nanostructures. The existence of SOP modes has been predicted theoretically and/or detected experimentally for ZnO nanostructures [16]. When the dimensions become extremely small, the only mode that persists is a surface mode, which is why the state of surface atoms plays a key role in determining their properties. In ZnO nanostructures, one can expect loss of long-range order and symmetry breakdown in the ZnO shell, which causes the appearance of forbidden Raman modes. With this in mind we can say that those forbidden Raman modes are SOP modes [17].

The aim of this work is to study sample characteristics, position of the Co ion in the ZnO lattice, formation of existing phases, presence of SOP modes and the sample quality dependence on CoO concentration, by applying micro-Raman spectroscopy.

SAMPLES AND CHARACTERIZATION

The nanocrystalline samples of ZnO doped with CoO were obtained by hydrothermal synthesis. In this method a mixture of cobalt and zinc hydroxides was obtained by addition of an ammonia solution or 2 M solution of KOH to the 20% solution of a proper amount of $Zn(NO_3)\cdot 6H_2O$ and $Co(NO_3)\cdot 4H_2O$ in water. Next, the obtained hydroxides were put in the reactor with microwave emission. The microwave-assisted synthesis was conducted under a pressure of 3.8 MPa for 15 min. The synthesized product was filtered and dried.

This method obtained a series of nanosized ZnO samples with nominal concentration of CoO from 5% to

50%. The morphology of the samples was investigated using scanning electron microscopy (SEM). In SEM images of samples of lower CoO concentration, one can notice particles of similar size that belong to both registered phases, ZnO and $ZnCo_2O_4$. With increase in CoO concentration, the particle size becomes quite different, so we can easily distinguish two types of particles with diverse sizes: bigger (100 nm or more) belonging to the ZnO phase, and smaller, belonging to the $ZnCo_2O_4$ phase.

X-Ray diffraction (XRD) ($Co_{K\alpha}$ radiation, X'Pert Philips) was used to determine the phase composition of samples. The detailed phase composition investigations, in samples prepared by hydrothermal method, revealed the presence of crystalline phases of hexagonal ZnO and spinel structure $ZnCo_2O_4$ (ICSD: 23-1390). XRD data, obtained in this way, allowed us to determine a mean crystalline size, using Scherrer's formula [18], in these samples. Here the mean crystalline sizes d were between 64 and 300 nm for ZnO phases and from 33 to 77 nm for $ZnCo_2O_4$ phases. The obtained results of XRD measurements, phase composition and mean crystalline size are gathered in Table 1.

Table 1. XRD Analysis results for samples prepared by hydrothermal method. The identified crystalline phases and mean crystalline size, d, were determined using Scherrer's formula

Concentration of CoO mass%	*d* / nm	
	ZnO phase	$ZnCo_2O_4$ phase
5	65	48
10	64	33
20	65	37
30	100	55
40	100	77
50	300	40

The results of SEM and XRD analyses indicate that the crystalline size of ZnO increased with increasing CoO concentration, while the second phase $ZnCo_2O_4$ did not have a monotonous dependence. Further, it is obvious that the relative change of crystaline size of the $ZnCo_2O_4$ phase is smaller than the corresponding change of the ZnO phase.

Here we present the investigation of all samples obtained by hydrothermal method. No other crystal phases have been observed in the samples.

Surface optical phonons

The presence of surface optical phonons (SOP) is common for samples containing particles of nanoscale dimensions and containing imperfections, impurity, valence band mixing, etc. These characteristics result in loss of long-range order and symmetry breakdown with a rise of new, previously forbidden, vibration modes in Raman spectra whose phonons have $l \neq 0$ [10,11,19,20]. Another important characteristic of SOP modes is that they exist in polar crystals and that the wavelength of the incident laser beam needs to be larger than the particle size [17]. To understand how SOP modes behave, their characteristics and properties, a physical model is needed. This physical model has to describe the macroscopic properties of a medium based on the properties and relative fractions of its components. This kind of model is found in effective medium theory (EMT) [21]. In the literature, many different approximations of EMT can be found, each of them being more or less accurate in distinct conditions [17,21]. For polar semi-insulating semiconductors, among many approximations and mixing models for the effective dielectric permittivity [22], it seems that the Maxwell-Garnet approximation and mixing rule are most prominent [23,24]. As the Maxwell-Garnet approximation is only valid for small volume fractions of inclusions, it is not appropriate for our samples. Another famous and prominent approximation is the Bruggerman approximation and mixing rule [25–27], which is more adequate in the case of our samples. The Bruggeman model is more suitable for high concentrations of inclusions, because there are no restrictions for volume fraction in it. According to the Bruggeman mixing rule, the effective dielectric function is given by:

$$(1-f)\frac{\varepsilon_1-\varepsilon_{\text{eff}}}{\varepsilon_{\text{eff}}+g(\varepsilon_1-\varepsilon_{\text{eff}})}+f\frac{\varepsilon_2-\varepsilon_{\text{eff}}}{\varepsilon_{\text{eff}}+g(\varepsilon_2-\varepsilon_{\text{eff}})}=0 \qquad (1)$$

where g is a geometric factor who depends on the shape of the inclusions. In the case of three-dimensional spherical particles g = 1/3 and in the case of two-dimensional circles g = 1/2. The method of preparation and derivation of our samples results in clusterized nanoparticles, which occupy a considerably important volume. With all this in mind it is clear that our nanoparticles, when g = 1/3 is applied, satisfy the Bruggeman formula conditions.

In this case, it is necessary to take into account two phonons, typical for ZnO nanoparticles, which are in the region of SOP modes appearance, $\omega_{A_{1LO}} = 577$ cm^{-1}, $\omega_{A_{1TO}} = 379$ cm^{-1}, $\omega_{E_{1TO}} = 410$ cm^{-1}, $\omega_{E_{1LO}} = 592$ cm^{-1}, with dielectric permittivity $\varepsilon_\infty = 3.7$ [28–30]. Our samples are characterized by low concentration of free carriers and their low mobilities, which permits us to neglect influence of plasmon-phonon interaction. Another consequence of the preparation method in our samples is the random distribution of nanoparticles in space and thus to the incident light. In the obtained Raman spectra, as will be seen later, there is no E1 symmetry phonon, while the existence of A1 symmetry phonon has been registered. This observation can point out the assumption that the E1 symmetry phonon participates in SOP creation. The Raman intensities due to

excitation of extraordinary phonons, for our sample, are given by:

$$I \sim \mathrm{Im}(-\varepsilon_{\mathrm{eff}}) \quad (2)$$

In the area of Bruggerman formula applicability, this manner of calculation predicts appearance of one asymmetric peak, with wavenumbers below $\omega_{E1}(LO)$. This is in good agreement with the experimental spectra of ZnO doped with CoO nanopowders prepared by the hydrothermal method. Therefore, as a result of variation in the main volume fraction and damping rate, there great difference in the intensities and line shapes of simulated SOP modes.

RESULTS AND DISCUSSION

The micro-Raman spectra were taken in the back-scattering configuration and analyzed using a Jobin Yvon T64000 spectrometer, equipped with a nitrogen cooled charge-coupled-device detector. As an excitation source, the 514.5 nm line of an Ar-iron laser was used. The measurements were performed at 20 mW laser power.

The obtained Raman spectra have been analyzed using Lorentzian type lines for all phonons [31] while for calculations of SOP lines we have used Eqs. (1) and (2) with $\varepsilon_1 = 1$ (air). The obtained Raman spectra for all samples of nanocrystaline ZnO doped with CoO are shown in Figure 1. In these samples, as mentioned earlier, only nanoparticles of ZnO and $ZnCo_2O_4$ were registered with XRD. We will start our analysis of the obtained Raman spectra with brief report about structural and vibration properties of all potentially present phases in the samples, typical for bulk materials, which is absolutely necessary for understanding the vibration properties of nanoparticles. As a consequence of the nano-nature (structure) of our samples, we expect that bulk modes will be shifted and broadening.

ZnO, the basic material in our samples, is one of the simplest uniaxial, hexagonal crystals; a semiconductor with wurtzite structure belonging to the C_{6v}^4 space group. It has four atoms per primitive cell, all occupying

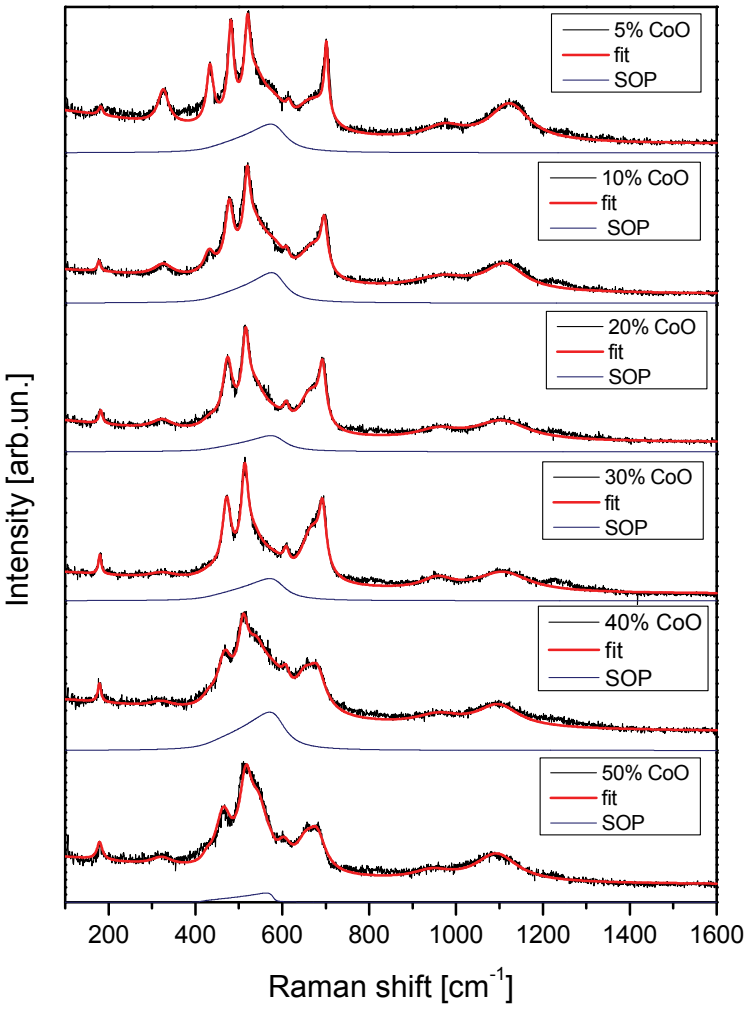

Figure 1. Fitted Raman spectra of nanocrystalline ZnO doped with CoO prepared by hydrothermal method. SOP modes are marked with solid lines.

C_{3v} sites. For a perfect ZnO crystal, only the optical phonons at the Γ point of the Brillouin zone are involved in first-order Raman scattering. Group theory predicts the existence of the following optical modes:

$\Gamma_{opt} = A_1 + 2B_1 + E_1 + 2E_2$

where A_1, E_1 and $2E_2$ modes are first-order Raman active, while the B_1 modes are Raman inactive modes [32,33]. Furthermore, the A_1 and E_1 modes are polar and can be further split into transverse optical (TO) and longitudinal optical (LO) phonons. The existence of macroscopic electric fields results in that the TO and LO phonons have different frequencies. Due to short-range interatomic forces, caused by dominances of electrostatic forces in this region, there is anisotropy for which the TO–LO splitting is larger than the A_1–E_1 splitting. The E_2 mode consists of two modes of low and high frequency phonons, assigned as $E_2^{(1)}$(low) and $E_2^{(2)}$(high), which are associated with vibrations of the heavy Zn sublattice and oxygen atoms, respectively. As a result of all of the above, in Table 2 we gather the most typical frequencies and assignation of ZnO Raman active modes [32,33].

Table 2. Frequencies and assignation of typical Raman active modes in ZnO

Frequency for bulk ZnO, cm^{-1}	Assignation of modes
102	$E_2^{(1)}$ (low)
330	Multi phonon
379	A_1(TO)
410	E_1(TO)
437	$E_2^{(2)}$ (high)
541	A_1(LA)
577	A_1(LO)
592	E_1(LO)
660	Multi phonon
1153	Multi phonon

$ZnCo_2O_4$, which has a cubic structure, is a typical representative of normal AB_2O_4 spinel and belongs to the Fd3m (O_h^7) space group with Z = 8. In an ideal AB_2O_4 spinel structure, A atoms are located on tetrahedral sites of T_d symmetry, while B atoms are on octahedral sites of D_{3d} symmetry and oxygen atom occupy C_{3v} sites [34]. In $ZnCo_2O_4$ the anions form a nearly ideal close-packed pseudo-face-center-cubic sublattice surrounded by tetrahedral and octahedral sites where cations occupy only 1/8 of the tetrahedrally coordinated sites and 1/2 of the octahedrally coordinated sites. Theoretical analysis based on factor-group approach predicts, for $ZnCo_2O_4$, five Raman-active bands ($A_{1g} + E_g + 3F_{2g}$) and four infrared-active bands F_{1u} [10,35–38]. In Table 3 we gathered frequencies and assignation of Raman active $ZnCo_2O_4$ modes, presented in [35]. Slightly different peak positions for bulk $ZnCo_2O_4$ at 488.0, 525.4, 623.4, 693.0 and ~705 cm^{-1} have been reported in [10] but quantitatively similar to those given in [35], except some of peaks are shifted by up to 10 cm^{-1}.

Table 3. Frequencies and assignation of Raman active modes of $ZnCo_2O_4$ phase

Frequency for $ZnCo_2O_4$ phase, cm^{-1}	Assignation of modes
185	F_{2g}
475	E_g
520	F_{2g}
610	F_{2g}
690	A_{1g}

Figure 1 shows all Raman spectra of samples obtained by hydrothermal method doped with 5 to 50% of CoO. In these spectra, there is an evident existence of modes that belong to both phases, ZnO and $ZnCo_2O_4$. The ZnO phase is represented with its characteristic single phonon modes at 379 (A_1(TO)), 437 ($E_2^{(2)}$), 577 (A_1(LO)), and multi phonons (2LO) at 330, 660 and ~1110 cm^{-1}. The most typical and most obvious representative of ZnO phase, especially in smaller concentrations of CoO, is the mode at 437cm^{-1}. This mode at 437 cm^{-1} behaves the same way as all other ZnO modes; its intensity decreases with increase in CoO concentration. In these spectra, the peak center position is at somewhat lower frequencies than in bulk crystals, due to the nanosized structure of the samples. Beside modes belonging to ZnO, modes such as 185 (F_{2g}), 475 (E_g), 520 (F_{2g}), 610 (F_{2g}) and 690 cm^{-1} (A_{1g}), which represent the $ZnCo_2O_4$ phase, can also be seen. Our results for $ZnCo_2O_4$ modes are in good agreement with results presented in [10] for smaller concentrations of dopant (CoO), while for higher concentration of dopant they are in good agreement with results presented in literature [35]. The intensity of $ZnCo_2O_4$ modes, oppositely from ZnO modes, increased with the increase of CoO concentration. These results of Raman spectroscopy are in good agreement with previously obtained XRD results. Apart from modes that belong to ZnO and $ZnCo_2O_4$, in each and every Raman spectrum of our samples prepared by hydrothermal method, the existence of an additional structure is also evident. This additional structure is the SOP mode, originating from ZnO nanoparticles as a consequence of the nanosize structure of the samples, as mentioned previously.

The effect of change of CoO concentration on the behavior of characteristic SOP modes is shown in Figure 2. It is clearly visible that the intensity of SOP modes decreases with the increase in CoO concentration, which is similar to the intensity behavior of ZnO modes and opposite to intensity behavior of $ZnCo_2O_4$. This conduction of SOP modes is an additional proof that they originate from ZnO.

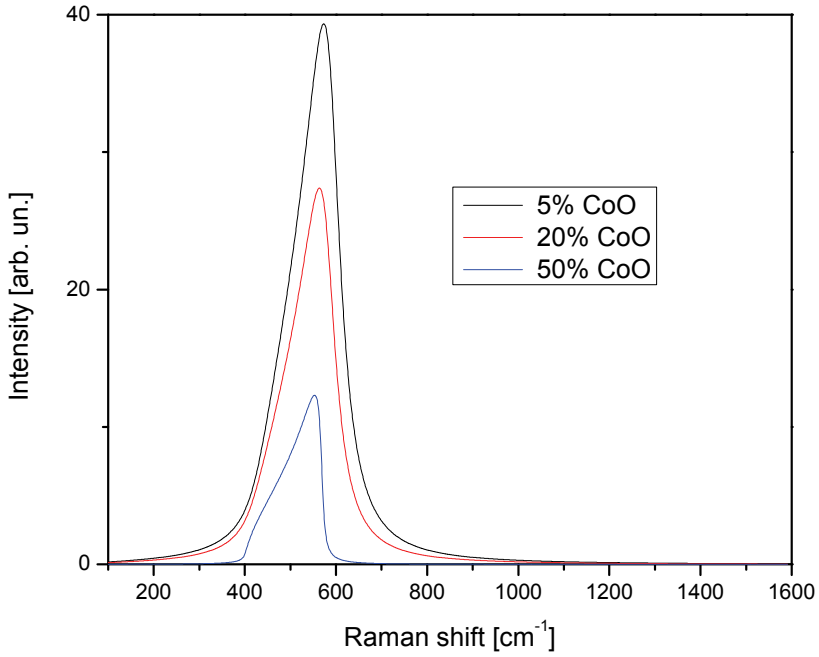

Figure 2. Change of intensity of characteristic SOP modes with CoO concentration.

CONCLUSION

The morphology of hydrothermally obtained samples was examined using SEM, showing particles of different sizes: smaller particles belonging to the $ZnCo_2O_4$ phase, and larger particles belonging to the ZnO phase. The following investigation of phase composition by X-ray diffraction revealed the existence of ZnO and $ZnCo_2O_4$ crystalline phases. In the Raman spectra of all prepared samples, the presence of ZnO was determined by the existence of characteristic single and multi phonons modes. The presence of $ZnCo_2O_4$ was determined by the existence of its typical phonon modes. Besides the modes that belong to $ZnCo_2O_4$ and ZnO phases, there is also evidence of surface optical phonons (SOP) modes. We have investigated the characteristics of the SOP modes and notice that their intensity, as the intensity of ZnO modes, decreased with the increases in CoO concentration, while the intensity of $ZnCo_2O_4$ modes showed the opposite behavior.

REFERENCES

[1] J. Gleize, E. Chikoidze, Y. Dumont, E. Rzepka, O. Gorochov, Superlat. Microstr. **42** (2007) 242–245.

[2] D.F. Wang, S.Y. Park, H.W. Lee, Y.S. Lee, V.D. Lam, Y.P. Lee, Phys. Stat. Sol. (a) **204** (2007) 4029–4032.

[3] Y. Chen, D.M. Bagnall, H. Koh, K. Park, K. Higara, Z. Zhu, T. Yao, J. Appl. Phys. **84** (1998) 3912–3918.

[4] J. Nemeth, G. Rodriguez-Gattorno, A. Diaz, I. Dekany, Langmuir **20** (2004) 2855–2860.

[5] J.M.D. Coey, M. Venkatesan, C.B. Fitzgerald, Nat. Mater. **4** (2005) 173–179.

[6] C. Sudakar, J.S. Thakur, G. Lawes, R. Naik, V.M. Naik, Phys. Rev., B **75** (2007) 054423–054426.

[7] T. Dietl, Acta Phys. Pol., A **111** (2007) 27–46.

[8] R. Cuscó, E. Alarcón-Lladó, J. Ibáñez, L. Artús, J. Jiménez, B. Wang, M.J. Callahan, Phys. Rev., B **75** (2007) 165202––165211.

[9] Y. Liu, J.L. MacManus-Drisoll, Appl. Phys. Lett. **94** (2009) 022503-3.

[10] J. Xu, W.Ji, X.B. Wang, H. Shu, Z.X. Shen, S.H. Tang, J. Raman Spectrosc. **29** (1998) 613–615.

[11] H. Zeng, W. Cai, B. Cao, J. Hu, Y. Li, P. Liu, Appl. Phys. Lett. **88** (2006) 181905-3.

[12] N. Romčević, R. Kostić, B. Hadžić, M. Romčević, I. Kuryliszin-Kudelska, W. Dobrowolski, U. Narkievicz, D. Sibera, JALLCOM **507** (2010) 386–390.

[13] M. Millot, J. Gonzalez, I. Molina, B. Salas, Z. Golacki, J.M. Broto, H. Rakoto, M. Gorian, JALLCOM **423** (2006) 224––227.

[14] R.P. Wang, G. Xu, P. Jin, Phys. Rev., B **69** (2004) 113303-4.

[15] R.Y. Sato-Berrú, A. Vázquez-Olmos, A.L. Fernández-Osorio, S. Sotres-Martínez, J. Raman Spectrosc. **38** (2007) 1073–1076.

[16] P.-M. Chassaing, F. Demangeot, V. Paillard, A. Zwick, N. Combe, C. Pages, M.L. Kahn, A. Maisonnat, B. Chaudret, Phys. Rev., B **77** (2008) 153306-4.

[17] G. Irmer, J. Raman Spectrosc. **38** (2007) 634–646.

[18] A.L. Patterson, Phys. Rev. **56** (1939) 978–982.

[19] A. Ghosh, R.N.P. Choudhary, J. Phys., D **42** (2009) 075416-6.

[20] F. Friedrich, N.H. Nickel, Appl. Phys. Lett. **91** (2007) 111903-3.

[21] C.G. Granqvist, O. Hunderi, Phys. Rev., B **18** (1978) 1554–1561.

[22] K. Karkkainen, A. Saviola, K. Nikoskinen, IEEE Transaction on geosciences and remote sensors **39**(5) (2001) 1013–1018.

[23] J.C.M. Garnett, Trans. R. Soc. Vol. CCIII, 1904, pp. 385––420.

[24] A. Saviola, I. Lindell, Dielectric Properties of Heterogeneous Materials, PIER 6 Progress in Electromagnetic Research, A. Priou, Ed., Elsevier, Amsterdam, 1992.

[25] D.A.G. Bruggeman, Ann. Phys. **24**(5) (1935) 636–679.

[26] J. Saarinen, E.M. Vartiainen, K. Peiponen, Opt. Rev. **10**(2) (2003) 111–115.

[27] X.C. Zeng, D.J. Bergman, P.M. Hui, D. Stroud, Phys. Rev., B **38** (1988) 10970–10973.

[28] J.D. Ye, S. Tripathy, F.F. Ren, X.W. Sun, G.Q. Lo, K.L. Teo, Appl. Phys. Lett. **94** (2009) 011913-3.

[29] I.M. Tiginyanu, A. Sarua, G. Irmer, J. Monecke, S.M. Hubbard, D. Pavlidis, V. Valiaev, Phys. Rev., B **64** (2001) 233317-3.

[30] M. Šćepanović, M. Grujić-Brojčin, K. Vojisavljević, S. Bernik, T. Srećković, J. Raman Spectrosc. **41** (2010) 914––921.

[31] H. Idink, V. Srikanth, W.B. White, E.C. Subbarao, J. Appl. Phys. **76** (1994) 1819–1823.

[32] N. Ashkenov, B.N. Mbenkum, C. Bundesmann, V. Riede, M. Lorenz, D. Spemann, E.M. Kaidashev, A. Kasic, M. Shubert, M. Grundmann, J. Appl. Phys. **93** (2003) 126––133.

[33] E.F. Venger, A.V. Melnichuk, L.L. Melnichuk, Yu.A. Pasechuk, Phys. Stat. Solidi, B **188** (1995) 823–831.

[34] C.M. Julien, M. Massot, J. Phys.: Condens. Matter **15** (2003) 3151–3162.

[35] M. Bouchard, A. Gambardella, J. Raman Spectrosc. **41** (2010) 1477–1485.

[36] X. Wang, R. Zheng, Z. Liu, H. Ho, J. Xu, S.P. Ringer, Nanotechnology **19** (2008) 455702–455708.

[37] O.N. Shebanova, P. Lazor, J. Solid State Chem. **174** (2003) 424–430.

[38] O.N. Shebanova, P. Lazor, J. Chem. Phys. **119** (2003) 6100–6110.

ИЗВОД

РАМАН СПЕКТРОСКОПИЈА ПОВРШИНСКИХ ОПТИЧКИХ ФОНОНА КОД НАНОЧЕСТИЦА ZnO(Co) ДОБИЈЕНИХ ХИДРОТЕРМАЛНОМ МЕТОДОМ

Бранка Хаџић[1], Небојша Ромчевић[1], Maja Ромчевић[1], Izabela Kuryliszyn-Kudelska[2], Witold D. Dobrowolski[2], Ursula Narkiewicz[3], Daniel Sibera[3]

[1]*Институт за физику, Универзитет у Београду, Београд, Србија*
[2]*Institute of Physics, Polish Academy of Science, Warsaw, Poland*
[3]*Institute of Chemical and Environment Engineering, Szczecin University of Technology, Szczecin, Poland*

(Naučni rad)

Узорци ZnO допирани CoO су добијени коришћењем хидротермалне методе. Овакав начин добијања узорака омогућио је настанак серије узорака са различитом концентрацијом допанта од 5 до 50% CoO. Овим узорцима је првобитно испитана морфологија коришћењем скенирајућег електронског микроскопа и при нижим концентрацијама допанта уочене су честице сличних величина, док је са порастом концентрације допанта јасно уочљиво постојање две врсте честица различите величине. Рентгеноструктурном анализом је утврђено порекло ових честица. У нашим узорцима коегзистирају две врсте честица, ZnO и $ZnCo_2O_4$. Такође, ова врста анализе је омогућила да коришћењем Шерерове формуле одредимо средњу величину кристалита ових честица. ZnO честице су величине од 64 до 300 nm, док су $ZnCo_2O_4$ честице величине од 33 до 77 nm. Видимо да величина ZnO честица расте са порастом концентрације допанта док промена величине $ZnCo_2O_4$ честица са концентрацијом није монотона. Вибрационе карактеристике узорака су испитиване коришћењем микро-Раман спектроскопије, зеленом линијом 514,5 nm аргон-јон ласера. Раман спектроскопија је изабрана јер је идеална недеструктивна метода која омогућује испитивање локалног атомског уређења, квалитета узорака, фонона, изотопских ефеката и електрон–фонон спаривања. Добијени Раман спектри су анализирани и фитовани коришћењем Лоренцове линије за све пикове. На овим спектрима, поред карактеристичних пикова за ZnO и $ZnCo_2O_4$ честице, јасно се уочава и додатна структура, за коју смо утврдили да потиче од ZnO, а последица је губитка дугодометне уређености и престанка важења правила симетрије услед нанодимензионалности узорака. Та додатна струкутра су површински оптички фонони (ПОФ). Испитали смо и утицај промене концентрације допанта CoO на понашање ПОФ модова и утврдили да њихов интензитет опада са порастом концентрације CoO, и то за карактеристичне ПОФ модове.

Кључне речи: Нано-материјали • Оптичке особине • Апсорпција и рефлексија светлости • Површински оптички фонони